

SEISMIC RETROFITTING OF REINFORCED CONCRETE STRUCTURES  
WITH STEEL BRACING SYSTEMS

APPROVED BY SUPERVISORY COMMITTEE:

*James O. Jusa*

*Jose W. Roedel*

*Michael S. Heger*

*John L. Tassoulas*

*Chun*

SEISMIC RETROFITTING OF REINFORCED CONCRETE STRUCTURES WITH STEEL  
BRACING SYSTEMS

BY

MARC ERIC BADOUX, B.S.C.E.

DISSERTATION

Presented to the Faculty of the Graduate School of  
The University of Texas at Austin  
in Partial Fulfillment  
of the Requirements  
for the Degree of  
DOCTOR OF PHILOSOPHY

THE UNIVERSITY OF TEXAS AT AUSTIN

May 1987

SEISMIC RETROFITTING OF REINFORCED CONCRETE STRUCTURES WITH STEEL  
BRACING SYSTEMS

Publication No. \_\_\_\_\_

Marc Eric Badoux, Ph.D.  
The University of Texas at Austin, 1987h

Supervising Professor: James O. Jirsa

The objectives of this study are first, to examine various aspects of the selection and design of steel bracing systems for the seismic retrofitting of reinforced concrete frame structures, and second, to study analytically the response of a steel braced reinforced concrete frame under cyclic lateral loading.

Concepts are introduced which are useful in determining a strategy for retrofitting seismically inadequate frame structures. The main steps of the retrofitting operation are outlined. The choice of the bracing system configuration is discussed. The importance of matching the relative deformability of the frame and the bracing system is demonstrated.

The behavior of a steel braced frame unit under static lateral loading, both monotonic and cyclic, is studied. The

influence of the brace design strength and slenderness ratio is investigated in a parametric study. Particular attention is given to frames with strong beams and weak short columns because such frames are likely candidates for seismic retrofitting. The possibility of improving the seismic quality of braced frames with weak short columns by weakening the beams is investigated.

The steel bracing scheme is found to be very well-suited for retrofitting operations aimed toward strengthening and/or stiffening reinforced concrete structures with inadequate lateral resistance. A variety of design objectives ranging from collapse prevention to drift control can be achieved. The retrofitted structure can be designed to respond primarily in the elastic range. Inelastic buckling of the braces is the main problem in achieving good inelastic cyclic behavior of the braced frame. Problems associated with inelastic buckling may be prevented by using braces which buckle elastically, such as cables, or by using braces which yield in compression.

To Him who alone does great wonders,  
For His loving kindness is everlasting

Psalms 136:4

To my Mother and Father,  
Myriam, Pierre, Luc and  
"L'Hirondelle"

## A C K N O W L E D G E M E N T S

The author wishes to express his gratitude to Dr. James O. Jirsa for his advice and encouragement throughout the time of their collaboration. Working under Dr. Jirsa's guidance has been a privilege and an invaluable learning experience. The author is also grateful to Dr. Jose Roesset, Dr. Michael Kreger, Dr. John Tassoulas and Dr. C.H. Lew for their involvement with this research.

Thankful appreciation goes to the many faculty, staff and students who contributed to the friendly and stimulating working environment which characterizes the Ferguson Laboratory and the fourth floor of ECJ. Special thanks go to Sharon Cunningham, Maxine DeButts, Ellen Forshage, Jean Gehrke, Laurie Golding and Carol Booth for their secretarial contribution and loving support. Many thanks also to coworkers Tommy Bush, Elizabeth Jones and Carol Roach for their friendship. The warm friendship of Dr. Jack Breen, Leo Linbeck III, Scott O'Brien and Troy Madeley contributed to make the author's time at the University particularly enjoyable.

This work was sponsored by the National Science Foundation.

## T A B L E O F C O N T E N T S

Chapter		Page
1	BACKGROUND .....	1
	1.1 Seismic Retrofitting .....	1
	1.2 Steel Bracing Technique .....	4
	1.3 Applications .....	7
	1.3.1 Sendai School Building .....	7
	1.3.2 Durango 49 Building .....	10
	1.3.3 Zaragoza Hospital .....	16
	1.4 Review of Research .....	21
	1.4.1 Experimental Research on Seismic Retrofitting .....	21
	1.4.2 Cyclic Inelastic Bucling of Steel Braces .....	22
	1.4.3 Design Guideline for Seismic Retrofitting .....	29
	1.4.4 Seismic Index, $I_S$ .....	33
	1.5 Object and Scope .....	36
2	SEISMIC RETROFITTING OF INADEQUATE STRUCTURES .....	38
	2.1 Introduction .....	38
	2.2 Evaluation of the Seismic Adequacy of a Structure .....	38
	2.2.1 Introduction .....	38
	2.2.2 Structural Properties of the Existing Structure .....	39
	2.2.3 Structural Requirements for the Existing Structure .....	40
	2.3 Inadequate Strength and/or Ductility .....	41
	2.4 Seismic Retrofitting .....	47
	2.4.1 Introduction .....	47
	2.4.2 Basic Retrofitting Approaches .....	47
	2.4.3 Optimum Retrofitting Approach .....	50
	2.5 Changes in the Natural Period of Vibration .	53
	2.5.1 Introduction .....	53
	2.5.2 Shortening of the Natural Period .....	58

T A B L E   O F   C O N T E N T S  
(continued)

<u>Chapter</u>	<u>Page</u>
2.5.3	Lengthening of the Natural Period ... 61
2.5.4	Change in Strength Ductility Period . 62
2.6	Change in Mass and Damping ..... 64
2.6.1	Change in Mass ..... 64
2.6.2	Change in Damping ..... 65
3	RETROFITTING WITH A STEEL BRACING SYSTEM ..... 67
3.1	Bracing Pattern and Configuration ..... 67
3.1.1	General ..... 67
3.1.2	Bracing Pattern ..... 68
3.1.3	Configuration of the Bracing System . 71
3.1.4	Spatial Distribution ..... 75
3.2	Modeling a Braced Frame ..... 78
3.2.1	Exact Model ..... 78
3.2.2	Approximate Model ..... 80
3.2.3	Overturning Forces of the Bracing System ..... 83
3.3	Deformability of the Bracing System ..... 85
3.4	Energy Dissipation in the Bracing System ... 92
3.5	Flowchart of the Retrofitting Process ..... 96
3.5.1	Decision to Brace a Structure ..... 96
3.5.2	Design of the Bracing System ..... 96
3.6	Braced Frame with Short Columns ..... 99
3.6.1	Introduction to Short Column Behavior ..... 99
3.6.2	Short Columns in a Braced Frame ..... 106
3.6.3	Axial Capacity of a Short Column Deflected Laterally ..... 109
4	DUPLICATION OF THE EXPERIMENTAL DATA ..... 115
4.1	Experimental Part of the Research Project .. 115
4.1.1	Introduction ..... 115
4.1.2	Model Frame ..... 115



T A B L E   O F   C O N T E N T S  
(continued)

<u>Chapter</u>	<u>Page</u>
4.1.3	Retrofitting with Reinforced Concrete Wing Walls ..... 121
4.1.4	Retrofitting with a Steel Bracing System ..... 122
4.2	The Computer Program ..... 128
4.3	Duplication ..... 132
4.3.1	The Bare Frame ..... 132
4.3.2	Braced Frame ..... 136
5	PARAMETRIC STUDY ..... 142
5.1	Introduction ..... 142
5.2	Subassemblage ..... 142
5.3	Analytical Model of the Subassemblage ..... 147
5.4	The n and m Ratios ..... 154
5.4.1	Design Ratio n ..... 154
5.4.2	Load Ratio m( $\delta$ ) ..... 156
5.5	Loadings and Variables of the Study ..... 158
5.5.1	Loadings ..... 158
5.5.2	Brace Variables ..... 159
5.5.3	Slenderness Ratios $kl/r$ ..... 161
6	RESULTS OF THE PARAMETRIC STUDY ..... 162
6.1	Monotonic Loading ..... 162
6.1.1	Failure Sequence ..... 162
6.1.2	Variation of n and $kl/r$ ..... 166
6.2	Reversed Loading ..... 172
6.2.1	Braces under Reversed Loading ..... 172
6.2.2	Failure Sequence ..... 174
6.2.3	Variation of n and $kl/r$ ..... 178
6.2.4	$kl/r = 0$ and $kl/r = \infty$ ..... 184
6.3	Cyclic Loading ..... 188
6.3.1	Development of the Inelastic Behavior ..... 188
6.3.2	Variation of n and $kl/r$ ..... 192

T A B L E O F C O N T E N T S  
(continued)

<u>Chapter</u>		<u>Page</u>
6.4	Evaluation of the Steel Bracing Scheme .....	203
	6.4.1 Introduction .....	203
	6.4.2 Strength .....	205
	6.4.3 Stiffness .....	206
	6.4.4 Ductility .....	206
	6.4.5 Design Implications for the Bracing System .....	209
6.5	Prevention of Inelastic Buckling .....	212
	6.5.1 Introduction .....	212
	6.5.2 Very Low Slenderness .....	212
	6.5.3 Very Large Slenderness Ratio .....	214
7	BEAM WEAKENING IN FRAMES WITH WEAK COLUMNS .....	221
	7.1 Introduction .....	221
	7.2 Weakening Parameters .....	224
	7.2.1 Conceptual Representation of the Idea .....	224
	7.2.2 The r and q Ratios .....	226
	7.2.3 Weakening Parameters .....	229
	7.3 Braced Frames with Weakened Beams .....	233
	7.4 Parametric Study .....	241
	7.4.1 Variation of Parameters u and v .....	241
	7.4.2 Choice of Parameters u and v .....	248
	7.5 Stiffness of the Weakened Frame .....	250
8	SUMMARY AND CONCLUSIONS .....	253
	8.1 Summary .....	253
	8.2 Conclusions .....	255
	8.2.1 Design Considerations .....	255
	8.2.2 Behavior and Analysis of the Braced Frame .....	256
	8.2.3 Nonstructural Considerations .....	259
	8.3 Suggestions for Research .....	260

T A B L E   O F   C O N T E N T S  
(continued)

<u>Chapter</u>	<u>Page</u>
A   APPENDIX .....	263
A.1   Beam Column Element EL7 .....	263
A.2   Buckling Element EL10 .....	269
REFERENCES .....	272

## L I S T   O F   F I G U R E S

<u>Figure</u>		<u>Page</u>
1.1.1	Retrofitting techniques .....	3
1.3.1	Sendai School, Japan; steel bracing retro- fitting .....	8
1.3.2	Sendai School, plan and elevation [2] .....	9
1.3.3	Detailing of the bracing system [2] .....	10
1.3.4	Test specimen for testing the spandrel beam beakening scheme [2] .....	10
1.3.5	Durango 49, Mexico City; steel bracing retro- fitting .....	12
1.3.6	Durango 49, plan and elevation [3] .....	14
1.3.7	Durango 49, connections .....	15
1.3.8	Zaragoza Hospital, Mexico City; steel bracing retrofitting .....	17
1.3.9	Zaragoza Hospital, plan .....	18
1.3.10	Zaragoza Hospital, elevation .....	19
1.3.11	Steel bracing unit in position .....	20
1.4.1	Experimental hysteresis curves for retrofitted frames [9] .....	23
1.4.2	Typical load-displacement relationships for different retrofitting techniques [5] .....	24
1.4.3	Hysteresis loops for steel braces with slender- ness ratios of 40, 80 and 120 [11] .....	26
1.4.4	Hysteresis curves from a cyclic coupon test [11] .....	27

## L I S T   O F   F I G U R E S

<u>Figure</u>		<u>Page</u>
1.4.5	Hysteresis loops for a brace with a slenderness ratio of 40 [11] .....	27
1.4.6	Envelopes of translated axial force-displacement curves [11] .....	28
1.4.7	Physical interpretation of a brace hysteretic loop [15] .....	28
1.4.8	Comparison of phenomenological models for steel braces [14] .....	30
1.4.9	Seismic retrofitting approaches [17] .....	32
1.4.10	Flowchart of design and construction for seismic retrofitting [17] .....	34
2.3.1	Strength reliant vs. ductility reliant structures .....	43
2.3.2	Seismic adequacy in the strength-ductility plane .....	46
2.4.1	Three basic retrofitting approaches .....	48
2.4.2	Retrofitting approaches for four structures ...	51
2.5.1	Elastic seismic design spectra, qualitative ...	55
2.5.2	Inelastic seismic design spectra, qualitative .	55
2.5.3	Seismic adequacy in the strength-period plane .	57
2.5.4	Undesirable shortening of the period .....	59
2.5.5	Desirable shortening of the period .....	59
2.5.6	Change in ductility and period .....	63

## L I S T   O F   F I G U R E S

<u>Figure</u>		<u>Page</u>
3.1.1	Bracing patterns .....	69
3.1.2	Bracing configurations .....	73
3.1.3	Deformation of a laterally loaded building with stiff perimeter braced frames .....	77
3.2.1	Modelling of a braced frame .....	79
3.2.2	Approximate model and response .....	81
3.2.3	Forces in a bracing system with X-pattern .....	84
3.3.1	Relative deformability of the frame and the bracing system .....	87
3.3.2	Initial stiffness of the bracing system for two levels of strength .....	91
3.4.1	Energy dissipation in the bracing system .....	93
3.5.1	Design flowchart for retrofitting with a bracing system .....	97
3.6.1	Seismic damage to short columns, Japan .....	100
3.6.2	Load-deflection relationships for short columns .....	102
3.6.3	Qualitative envelopes of a short column under cyclic lateral loading .....	103
3.6.4	Short column with strength equation .....	105
3.6.5	Lateral load-drift relationship for a braced frame with short columns .....	107

L I S T   O F   F I G U R E S

<u>Figure</u>		<u>Page</u>
3.6.6	Axial failure of a short column deformed laterally .....	110
3.6.7	Qualitative influence of axial compression on ultimate lateral drift .....	113
3.6.8	Qualitative influence of axial compression and confinement on ultimate lateral drift .....	113
4.1.1	Example building .....	116
4.1.2	Prototype building, plan and elevation [29] ...	117
4.1.3	Detailing of spandrel beam and column .....	119
4.1.4	Frame model, boundary conditions and test set up [29] .....	120
4.1.5	Steel bracing scheme for model frame [29] .....	123
4.1.6	Braced frame after test .....	125
4.1.7	Damage to the braced frame .....	126
4.1.8	Experimental load-drift relationship for the braced frame model [29] .....	127
4.1.9	Composite column .....	129
4.3.1	Analytical models .....	133
4.3.2	Comparison of initial stiffness .....	135
4.3.3	Analytical load-drift relationship for the braced frame .....	138
4.3.4	Experimental and analytical load-drift envelopes .....	139

## L I S T   O F   F I G U R E S

<u>Figure</u>	<u>Page</u>
5.2.1	Subassemblage ..... 143
5.2.2	Braced column of the prototype frame ..... 145
5.3.1	Analytical model of the subassemblage ..... 148
5.3.2	Experimental load-deflection relationship for a short column similar to the prototype column [23] ..... 150
5.3.3	Assumed load-drift relationship for the proto- type column ..... 151
5.3.4	Moment-rotation relationship for the beam in- elastic spring ..... 151
5.4.1	Ratio $n$ for a frame retrofitted with a steel bracing system ..... 155
5.4.2	Design ratio $n$ and load ratio $m$ ..... 157
6.1.1	Bare frame and column under monotonic loading . 163
6.1.2	Bracing system under monotonic loading ..... 163
6.1.3	Normalized load-drift relationship for a braced frame under monotonic loading ..... 165
6.1.4	Braced frame under monotonic loading - $n = 1, 2, 3$ and $4$ , and $kl/r = 40$ ..... 167
6.1.5	Braced frame under monotonic loading - $n = 1, 2, 3$ and $4$ , and $kl/r = 80$ ..... 168
6.1.6	Braced frame under monotonic loading - $n = 1, 2, 3$ and $4$ , and $kl/r = 120$ ..... 169



L I S T   O F   F I G U R E S

<u>Figure</u>	<u>Page</u>
6.1.7	Braced frame under monotonic loading - n = 1, 2, 3 and 4, and $kl/r = 40, 80$ and 120 .. 171
6.2.1	Brace under reversed loading - $kl/r = 40, 80$ and 120 ..... 173
6.2.2	Braced frame under reversed loading ..... 175
6.2.3	Frame and brace contributions under reversed loading ..... 176
6.2.4	Braced frame under reversed loading - n = 1, 2, 3 and 4, and $kl/r = 40$ ..... 179
6.2.5	Braced frame under reversed loading - n = 1, 2, 3 and 4, and $kl/r = 80$ ..... 180
6.2.6	Braced frame under reversed loading - n = 1, 2, 3 and 4, and $kl/r = 120$ ..... 181
6.2.7	Braced frame under reversed loading - n = 4, and $kl/r = 40$ and 120 ..... 183
6.2.8	Braced frame under reversed loading - n = 2, and $kl/r = 0$ ..... 185
6.2.9	Braced frame under reversed loading - n = 2, and $kl/r = \text{infinity}$ ..... 186
6.2.10	Braced frame under reversed loading - n = 2, and $kl/r = 0, 80$ and infinity ..... 187
6.3.1	Cyclic loading history ..... 189
6.3.2	Braced frame under cyclic loading ..... 190
6.3.3	Frame contribution under cyclic loading ..... 191

## L I S T   O F   F I G U R E S

<u>Figure</u>		<u>Page</u>
6.3.4	Bracing system contribution under cyclic loading .....	191
6.3.5	Braced frame under cyclic loading - n = 2 and $kl/r = 40$ .....	193
6.3.6	Braced frame under cyclic loading - n = 3 and $kl/r = 40$ .....	194
6.3.7	Braced frame under cyclic loading - n = 4 and $kl/r = 40$ .....	195
6.3.8	Braced frame under cyclic loading - n = 2 and $kl/r = 80$ .....	196
6.3.9	Braced frame under cyclic loading - n = 3 and $kl/r = 80$ .....	197
6.3.10	Braced frame under cyclic loading - n = 4 and $kl/r = 80$ .....	198
6.3.11	Braced frame under cyclic loading - n = 2 and $kl/r = 120$ .....	199
6.3.12	Braced frame under cyclic loading - n = 3 and $kl/r = 120$ .....	200
6.3.13	Braced frame under cyclic loading - n = 4 and $kl/r = 120$ .....	201
6.3.14	Braced frame under cyclic loading - n = 4 and $kl/r = 40, 80$ and 120 .....	202
6.3.15	Last two cycles of the loading history - n = 4 and $kl/r = 40$ and 120 .....	204
6.4.1	Retrofitting with a steel bracing system .....	208

## L I S T   O F   F I G U R E S

<u>Figure</u>		<u>Page</u>
6.5.1	Qualitative influence of brace slenderness ratio $k\ell/r$ on hysteretic behavior .....	213
6.5.2	Prestressing forces in the braced frame .....	216
6.5.3	Load deformation curve for a cable, nonpre-stressed and prestressed .....	216
6.5.4	Effect of prestressing .....	218
7.1.1	Frame lateral failure mechanism .....	222
7.2.1	Retrofitting with and without beam weakening ..	225
7.2.2	Ratio $q$ for a member in double curvature .....	227
7.2.3	Ratio $r$ for a beam column joint .....	227
7.2.4	Weakening parameters $u$ , $v$ and $w$ .....	230
7.2.5	Beam weakening schemes for prototype frame ....	232
7.2.6	Shear transfer in weakened beam .....	234
7.3.1	Altered frame under monotonic loading .....	236
7.3.2	Altered frame under reversed loading .....	236
7.3.3	Braced frame under monotonic loading, with and without beam weakening .....	237
7.3.4	Braced frame under reversed loading, with and without beam weakening .....	239
7.3.5	Braced frame under cyclic loading, with and without beam weakening .....	240

CHAPTER 1  
BACKGROUND

1.1 Seismic Retrofitting

Our ability to build seismically safe structures with adequate seismic resistance has increased significantly in the past two decades. One aspect of earthquake engineering which has received comparatively little attention is the seismic retrofitting of existing structures. Many reinforced concrete frame structures built in seismically active areas are expected to perform inadequately in a seismic event. Reconnaissance studies following major earthquakes have documented collapse or severe damage of numerous multistory reinforced concrete frames. For life safety and for economic reasons, structures expected to perform inadequately must be replaced or retrofitted.

Wyllie [1] defines seismic retrofitting of an existing building as "the judicious modification of its structural properties in order to improve its performance in future earthquakes." The aim of the retrofitting may be to increase the strength and/or ductility and/or stiffness. The engineering task of improving the seismic performance of a structure is often referred to in the literature as "seismic strengthening." The term "seismic retrofitting" is used in this study because it

better describes a task in which strengthening is only one aspect.

The most likely candidate for seismic retrofitting is a building with a satisfactory gravity load capacity, but a seismically deficient lateral resistance. The lateral resistance of a structure may be inadequate for various reasons:

- upgrading of the code seismic provisions
- damage in a previous earthquake
- design or construction errors
- changes in building occupancy
- additions to the building

Corresponding to the variety of structures and of their deficiencies, there are many retrofitting techniques. The four major techniques to improve the seismic lateral resistance of a space frame are shown in Fig. 1.1.1:

a) Column strengthening - The columns lateral capacity and ductility are increased by steel or reinforced concrete encasement.

b) Wing walls - The columns are strengthened by the arrangement of cast-in-place or precast wing elements. The goal is often to produce a better frame failure mechanism by forcing failure away from the columns into the beams.

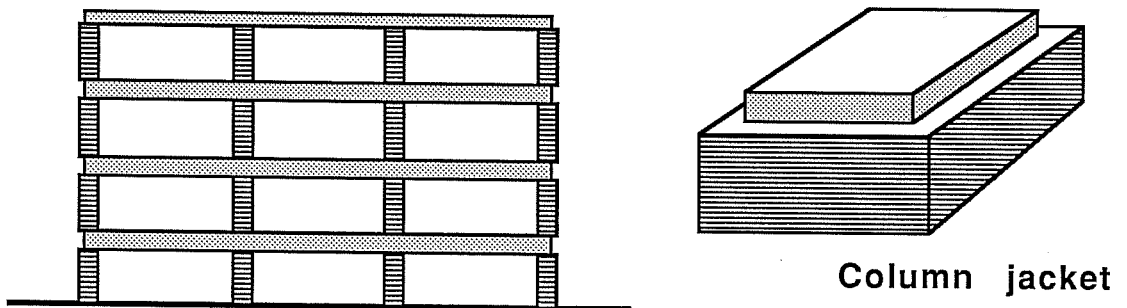
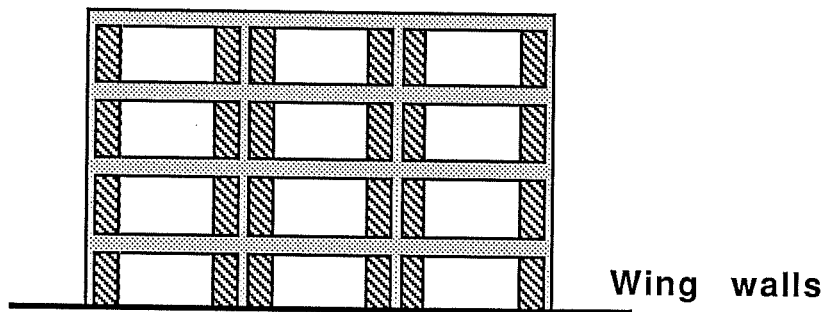
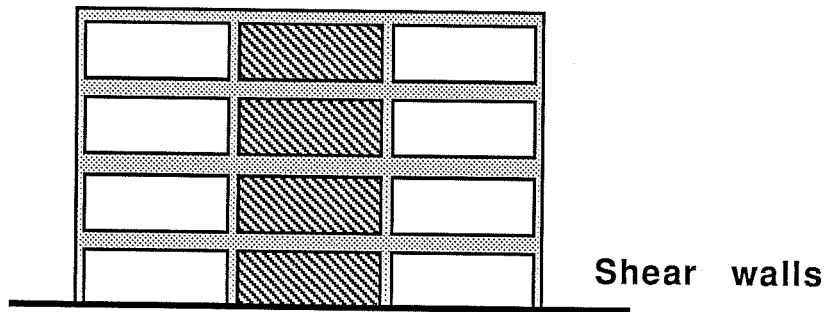
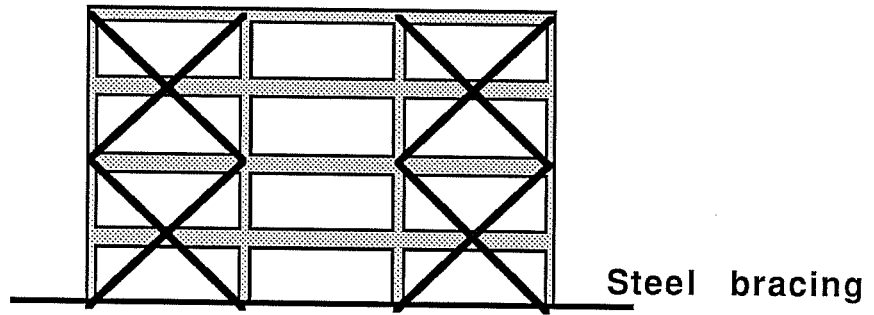


Fig. 1.1.1 Retrofitting techniques

c) Shear walls - Shear walls are created by the infilling of certain bays, usually bays of interior frames. This is an efficient way to strengthen and stiffen a building.

d) Bracing system - A steel bracing system is typically attached on the exterior of the perimeter frames.

Research is needed to evaluate the reliability of the retrofitting techniques and improve their effectiveness. Design and construction guidelines must be developed to meet the future need for retrofitting. In this study the retrofitting schemes using steel bracing systems is investigated. Much of the research on seismic retrofitting can be applied to retrofitting for other types of lateral loading, such as wind loads. Adequate lateral strength and stiffness are need for wind resistance. For seismic loading, ductility is an additional consideration for adequate structural performance.

## 1.2 Steel Bracing Technique

Braced frames are known to be efficient structural systems for buildings under high lateral loads such as seismic or wind loadings. The fact that the lateral resistance of a frame can be significantly improved by the addition of a bracing system has led to the idea of retrofitting seismically inadequate reinforced concrete frames with steel bracing systems. Three

applications of this retrofitting technique are presented in Section 1.4.

Retrofitting a structure with a steel bracing system is particularly well suited for multi-story space frames in need of lateral strengthening and/or stiffening at every story. The interior frames can be braced, but in general the bracing system is added to the perimeter frames. Unless specified otherwise, it is assumed in this study that the bracing system is external.

The bracing scheme has architectural advantages. In the case of an external bracing system, all or most of the work can be performed on the exterior of the building. Therefore the disruption during construction and the loss of room and accessibility in the retrofitted structure are minimized. This represents a major economical and functional advantage of bracing schemes.

Less tangible aspects such as the impact of external bracing on the aesthetics of the structure must be considered. The bracing system often damages the appearance of the building. But if the bracing system is carefully shaped, it can enhance the aesthetics of the building. The application described in Section 1.3.3 is a good example of a retrofit with a positive aesthetic impact. The bracing is a visible sign of strength and can be used to convey a sense of confidence to users.



The main disadvantage of the bracing technique is the cost. Typically, the bracing system is prefabricated in small components and assembled on the existing structure. Much work is necessary to connect the bracing system to the existing structure. The construction is labor intensive, and fabricated steel is expensive to install and to maintain. A further drawback is the lack of data and experience supporting the reliability of the technique.

In many applications the bracing of the building is best combined with other retrofitting operations. Bracing the perimeter frames may be used together with column strengthening in interior frames or the creation of infill shear walls. In the case of a structure damaged in an earthquake the bracing may be mixed with a variety of repair and strengthening work.

A retrofitting scheme using a steel bracing system has many structural advantages:

- The level of strength and stiffness increase can be tuned relatively easily by the choice of the number and size of the braces.
- If adequately detailed, satisfactory ductility and hysteretic behavior can be obtained from the bracing system.
- The new lateral resisting system can be designed to carry the entire lateral load. The reinforced concrete

can be relieved of any lateral load-carrying function. This is particularly advantageous if the frame has a defective failure mechanism.

- The designer has adequate control over the flow of force. Local force concentrations can thus be kept to a minimum in a good design.

- The additional mass is small.

### 1.3 Applications

1.3.1 Sendai School Building. The reported number of reinforced concrete buildings retrofitted with steel bracing systems is low. But the number of applications is increasing as the need for seismic retrofitting grows and as designers become more familiar with the advantages of the bracing scheme. The technique was first used in Japan. In some cases the bracing had a preventive character while in others it was part of the repair process of a structure damaged in an earthquake. The Sendai school building [2] is an example of the bracing of a damaged structure. A poor design produced perimeter frames with deep spandrel beams and short columns. Following shear failure of many columns in the 1978 Miyagi-Ken-Oki earthquake the perimeter frames were retrofitted with steel bracing systems. The configuration of the bracing system is shown in Figs. 1.3.1 and 1.3.2 and the detailing in Fig. 1.3.3. The braces and

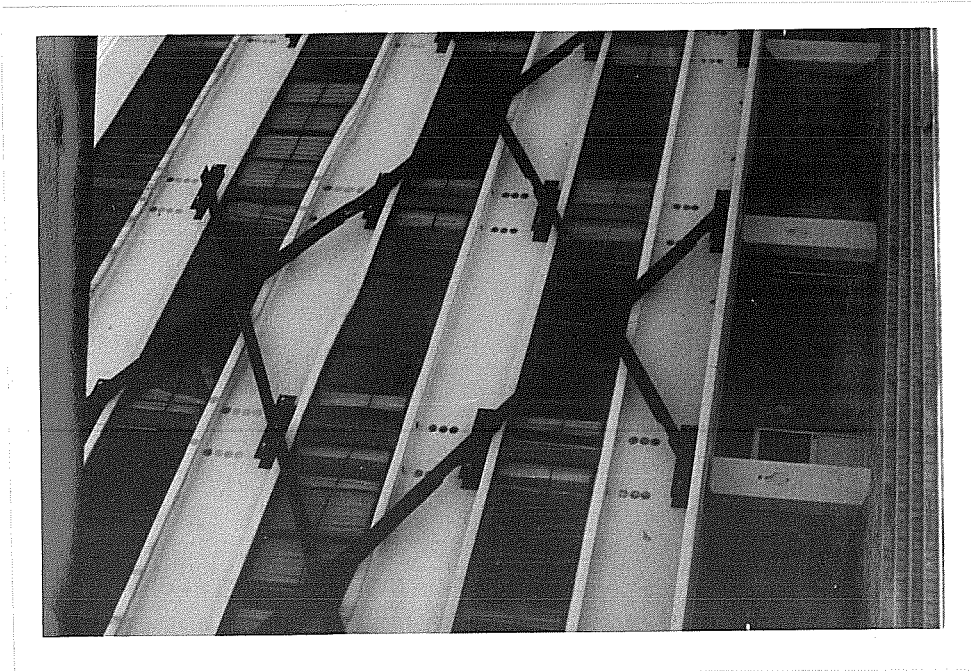


Fig. 1.3.1 Sendai School, Japan; steel bracing retrofitting

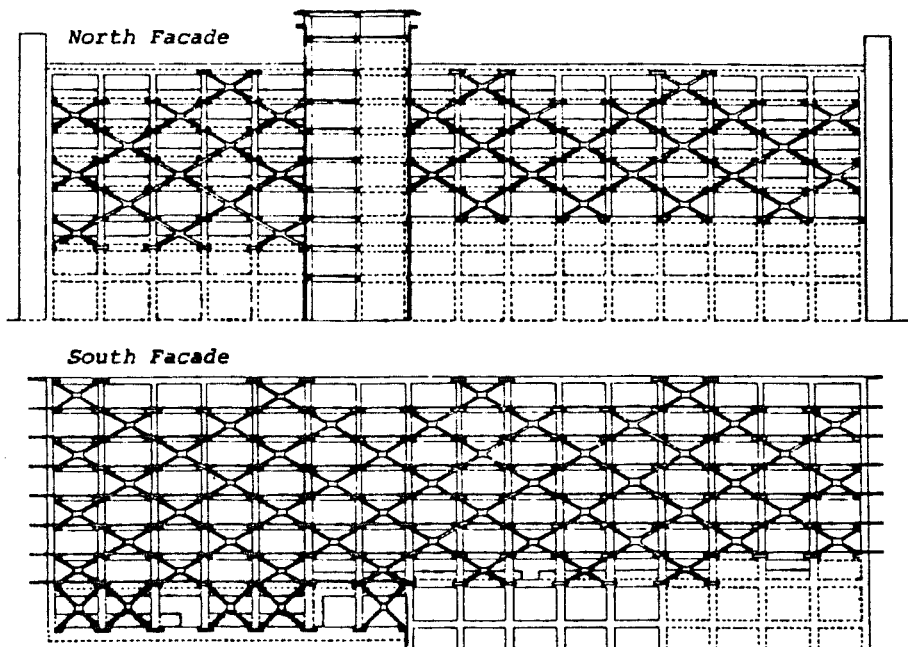
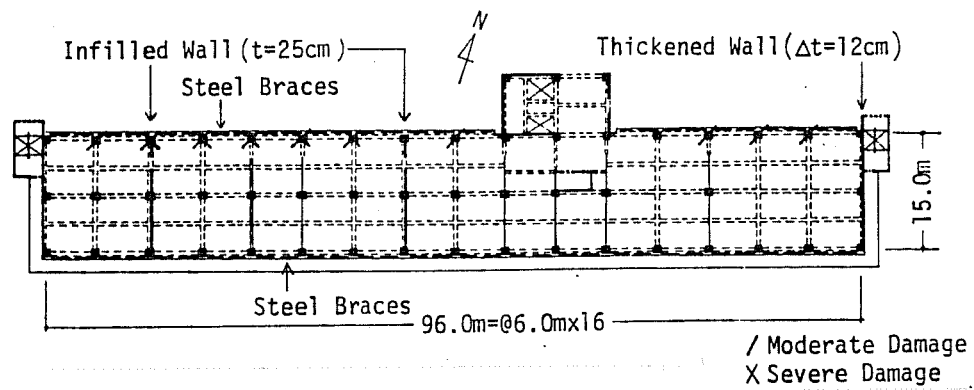


Fig. 1.3.2 Sendai School, plan and elevation [2]

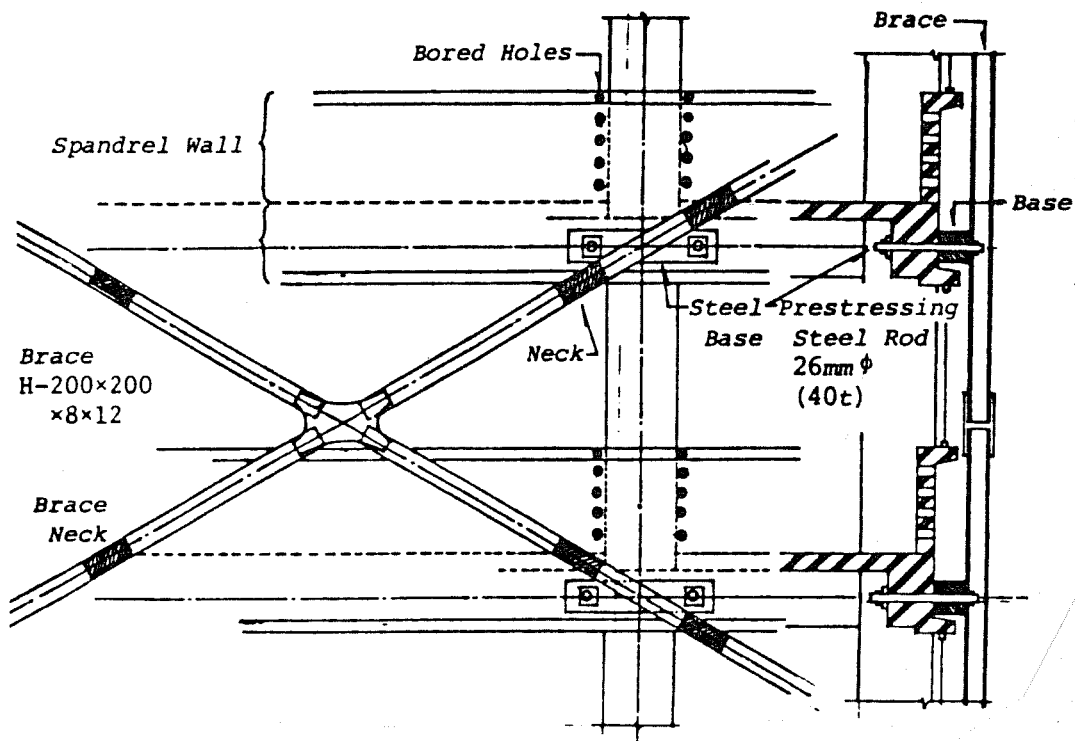


Fig. 1.3.3 Detailing of the bracing system [2]

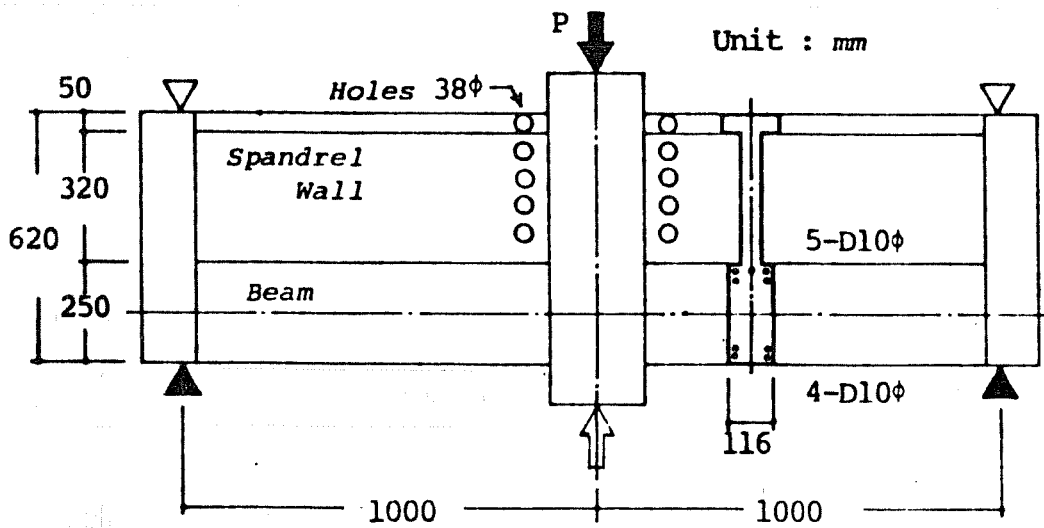


Fig. 1.3.4 Test specimen for testing the spandrel beam weakening scheme [2]

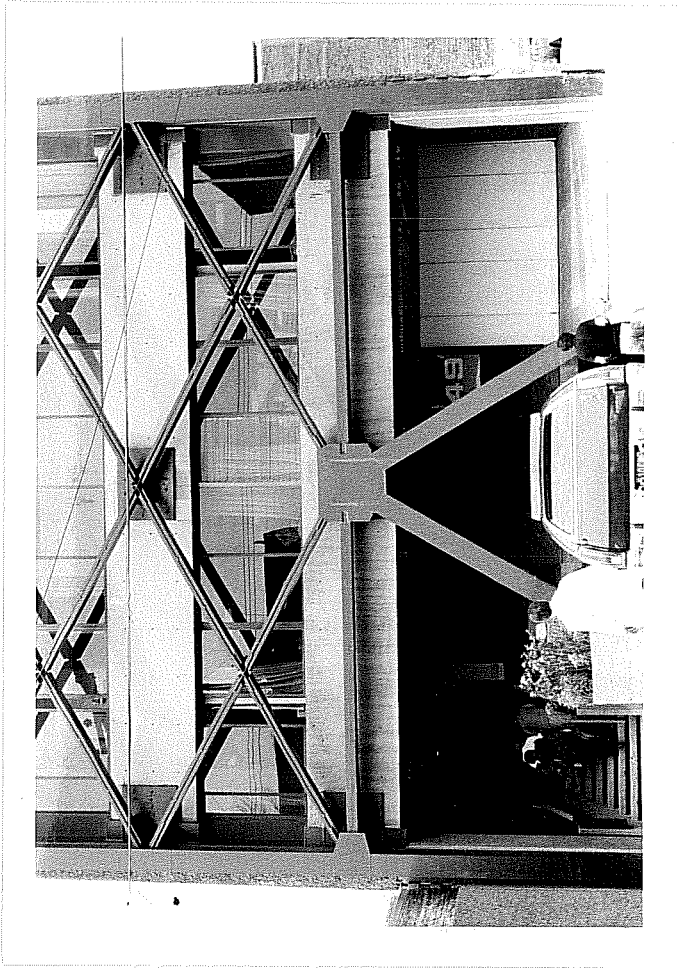
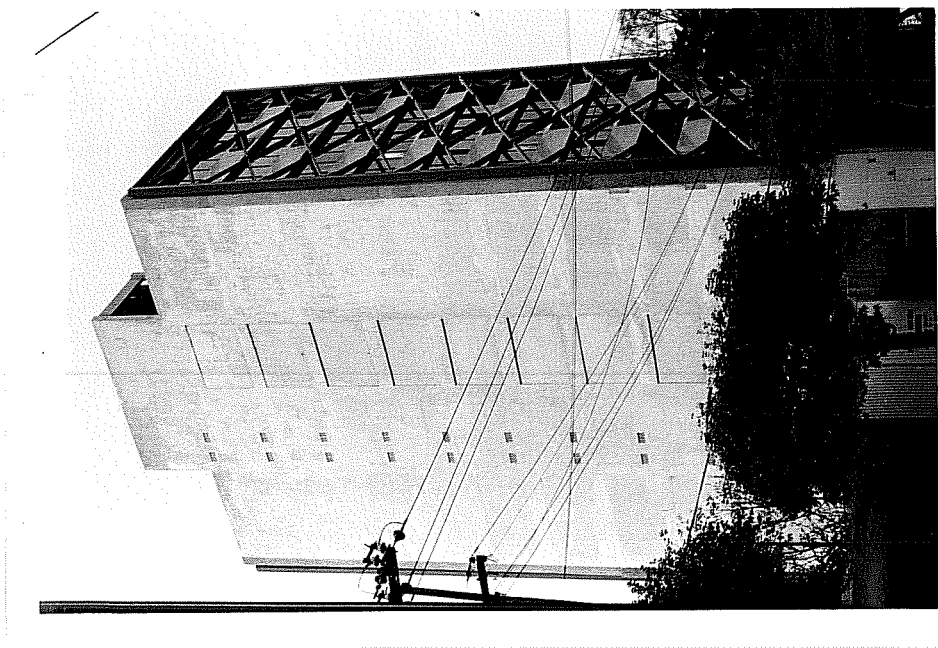


Fig. 1.3.5 Durango 49, Mexico City; steel bracing retrofitting

connections were detailed to guarantee good energy dissipation under cyclic loading in the inelastic range. The bracing system and the frame are very well matched in regard to their damage drift levels. The bracing system stiffness compensated for the large loss of stiffness ( $\approx 70\%$ ) resulting from the seismic damage to the columns. The period of the building in the longitudinal direction was increased from 0.34 sec. to 0.53 sec. as a result of the column damage and reduced to 0.35 sec following the retrofitting.

It is likely that it was not considered in the design that the inclusion of deep spandrel walls produced strong beams and weak short columns. The retrofitting included coring the spandrel beams to reduce their strength. Experimental tests [2] on models of the beam column assemblage (Fig. 1.3.4) showed that coring reduced the positive flexural capacity of the beams by about 70%. This was sufficient to transfer failure from the columns into the beams. Weakening thus transformed a weak column strong beam frame into a strong column weak beam frame with a ductile failure mechanism. Weakening of the spandrel beams was possible because of the additional strength and stiffness of the bracing system.

1.3.2 Durango 49 Building. The twelve story medical building shown in Fig. 1.3.5 was built in the 1970's. It is a reinforced concrete frame with an asymmetrical floor plan

(Fig. 1.3.6). The perimeter frames in the narrow direction feature deep facade beams. During the 1979 earthquake, several columns and beams of the first three stories were damaged. The structure was subsequently repaired and retrofitted with two external steel trusses "in order to reduce the seismic effects on the affected members" [3]. Except at ground level where the bracing pattern is different to preserve accessibility to the building and the underground parking garage, the bays are braced with an x pattern (See Fig. 1.3.6). Strong steel columns help the slender structure resist the high overturning moments. The braces are made of U-shaped sections, and connected as shown in Fig. 1.3.7. A steel plate connected to the bracing system is clamped to the beams with post-tensioned bolts. The seismic forces are transferred to the bracing system through friction. "The slabs were reinforced in order to transmit the seismic shear forces to the new very stiff facade" [3]. The foundation had to be strengthened with new steel piles at the foot of the bracing system.

Retrofitting was completed in 10 months at approximately 20% of the replacement cost and with minimal disturbance to the users. Unlike numerous surrounding buildings of similar height, the retrofitted structure performed very well in the devastating 1985 Mexico City earthquake.



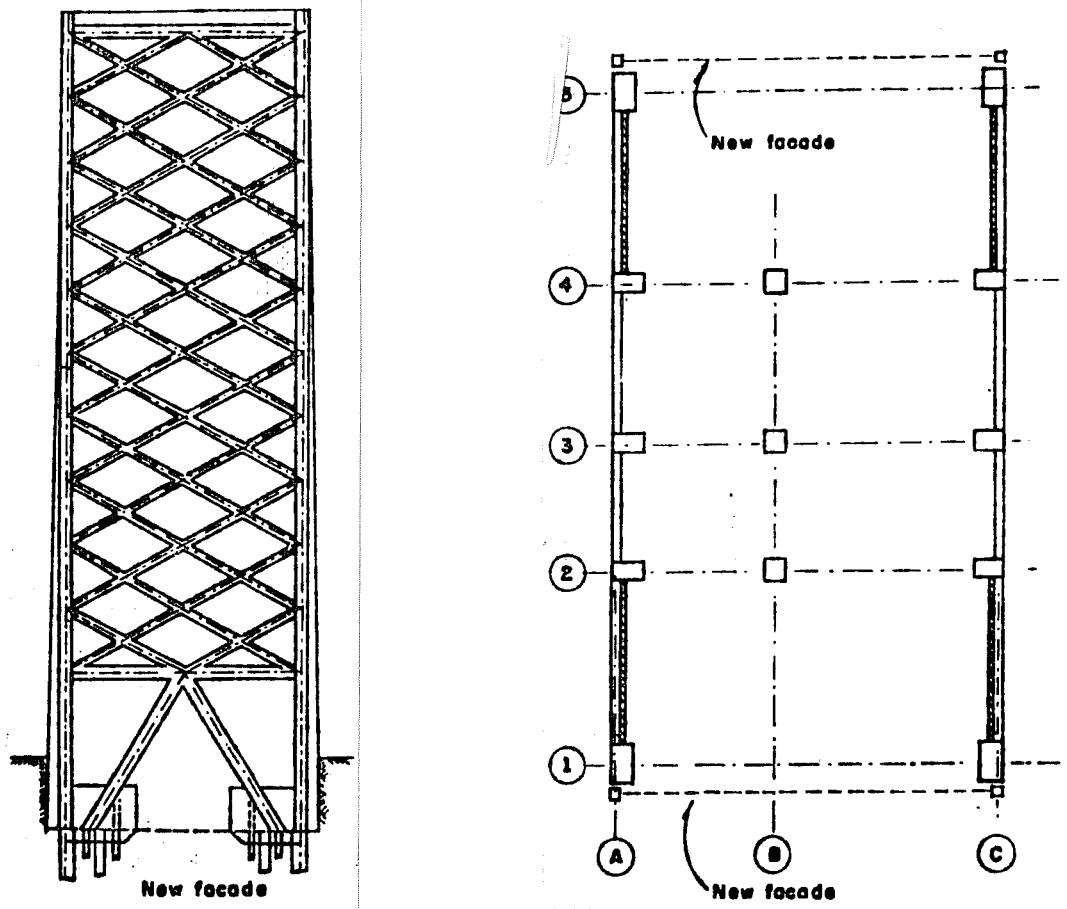


Fig. 1.3.6 Durango 49, plan and elevation [3]

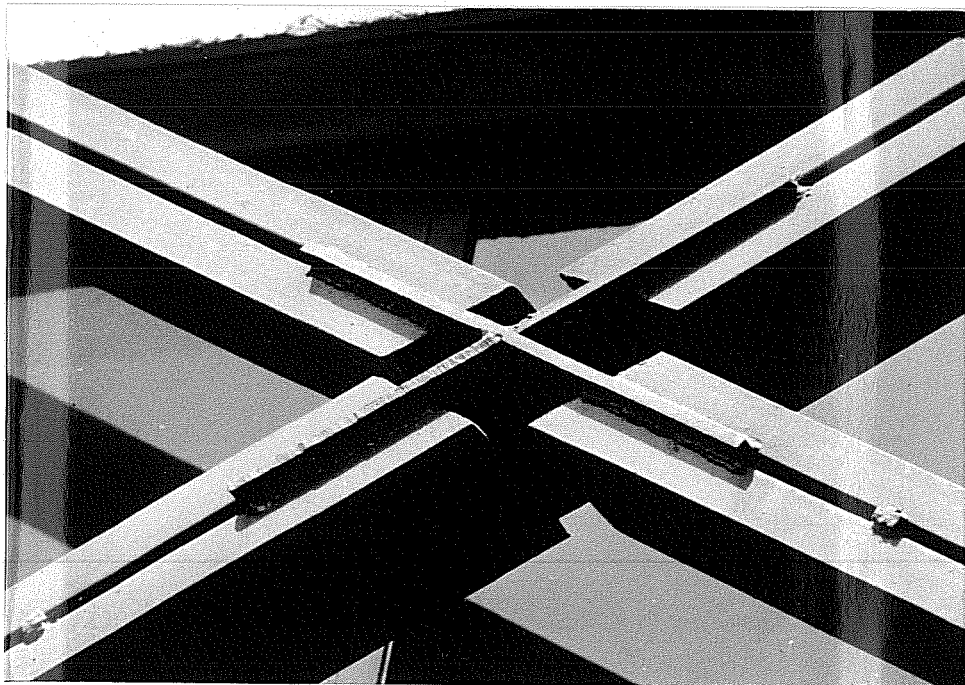
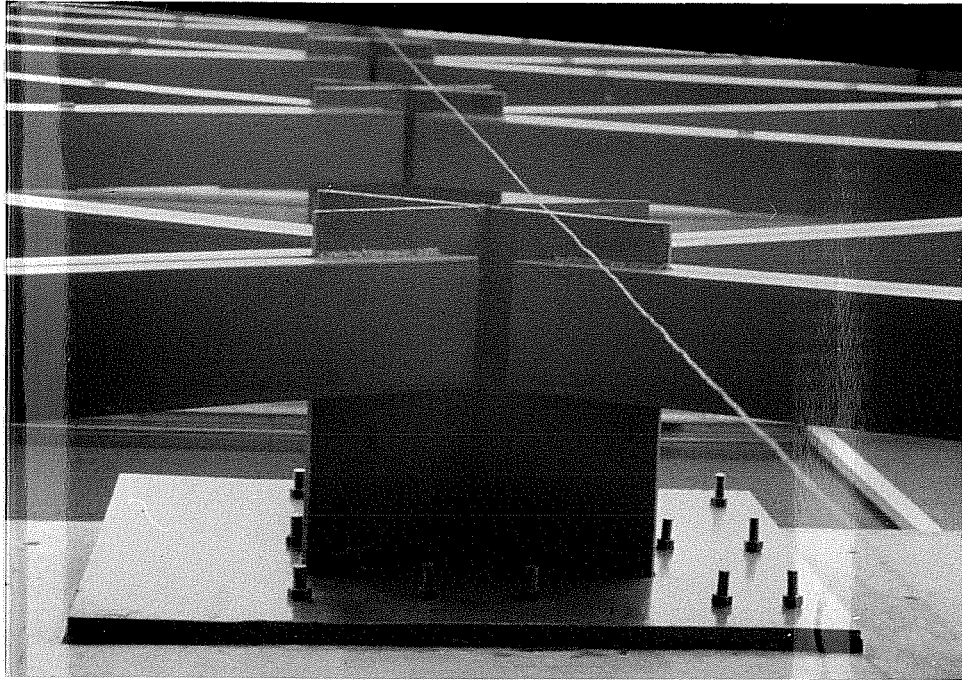


Fig. 1.3.7 Durango 49, connections

1.3.3 Zaragoza Hospital. The Zaragoza Hospital (Figs. 1.3.8 to 1.3.11) is another building situated in the seismically unfavorable lake bed zone of Mexico City. Although the building suffered only minor damage (light cracking in some of the masonry walls of the staircase), in the 1985 earthquake it was decided to retrofit it to reduce the possibility of structural and nonstructural damage in future events. The retrofitting operation had to be quick and economical, and had to be concentrated on the perimeter elements in order to keep the inside of the hospital clear. The plan of the structure (Fig. 1.3.9) shows that it is a space frame with perimeter shear walls in the short direction. The designer chose to strengthen the existing shear walls and to create two strong longitudinal braced frame by inserting steel bracing units in the bays of the perimeter frames (Fig. 1.3.10). The prefabricated bracing units were positioned and concrete was cast between the steel bracing unit and the existing concrete frame (Fig. 1.3.11). Shear is transferred by dowels welded to the bracing unit and epoxy grouted into the concrete frame. The braces are square, built-up sections designed to yield rather than buckle in compression (the effective slenderness ratio is  $kl/r \approx 16$ ). The foundations of the perimeter frame were strengthened with precast segmental friction piles. The aesthetic of the retrofitted building is very

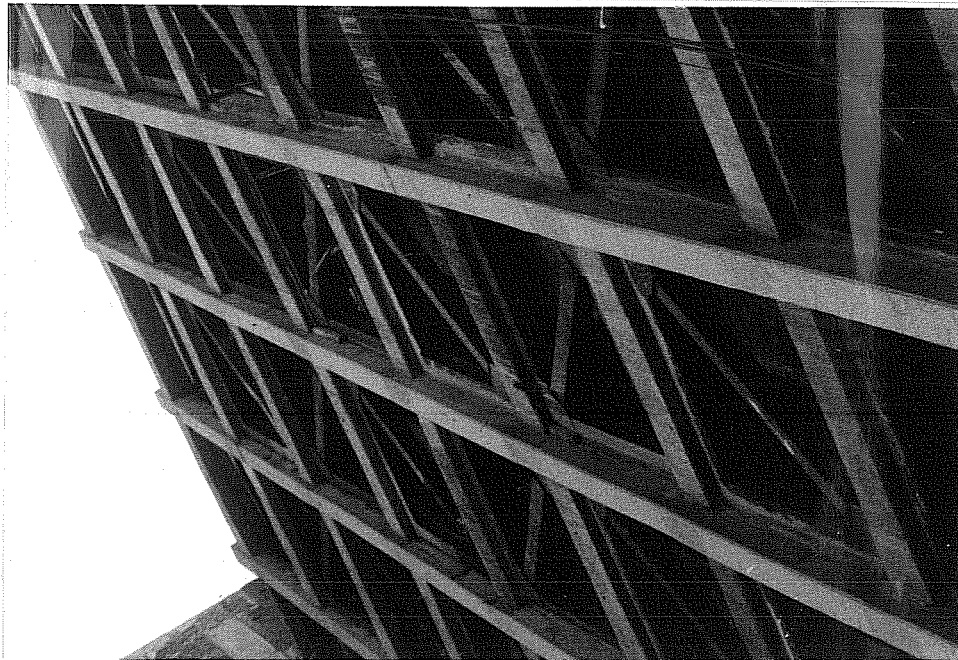


Fig. 1.3.8 Zaragoza Hospital, Mexico City;  
steel bracing retrofitting

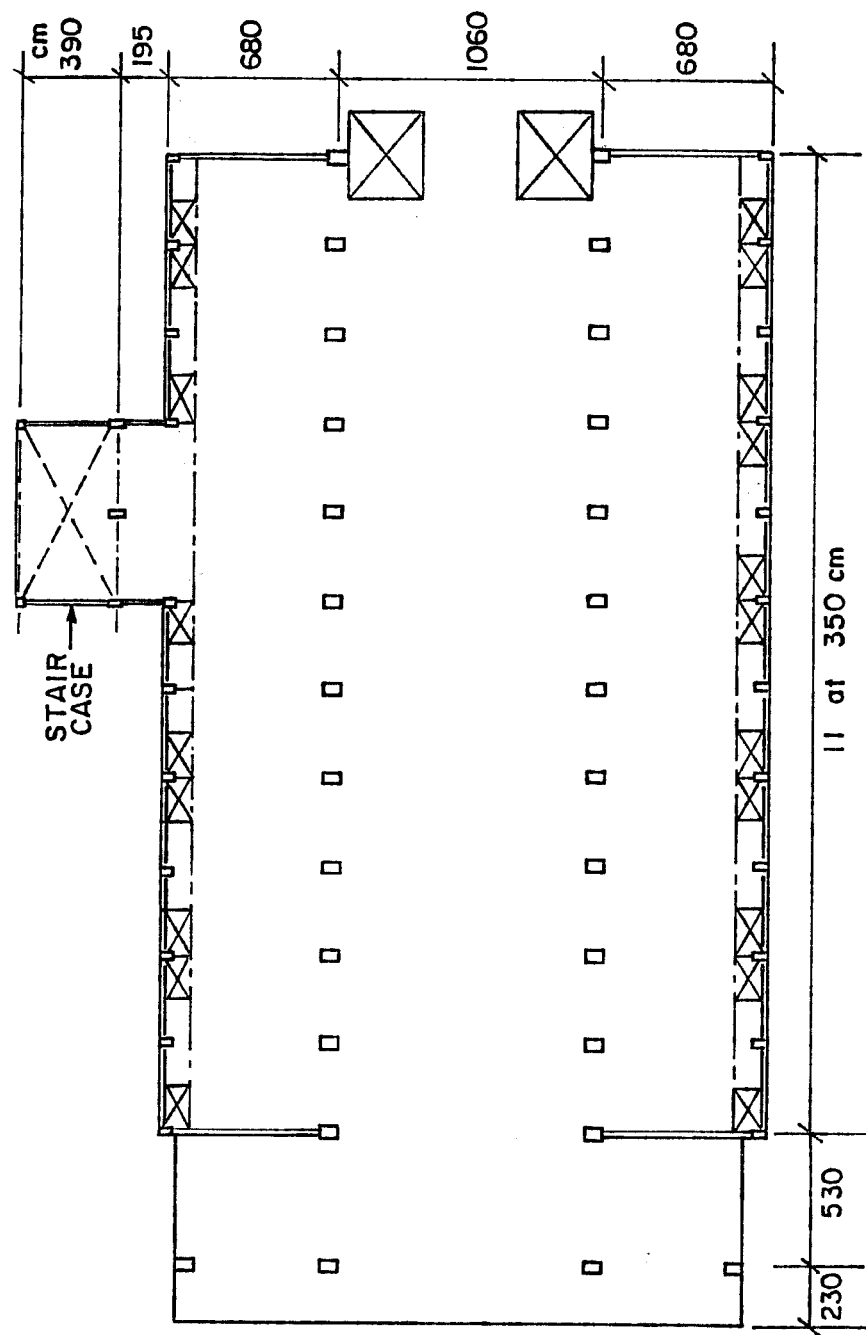


Fig. 1.3.9 Zaragoza Hospital, plan

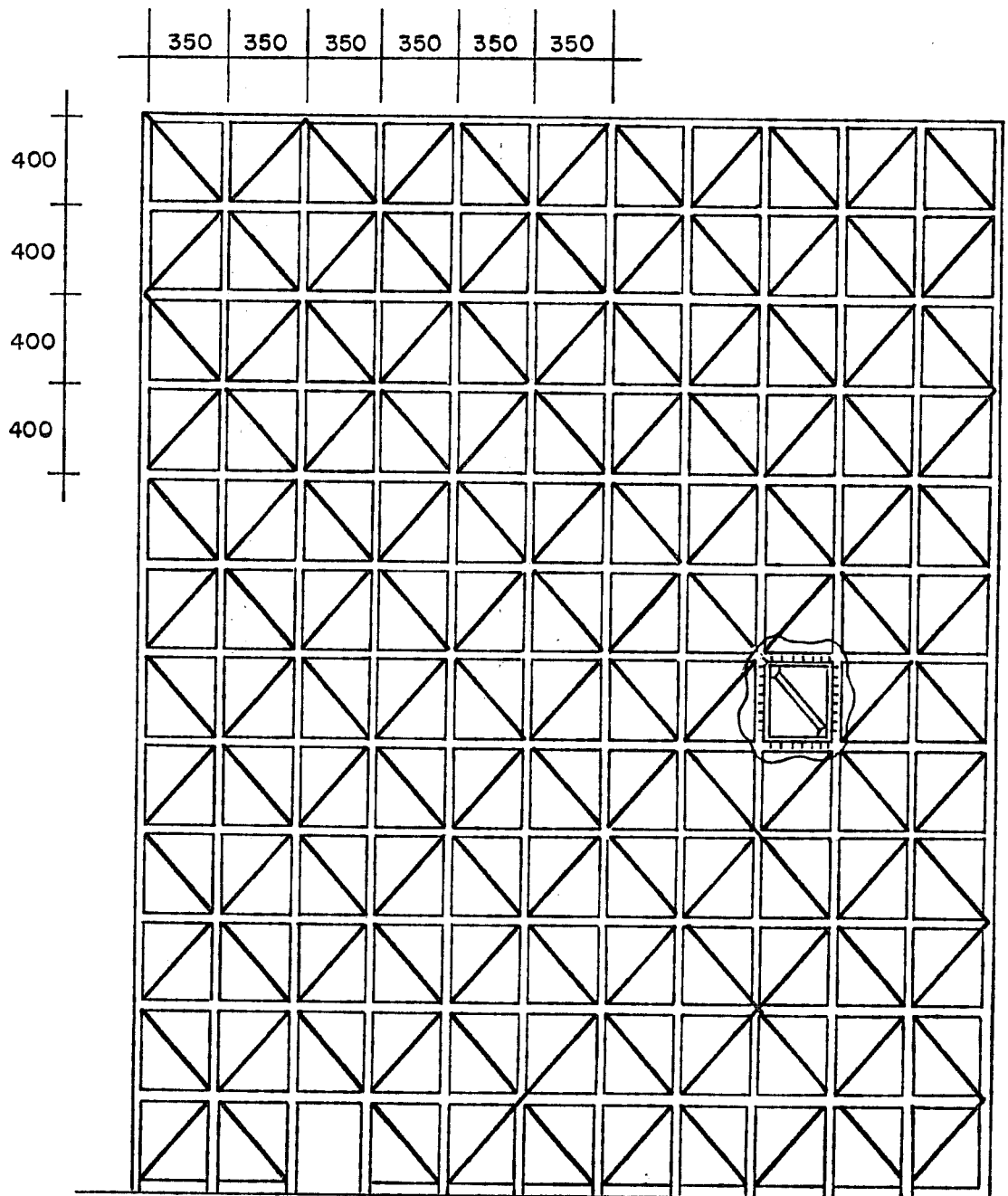


Fig. 1.3.10 Zaragoza Hospital, elevation

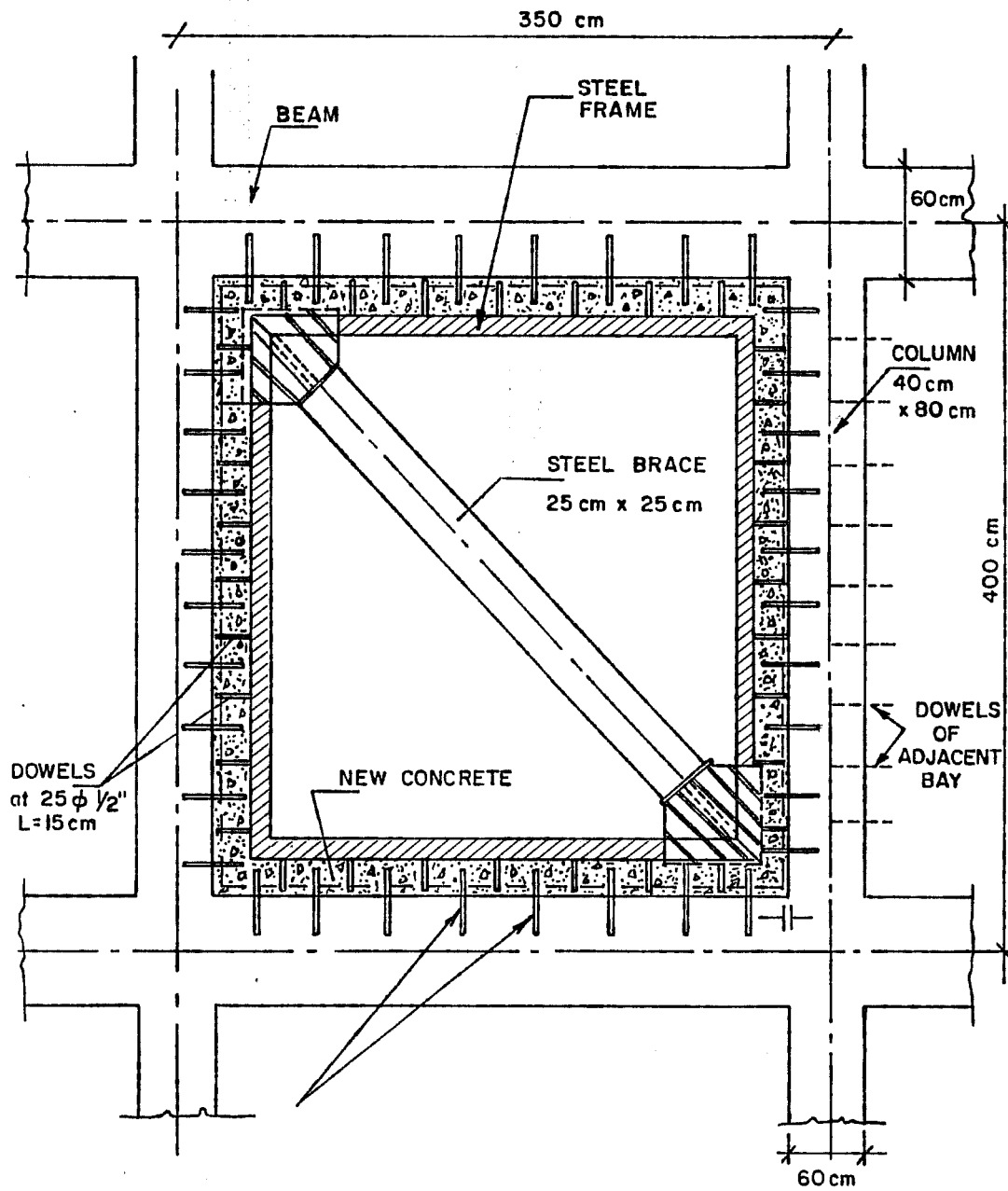


Fig. 1.3.11 Steel bracing unit in position

satisfying, the bracing units appear to have been part of the original structure.

#### 1.4 Review of Research

##### 1.4.1 Experimental Research on Seismic Retrofitting.

Much of the research on seismic retrofitting has been conducted in Japan following destructive earthquakes [4, 5, 6, 7, 8, 9, 10]. Buildings were retrofitted either to repair damage or to prevent damage in future earthquakes. Most damaged structures were low to middle rise buildings with columns which failed in shear. Many buildings expected to perform as emergency centers, especially hospitals in case of an earthquake were retrofitted to satisfy upgraded provisions. For low rise structures, cast-in-place infilled walls were the most common technique. Wing walls and column strengthening were used in most other cases. Steel bracing systems were used in very few cases. Retrofitting designs were based mostly on engineering judgement. Research was undertaken to evaluate the various retrofitting techniques and provide design guidelines.

An extensive experimental test program involving retrofitting columns and frames was carried out. Most of the column tests were aimed at improving ductility. Various techniques for encasing columns with steel and reinforced



concrete were investigated. Dramatic improvements in column deformation capacity and hysteretic behavior were attained.

The results of a series of frame tests by Sugano and Fujimura [4] are presented in Fig. 1.4.1. The frames were one-third scale, single bay, single story retrofitted using various techniques and submitted to static cyclic lateral loading. The frame infilled with a concrete wall displayed little ductility but was the strongest and the stiffest. The infilled frame reached 80% of the monolithic wall strength and more than five times the bare frame strength. The diagonally braced frames performed very well. The frame with tension braces displayed the largest energy dissipation capacity. The frame with compression braces was somewhat less strong because of sliding in the connections between the frame and the braces. Sugano [5] summarized these and other test results in Fig. 1.4.2. The steel bracing technique is found to "indicate moderate increases in strength, but adequate ductility and ability to dissipate energy." Also, "connection details require careful attention as they might strongly influence the overall hysteretic response." X and k bracing patterns were found to be superior to diamond patterns [6].

1.4.2 Cyclic Inelastic Buckling of Steel Braces  
Experimental Work. Black, Wenger, and Popov [11] investigated experimentally the inelastic buckling of steel members subjected

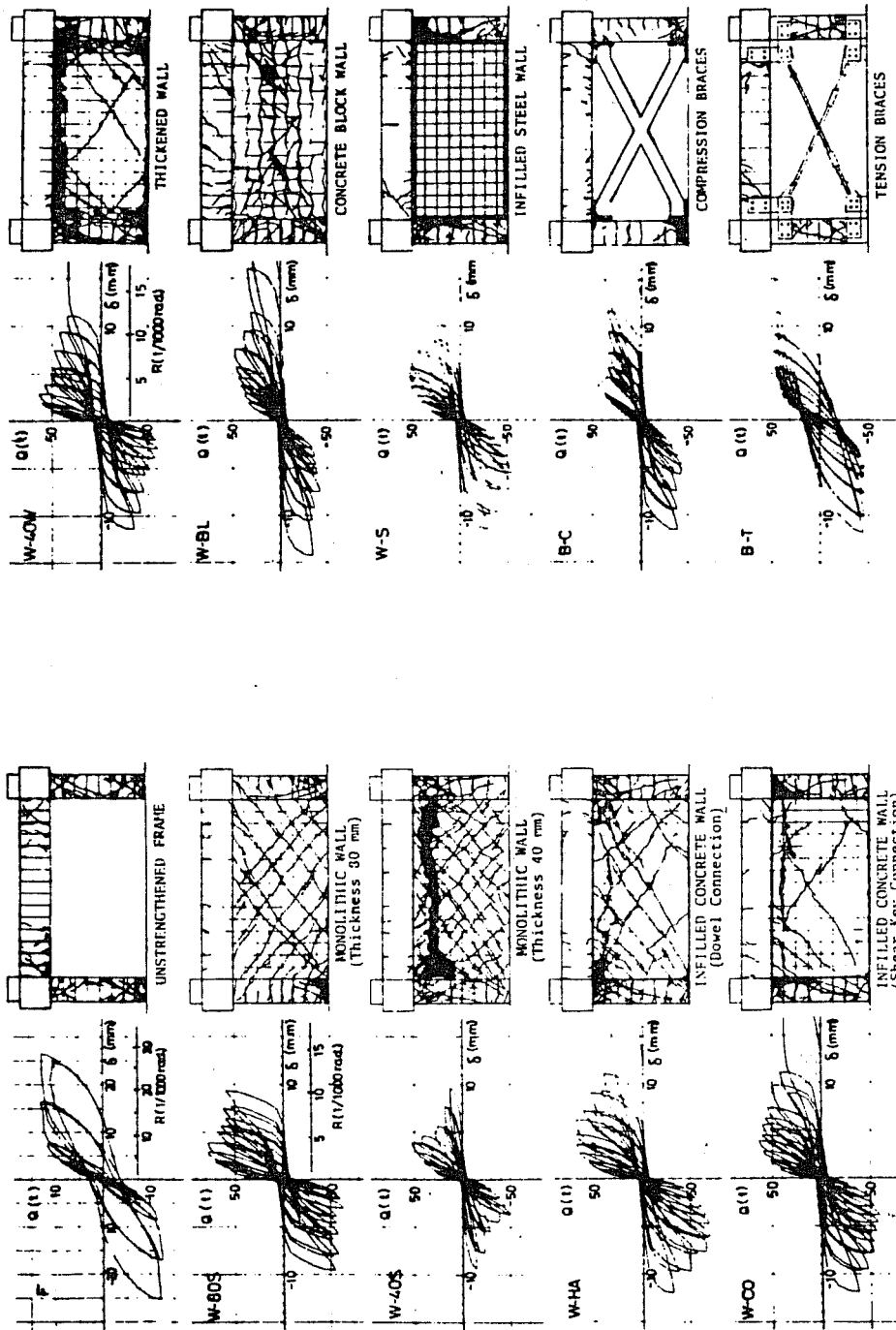


Fig. 1.4.1 Experimental hysteresis curves for retrofitted frames [9]

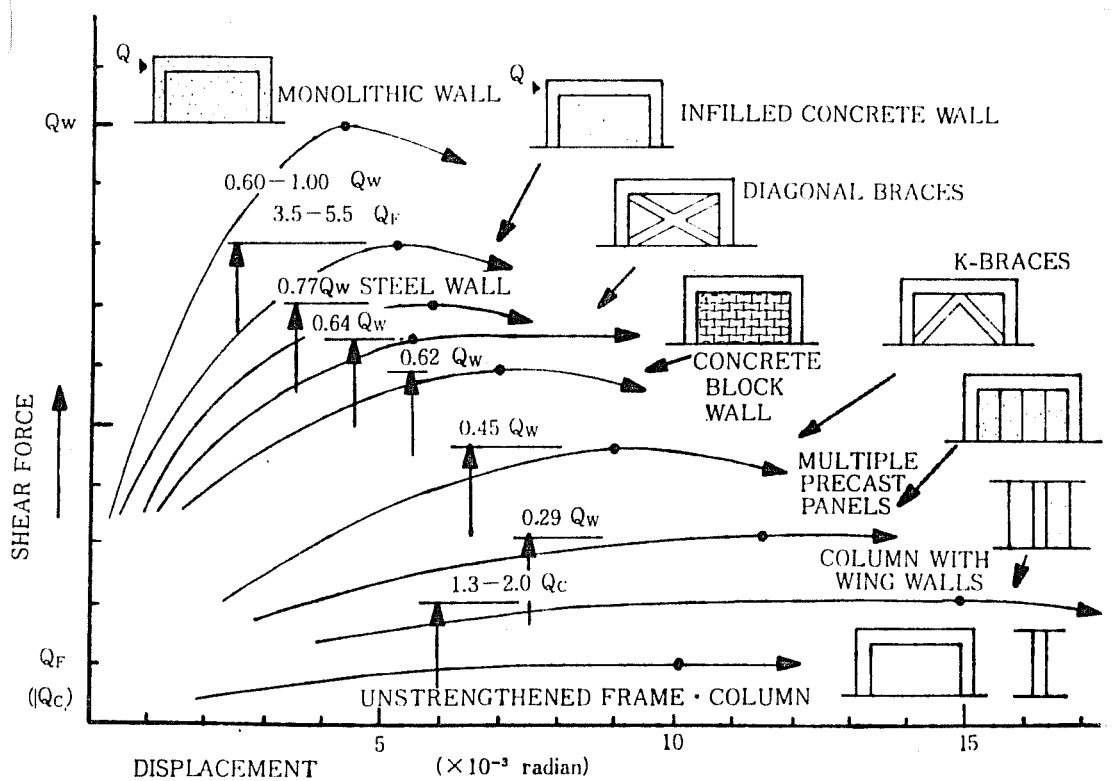


Fig. 1.4.2 Typical load-displacement relationships for different retrofitting techniques [5]

to cyclic axial loading. Normalized axial load versus axial deflection curves for three wide flange sections with an effective slenderness ratio  $kl/r$  of 40, 80, and 120 are shown in Fig. 1.4.3. The hysteresis curve for a cyclic coupon test is shown in Fig. 1.4.4 for comparison. Slenderness was found to be the single most important parameter determining hysteretic behavior. The stockier brace generated fuller loops than the more slender ones. Figure 1.4.5 shows deterioration of the buckling load during inelastic cyclic loading. The envelopes of Fig. 1.4.6 indicate the influence of  $kl/r$  on the compressive load capacity.

Gugerli and Goel [12] tested a series of wide flanges and structural tubes under inelastic cyclic axial loading. The specimens had rigid connections and covered a range of effective slenderness ratios from 47 to 87. All buckled in a symmetric mode similar to a member with fixed ends ( $k = 0.5$ ). Fuller hysteresis loops were also observed at lower  $kl/r$  values. But members with lower  $kl/r$  experienced more severe local buckling. Shorter hysteretic fracture life was observed with increased amount of local buckling.

Analytical Models - Phenomenological models are based on simplified hysteresis rules that mimic observed behavior. They are not based on theoretical considerations. The brace hysteresis behavior is interpreted in Fig. 1.4.7 for

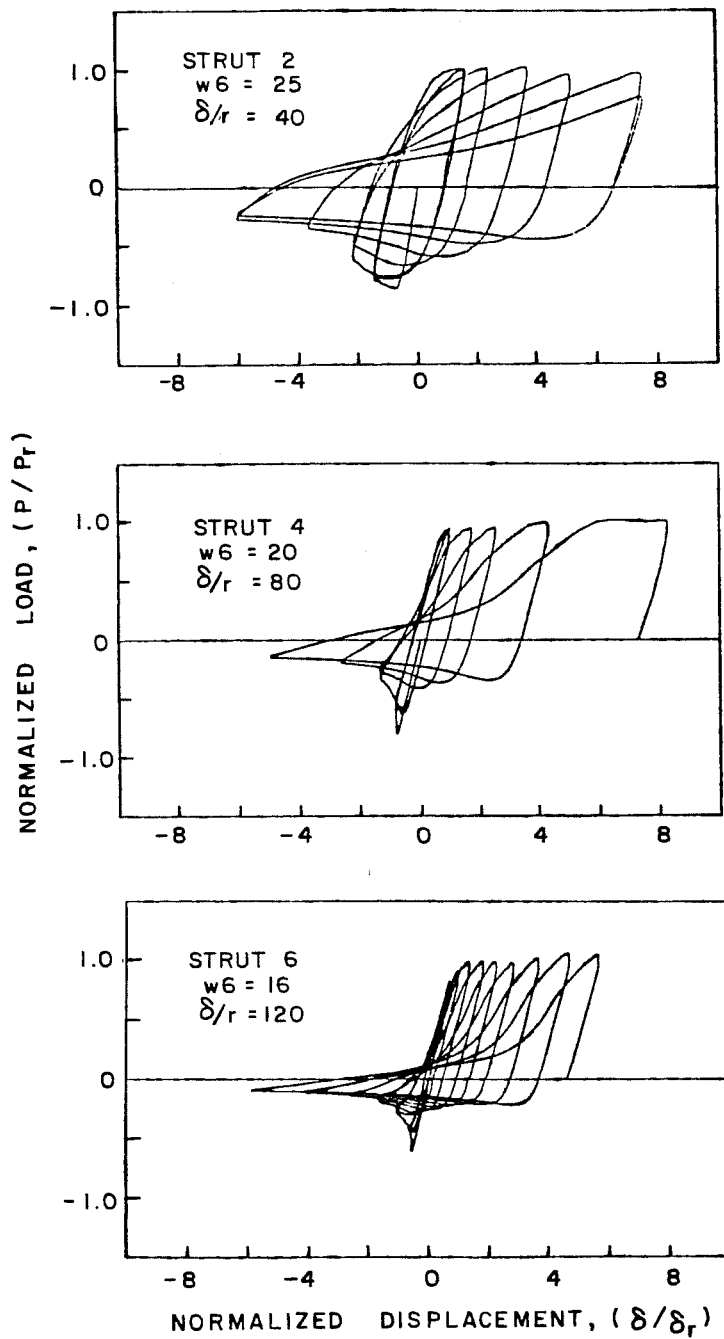


Fig. 1.4.3 Hysteresis loops for steel braces with slenderness ratios of 40, 80 and 120 [11]

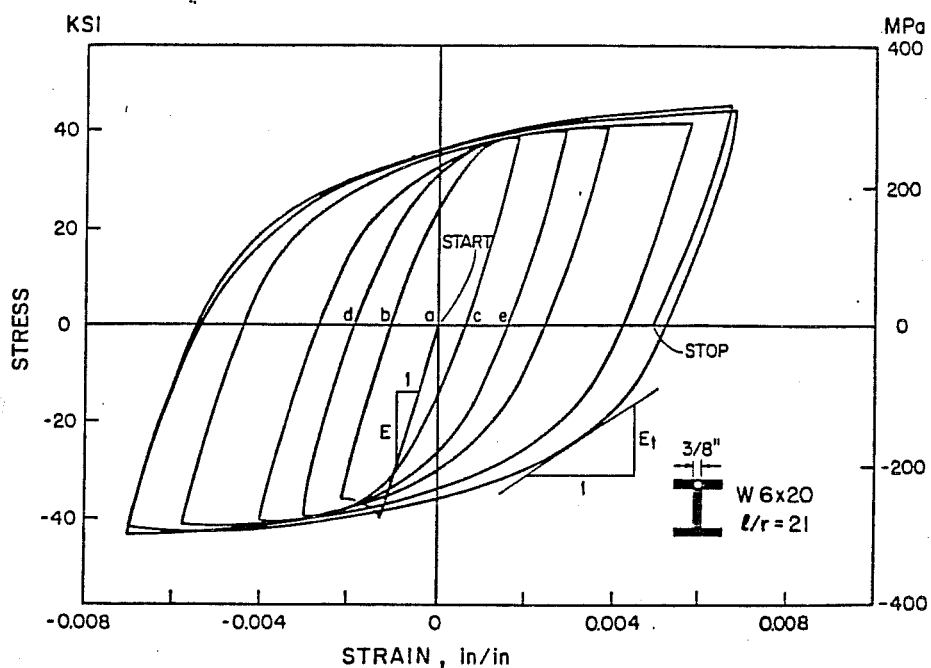


Fig. 1.4.4 Hysteresis curves from a cyclic coupon test [11]

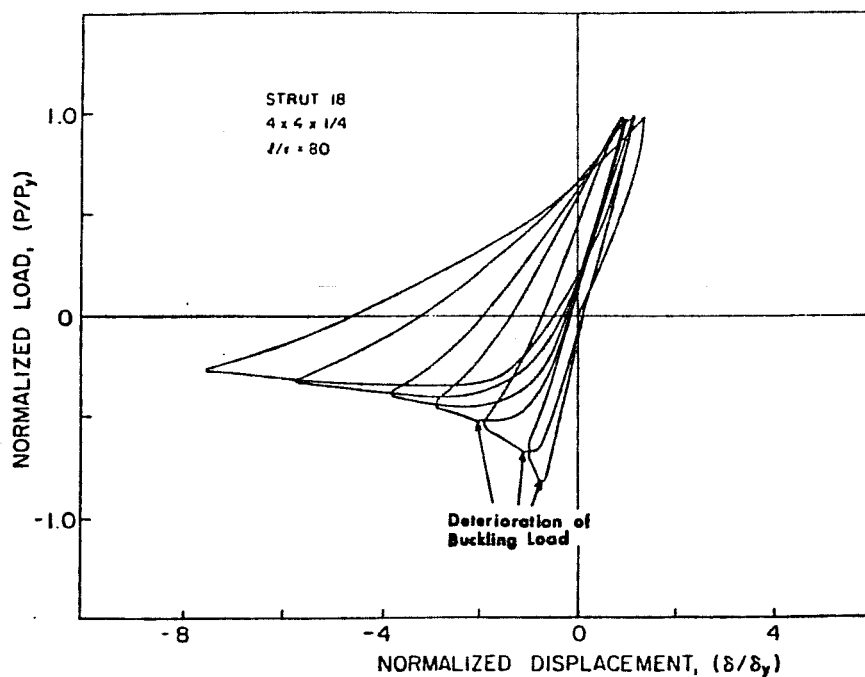


Fig. 1.4.5 Hysteresis loops for a brace with a slenderness ratio of 40 [11]

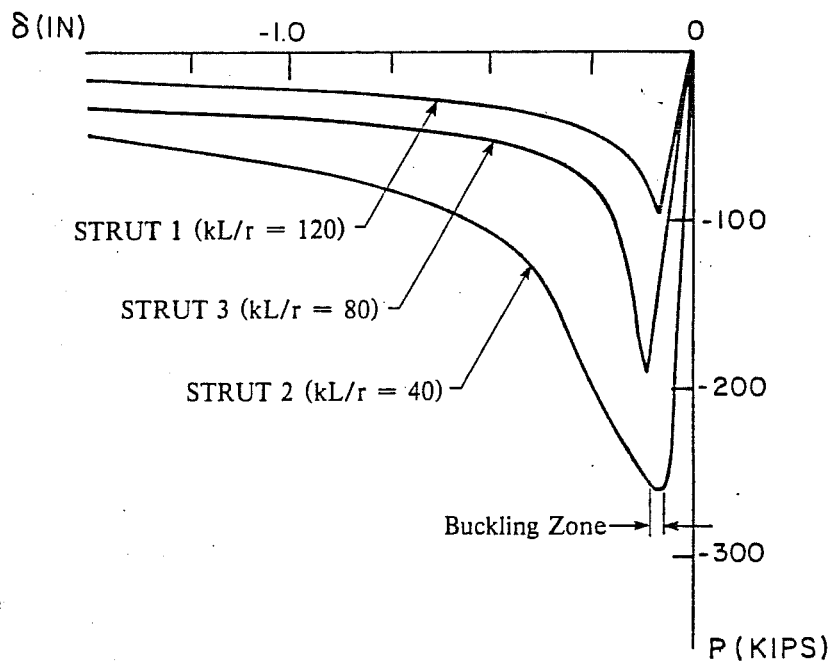


Fig. 1.4.6 Envelopes of translated axial force-displacement curves [11]

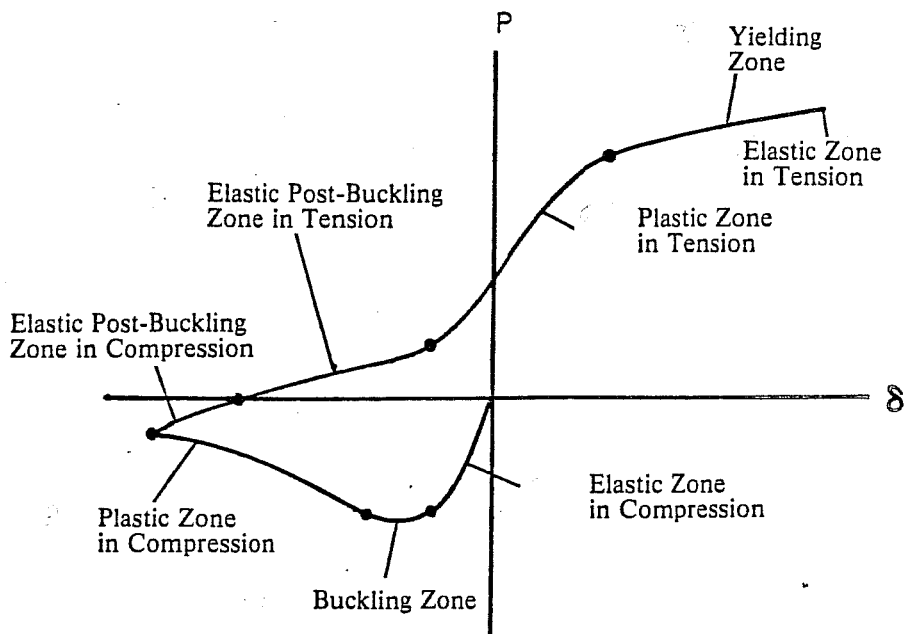


Fig. 1.4.7 Physical interpretation of a brace hysteretic loop [15]

phenomenological modeling [14]. Several phenomenological models developed to reproduce cyclic inelastic buckling behavior of steel braces are compared in Fig. 1.4.8 [13]. Models differ in the number of linear segments employed to define the hysteretic curve and in the number and nature of the input parameters. The fewer the segments the more computationally efficient a model tends to become. With more segments, the complex hysteresis behavior can be replicated better. The most refined model to date has been developed by Ikeda and Mahin [15]; it is based on the approach taken by Maison (See Fig. 1.4.8). The model by Jain [16] was selected for this study because it strikes a good balance between numerical simplicity and complex experimental behavior; it is described in detail in Appendix A.

1.4.3 Design guidelines for seismic retrofitting. The Japanese experimental research (See Sec. 1.4.1) lead to the development of the "Guideline for seismic Retrofitting (Strengthening, Toughening and/or Stiffening) Design of existing Reinforced Concrete Structures" [17]. The guideline is intended to complement established Japanese Building Codes. Detailed design equations and recommendations are provided for the retrofitting techniques which have been studied most extensively (infilled walls and wing walls). Only conceptual recommendations are given for bracing techniques. Some features of the



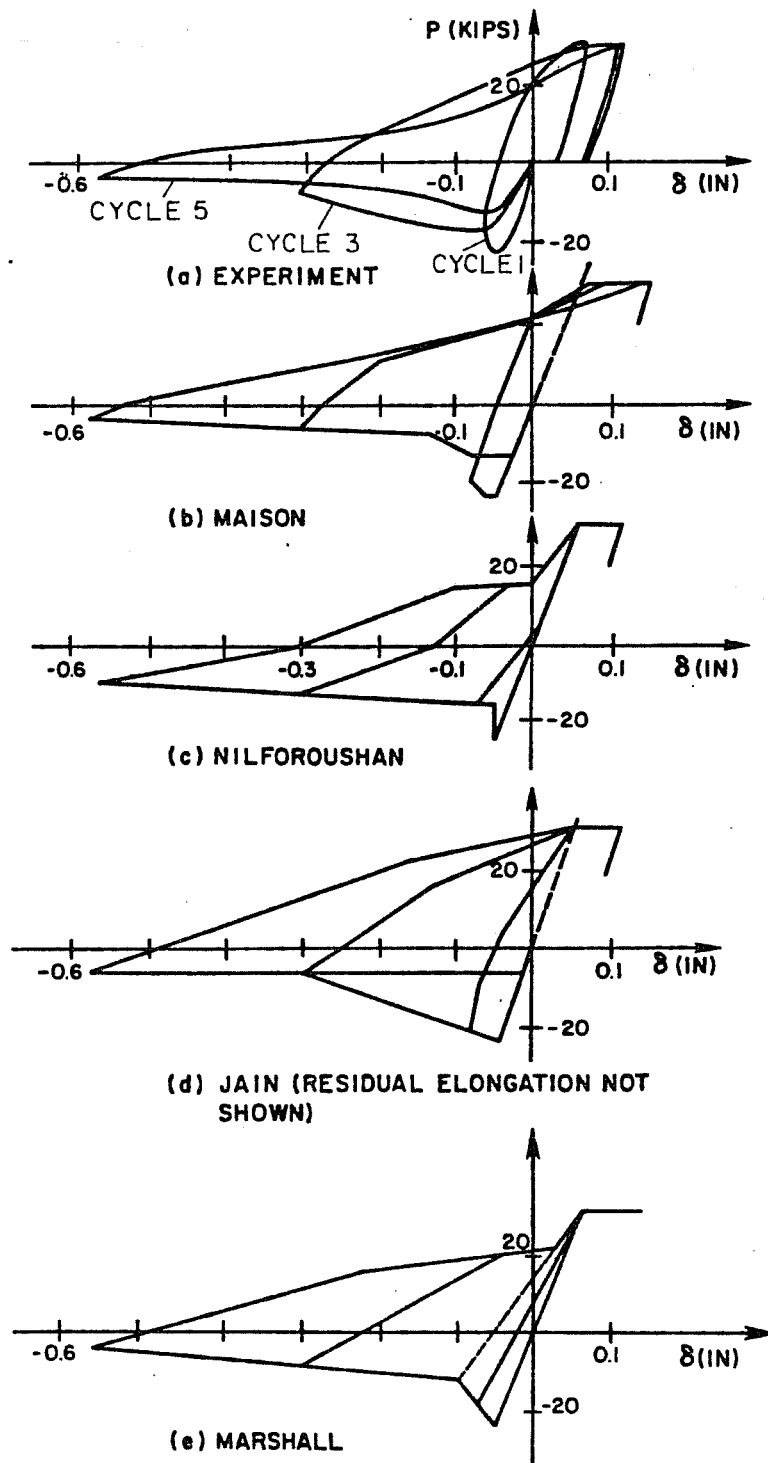
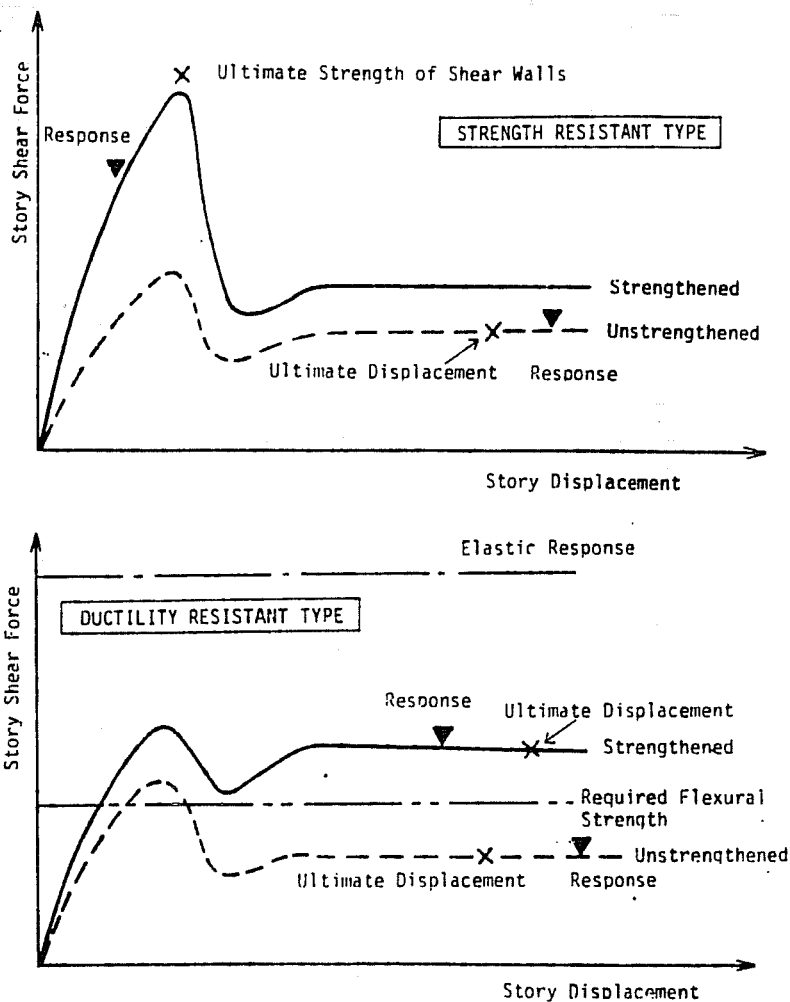


Fig. 1.4.8 Comparison of phenomenological models for steel braces [14]

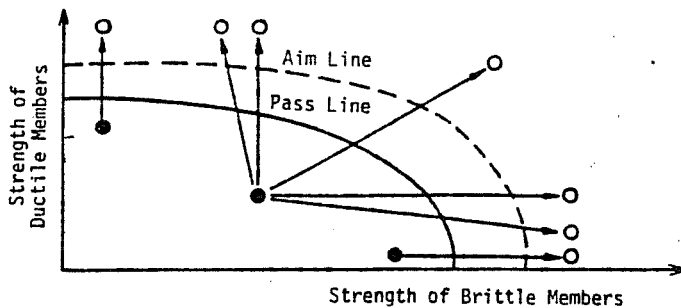
guidelines are presented below:

- A so-called seismic index  $I_S$  (described in Sec. 1.4.4) is used for the evaluation of the seismic adequacy of structures.
- The retrofitting operation is illustrated in a strength-ductility plane (Fig. 1.4.9b). An additional factor of safety of 1.20 for retrofitting problems is required. The "aim line" is therefore more demanding than the "pass line".
- Two retrofitting approaches are differentiated and illustrated in Fig. 1.4.9a. The dashed line is the load deformation curve of the unstrengthened structure. The response point is the computed displacement for the design earthquake. The unstrengthened structure is considered seismically inadequate since the computed response displacement is larger than the expected ultimate displacement capacity.

In the first retrofitting approach the structure resists the design earthquake by relying on its strength (strength resistance type). The structure is brittle and must remain in the elastic range. The design must be based on providing ultimate strength larger than the computed seismic forces. In the second approach the



(a) Type of Earthquake Resistance



(b) Aim of Strengthening

Fig. 1.4.9 Seismic retrofitting approaches [17]

structure withstands the design earthquake by deforming in the inelastic range. Large ductility is required (ductility resistance type). The structure must be designed for the ultimate displacement capacity to be larger than the maximum computed displacement under the design earthquake.

- A general flowchart for seismic retrofitting is provided (Fig. 1.4.10).

1.4.4 Seismic Index,  $I_S$ . Research has been conducted in Japan in the area of the evaluation of the expected seismic performance of existing structures. Such research is relevant to the seismic retrofitting problem since a structure must first be evaluated to determine its need for retrofitting. Aoyama [18] has defined the "seismic performance index",  $I_S$ , as follows:

$$I_S = E_O G S_D T$$

where:  $E_O$  = basic seismic index  
 $G$  = geological index  
 $S_D$  = structural design index  
 $T$  = time index

$E_O$  is the main factor in the computation of  $I_S$ ; it is a combined measure of the strength, ductility, and reliability of the structure. The influence of the structure's dynamic properties can be included in the determination of  $E_O$ . Procedures of

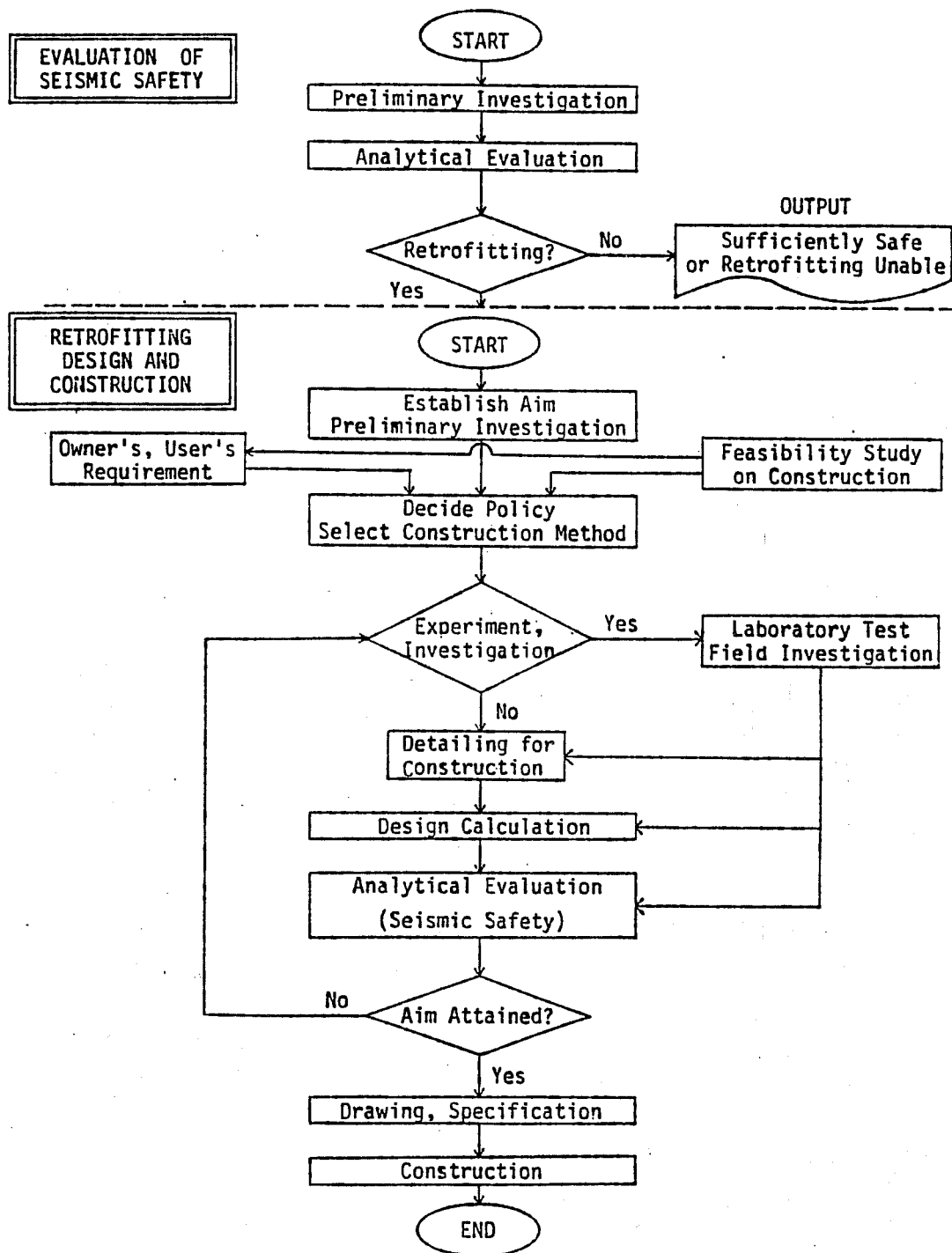


Fig. 1.4.10 Flowchart of design and construction for seismic retrofitting [17]

varying complexity and accuracy have been developed to calculate  $E_0$  for different types of reinforced concrete structures. The geological index,  $G$ , takes into account the effect of local soil conditions on the seismic loading. Unfavorable effects of unbalanced spatial distribution of strength and stiffness are accounted for with the structural index,  $S_D$ . The loss of strength and quality linked with age is introduced through the time index,  $T$ .

$I_S$  is a refined measure of the seismic quality of a structure. Data from extensive field and analytical studies was used to define a quantitative correlation between the computed seismic index  $I_S$  and effective seismic performance. Most buildings with  $I_S$  smaller than a certain critical value suffered extensive damage in a given earthquake, while all structures with  $I_S$  above that value performed adequately. The seismic performance of a structure in future earthquakes with similar characteristics can thus be evaluated by calculating the seismic index  $I_S$ .

A seismic index for retrofitted structures,  $I_{SR}$ , could be introduced and used to set minimum performance requirements for retrofitting.  $I_{SR}$  could also serve to compare the impact of various retrofitting schemes on the seismic quality of a structure. The comparatively large effort needed to determine  $I_S$  should not be viewed as a flaw of the method, but rather as a

consequence of the complexity of the seismic evaluation of an existing reinforced concrete structure. The introduction in the U.S. of the seismic index would require an extensive calibration effort. The index would need to be adapted to the different seismic conditions, building and foundation types, and construction techniques.

### 1.5 Object and Scope

This study has two related objectives:

- To examine various aspects of the selection and design of steel bracing systems for the seismic retrofitting of reinforced concrete frame structures.
- To study analytically the behavior of a steel braced reinforced concrete frame under cyclic lateral loading.

Concepts are introduced which are useful in determining a retrofitting strategy for a seismically inadequate frame structure. The choice of the bracing system configuration is discussed. The importance of matching the relative deformability of the frame and the bracing system is demonstrated. The study of the energy dissipation mechanism in the braced frame leads to the investigation of ways to improve the hysteretic behavior of the braced frame by preventing inelastic buckling. Finally, a flowchart is developed which outlines the main step of the retrofitting operation.

The behavior of a laterally loaded steel braced frame unit is studied analytically. Monotonic and cyclic, static, loading is considered. The influence of the brace design strength and slenderness ratio is investigated in a parametric study. The braced unit consists of two beams, a column and two braces. This two dimensional subassemblage models a prototype frame structure which features weak columns expected to fail in shear. Particular attention is given to the bracing of frames with weak short columns because they are likely candidates for seismic retrofitting. The possibility of improving the seismic quality of braced frames with weak short columns by weakening the beams is investigated.

This work is part of a research project entitled "Repair and Strengthening of Reinforced Concrete Buildings" is sponsored by the National Science Foundation. The goal of the project is to provide data for the development of design guidelines for seismic retrofitting of existing buildings. In the initial phase, a large scale model of a portion of the prototype frame was retrofitted with a steel bracing scheme and tested. The computer program used in this study was calibrated with the data from the braced frame test.



## C H A P T E R 2

### SEISMIC RETROFITTING OF INADEQUATE STRUCTURES

#### 2.1 Introduction

Seismic retrofitting is examined qualitatively and conceptually in this chapter. The evaluation of the seismic adequacy of a structure is discussed. A structure can be deficient in strength or ductility or stiffness or a combination of those properties. The aim of the retrofitting is to correct or compensate for the deficiencies. Retrofitting of a structure inadequate in strength and/or ductility is studied.

The seismic response of a structure depends on its dynamic properties. The most important being the first period of vibration. The period is a function of the mass and stiffness of the structure. The mass and stiffness, and therefore the period, are typically changed as a result of the retrofitting. The influence of a change in period on the strength requirement is investigated, first assuming unchanged ductility, then including changes in ductility.

#### 2.2 Evaluation of the Seismic Adequacy of a Structure

2.2.1 Introduction. A structure is seismically inadequate if the observed or expected seismic performance does not satisfy minimum performance requirements. The concept of seismic inadequacy is simple, but evaluation of the adequacy of a

given structure is difficult. The expected seismic performance of the structure must be determined and an acceptable minimum performance decided on. The evaluation of the seismic adequacy of a structure combines two distinct tasks:

- 1) Determination of the structural properties (Sec. 2.2.2), and
- 2) Determination of the minimum structural requirements (Sec. 2.2.3).

The first one is an engineering task, whereas the second one involves both non-engineering and engineering considerations. The seismic adequacy of the structure can be determined by comparing the structural properties with the structural requirements. Evaluation of the seismic adequacy of a structure is the prerequisite to any retrofitting operation. Before retrofitting an inadequate structure it is necessary to understand thoroughly the nature and degree of the inadequacy.

#### 2.2.2 Structural Properties of the Existing Structure.

There are two main problems in determining the structural characteristics of an existing reinforced concrete structure:

- Collecting the necessary structural data is often difficult. The material properties may not be available. The amount and detailing of the reinforcement may be unknown if construction plans are missing or if the reinforcement was not placed

according to plans. In the case of a structure damaged in a previous earthquake, it takes much engineering judgement to quantify the structural impact of the damage.

- Nonstructural elements may significantly affect the structural characteristics. For example, infill walls can add stiffness and brittle strength to the structure.

2.2.3 Structural Requirements for the Existing Structure. The minimum structural requirements for an existing structure depend on the required level of safety against human and economic losses. Defining the required safety means determining an acceptable risk level. Such a task has economical, social and political implications. Acceptable risk levels vary with the structure's function and should be determined by the owner and the user in accordance with requirements protecting the public interest. The engineer's role is primarily to provide the necessary technical data, especially concerning feasibility, reliability, and cost. If the engineer participates in the determination of the required seismic safety he must have a clear understanding of the non-engineering dimension of the task. The translation of the safety

requirements into structural requirements (such as strength, ductility, and drift requirements) is an engineering task.

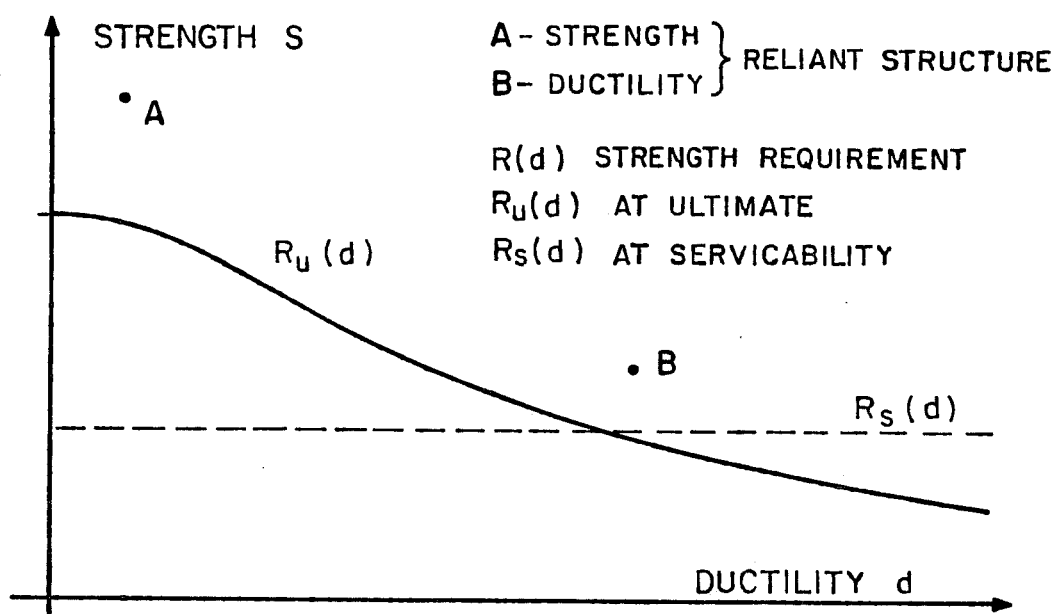
When no specific guidelines for the evaluation of existing buildings are available, the seismic requirements of building codes for new construction can be used for the evaluation of existing buildings. There are, however, problems in using code requirements intended for new design. An existing structure which does not satisfy a particular seismic code requirement is not automatically inadequate. For example a reinforced concrete frame structure may not satisfy code requirements intended to produce a weak beam-strong column structure and may nevertheless, perform adequately under seismic loading because it has high lateral strength. This leads to the idea that specific structural parameters need to be developed for seismic evaluation of existing structures. Such a parameter, the seismic performance index,  $I_S$ , was described in Sec. 1.4.4.

### 2.3 Inadequate Strength and/or Ductility

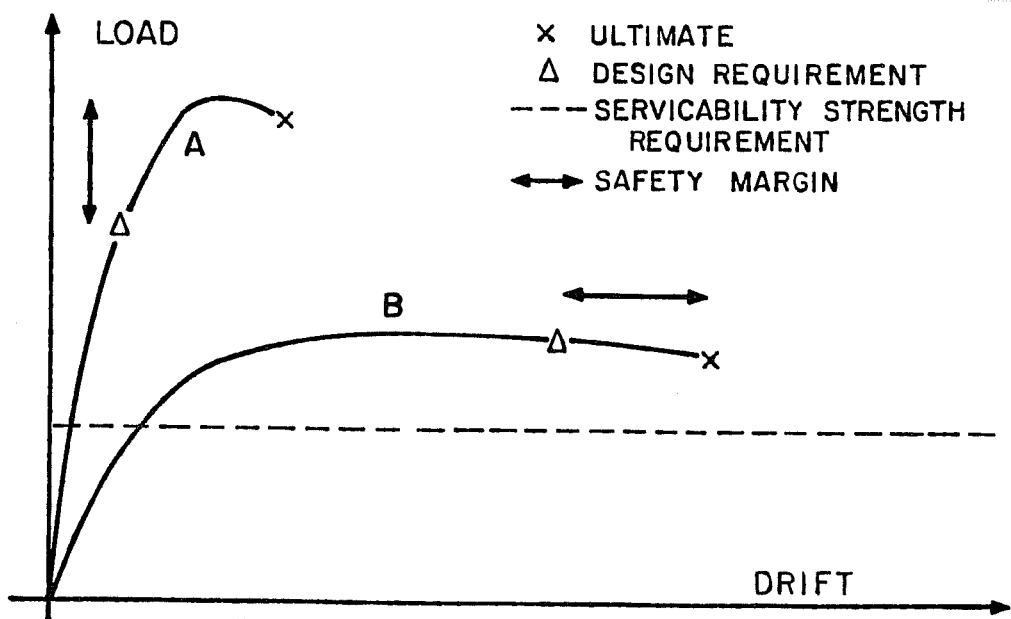
From a seismic point of view, strength and ductility can not be separated, and inadequacy in strength and/or ductility must be approached as one problem. Ductility is the ability to maintain strength under large deformations in the inelastic range. Brittle structures rapidly lose capacity when subjected to inelastic deformations. The "seismic quality" of strength is

a function of the ductility associated with it. Because of the energy dissipation which can be realized, a structure with ductile strength is seismically superior to a brittle structure, with similar strength. The higher the ductility, the lower the strength required to prevent collapse of a structure. Figure 2.3.1a shows qualitatively the influence of the ductility,  $d$  of a structure on its seismic strength requirement  $R_u(d)$  at ultimate state. If the structure has no inelastic deformation capacity, the strength requirement is the elastic design forces.  $R_u(d)$  decreases with increasing ductility. Theoretically, a structure with very large ductility requires low strength to survive a ground motion. The displacements, however, will be very large and unacceptable. Figure 2.3.1a is qualitative because  $S$  and  $d$  are qualitative measures of the strength and ductility. Also, the influence of the natural period on  $R_u(d)$  is not considered (See Sec. 2.5). The strength of the structure and the required strength  $R(d)$  are defined per unit of mass (for reasons discussed in Sec. 2.5.5).

Points A and B in Fig. 2.3.1a represent two structures which satisfy strength requirements. Structure A has little ductility and relies on strength to withstand earthquakes whereas Structure B relies on ductility. The load deformation curve for both structures is shown in the Fig. 2.3.1b. A strength reliant structure is designed so that the ultimate strength is larger



a) Strength requirement curve at ultimate, qualitative



b) Load-drift relationships

Fig. 2.3.1 Strength reliant vs. ductility reliant structures

than the seismic forces generated by the selected earthquake. A reinforced concrete structure with shear walls as the principal lateral load carrying system is such a structure. A ductility reliant structure is designed to deform in the inelastic range and is safe as long as its ultimate deformation capacity is not exceeded. A ductile moment-resisting frame is an example of a ductility reliant structure. Many structures are neither pure strength nor pure ductility reliant, but combine advantageously the characteristics of both types by having intermediate strength and ductility.

Next to surviving a major earthquake without collapsing, a structure should resist smaller earthquakes with minimal damage. High ductility, low strength structures tend to undergo large displacements, even in smaller earthquakes, and the resulting nonstructural damage may be so important that the building, although structurally sound, has to be replaced. A minimum strength requirement, is therefore introduced to guarantee adequate behavior in small earthquakes. It is the serviceability state strength requirement,  $R_S$ , which is independent of the ductility (see Fig. 2.3.1).  $R_S$  may control the design of a ductile structure.

The combination of the strength requirement for ultimate and serviceability states produces a "pass line" which divides the strength ductility plane into seismically adequate and

seismically inadequate zones (Fig. 2.3.2). If the point representing a structure in the strength-ductility plane ( $S,d$ ) is below the line of minimum strength requirement  $R(d)$ , the structure is seismically inadequate. If the point is above the line, the structure is seismically adequate in strength and ductility. Figure 2.3.2 thus illustrates the concept of seismic adequacy. The weakness of such a representation is that it implies that seismic inadequacy of a given structure can be uniquely quantified, whereas it is in fact a relative judgment because the possible seismic performance ranges from no damage to collapse and the earthquakes from small and frequent to major and rare. This representation is nevertheless useful for the discussion of the retrofitting of seismically inadequate structures.

A structure with little ductility risks catastrophic failure with comparatively little warning if deformations in the inelastic range are experienced. Because of the unpredictable nature of seismic loading, it is not possible to guarantee that the structure will not enter the inelastic range. It is thus desirable for a structure to have a minimum ductility. If such a requirement is included in the representation of Fig. 2.3.2, a zone of the strength ductility plane is defined in which the structure has adequate but "undesirable strength-ductility".



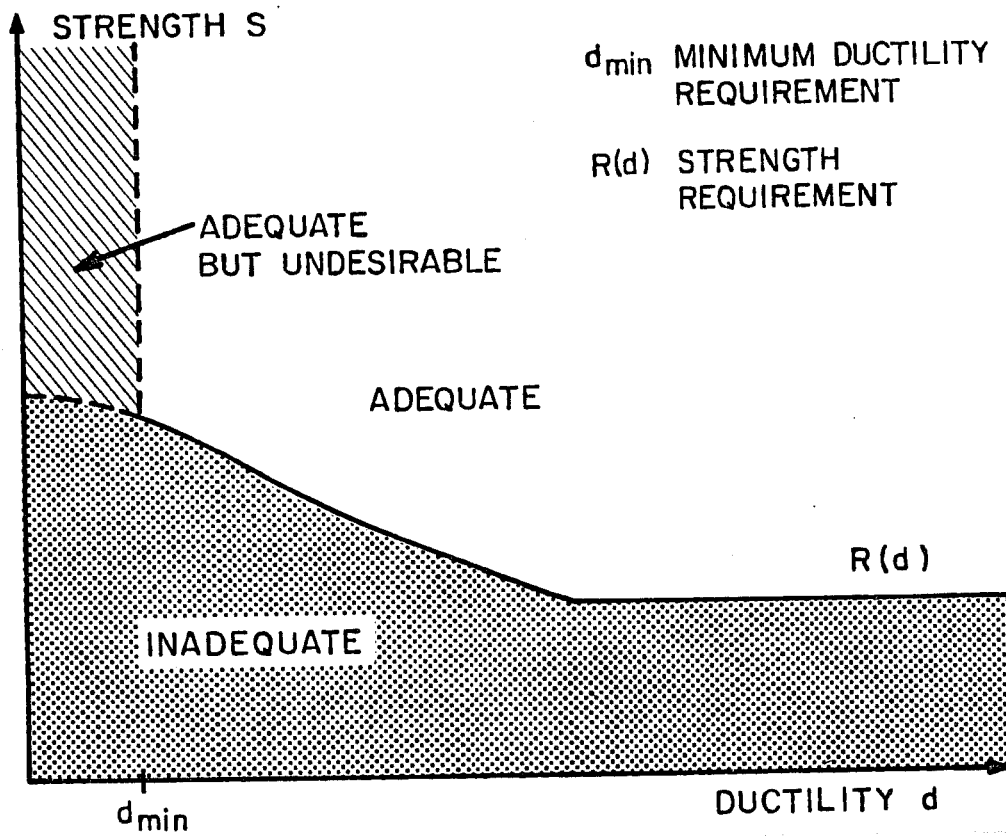


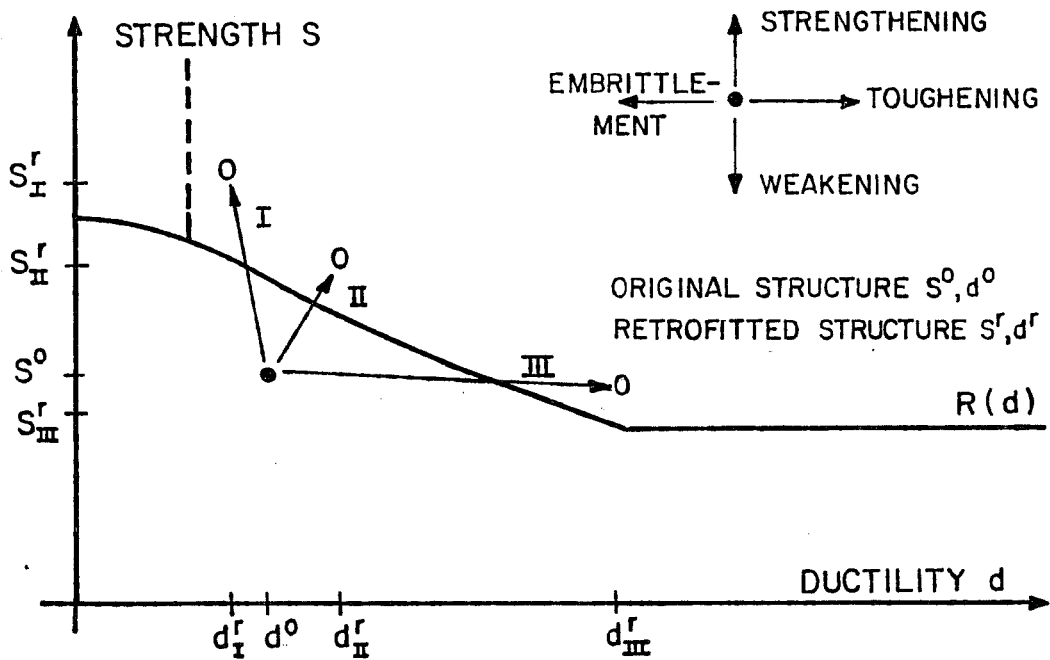
Fig. 2.3.2 Seismic adequacy in the strength-ductility plane

## 2.4 Seismic Retrofitting

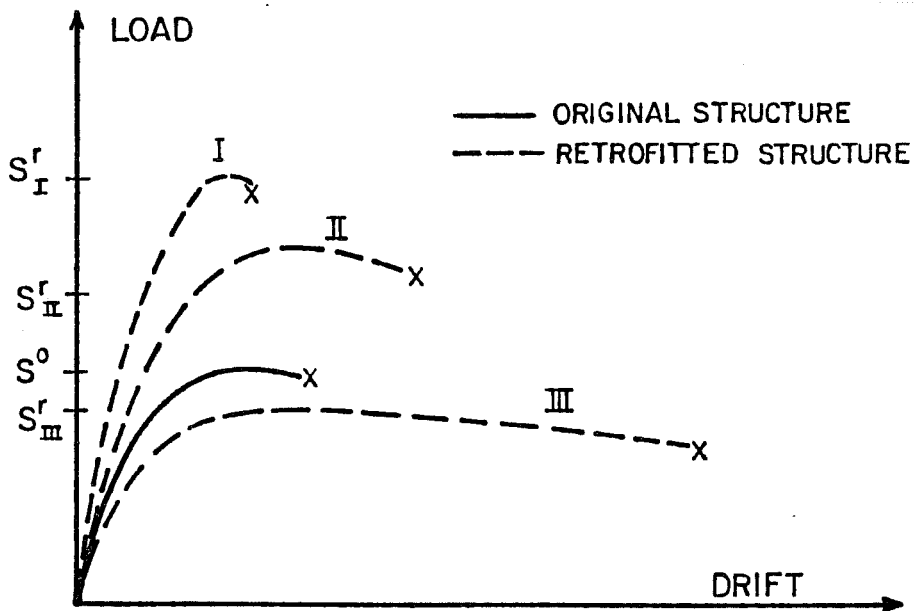
2.4.1 Introduction. The goal of a seismic retrofitting operation is to improve the seismic quality of a structure to a desired level. This section focuses on various retrofitting approaches for structures inadequate in strength and/or ductility. The discussion is simplified by assuming that strength requirements for the initial and retrofitted structure are the same. This assumption implies that the effect on the seismic strength requirement of changes in the structure's natural period are not considered. The effect of such changes are studied in section 2.5.

2.4.2 Basic Retrofitting Approaches. Consider a reinforced concrete structure with strength  $S^0$  and ductility  $d^0$  placing it in the seismically inadequate zone of Fig. 2.3.2. A retrofitting operation is aimed at modifying the structure so that it is in the seismically adequate zone. The strength  $S^0$  and ductility  $d^0$  for the original structure become  $S^r$  and  $d^r$  for the retrofitted structure. Three basic retrofitting approaches for a structure with inadequate strength/ductility are shown in Fig. 2.4.1.

I "Strengthening and embrittlement". Strength increase ( $S^r > S^0$ ) and ductility decrease ( $d^r < d^0$ ).



a) Strength-ductility plane



b) Load-drift relationships

Fig. 2.4.1 Three basic retrofitting approaches

- II "Strengthening and toughening." Strength increase ( $S^r > s^o$ ) and ductility increase ( $d^r > d^o$ ).
- III "Weakening and toughening." Strength decrease ( $S^r < S^o$ ) and ductility increase ( $d^r > d^o$ ).

The most common example of Approach I is the addition of shear walls to a ductile frame. The structure is strengthened and stiffened but its overall ductility may be reduced. Approach I is well suited for retrofitting operations aiming at limiting drifts during earthquakes.

The required strength increase is less for Approach II than for Approach I because of the simultaneous increase in ductility. Approach II is well-suited for brittle structures as demonstrated by retrofitting with a steel bracing system (See Sec. 4.1) Both the strength and ductility of the brittle reinforced concrete frame are increased by the addition of steel braces.

Retrofitting Approach III is theoretically attractive for brittle structures, but rarely practical. Usually, when a structure is toughened, it is strengthened also (Approach II), as in the case of brittle column made ductile by an encasing technique. There are exceptions such as a case where a slight weakening of some elements of the structure results in a large increase in ductility (See Chapter 7).

2.4.3 Optimum Retrofitting Approach. The optimum retrofitting approach is a function of the deficiencies which are to be corrected. Various retrofitting approaches are shown in Fig. 2.4.2 for four structures of different inadequacy. All the points representing the retrofitted structures are located on a so called "aim line". This line depends on the desired safety factor for the retrofitted structure. In each case, one approach is to improve the structure on a line normal to the limit of acceptability. The "normal line approach" requires the smallest increase in strength-ductility and is thus theoretically the most efficient one. Practically, however, it may not be the optimum solution; alternative approaches are therefore included.

Structure 1 (Fig. 2.4.2) has large ductility, but the strength must be increased to satisfy serviceability requirements. The "normal line approach" would consist of adding ductile strength. But the most economical way to provide the required additional strength may be to add shear walls, which reduce the overall ductility.

For structure 2 different retrofitting approaches, combining changes in strength and ductility, are possible. Although the required strength increase is significantly more than for the "normal line approach", adding brittle strength in the form of shear walls may again be the most economical.

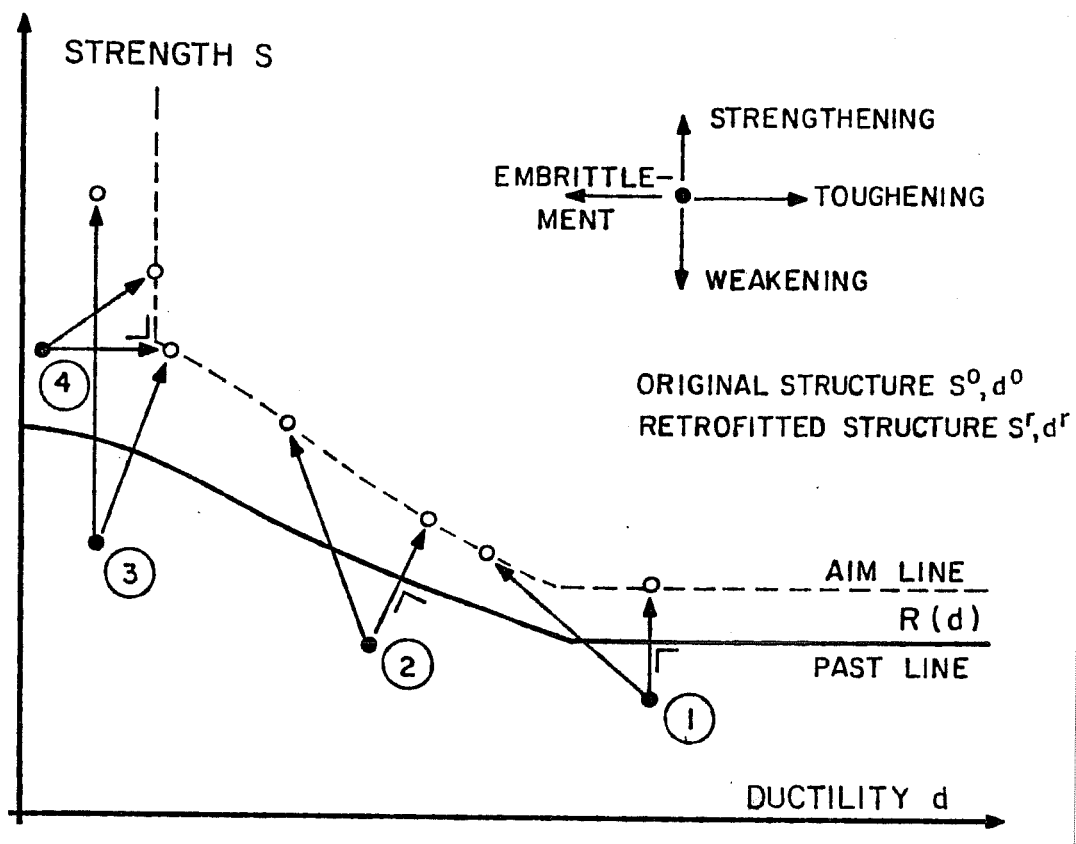


Fig. 2.4.2 Retrofitting approaches for four structures

Structure 3 is a strength reliant structure with inadequate strength. Retrofitting with brittle shear walls for example would place the retrofitted structure in the zone of undesirably low ductility. If this approach is nevertheless chosen, because it is the most economical or the only feasible one, the safety margin for the retrofitting technique should be high to reduce the probability that the structure enters the inelastic range. It may however be possible to bring this structure into the desirable strength-ductility zone by combining strengthening and toughening. Bracing the steel structure with a ductile steel truss is an example of such retrofitting.

Structure 4 has adequate strength but is very brittle. The seismic quality of this structure can be significantly improved by an increase in ductility, no strengthening is needed. If feasible, Approach III of Fig. 2.4.1 is attractive in such a situation.

The discussion of various retrofitting approaches for structures with inadequate strength/ductility can be concluded by observing that retrofitting is primarily a strengthening operation. Substantial toughening of an existing structure is limited to special cases.

## 2.5 Changes in the Natural Period of Vibration

2.5.1 Introduction. The response of a structure to an earthquake depends on its natural periods of vibration. Typically, the first mode of vibration controls the response. The closer the dominant period of the seismic excitation is to the first natural period of the structure, the higher is the response. Wherever the frequency content of future earthquakes is predictable, the design forces are a function of the first natural period of the structure. The "first natural period T" is simply referred to as "period" in the following. The period is itself a function of the stiffness and mass of the structure,  $T \approx 2\pi\sqrt{m/K}$ . The stiffer and lighter a structure, the lower its natural period.

Retrofitting typically results in a change in stiffness which, together with changes in the mass, result in a change of the period. Changes in the period must be considered because they may modify the strength requirement for the structure. The effect of changes in the period on the strength requirement for the retrofitted structure is discussed qualitatively in this section. It is assumed that a change in stiffness is linked with a parallel change in strength and that the change in stiffness is larger than the change in mass. This means that a strengthening operation shortens the period of a structure, while weakening lengthens the period.



Figure 2.5.1 shows how the elastic seismic strength requirement  $R_e(T)$  varies with the period  $T$ . Like  $R(d)$  in Sec. 2.3,  $R_e(T)$  is defined as a seismic strength requirement per unit of mass. This typical elastic spectra has three period ranges: a medium period range of high response, a long period range where the strength requirement decreases as the period moves away from the resonant period and a short period range where the structure is too stiff to be excited.

If the structure is allowed to deform inelastically, the strength requirement for a given earthquake is reduced (Sec. 2.3). Inelastic design spectra can be obtained by modifying the elastic design requirement. The modification factor is a function of the available ductility and of the period range. In the short period range, very high ductility is necessary to substantially reduce the strength requirement. At first inelastic behavior increases the response because it brings the period closer to the resonant period. Very large inelastic deformations are necessary to move the structure to the range of lesser response. A structure in the short period range is therefore designed to remain elastic, and ductility - i.e. inelastic deformation capacity - does not affect the seismic strength requirement in this range.

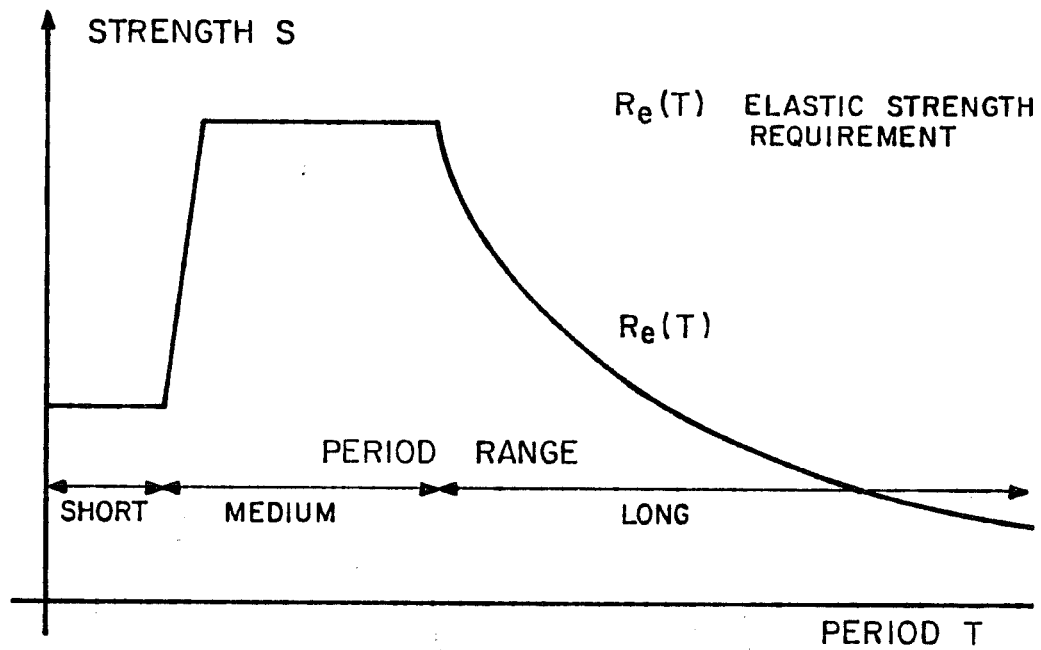


Fig. 2.5.1 Elastic seismic design spectra, qualitative

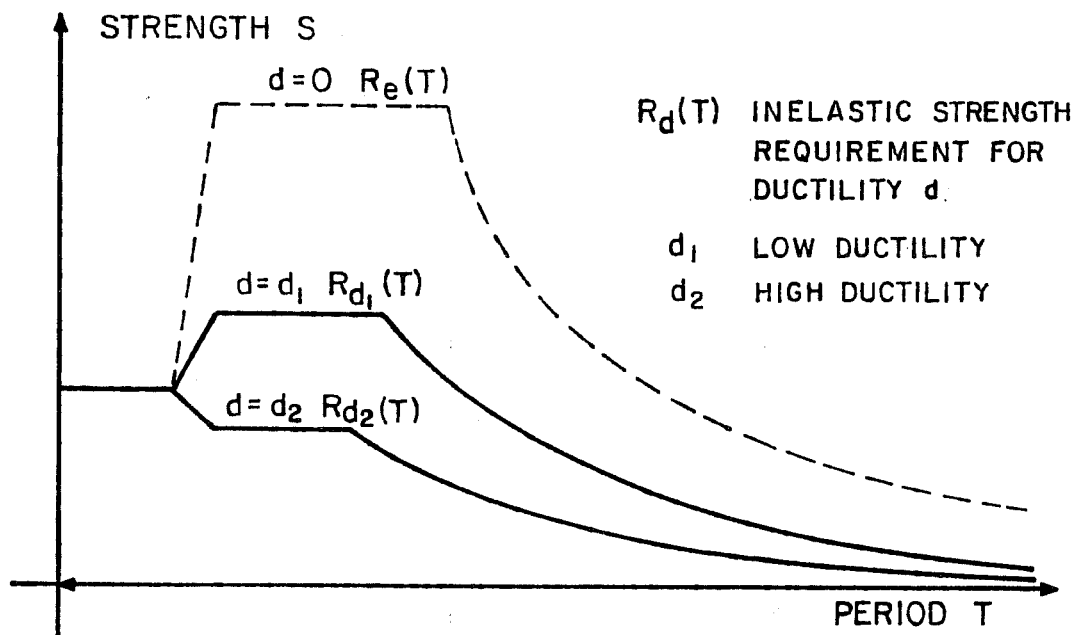


Fig. 2.5.2 Inelastic seismic design spectra, qualitative

In the medium and long period ranges ductility significantly reduces the ultimate strength requirement. Newmark [19] set the inelastic strength requirement in the medium period range at  $1/\sqrt{2\mu-1}$  of the elastic requirement and at  $1/\mu$  in the long period range, where  $\mu$  is a measure of the ductility. Figure 2.5.2 shows qualitatively the derivation of an inelastic design spectra from a elastic one for two values of the ductility  $d$ . The inelastic strength requirement  $R_{d1}(T)$  is for a system of low ductility. Curve  $R_{d2}(T)$  is for a system of high ductility such as a ductile frame. For high ductility values the shape of the inelastic spectrum is such that the lower the period, the higher the required strength. If limit state design is used, an elastic design spectra for a small earthquake may be used for the serviceability state and an inelastic design spectrum, derived from the elastic design spectra for a strong earthquake, may be used for the ultimate state. The structure must then satisfy both the elastic and inelastic requirement. The inelastic requirement is used in the discussion of the influence of changes in the period on the strength requirement.

Figure 2.5.3 illustrates that the seismic adequacy of a structure with strength  $S$  depends on its period  $T$ . The structure has adequate elastic strength if the point  $(S,T)$  is above the inelastic strength requirement line  $R_d(T)$ . If the point is below

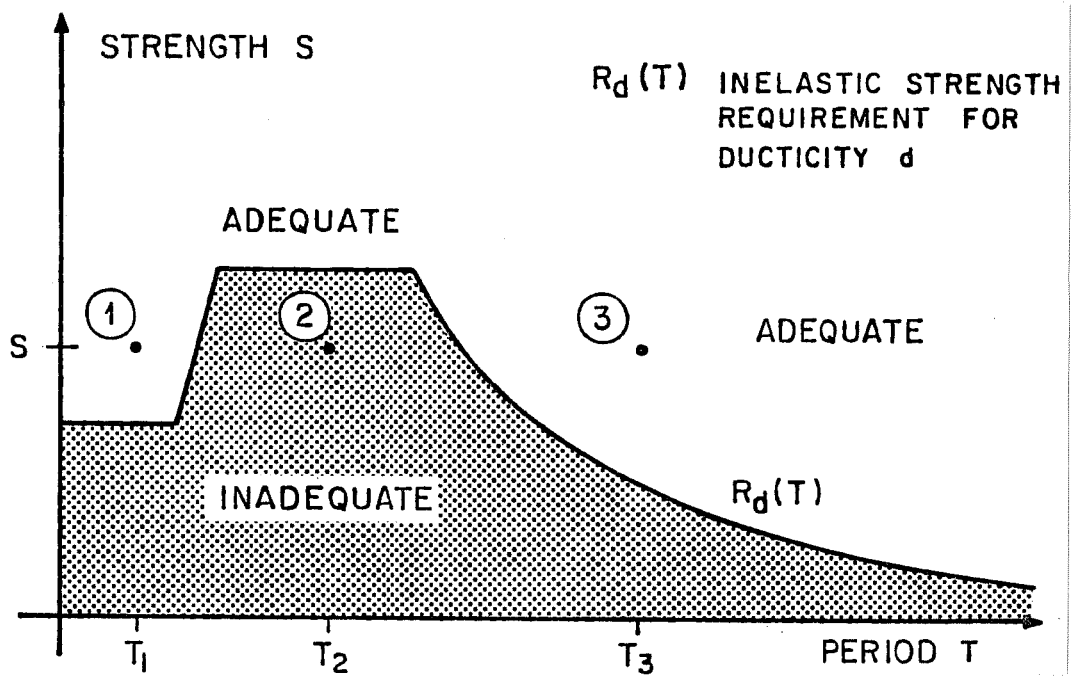


Fig. 2.5.3 Seismic adequacy in the strength-period plane

the line, the structure is seismically inadequate and a candidate for retrofitting. The goal of retrofitting is to move the point  $(S,T)$  representing an inadequate structure into the zone of adequate strength. The strength and natural period  $(S^0, T^0)$  of the original structure becomes  $(S^r, T^r)$  for the retrofitted structure. Since the strength requirement for a structure depends on its period, the effect of a change in period from  $T^0$  to  $T^r$  must be considered. This is discussed first for the case of a shortening of the period ( $T^r < T^0$ ) (Sec. 2.6.2) and then for a lengthening of the period ( $T^r > T^0$ ) (Sec. 2.6.3). For simplification, it is assumed in both cases that the ductility of the original and retrofitted structure are the same ( $d^r = d^0 = d$ ), so that the strength requirement is unchanged ( $R_d^r(T) = R_d^0(T) = R_d(T)$ ). The effect of a change in ductility is included in section 2.6.4. A retrofitting operation with a change in strength, ductility and period is illustrated ( $S^r \neq S^0, d^r \neq d^0, T^r \neq T^0$ ).

2.5.2 Shortening of the Natural Period. Most retrofitting operations involve stiffening the structure and result in a shortening of the natural period. The shortening may result in a smaller seismic strength requirement, and thus be desirable, or in a higher requirement, and thus be undesirable.

Figure 2.5.4 illustrates a situation with an undesirable shortening of the period. The inelastic strength requirement for the structure is increased as a result of the retrofitting. If

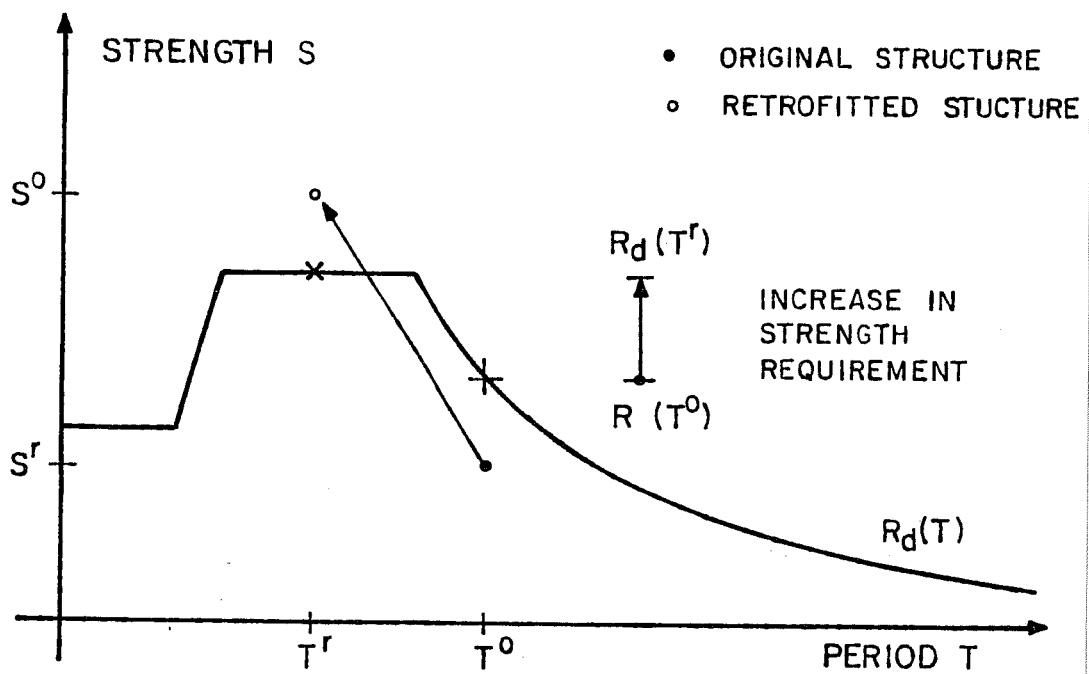


Fig. 2.5.4 Undesirable shortening of the period

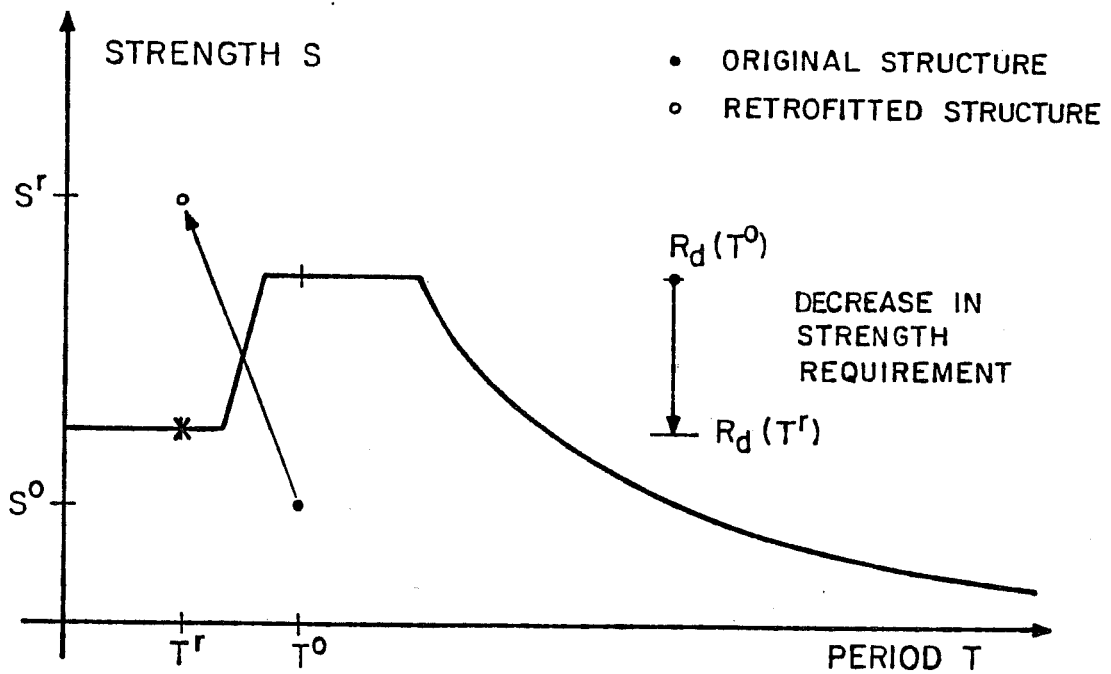


Fig. 2.5.5 Desirable shortening of the period

this effect is overlooked, the seismic safety of the retrofitted structure will be significantly less than expected. In theory, it is even possible to imagine a case where a structure would be seismically less safe after retrofitting because the strength increase would be less than the increase in seismic forces.

Fig. 2.5.5 illustrates a situation where shortening the period is desirable. The period of the structure is moved from the zone of high response to a range of lesser response thus reducing the elastic strength requirement. This reduction combined with the strength increase significantly improves the seismic quality of the structure.

Mexico City offers many examples of structures for which a shortening of the natural period would be desirable. A number of 10 to 20-story reinforced concrete frames founded on soft soil have a natural period close to the critical period of vibration for Mexico City earthquakes ( $T_{crit}$  about 2 sec.). The seismic forces could be substantially reduced by shortening the period away from the resonant period range. The bracing of the building described in Sec. 1.3.2 is an example of retrofitting which shortened the period to a more favorable period range.

Retrofitting which relies on the stiffening of a structure to reduce the seismic force requirement is to be approached carefully. If the structure enters the inelastic

range it loses stiffness and the improvement could be canceled. Therefore, a retrofitting scheme moving a structure into the short period range must be designed to resist even strong earthquakes elastically.

2.5.3 Lengthening of the Natural Period. The structure and the local seismic conditions are often such that lengthening the period reduces the seismic forces. One way to lengthen the natural period of a structure is to reduce its stiffness by taking away or softening the stiffer members of the lateral resisting system; this weakens the structure. In general the negative aspect of weakening and softening override the advantages of the change in period.

One way to lengthen the natural period of an existing structure could be to apply the concept of "base isolation" to retrofitting. The idea is to place the building on elastomeric bearings which isolate the structure from lateral ground motions. A retrofit using base isolation has the advantage of making the building seismically safe with retrofit work limited to the foundation level. The building itself may not need to be altered. However, base isolation has not been commonly as a retrofitting technique, thus leaving its reliability and its economical and technical feasibility unproven [20].

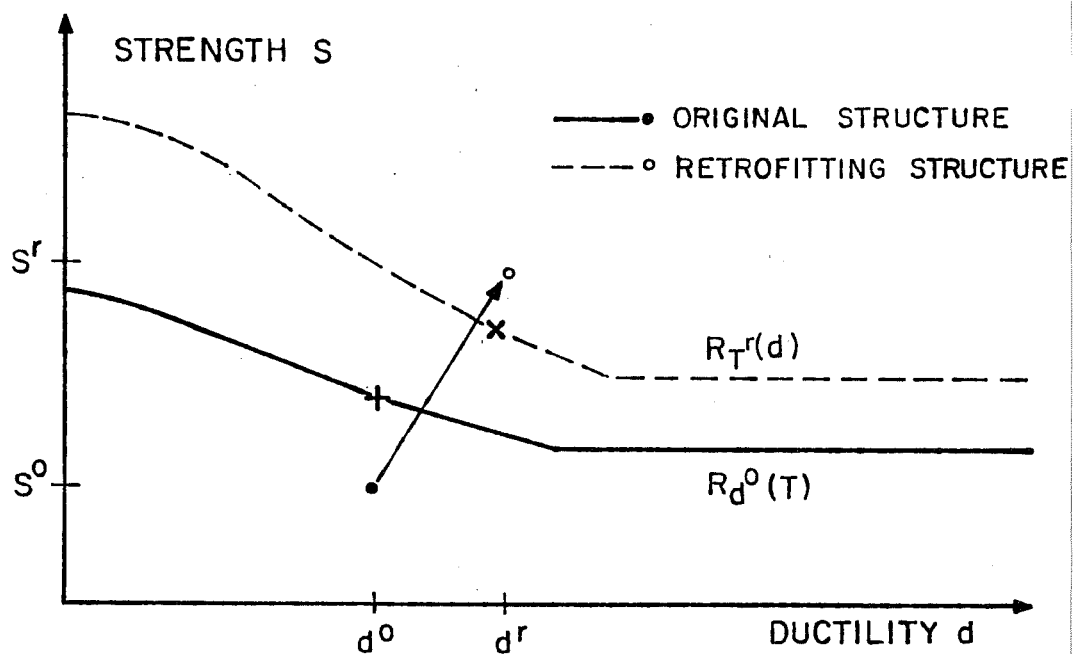
In summary, it can be said that the problems linked with the reduction of the lateral stiffness of an existing structure



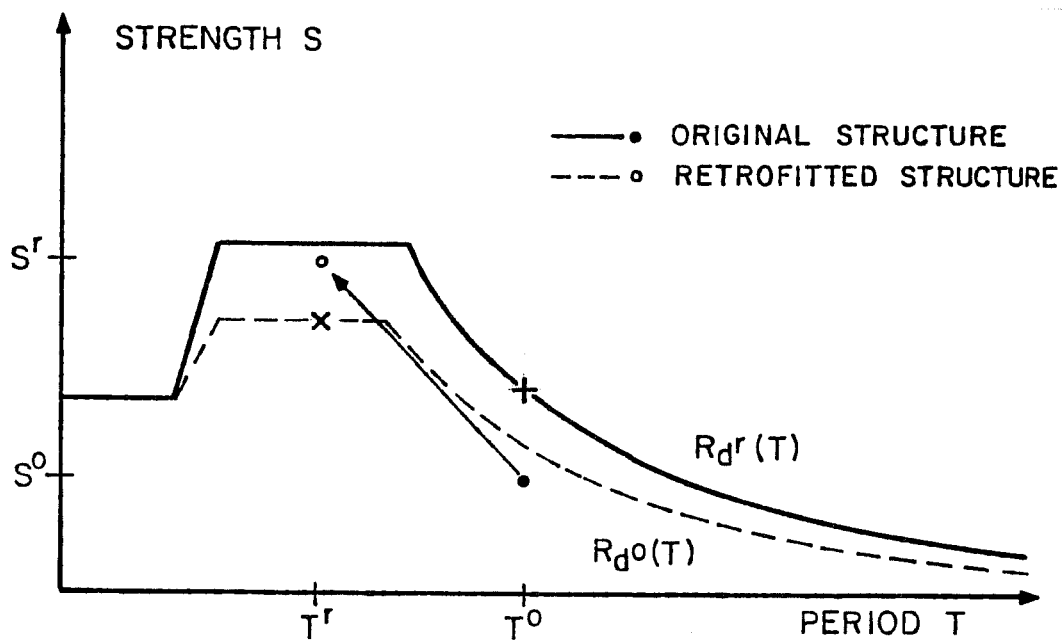
make lengthening its natural period an unlikely way to improve its seismic behavior.

2.5.4 Change in Strength, Ductility and Period. In Section 2.4, the passage from the original to the retrofitted structure was shown in the strength-ductility plane and the effect of a change in the period of the structure was not considered. In Sections 2.5.2 and 2.5.3 the strength-period plane was used and the ductility was assumed to remain unchanged. An example is discussed here where a change in all three parameters - strength, ductility and period - is considered. The two representations used earlier are combined to illustrate the retrofitting operation.

Consider a retrofitting operation like the one illustrated with Curve II of Fig. 2.4.1b. The structure is strengthened, toughened and stiffened so that  $S^r > S^o$ ,  $d^r > d^o$  and  $T^r > T^o$ . The retrofit is shown in the strength-ductility plane in Fig. 2.5.6a. Because of the change in the period from  $T^o$  to  $T^r$ , the required strength curves for the original and retrofitted structures are different ( $R_{T^o}(d) \neq R_{T^r}(d)$ ). The same operation is illustrated in the strength-period plane in Fig. 2.5.6b. The shortening of the period is undesirable and results in a higher strength requirement for the retrofitted structure [ $R(d^r, T^r) > R(d^o, T^o)$ ]. The increase in required strength due to the



a) Strength-ductility plane



b) Strength-period plane

Fig. 2.5.6 Change in ductility and period

shortening of the period is partly compensated by the improvement in ductility.

This example shows that in terms of strength, the retrofitting aim depends on how the retrofitting scheme affects the ductility and the period. The retrofitting operation shown in Fig. 2.5.6a and b is best illustrated in a three dimensional space with axes for strength,  $S$ , ductility,  $d$ , and period,  $T$  and where the strength requirement is represented by surfaces  $R(d,T)$ .

## 2.6 Change in Mass and Damping

2.6.1 Change in Mass. The seismic strength requirement for a structure is proportional to its mass. In a retrofitting operation, the mass is changed (typically increased) and so is the required strength. This means that a structure is only effectively strengthened by retrofitting insofar as the strength is increased more than the mass, it is effectively weakened otherwise. Any strength increase has to be compared with the mass increase. In most situations a light retrofitting scheme (such as a bracing system) has a definite advantage over a heavier scheme (using reinforced concrete infill walls, for example). A lighter system is also better for the foundations.

In the previous sections,  $R(d)$  and  $R(T)$  were defined as strength requirement curves per unit mass. They are not affected

by changes in mass resulting from the retrofitting. Changes in strength,  $S$ , are per unit of mass, any change in  $S$  is therefore an effective change in seismic resistance.

If shear walls or bracing systems are used, it is particularly important to consider the increase of mass in the direction perpendicular to the plane of the retrofitting system. In the perpendicular direction, the strength is not increased, but the seismic forces are. It must, therefore, be checked that the retrofitted structure can resist the increased seismic forces in that direction.

2.6.2 Change in Damping. The energy dissipated by inelastic deformation is the primary source of damping in a reinforced concrete structure during an earthquake. The area within the hysteretic loops of the force-resisting components is a measure of the inelastic damping. From a dynamic analysis perspective, changes in the hysteretic ductility (i.e. in the inelastic deformation capacity under cyclic loading) of the structure are therefore changes in the inelastic damping characteristics. The influence of changes in ductility on the strength requirement is discussed in Section 2.4. If retrofitting increases the ductility, and thus the inelastic damping, the seismic response of the structure is improved and the required strength decreases.

Increasing the elastic damping could be favorable for serviceability state design. Typical retrofitting techniques do not significantly affect the elastic damping characteristics of a structure. One way to increase the elastic damping is to introduce dampers, or dash pots. Such devices have been used with success in new structures to reduce the response of structures to wind excitation and can be used for seismic loading also [21]. But use of dampers for a retrofitting operation has not been reported.

## C H A P T E R 3

### RETROFITTING WITH A STEEL BRACING SYSTEM

#### 3.1 Bracing Pattern and Configuration

3.1.1 General. The following three terms are used in this section in discussing the layout of a bracing system for retrofitting a frame structure:

- Bracing spatial distribution refers to the distribution of the braced frames within the building (Sec. 3.1.4).
- Bracing configuration refers to the distribution of the braced bays in the plane of the frames (Sec. 3.1.3).
- Bracing pattern refers to the geometry of the braces within a braced bay or a group of braced bays (Sec. 3.1.2).

The selection of the bracing spatial distribution, configuration and pattern is a critical component of the design of a braced retrofitting scheme. Structural, architectural and construction considerations are basic to the selection. From a structural point of view, it is usually desirable to distribute the required increase in strength and stiffness as evenly as possible throughout the structure. It is, however, necessary for construction reasons to limit the number of bracing members and connections. This means limiting the number of braced bays. A

change in the stiffness distribution within the structure results in a new load path which may overload some of the members of the existing structure. The designer must thus control the effect of the change in the strength and stiffness distribution on the seismic forces in the unstrengthened parts of the structure. For example if the top story of a building is left unbraced an earthquake may generate higher forces in this story than if the structure were not braced at all. The bracing may create new, undesirable, weak links in the building.

Architectural considerations are important in the choice of a bracing geometry. Possible loss of space and accessibility influences the choice of what bay to brace, and what bays to leave unbraced. For an exterior bracing system the impact of the retrofit on the aesthetic value of the structure depends on its configuration.

3.1.2 Bracing Pattern. Four common patterns used in braced frames are presented in Fig. 3.1.1.

X-Bracing Pattern. X-shaped patterns are the most common because of their structural simplicity and ease of fabrication. Pattern 1 tends to be superior to Pattern (2) for two reasons. First, in many reinforced concrete frames the interstory height is about half the column spacing. In such a geometry the braces of Pattern 1 are inclined at about  $45^\circ$ , and are therefore more efficient in providing strength and stiffness.

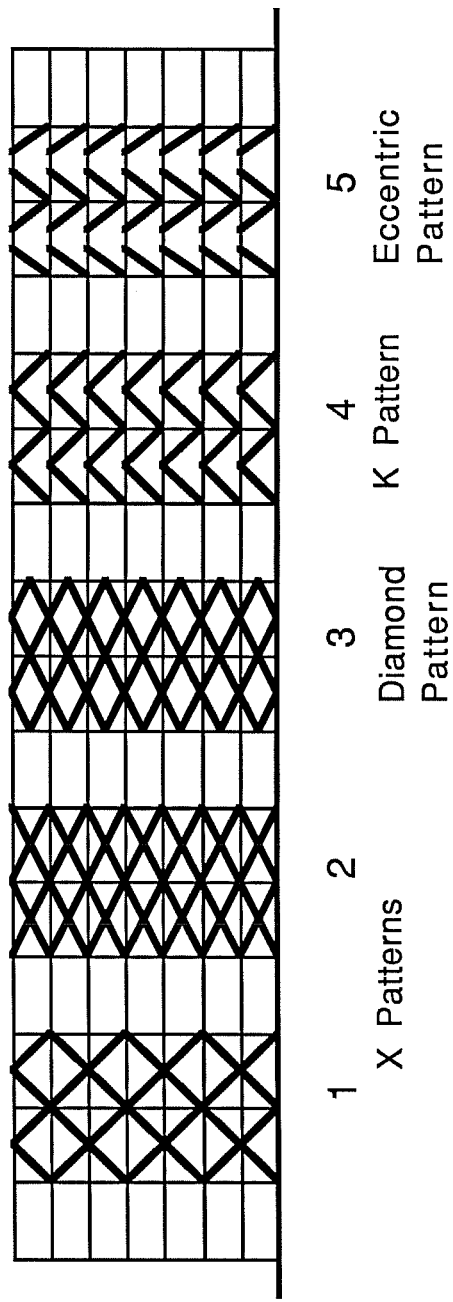


Fig. 3.1.1.1 Bracing patterns



Second, Pattern 1 features a smaller number of members. This reduces construction costs and also means less visual obstruction of windows in the case of an exterior bracing system. Pattern 1 of Fig. 3.1.1 was proposed for retrofitting the prototype structure on which experimental test was based (See Sec. 4.1.4). It is the bracing pattern used for the rest of this study.

Diamond-bracing Pattern. This pattern is identical to Pattern 2 except that it is connected at the beam midspan and the column midheight instead of the beam-column joint. This typically reduces the buckling length of the braces, which can be considered fixed at both ends. This pattern also has aesthetic advantages when used as an exterior bracing pattern. It is, however, seldom used because of the large construction effort required to connect the bracing system to the frame. Also, there is the risk with such a bracing pattern of introducing an unwelcome horizontal force in the column at midheight.

K-bracing Pattern. This pattern can be seen as a modified pattern 1. The braces are inclined with the same angle and have the same buckling length, but they are not continuous from one story to another. This modification has negative structural consequences: if the load in the two braces of a bay are different, there is a resulting vertical force acting on the beam at midspan. Such an unbalance can occur in the inelastic

range for example, when the compression brace has buckled and the tension brace has yielded. For braces with a high slenderness ratio the difference in post-buckling and yielding capacity is large, resulting in a large downward oriented force on the beam. In a retrofitting situation, this force is undesirable because it probably was not accounted for in design. This pattern is therefore not recommended for retrofitting operations, especially for braces with a high slenderness ratio.

Eccentric-Bracing Pattern. It has been shown that eccentrically braced steel frames can display, if proportioned adequately, very favorable seismic behavior. The favorable seismic behavior relies on inelastic deformations in so-called "shear links" in the beams. The shear links are detailed for good energy dissipation under hysteretic shear loading. The use of eccentric bracing for the retrofitting of reinforced concrete frames is problematic. The beams of an existing reinforced concrete building cannot be used to develop shear links. It becomes necessary to provide horizontal steel members to protect the reinforced concrete beams. The advantage of using the existing reinforced concrete beams as horizontal members of the braced frame thus disappears.

3.1.3 Configuration of the Bracing System. Retrofitting a frame of a multistory building may not require the bracing of all bays. The designer thus has freedom in the choice

of a bracing configuration. Consider for example the prototype structure described in Sec. 4.1. The longitudinal frames have eleven bays and seven stories. The story height is 10 ft, the column spacing is 21 ft, except for the 2 end bays where it is 19 ft 6 in. A possible retrofitting scheme for this seismically inadequate structure is bracing its perimeter frames; six alternative configurations are presented in Fig. 3.1.2.

Configuration 1. The 5 center bays of the frame are braced at every story. The number of braced bays depends on the strength and stiffness requirement for the bracing system. The bracing system should preserve the symmetry of the frame. It is often advantageous not to brace the two end bays. The main reason is that it is common for the two end spans to be shorter than the intermediate ones. The bracing geometry of the end bays would therefore be different from the rest of the structure, which would have structural and construction disadvantages. A further reason is that an interior column of the frame can better help carry some of the overturning forces than the exterior columns of the bracing system. First, because a frame interior column carries the gravity load from two half bays, instead of one for an exterior column, and can thus better help resist uplift forces. Second, because in a typical frame, the outermost

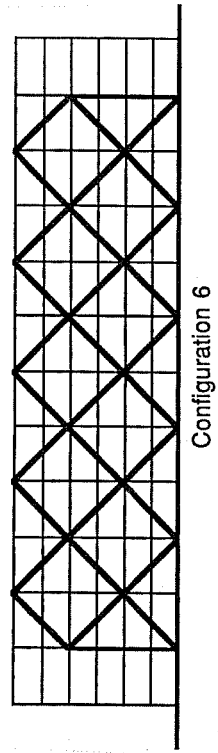
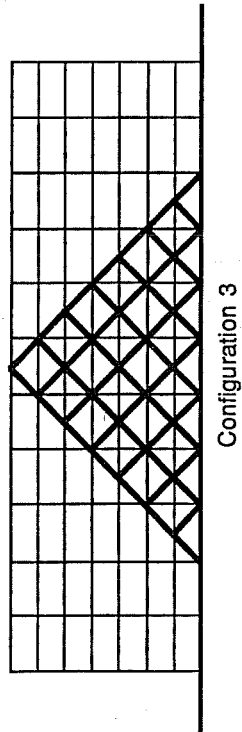
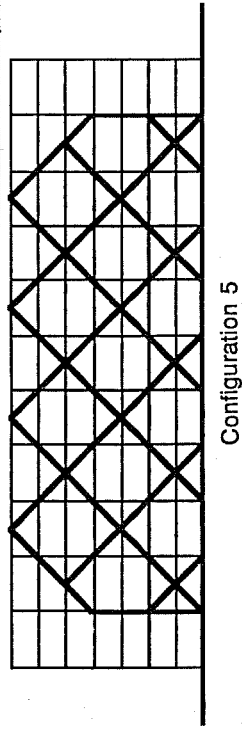
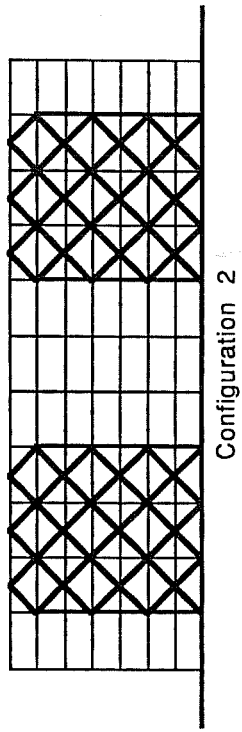
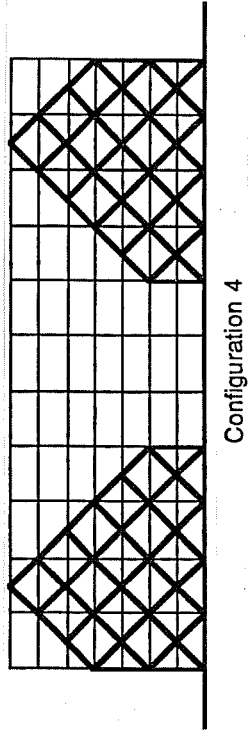
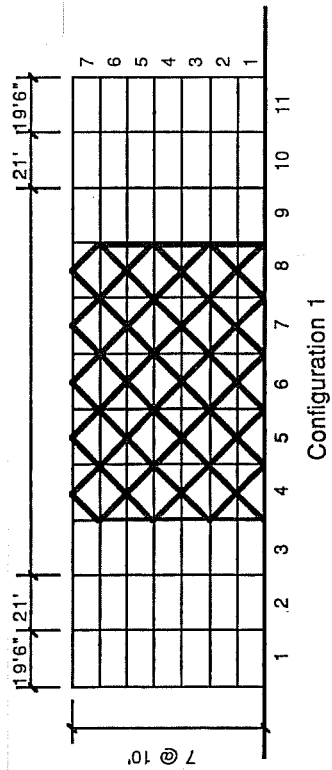


Fig. 3.1.2 Bracing configurations

columns resist greater vertical forces from frame overturning moments than the interior columns.

Configuration 2 This configuration is similar to the first one except for the distribution of the bracing system in two separate halves. This has the structural advantage of a better distribution of the strength and stiffness in the plane of the frame.

Configuration 3 Because of its pyramidal shape, this bracing system may satisfy the seismic strength requirement more efficiently. The bracing system decreases in strength at higher story levels where the seismic story shear is less. This can also be done with other configuration by decreasing the brace section, but it is preferable for structural and construction reasons to have only one brace size. Also, in this configuration, no columns are necessary in the bracing system to carry overturning forces. Finally, this configuration may be aesthetically superior.

Configuration 4. This configuration combines the advantages of the two previous ones. Splitting the bracing system in two halves allows a good planar distribution of the strength increase. The vertical distribution of the strength of the retrofit system typically corresponds very well to that of the diagram of design story shear. This configuration may also be attractive architecturally. Bracing the two end bays may be

disadvantageous for the reasons mentioned above. If this is a problem, the two halves of the bracing system can be moved inward.

Configuration 5. In this configuration the braced and unbraced bays alternate in a "checker-board" fashion. This allows a better distribution of the strength than Configuration 1 for example. The main structural disadvantage of this configuration is that lateral loads introduced at the second, fourth and sixth floors result in axial loading of the interior columns. Because of this axial load the columns may need to be strengthened with vertical members.

Configuration 6. As for the previous case, in this configuration the strength increase is distributed over the entire frame and a minimum number of members is needed. Every bay is braced, but with one brace only. Unlike Configuration 5, this bracing system does not generate axial load in the interior column when subjected to lateral loading in the inelastic range. For structural and aesthetic reasons, this configuration is only well suited for a frame with an even number of bays and stories. It is therefore illustrated for a frame with twelve bays and six stories.

3.1.4 Spatial Distribution. An adequate spatial distribution of the bracing system helps limit the amount of

torsion on the structure during an earthquake. Keeping the torsional eccentricity to a minimum should be a primary goal in retrofitting. It is, in this respect, best for the retrofitting scheme to maintain whatever symmetry the structure has, so that the structure's center of torsion and center of mass coincide. The further apart the braced frames, the greater the improvement of the torsional strength and stiffness of the structure. The designer of the retrofitting system for the Mexican structure presented in Section 1.3.2 chose to brace the two perimeter frames. This maintained symmetry and significantly increased torsional strength and stiffness.

If only the exterior frames are strengthened, the slabs have to carry part of the seismic shear from the interior frames to the exterior frames. The slabs have probably not been designed and detailed for this diaphragm function. They may suffer damage from the additional in-plane shear and bending. If the slabs are not stiff and strong enough, their distortion is such that the interior frames deform considerably more than the exterior ones (See Fig. 3.1.3). This may be the case with waffle slabs for example. Retrofitting may thus fail to prevent damage to the interior frames. A possible remedy to this problem is to strengthen the slabs so that they can transfer the required loads from the interior frames to the exterior ones with minimum shear or flexural distortion. Such slab retrofitting is often

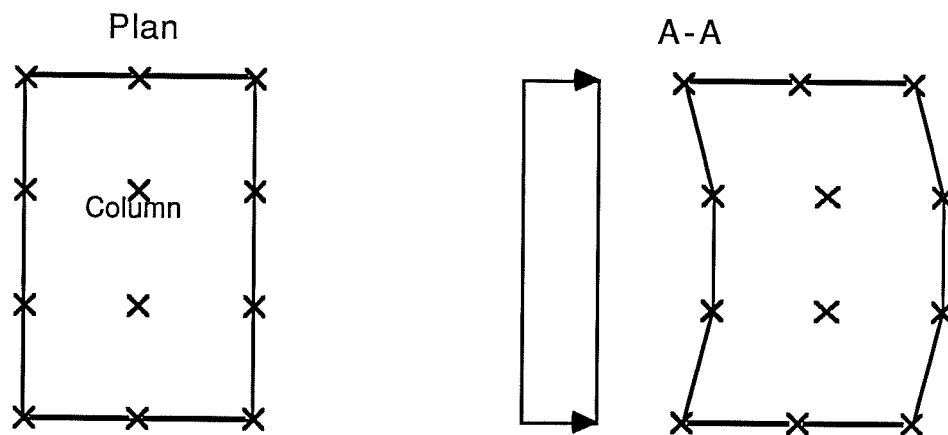
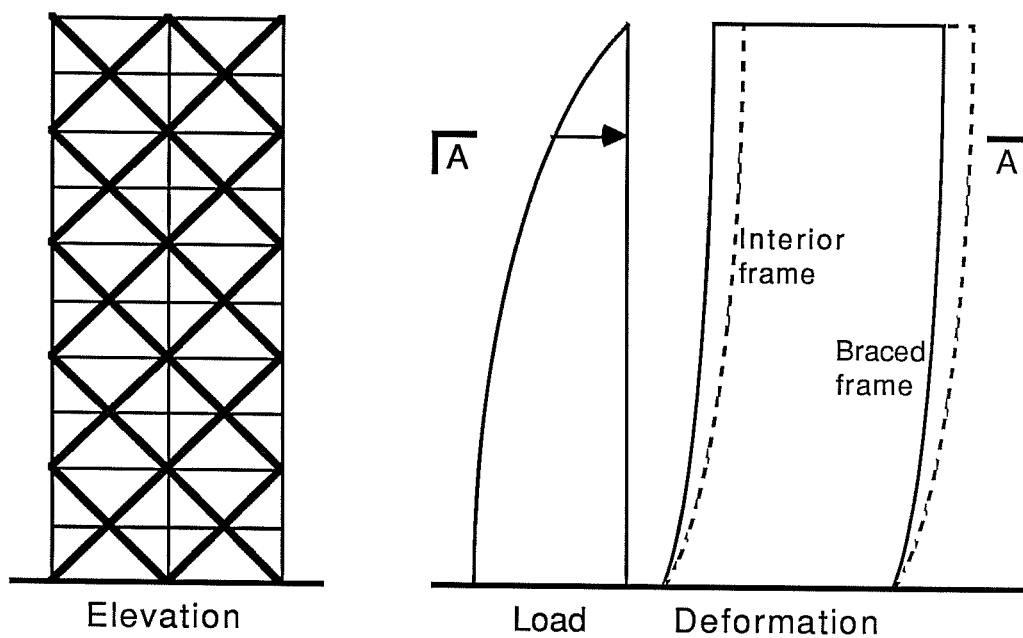


Fig. 3.1.3 Deformation of a laterally loaded building with stiff perimeter braced frames



impractical or very expensive. An alternative is to complement the bracing of the perimeter frames with the strengthening of one or several interior frames. Interior frames can be strengthened with a bracing system also, but in most cases it is probably better to use shear walls or column strengthening techniques. A mixed retrofitting scheme using a bracing system on the perimeter frames and another retrofitting technique for the interior frame may be a good solution for large frame structures in need of extensive improvement.

### 3.2 Modeling a Braced Frame

3.2.1 Exact Model. Consider the steel braced reinforced concrete frame of Fig. 3.2.1a. A model of the braced frame under lateral loading is shown in Fig. 3.2.1b. The connections between the frame and the bracing system are rigid connections, i.e. moment connections. They impose compatibility of displacements and rotations between the braces and the frame at the joints. The deformed shape of the braced frame in the inelastic range is shown in Fig. 3.2.1c. The frame columns and beams deform primarily in flexure and therefore in double curvature. The brace behavior is dominated by axial loads, but as a result of the rotation compatibility at the joint, the braces experience double curvature deformation in the elastic range. In the inelastic range tension brace B1 yields and

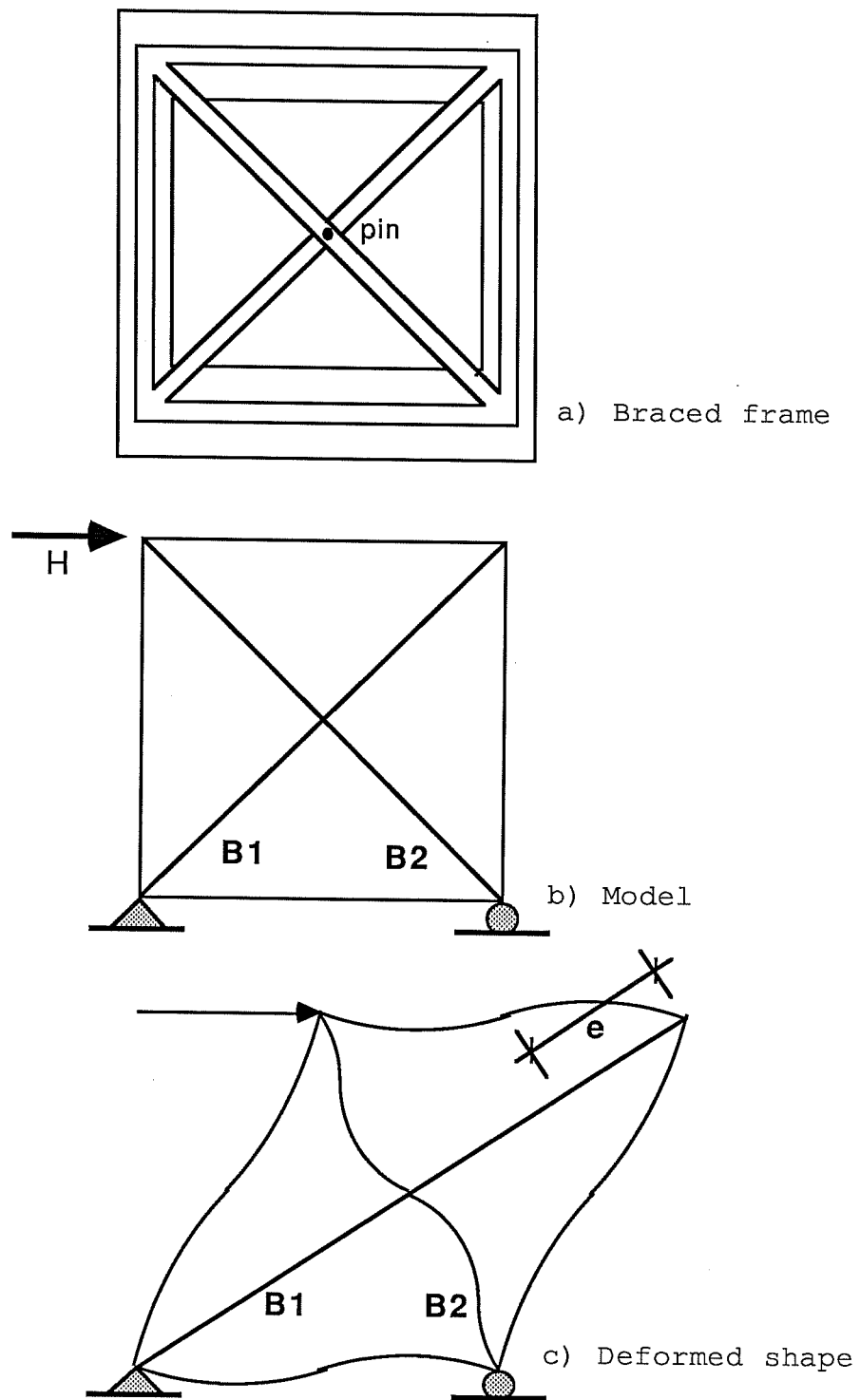


Fig. 3.2.1 Modelling of a braced frame

compression brace B2 buckles. The main effect of the rotation compatibility at the joint is the end restraint provided to the brace. The buckling length is significantly reduced in comparison to the unrestrained case. Tests show that the buckling shape of the brace is close to the fixed end case. Therefore, the  $k$  factor for the effective buckling length is close to 0.5.

3.2.2 Approximate Model. An approximate model for the braced frame of Fig. 3.2.1a is presented in Fig. 3.2.2. The frame and the bracing system are separated and coupled with a pinned bar. The coupling of the two systems with a pinned link bar only reproduces the lateral displacement compatibility. The compatibility of rotations between the members of the bracing system and the beam column joints is not reproduced. The model is, therefore, only approximate.

The main effect of the rotation compatibility is the end restraint provided to the compression brace. This effect can be accounted for in the approximate model by reducing the buckling length of the braces. The effective buckling length factor  $k$  can be evaluated by comparing the flexural stiffness of the beam column joint and of the braces. The other effect of the rotation compatibility is the contribution of the braces to the rotational stiffness of the braced frame joints. This effect is not

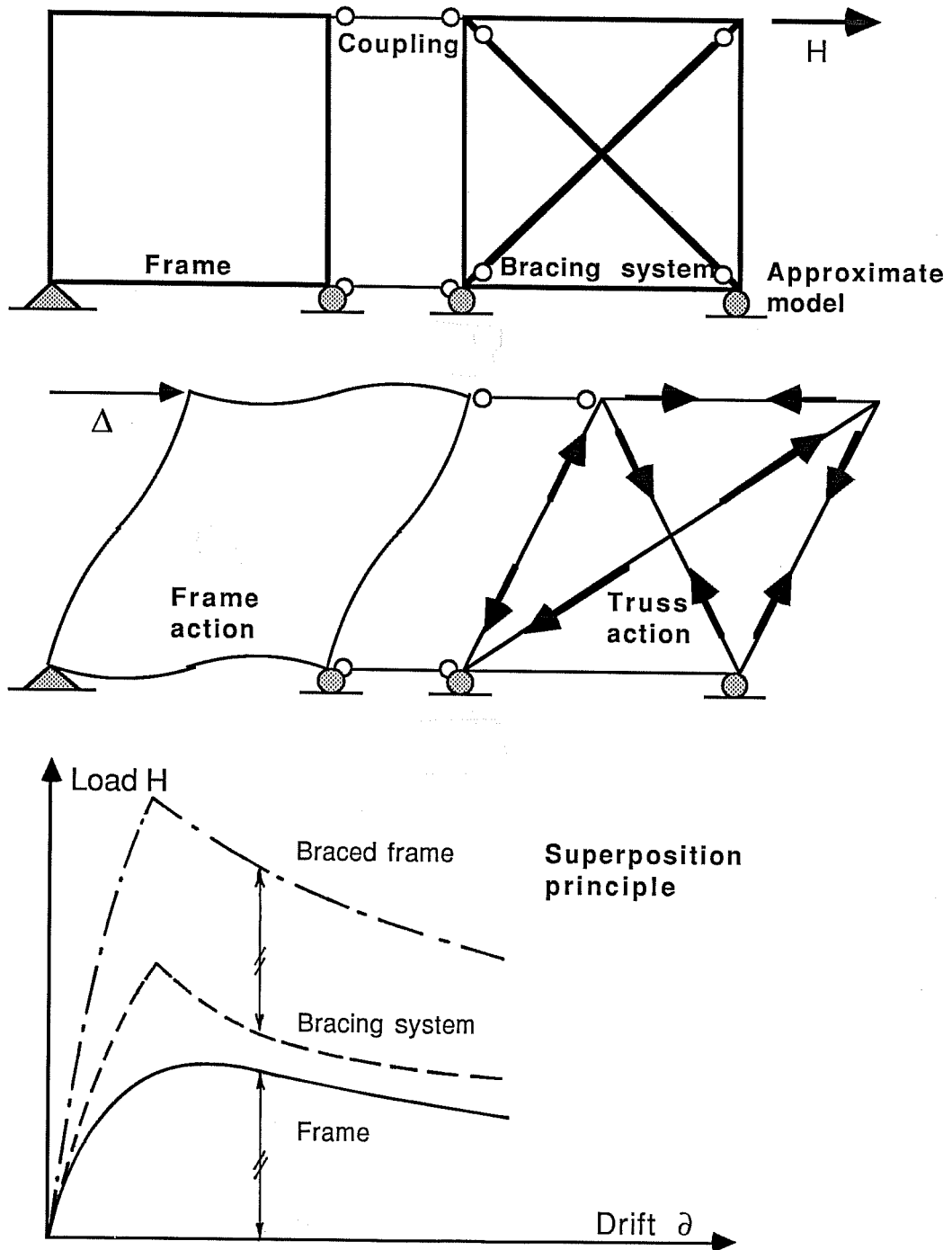


Fig. 3.2.2 Approximate model and response

accounted for in the approximate model. In most retrofitting cases, however, the ratio of the flexural stiffness of the steel braces to that of the reinforced concrete beams and column is small. In such a case, neglecting the contribution of the flexural stiffness of the braces to the braced frame lateral stiffness is not very significant. A good approximation of the braced frame behavior can be obtained with the approximate model.

The advantage of the approximate model is its simplicity. "Frame action" and "truss action" are clearly separated (See Fig. 3.2.2b). The frame resists lateral loads by developing flexure and shear in its members. The bracing system lateral resistance is based on axial forces in the braces. The lateral load-drift curve of the approximate model is obtained by superposition of the load-drift curve of the frame and bracing system. Figure 3.2.2 illustrates the principle of superposition. The load is distributed to the two systems according to their lateral stiffness. The principle of superposition is valid because the two systems are coupled in statically determinate fashion. In the exact model of Sec. 3.2.1, the two systems are coupled in a statically indeterminate way.

The approximate model is used in this study to investigate braced frame behavior qualitatively. The exact model is used when quantitative load drift response is studied.

### 3.2.3 Overturning forces of the Bracing System.

Consider a bracing system composed of three bays with identical braces. Figure 3.2.3 shows this truss under lateral loading. At the foundation level overturning generates an uplift force, T, at one extremity of the frame and a downward force, C, at the other end. The intermediate foundations are not loaded. The foundation forces T and C for a bracing system with m stories and n bays can be calculated as follows:

$$T=C= \frac{\sum_{j=1}^m H_j \cdot h_j}{\sum_{i=1}^n l_i}$$

T, C: Upward and downward forces due to overturning  
 $H_j$ : Overturning force  
 $h_j$ : Height above foundation level of  $H_j$   
 $l_i$ : Column spacing

The higher and the narrower the bracing system, the higher the overturning forces on the foundations.

Only the exterior vertical members of the truss of Fig. 3.2.3 are loaded. The interior columns are not loaded because the forces in the compression and tension brace are equal and compensate each other at the joint. Bracing systems used in retrofitting operations often feature external steel columns because the overturning forces from the bracing system are too large to be carried by the columns of the existing frame.

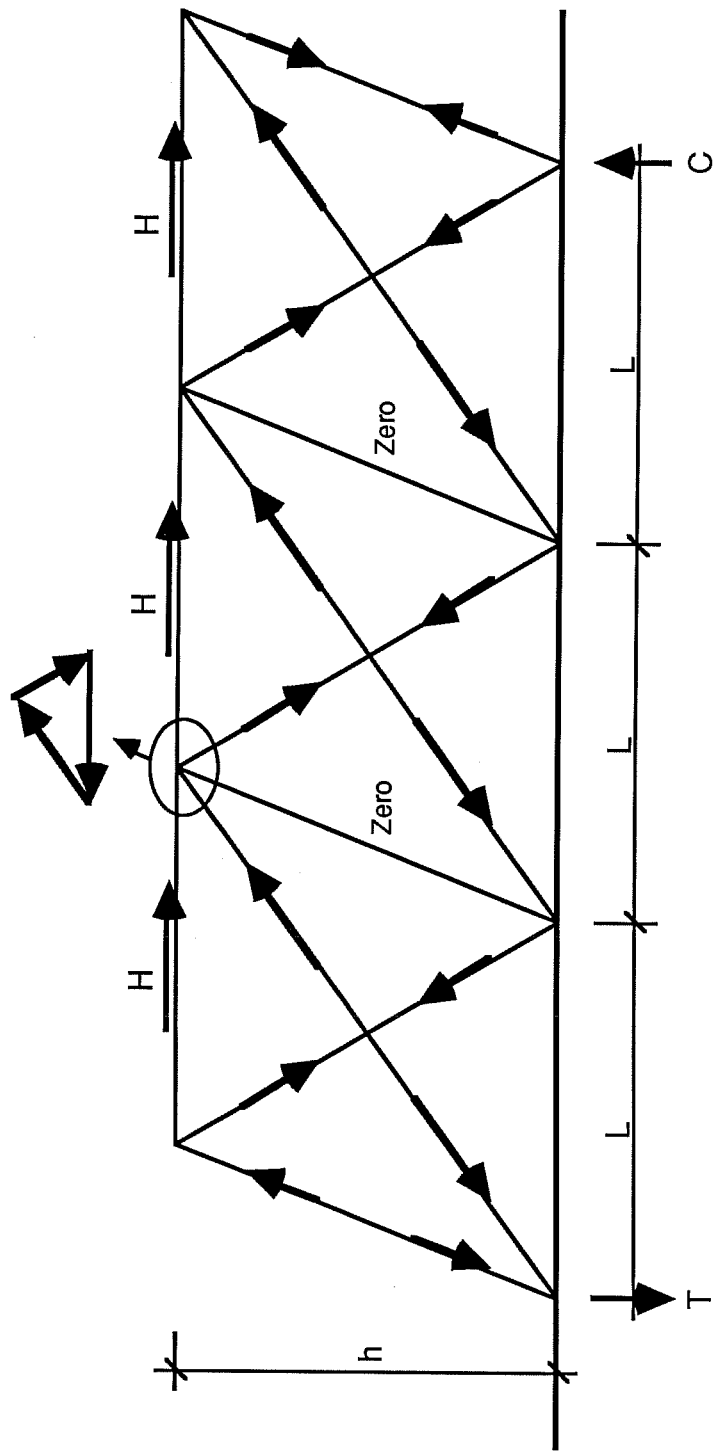


Fig. 3.2.2.3 Forces in a bracing system with X-pattern

The axial load on the interior columns of the truss is not zero in the inelastic range. Typically the brace post buckling capacity is smaller than its tensile yield capacity, in which case vertical components do not cancel. If the vertical resultant is too high to be carried by the column of the existing frame, it is necessary to include vertical steel members in the bracing system. But if the maximum possible vertical resultant can be carried by the existing reinforced concrete column, a much simpler bracing scheme can be designed. The columns of the existing structure can be used as vertical members of the bracing system. By keeping the brace slenderness ratio low, buckling of the compression braces is delayed or prevented and a large imbalance of compression and tension forces in the bracing system does not occur. Low slenderness increases the probability that interior vertical elements will not be necessary in the bracing system.

### 3.3 Deformability of the Bracing System

The question of the optimum deformability or damage drift level of the bracing system for a given reinforced concrete frame is investigated qualitatively.

The drift  $\delta^f$  is defined as the drift level at which a reinforced concrete frame suffers unacceptable structural damage.  $\delta^f$  varies from one frame to another. The lateral load-drift



curve of Fig. 3.3.1 (solid line) is for a reinforced concrete frame with short columns like the prototype structure (Sec. 4.1.1). For the prototype structure  $\delta^f$  is the drift at which the columns fail in shear and the peak lateral strength is reached. In this case, interstory drift  $\delta^f$  is small, about half a percent. In a ductile frame  $\delta^f$  would be larger.

The load-drift curve of the bracing system for retrofitting is also plotted in Fig. 3.3.1. For simplification it is assumed that the compression and tension braces buckle and yield simultaneously at drift  $\delta^{bs}$  when the bracing system enters the inelastic range. This is a reasonable assumption for low  $kl/r$  ratios. As will be seen in Sec. 6.4, it is desirable for the bracing system to remain in the elastic range under the design seismic loads. Drift,  $\delta^{bs}$ , is like  $\delta^f$  for the frame, the drift of unacceptable damage as well as the peak strength drift for the bracing system.  $\delta^{bs}$  and  $\delta^f$  can be interpreted as measures of the deformability of the bracing system and the frame.

In the retrofitting operation, the bracing system is attached to the frame and a braced frame is produced. As was established in Sec. 3.5 and confirmed by the analytical study (Sec. 6.1), a good approximation of the load-drift curve for the braced frame can be obtained by superposition of the load-drift

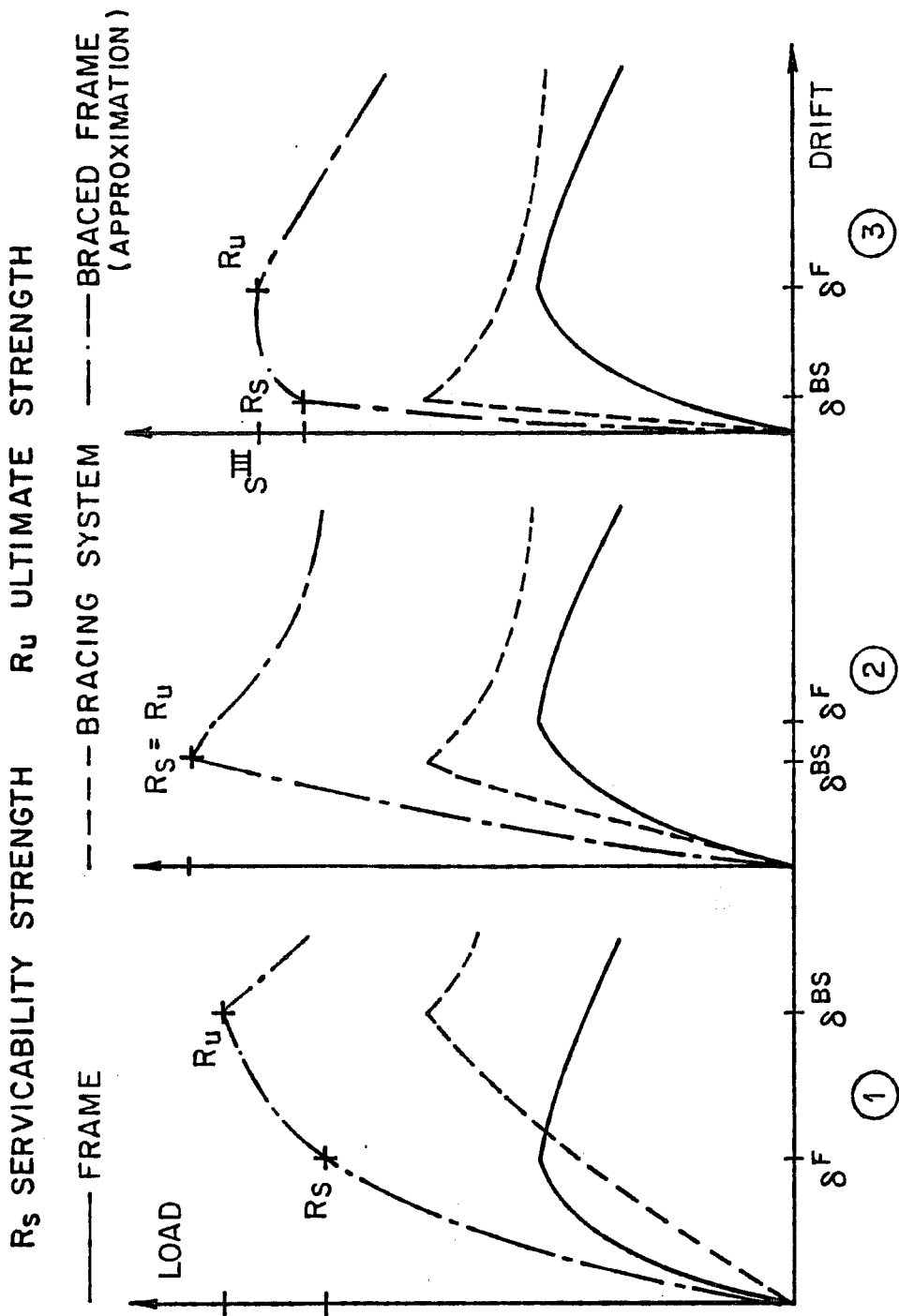


Fig. 3.3.1 Relative deformability of the frame and the bracing system

curves for the frame and bracing system. Superposition is used in Fig. 3.3.1 to obtain the braced frame load-drift curve. If the "serviceability strength" is defined as the strength which can be mobilized without significant structural damage, the serviceability strength for the braced frame is the strength at the smallest of the drifts  $\delta^{bs}$  and  $\delta^f$ . Figure 3.3.1 shows the influence of the relative values of  $\delta^{bs}$  and  $\delta^f$  on the serviceability strength  $R_s$  and the peak or ultimate strength  $R_u$  of the braced frame, for three values of  $\delta^{bs}$ .

1) Damage Drift Level  $\delta^{bs}$  Larger than  $\delta^f$ . Only half of the bracing system elastic strength is mobilized when the frame reaches its peak strength. As a result the frame suffers heavy structural damage before the bracing system lateral resistance is fully used. The serviceability strength  $R_s$  is low. The bracing system is inefficient in protecting the frame against lateral overload because its deformability does not match frame deformability.

2) Damage Drift Level  $\delta^{bs}$  Somewhat Smaller than  $\delta^f$ . When the bracing system enters the inelastic range, most of the frame lateral strength is mobilized and contributes to the overall lateral strength. Both systems enter the inelastic range in parallel the serviceability strength  $R_s$  of the braced frame is maximized. The two systems are well-matched in their lateral deformability.

3) Damage Drift Level  $\delta^{bs}$  Much Smaller Than  $\delta^f$ . The bracing system reaches the inelastic range and peak strength before the frame can contribute significantly to the lateral resistance. The frame is well protected against lateral overloading but the two systems do not work together. As a result, the braced frame has low serviceability and ultimate strength.

Figure 3.3.1 shows that the bracing system should not be designed on the basis of strength only. The relative deformability of the bracing system and the frame should be considered in order to avoid an unfavorable failure sequence of the braced frame. To prevent substantial damage to the frame, damage drift level  $\delta^{bs}$  should not be greater than  $\delta^f$ . The braced frame serviceability and ultimate strength is maximized if  $\delta^{bs}$  and  $\delta^f$  are equal. It is, however, desirable to design a bracing system with a damage drift level  $\delta^{bs}$  somewhat smaller than  $\delta^f$ . The resulting small loss of braced frame strength is outweighed by the additional margin against overloading the frame. If the bracing system deformability is much less than the frame deformability, the braced frame is not optimum in terms of strength and composite action. When the two systems are well matched, most of the lateral strength of the retrofitted structure is mobilized with only minor cracking of the frame.

The retrofitted frame remains basically elastic until the peak strength is reached, so that the serviceability strength is maximized.

If the two systems are ill-matched in their deformability the designer should consider changing the bracing system  $\delta^{bs}$  (changing  $\delta^f$  is difficult since it implies modifying the frame). For a given bracing configuration and brace slenderness  $\delta^{bs}$  is independent of the brace strength. To change  $\delta^{bs}$  the configuration and/or the slenderness must be changed. If this is not possible or desirable, the bracing system must then be carefully designed to insure proper performance. If  $\delta^{bs} > \delta^f$ , only the part of the bracing system strength which is mobilized at drift  $\delta^f$  can be used in the design of the bracing system. If  $\delta^{bs} \ll \delta^f$  the frame does not contribute significantly to the elastic strength of the braced frame, the bracing system must carry the entire design lateral load.

Matching bracing system and frame deformability could also be expressed in terms of stiffness. But the stiffness of the reinforced concrete frame is not uniquely defined in the drift range preceding  $\delta^f$ , so that damage drift level  $\delta^f$  would have to be introduced anyway to define a secant stiffness. It is interesting, however, to look at the implication of the matching criteria for  $\delta^{bs}$  on the required bracing system stiffness. Figure 3.3.2 shows that the stronger the bracing system, the

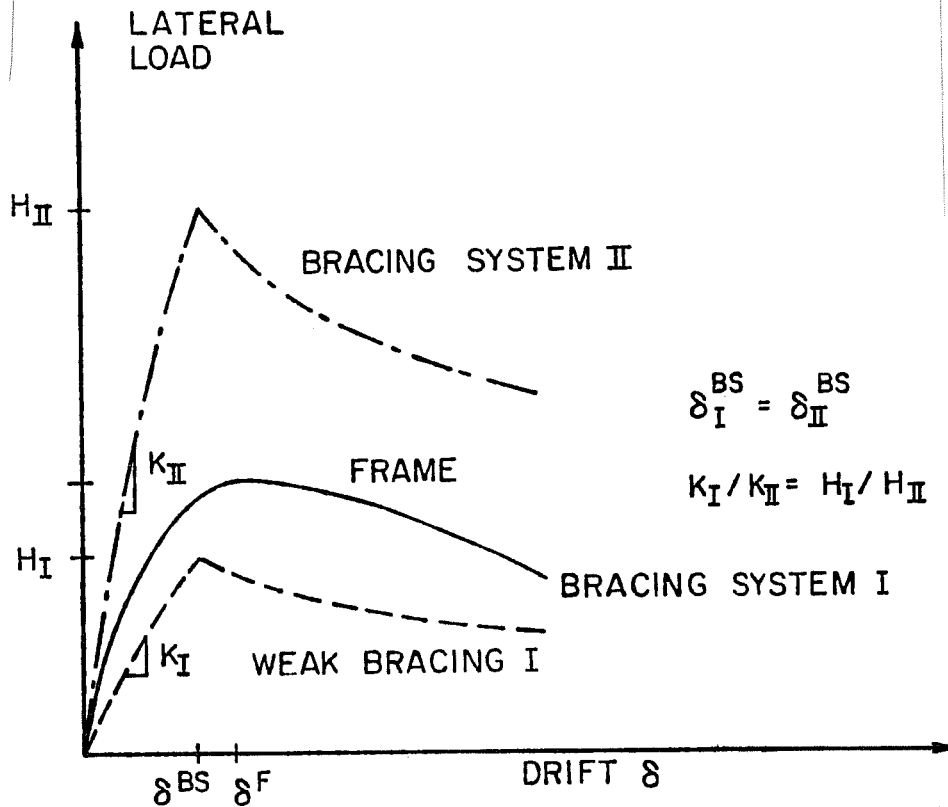


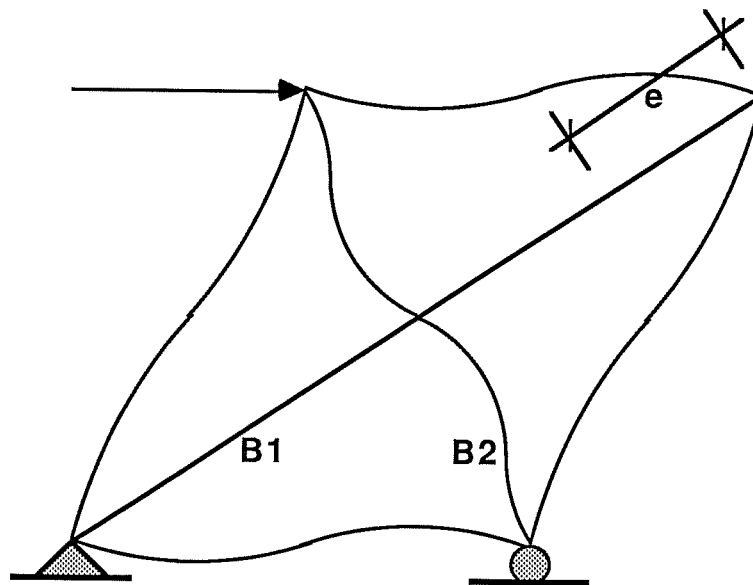
Fig. 3.3.2 Initial stiffness of the bracing system for two levels of strength

greater the required stiffness for the bracing system to attract its share of the load. The general principle can thus be formulated that the relative ratio of the stiffness of the two systems should be about the same as their relative strengths. This guarantees that the two systems enter the damage drift range at about the same drift level.

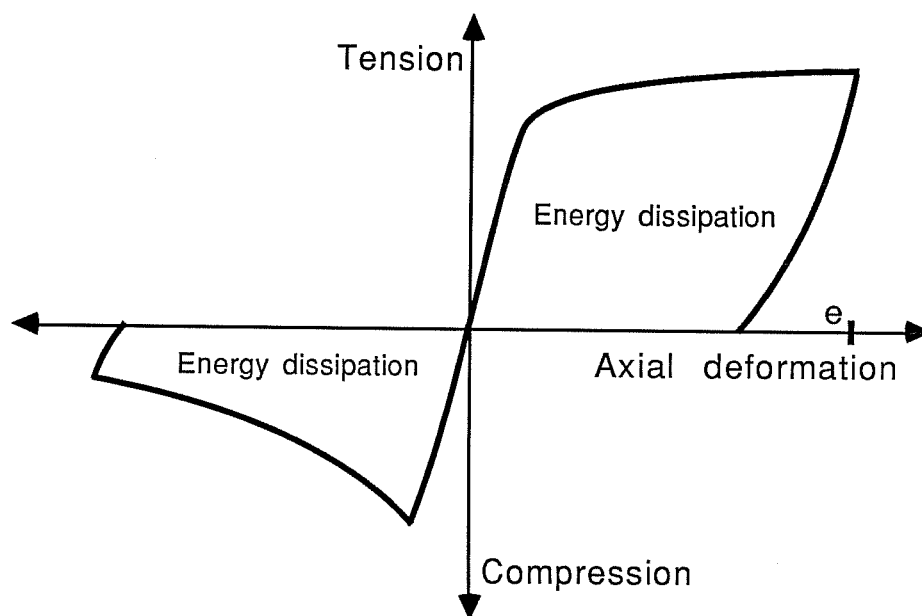
### 3.4 Energy Dissipation in the Bracing System

The impact of seismic retrofitting on the energy dissipation capacity (i.e. ductility) of a structure is of primary interest in seismic applications. The energy dissipation mechanism of the bracing system must be studied.

Ductile members failing in flexure exhibit good energy dissipation capacity. They develop flexural hinges in which much energy is dissipated by the gradual yielding of the steel. Ductile frames have high energy dissipation capacity if detailed adequately. In a bracing system the energy dissipation capacity has to be provided by inelastic deformation of the braces under axial load. Consider the braced frame of Fig. 3.4.1. There is energy dissipation in both braces when the structure is subjected to lateral deformation in the inelastic range. The load deformation curve of a brace under monotonic axial compression and tension is shown in Fig. 3.4.1b. The area under the load deformation curve is the energy dissipated by the braces.



a) Deformed shape



b) Load deformation curve for the braces

Fig. 3.4.1 Energy dissipation in the bracing system



Tests show that tension braces exhibit good energy dissipation capacity. Yielding develops in a section of the brace and the zone of yielding spreads with increased elongation because of strain hardening. Large elongations can be reached before failure if the connections are adequate. In compression the brace typically exhibits limited energy dissipation capacity. If the brace is prevented from buckling and yields, the energy dissipation in compression is similar to that in tension, but in most cases the brace buckles and loses capacity with increased axial deformation. The higher the slenderness ratio, the more pronounced the buckling behavior and the smaller the energy dissipation capacity. Compression braces with slenderness ratios above 100 contribute little to the energy dissipation capacity of the bracing system.

It is the energy dissipation capacity under repeated cyclic loading ("hysteretic ductility" in this study), rather than under monotonic loading, which is important. The hysteretic behavior of the braced frame is more relevant than the monotonic behavior for the seismic performance. In a well-detailed ductile frame the favorable energy dissipation capacity under monotonic loading is maintained under repeated cyclic loading. For the bracing system, the cyclic loading case is much more severe than the monotonic case because the braces switch from compression to tension and vice versa. In the inelastic range, they may undergo

several cycles of buckling and yielding, a kind of low cycle fatigue with large local deformations. The repeated passage from buckling to yielding can lead to failure of the connections or braces.

The study of the energy dissipation capacity of the bracing system shows the importance of making the distinction between "material ductility" and "system ductility." In the case of a steel bracing system, the material hysteretic ductility is excellent, but the system ductility may be significantly less favorable. This is illustrated by the comparison of the hysteresis loops of a brace with those of a coupon from the same brace (See Figs. 1.3.4 and 1.3.5). The difference is the result of the influence of the structural geometry of the system on ductility. In a material test the steel yields in compression whereas the steel braces of the bracing system buckle in compression. The buckling has a double negative effect on the system ductility. First, the energy dissipation in the compression brace is substantially lower in buckling than yielding. Second, buckling can, under repeated load reversals, lead to failure and terminate the energy dissipation of the brace in tension.

### 3.5 Flowchart of the Retrofitting Process

3.5.1 Decision to Brace a Structure. The main steps in the process leading to retrofitting a structure with a steel bracing scheme are outlined in the flowchart of Fig. 3.5.1.

The evaluation of the seismic adequacy of the structure (Step 1) consists of comparing the seismic performance requirements with expected behavior under seismic loading. This is a difficult task which requires much engineering judgment and include nonengineering considerations (Sec. 2.1). If the structure is found inadequate (Step 2), a responsible owner must choose between retrofitting or replacement (Step 3). If the retrofitting alternative is chosen, the "aim of the retrofitting" in terms of strength, stiffness and ductility of the retrofitted structure is defined (Step 4). The aim of the retrofitting depends on the structural characteristics and deficiencies of the structure (see Sec. 2.4). The selection of a retrofitting scheme (Step 5) is based on economy, constructibility and aesthetic quality. Disruption of usage during and after the retrofitting operation is an important consideration also. The rest of the flowchart is for the case where a steel bracing system best meets the structural and nonstructural requirements. Bracing may be combined with other retrofitting techniques.

3.5.2 Design of the Bracing System. The choice of the bracing system (Step 6) configuration includes selecting frames

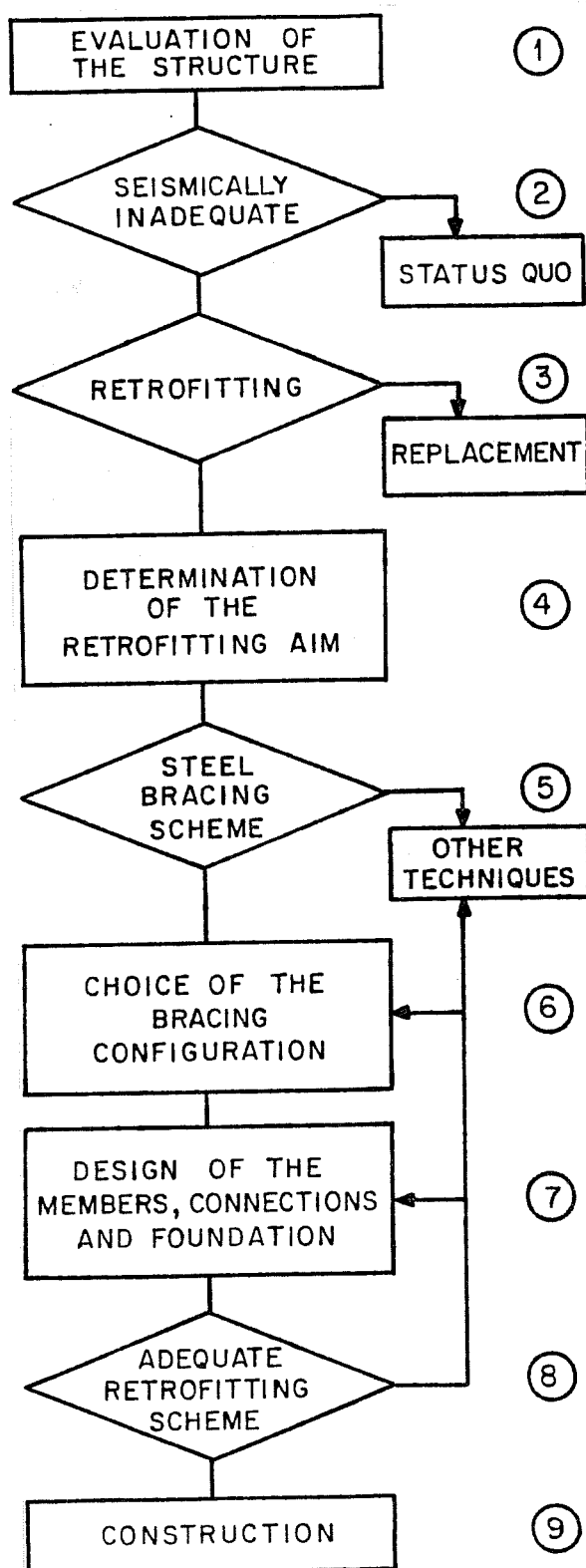


Fig. 3.5.1 Design flowchart for retrofitting with a bracing system

and bays to be braced and selecting the bracing pattern (see Sec. 3.1). For this choice, the three-dimensional response of the retrofitted structure must be considered. The introduction of torsional eccentricities in the plan of the structure or within the braced frames should be avoided. Also, it must be considered that in the direction perpendicular to the bracing, the lateral resistance is not increased, but the seismic forces are because of the increase in mass. Changes in force distribution in the existing structure must be checked to avoid overloading certain members, or creating local force concentrations.

Once a configuration has been chosen, the bracing system can be designed and detailed (Step 7). To maximize the drift range in which the braced frame responds elastically, the bracing system and the frame should be matched in terms of their relative deformability (Sec. 3.3). If columns function as vertical elements of the bracing system, they must be checked for their ability to carry the additional loads. The connections of the bracing system must be detailed carefully to avoid local failure under inelastic cyclic deformations. The foundations of the braced frames may need strengthening because the retrofitted structure typically transfers greater seismic forces on the foundations.

If the retrofitting design found is inadequate (Step 8), a new bracing configuration and/or design is necessary, or another retrofitting technique must be used. In the construction phase, allowance should be made for higher fitting tolerances and for in situ modifications. The boundary conditions are more narrowly defined than in new construction; special construction problems should therefore be expected.

### 3.6 Braced Frame with Short Columns.

#### 3.6.1 Introduction to Short Column Behavior.

Understanding the behavior of reinforced concrete short columns is important in many retrofitting applications. Because of the brittle nature of failure and poor hysteretic performance of short columns, structures featuring short columns are often seismically deficient and in need of retrofitting. For that reason, a building with short columns was chosen as the prototype for this study. Two examples of short column failure under seismic loading are shown in Fig. 3.6.1.

A laterally loaded slender column fails by developing flexural hinges at its extremities. In short columns the shear resistance is reached before flexural hinges develop. Because the failure is shear dominated, reinforced concrete short columns exhibit brittle behavior under lateral loading. A typical load deformation curve for an axially loaded reinforced concrete short

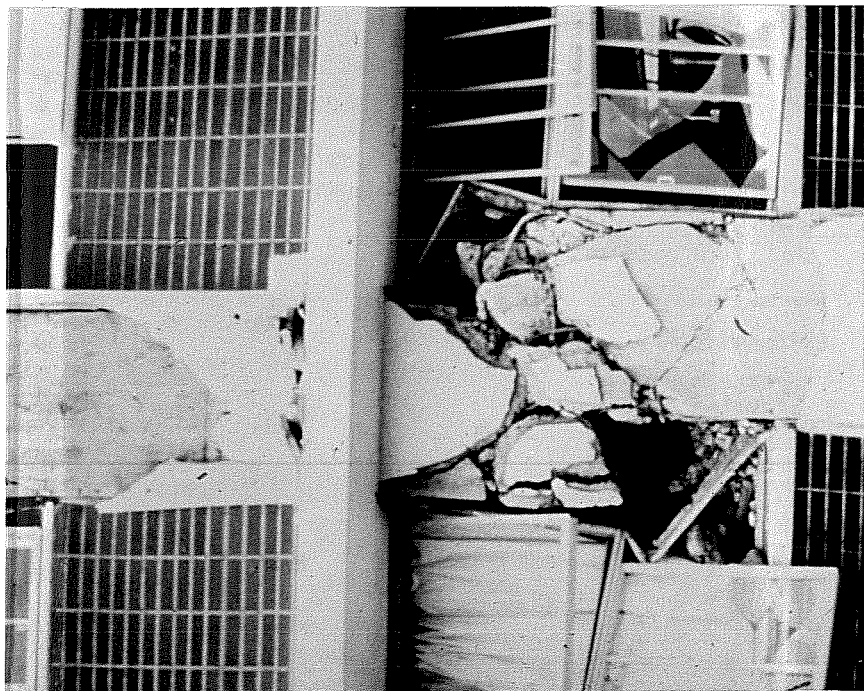
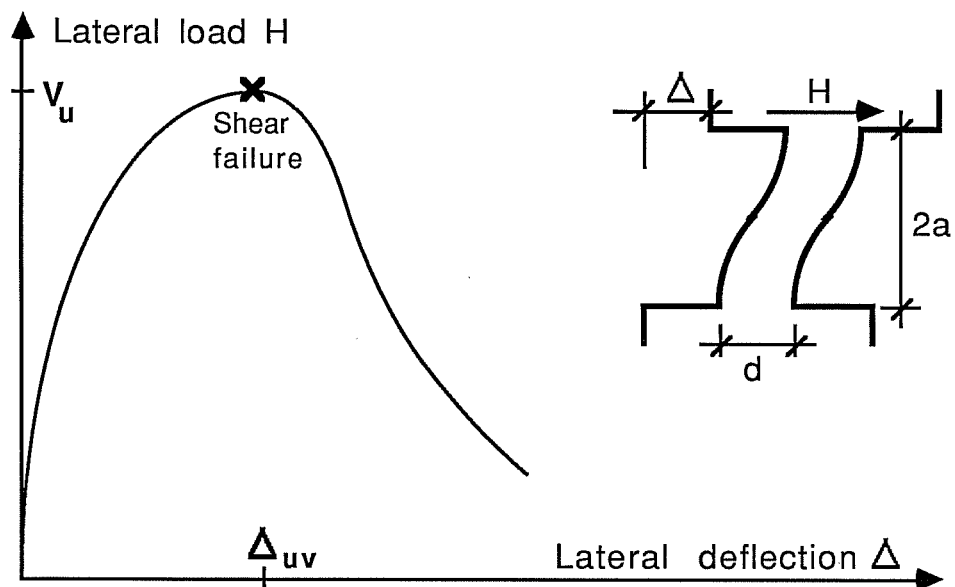


Fig. 3.6.1 Seismic damage to short columns, Japan

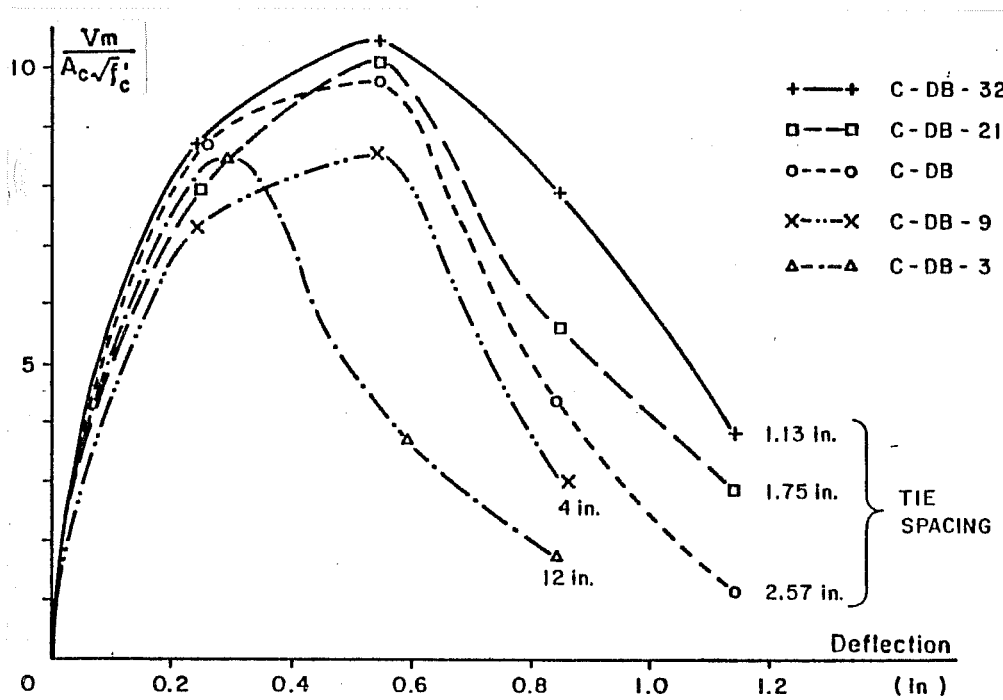
column is shown in Fig. 3.6.2a. The ultimate shear capacity  $V_u$  is reached at a relatively low deflection level  $\Delta_{uv}$ . The short column lateral capacity decreases with increased lateral deflection. Experimental curves from a test series of reinforced concrete short columns under cyclic lateral loading are presented in Fig. 3.6.2b [23]. The behavior of a short column under lateral loading depends on the span to depth ratio  $2a/d$ , the level of axial compression  $P$ , and the confinement ratio  $\beta$ . Short column behavior is generally limited to shear span-to-depth ratios less than 3 for typical reinforced concrete columns. At higher shear span-to-depth ratios, the failure is dominated by flexure rather than shear. The greater the amount of longitudinal reinforcement, the higher the critical shear span-to-depth ratio for short column behavior.

Umehara [24] studied axially loaded short columns under cyclic lateral loading. The axial compression  $P$  was varied from test to test but kept under the balance load  $P_b$ . He found that a compression load significantly increases the column strength, but also accelerated the strength degradation past ultimate. In other words, an axially loaded short column is stronger but more brittle. The influence of axial compression on the load deformation curve of a short column is presented qualitatively in Fig. 3.6.3.





a) Qualitative



b) Experimental [23]

Fig. 3.6.2. Load-deflection relationships for short columns

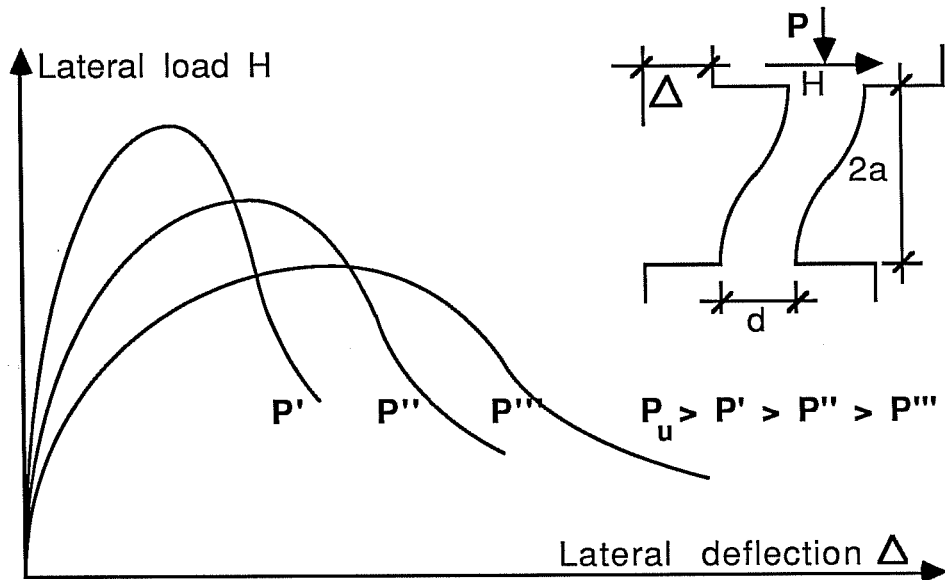
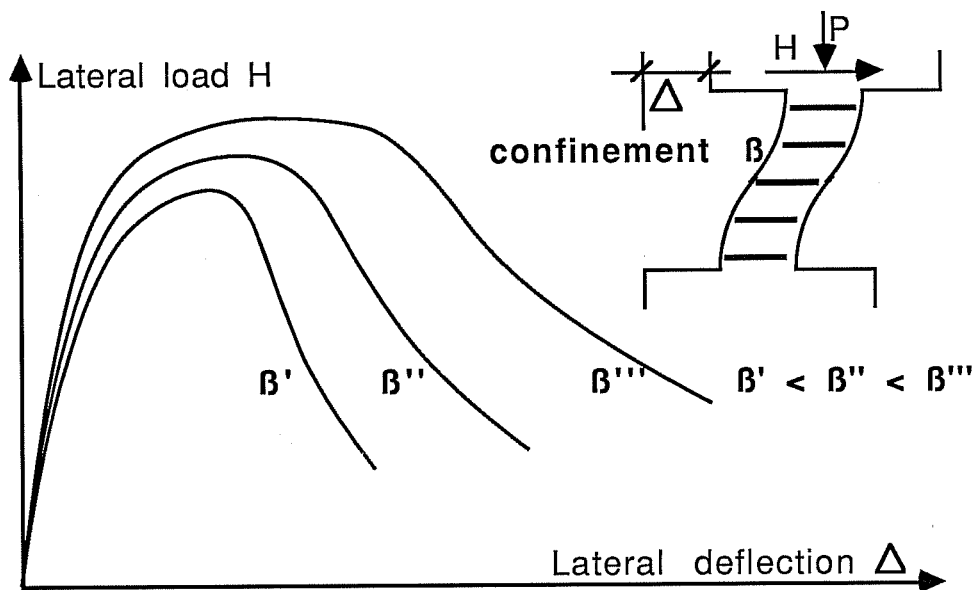
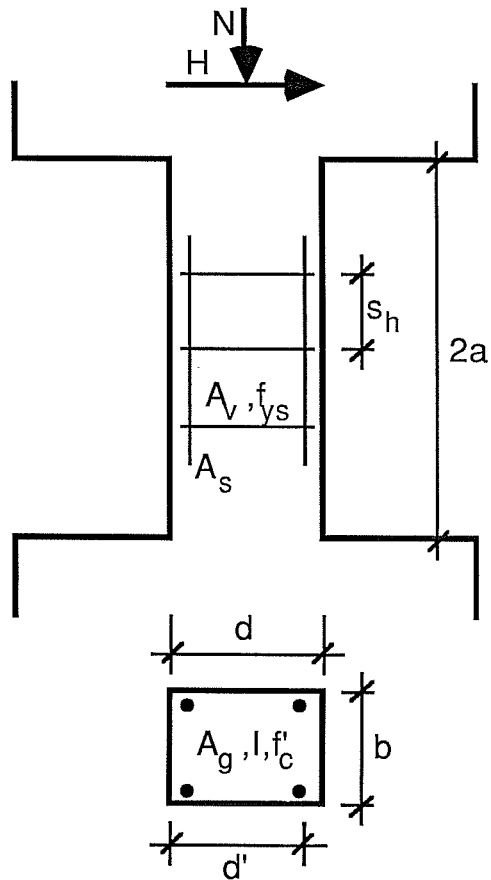
a) Influence of the axial compression  $P$ b) Influence of the confinement ratio  $B$ 

Fig. 3.6.3 Qualitative envelopes of a short column under cyclic lateral loading

A column without lateral reinforcement displays no ductility under lateral loading. Confinement increases the ability of the column to maintain strength in the inelastic range. But confinement reinforcement can only slow, not prevent degradation after the maximum strength has been reached. Confinement does not significantly increase column strength [24]. Fig. 3.6.3b shows qualitatively the influence of the confinement ratio  $\delta$  on the load deformation curve of an axially loaded column.

The shear strength of short columns is underestimated if calculated according to Chap. 11 of the ACI code [25]. The equation in Fig. 3.6.4 was developed for lateral strength of an axially loaded short column [24]. It is based on experimental data and applies for values of  $2a/d$  between 2.0 and 5.0, and for axial compression lower than the balance load. The first term of the equation represents the contribution of the compression strut which develops in the concrete. It is by far the largest contribution to the lateral capacity of columns with low shear span-to-depth ratios. The input of an axial load on the shear capacity is included through the second term. The third term represents the influence of column lateral reinforcement.

In addition to their brittle response, reinforced concrete short columns exhibit poor hysteretic behavior. Short columns dissipate little energy under cyclic loading, because the



$$V_u = (7.3 - 2.6 a/d' + 1.7 \sqrt{A_s/A_g}) b d' \sqrt{f'_c} + 2 N I / (a A_g h) + 0.61 A_v f_{ys} d' / s_h$$

Fig. 3.6.4 Short column with strength equation

hysteresis loops are characterized by severe pinching and rapid strength degradation from cycle to cycle.

3.6.2 Short Columns in a Braced Frame. In an unbraced frame, the columns have a double function: they carry the vertical loads (gravity) and the lateral loads (wind, earthquake). The frame relies on both the vertical and lateral carrying capacity of the columns, loss of either constitutes failure. If the short columns undergo a lateral deflection  $\Delta$  much above  $\Delta_{UV}$  in an earthquake, most of the lateral carrying capacity is lost (Fig. 3.6.2), and the frame fails. The level of vertical load-carrying capacity remaining in the columns at that point is irrelevant.

The situation is different in a braced frame. If detailed adequately, the bracing system can maintain the required lateral capacity up to a large interstory drift. In a reinforced concrete frame with short columns, the ultimate interstory drift,  $\delta_U^{bs}$  for the bracing system, is typically several times larger than drift  $\delta_{UV}^f$  for the frame. Interstory drift  $\delta_{UV}^f$  is the drift at which the short columns reach the ultimate lateral deflection  $\Delta_{UV}$  and fail in shear. The load-drift curve for a reinforced concrete frame with short columns and for the steel bracing system are shown qualitatively in Fig. 3.6.5. The curve for the

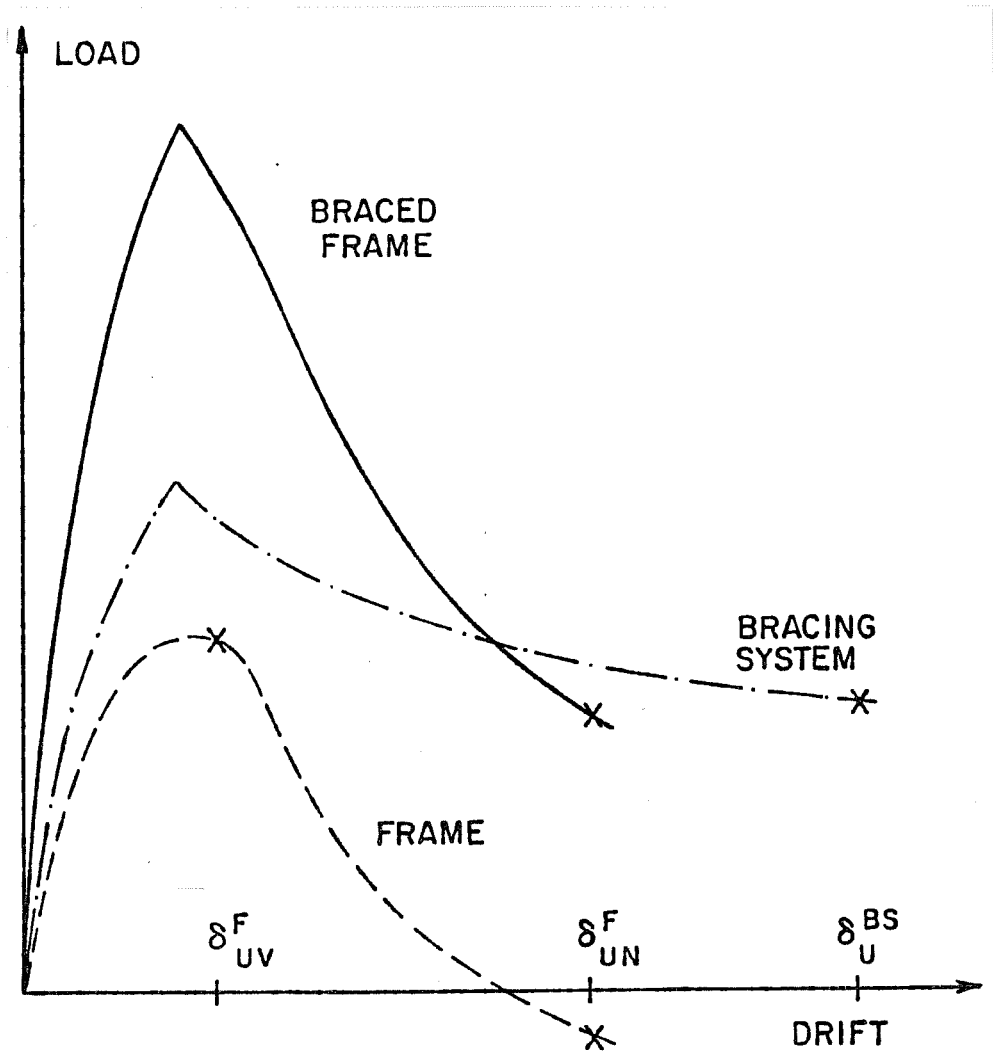


Fig. 3.6.5 Lateral load-drift relationship for a braced frame with short columns

composite system is obtained by superposition of the curves for its two components.

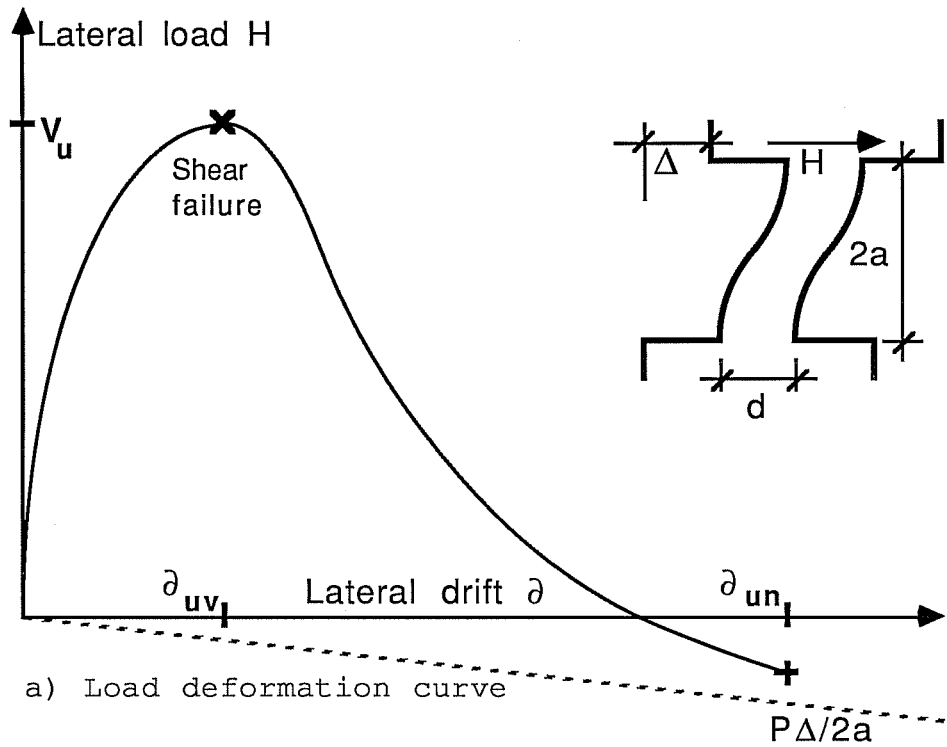
At an interstory drift much above  $\delta_{uv}^f$ , the frame has lost most of its lateral capacity. But the bracing system still provides large lateral resistance until reaching ultimate drift  $\delta_u^{bs}$ , which is large if the bracing system is detailed adequately. If the bracing system is designed to carry all the lateral load, the braced frame can be considered sound up to lateral drift  $\delta_u^{bs}$ . This means that a reinforced concrete frame retrofitted with a steel bracing system does not have to rely on columns for lateral resistance. But, the columns still have to carry the vertical loads. The lateral deformation capacity of the bracing system is useless if the vertical load-carrying system is lost. Assume that there is a lateral drift  $\delta_{un}^f$  at which the columns cannot carry their vertical load. The braced frame reaches ultimate when the bracing system fails laterally or when the columns fail axially, whichever comes first. The ultimate drift  $\delta_u^{bf}$  for the braced frame is the smaller of  $\delta_u^{bs}$  and  $\delta_{un}^f$ .

The determination of  $\delta_u^{bs}$  can be based on some experimental data on braces and bracing systems. The drift level for axial failure of the frame columns,  $\delta_{un}^f$ , is more difficult to determine. In a ductile frame, failure develops in the beams; the columns remain intact and  $\delta_{un}^f$  is generally large. In a frame with short columns the columns suffer substantial damage if the

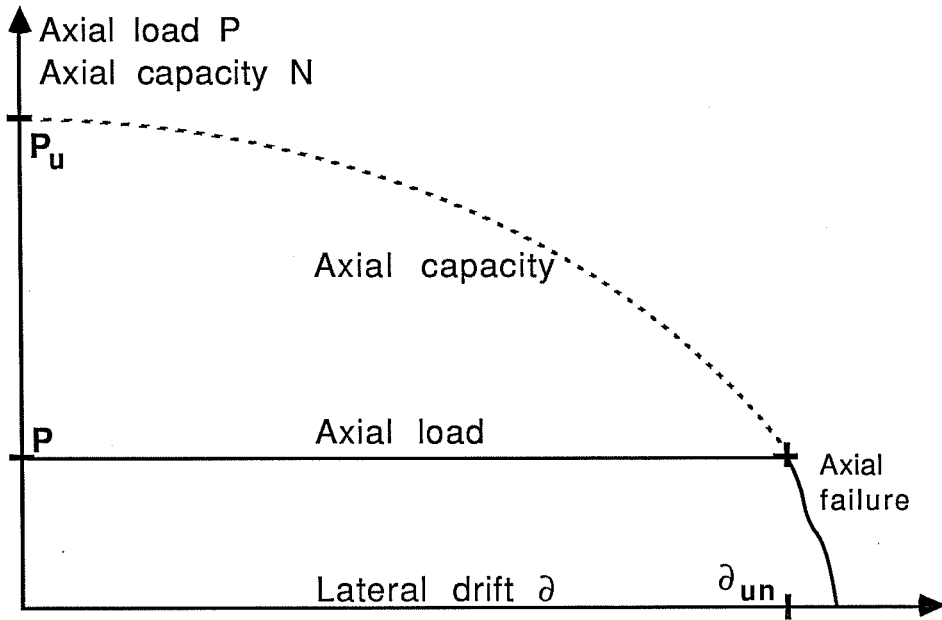
lateral drift is increased past  $\delta_{uv}^f$  (See Fig. 3.6.5). Determining  $\delta_{un}^f$  means evaluating how the axial load-carrying capacity of the short columns is affected by the damage. This problem has not been addressed experimentally. The reason is that, as was shown above, the question of how much axial capacity remains in a short column at drifts larger than the drift at shear failure only becomes relevant in the special case of a braced frame. Such a frame can survive the loss of the lateral capacity of the columns but not of their axial capacity. The problem of the axial failure of short columns submitted to lateral drift is discussed below. Due to the lack of pertinent experimental data, such a failure is academic and can only be studied qualitatively at that point. The discussion is nevertheless based partly on the observed behavior of axially loaded short columns tested under cyclic loading [23, 24].

3.6.3 Axial Capacity of a Short Column Deflected Laterally. Consider a short column with a compression load  $P$  submitted to lateral loading (See Fig. 3.6.6). At a drift  $\delta_{un}$ , the column fails in shear. If the lateral drift is increased further, the column shear mechanism deteriorates and the column suffers increasing damage. The damage results in a reduction of the available section for axial load. Axial failure occurs if a drift is reached at which the axial capacity  $N$  becomes less than





a) Load deformation curve



b) Deterioration of the axial capacity

Fig. 3.6.6 Axial failure of a short column deformed laterally

the axial load  $P$ . The drift at which an axially loaded short column is unable to carry the axial load is denoted as  $\delta_{un}$ . Figure 3.6.6b illustrates the concept. The dashed line represents the axial capacity  $N(\delta)$  of the column. With increasing drift beyond  $\delta_{uv}$ , i.e. with increasing column shear damage, the axial capacity  $N(\delta)$  decreases. It is assumed to be an accelerating process. At  $\delta = \delta_{un}$  the axial capacity  $N(\delta)$  is equal to the column compressive load  $P$ , and additional lateral drift leads to axial failure.

In a typical short column situation,  $\delta_{un}$  is several times larger than  $\delta_{uv}$ . It is difficult to give a quantitative assessment of  $\delta_{un}$ . Tests on axially loaded short columns submitted to lateral drift have focused on the shear strength and were stopped when the lateral capacity deteriorated to a given level. No quantitative data on the remaining axial capacity at that drift level is available. In Umehara's test, the axial load was 15-20% of the ultimate load  $N_u$  and the maximum imposed lateral deflection was above 3% of the column free height. None of the axially loaded columns showed any sign of failing axially. This indicates that  $\delta_{un}$  is indeed several times larger than  $\delta_{uv}$  for a typical short column.

The following qualitative comments can be made about  $\delta_{un}$ . It is expected that  $\delta_{un}$  is a function of the axial compression. The higher the axial load, the smaller the drift

$\delta_{un}$  for axial failure. First, because the level of damage leading to axial failure is less. Second, because a short column with large compression is more brittle, i.e. degrades more rapidly beyond  $\delta_{uv}$  (See Fig. 3.6.3). A short column loaded with  $P_u$  equal to its maximum axial capacity fails at a lateral drift  $\delta$  of zero. The other limit is for a column with no axial load. For  $P = 0$ ,  $\delta_{un}$  theoretically tends to infinity. The column can undergo a large lateral drift without failing axially. In Fig. 3.6.7, the two limits are shown in the  $P$ - $\delta_{un}$  plane and a curve  $\delta_{un}(P)$  is fitted between the points. The curve is speculative but provides an indication of the relation between drift  $\delta_{un}$  and axial compression  $P$ .

In Fig. 3.6.8, the influence of the confinement ratio  $\beta$  on the  $\delta_{un}(P)$  curve for a reinforced concrete short column is presented. It is expected that a high confinement ratio reduces the rate of damage associated with the lateral loading of the short column (See Fig. 3.6.3b). Therefore, the higher the confinement, the higher the drift  $\delta_{un}$  at which the damage to the column becomes critical for the axial capacity.

Experimental tests are necessary if a better understanding of the axial failure of reinforced concrete short columns deflected laterally is to be attained. An important experimental effort would be necessary to obtain quantitative

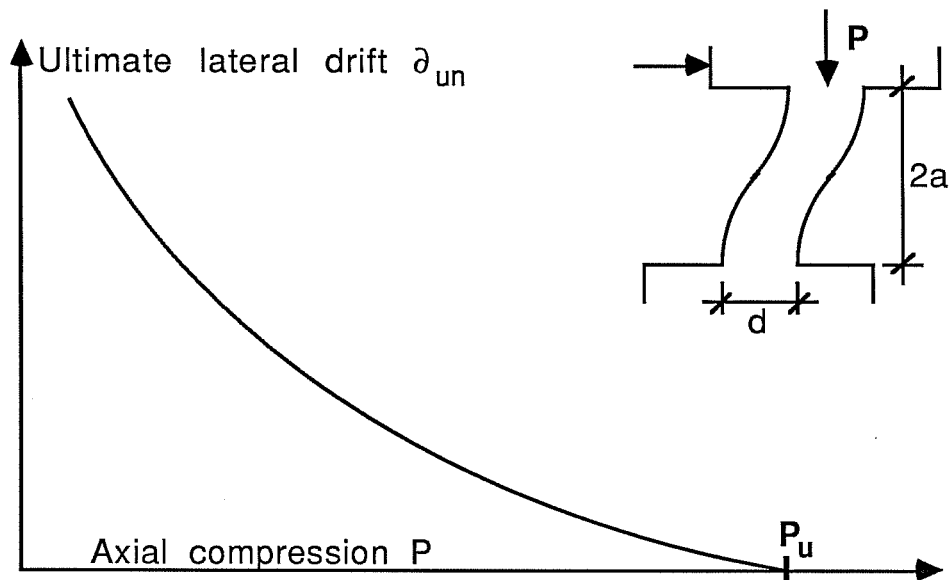


Fig. 3.6.7 Qualitative influence of axial compression on ultimate lateral drift

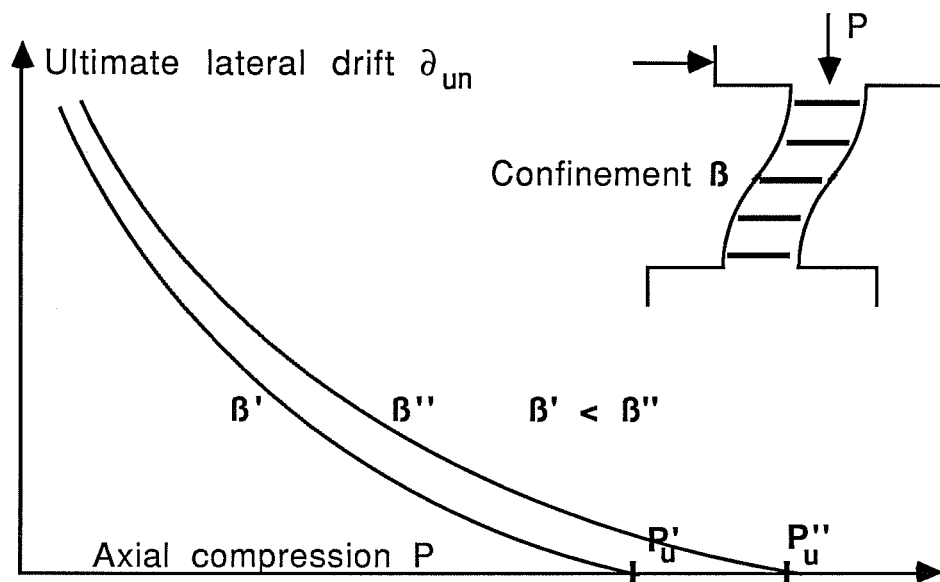


Fig. 3.6.8 Qualitative influence of axial compression and confinement on ultimate lateral drift

data for the  $\delta_{un}(P)$  curves. They would have to be determined point by point, each point requiring a column with a given axial load  $P$  and confinement ratio  $\beta$  to be deflected laterally until axial failure. A sophisticated load control mechanism would be needed to maintain the desired axial load on the column at all lateral drift levels. Further investigation could include the effect of cycling the lateral loading and even the axial compression to reproduce seismic loading characteristics. A quantitative assessment of the  $\delta_{un}(P)$  curves would help make possible the determination of the maximum allowable lateral drift for a steel braced reinforced concrete frame with short columns.

## CHAPTER 4

### DUPLICATION OF THE EXPERIMENTAL DATA

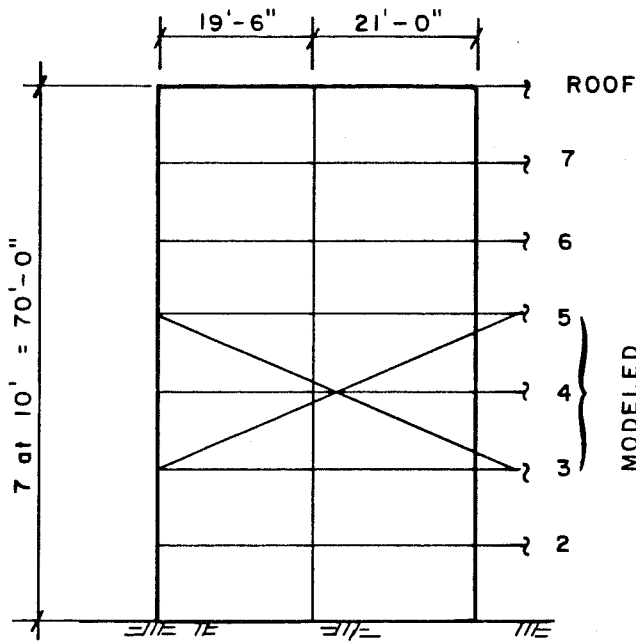
#### 4.1 Experimental Part of the Research Project

4.1.1 Introduction. This conceptual and analytical study, complements an experimental study in which a reinforced concrete frame model was retrofitted, first with reinforced concrete wing walls and then with a steel bracing system and subjected to static cyclic lateral loading. The tests are described briefly below and in detail in [26, 27, 28, 29]. The data from the test of the steel braced frame is used in Section 4.3 to calibrate the analytical model used in Chapters 6 and 7.

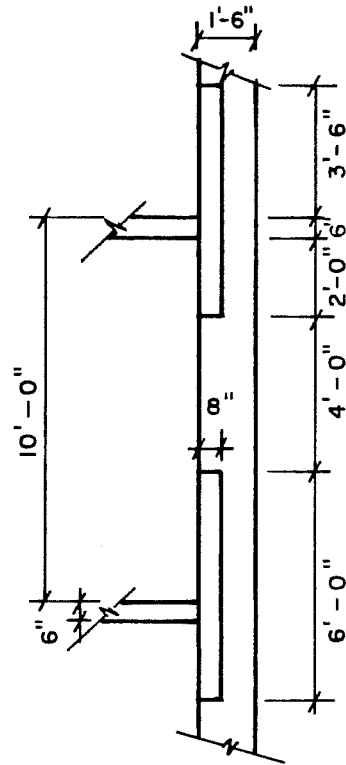
4.1.2 Model Frame. The reinforced concrete frame used in the evaluation of the retrofiting techniques was modeled after a prototype building. The prototype was chosen because it is a typical structure in need of seismic retrofitting. It is representative of a class of reinforced concrete buildings constructed commonly in California in the 1950's and 1960's. The perimeter frames were the primary lateral resisting system of the structure in the longitudinal direction, as can be seen on the example building shown in Fig. 4.1.1. The plan and elevation of the prototype building are shown in Fig. 4.1.2. Those frames were characterized by deep spandrel beams and short columns. The specified concrete compressive strength was 3000 psi. The



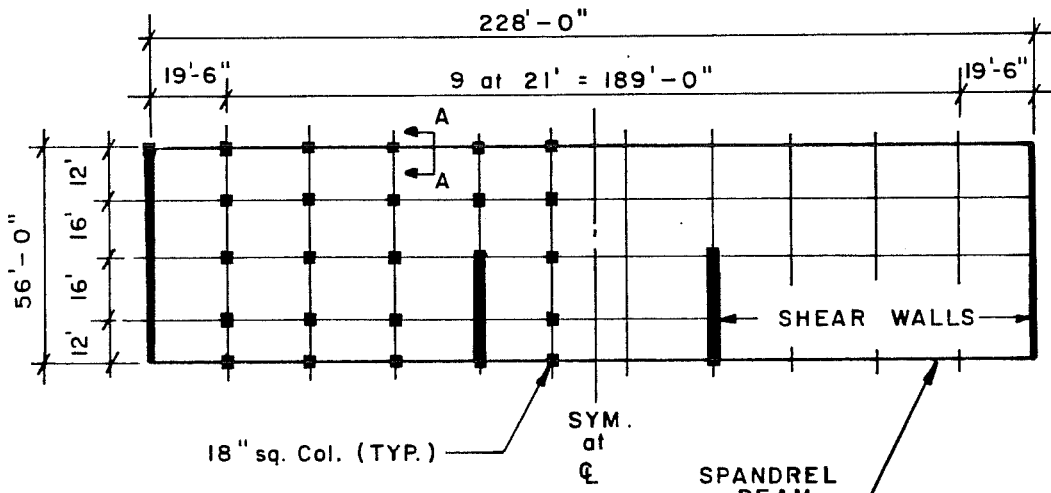
Fig. 4.1.1 Example building



ELEVATION



SECTION A-A



PLAN

prototype building, plan and elevation [29]



specified yield strengths of the reinforcement was 60 ksi for longitudinal column bars and 40 ksi for all other bars. The reinforcement of the prototype frame is shown in Fig. 4.1.3a. The columns transverse reinforcement was very low (#3 @ 18").

The prototype building is seismically inadequate for two reasons. First, the lateral strength is inadequate because seismic design loads have more than doubled since the building was originally designed. Second, the lateral failure mechanism of the perimeter frames is deficient, because the columns are the weak link of the structure. The energy dissipation capacity in a weak column strong beam frame is usually small. The expected energy dissipation capacity of the prototype frames is particularly small because the weak columns are short columns which exhibit a brittle, shear dominated, failure (See Sec. 3.6).

The prototype building, deficient both in strength and ductility, is a prime candidate for retrofitting. Structure 3 of Fig. 2.4.2 is representative of its structural inadequacy and its retrofitting needs. In order to test the two retrofitting schemes, a model of a portion of the prototype building was constructed. It was a 2/3 scale model of the third and fourth levels of the prototype perimeter frames. The geometry and reinforcement detailing of the frame model are shown in Figs. 4.1.3b and 4.1.4. The boundary conditions were chosen to

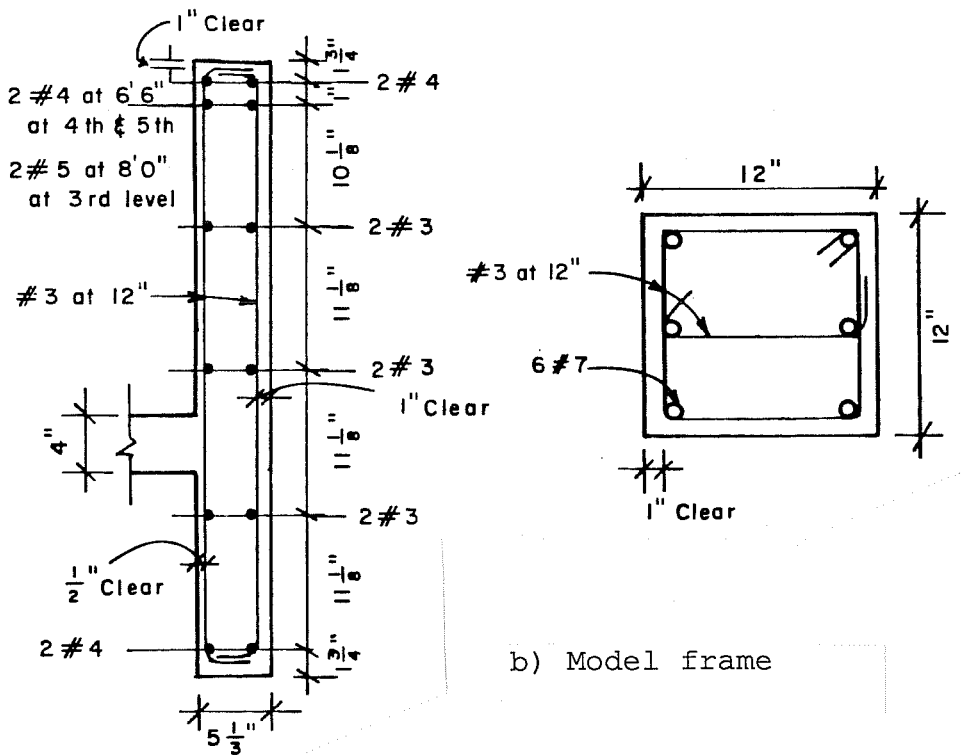
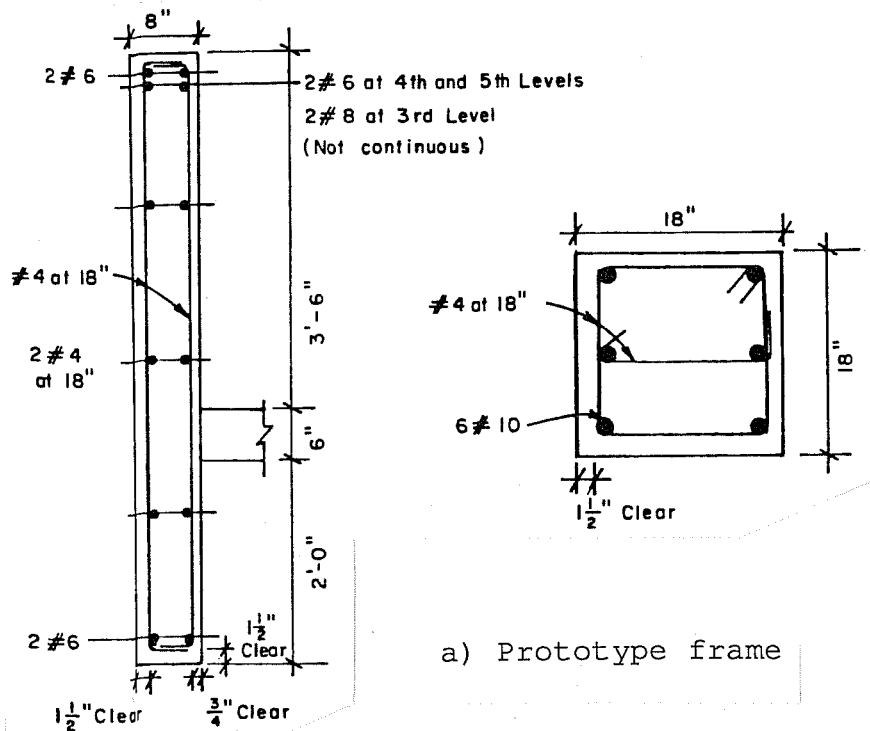


Fig. 4.1.3 Detailing of spandrel beam and column

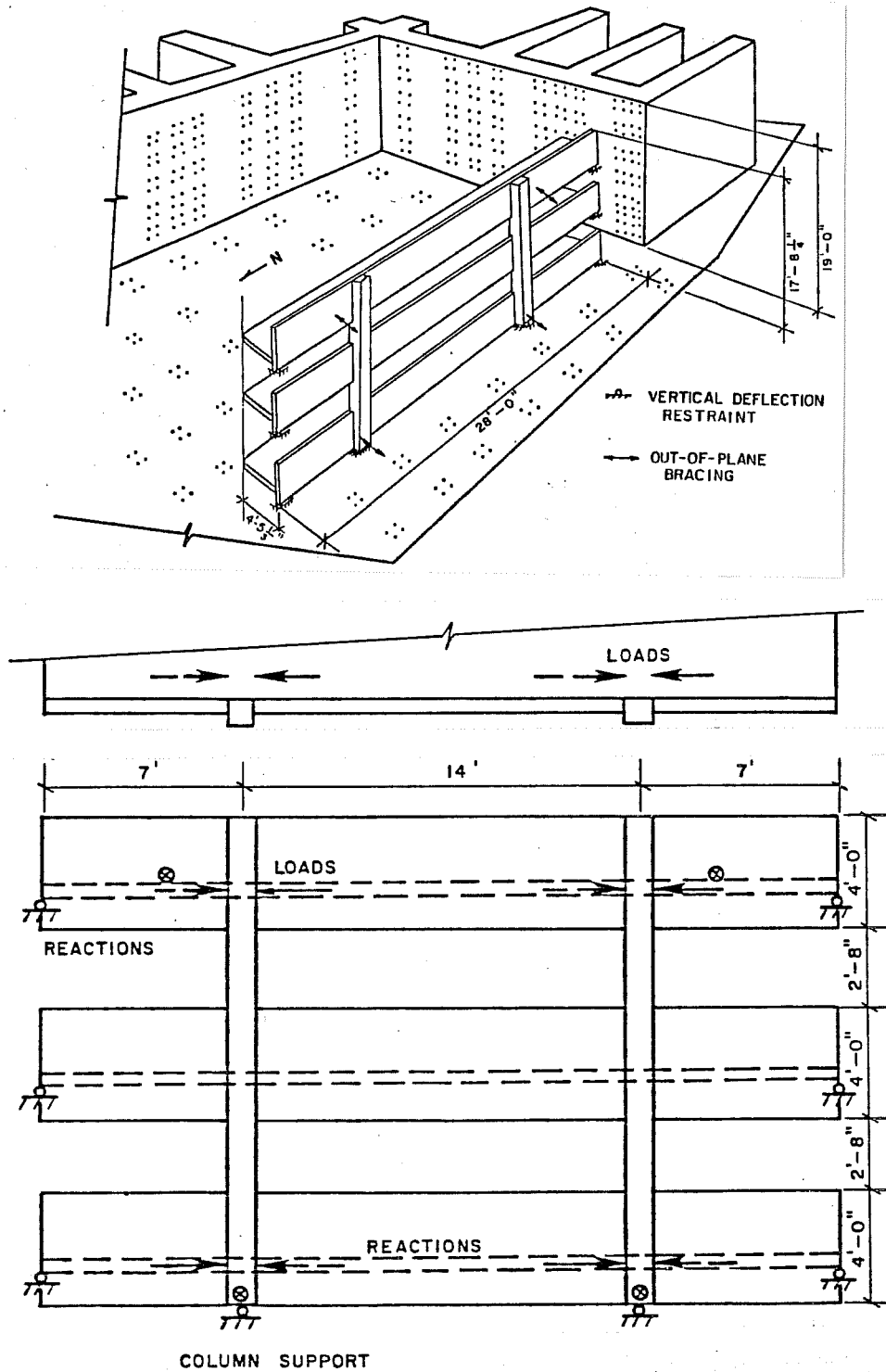


Fig. 4.1.4 Frame model, boundary conditions and test set up [29]

reproduce the situation in the original structure under lateral loading. Before the first retrofitting operation, the bare frame was loaded to obtain the initial stiffness. The loading was kept at a low level to avoid damaging the columns.

#### 4.1.3 Retrofitting with Reinforced Concrete Wing Walls.

First, the bare frame was retrofitted with the wing wall scheme [27]. Cast in-situ reinforced concrete was attached to the columns and spandrel beams with epoxy grouted dowels. A strong pier was created which proved to behave monolithically, i.e. the wing walls and original columns deformed as a unit. The retrofitted frame was subjected to static lateral loading. Cyclic loading was applied to simulate seismic loading. The wing wall retrofitting scheme substantially increased the expected strength and the initial stiffness of the bare frame. Failure was transferred from the columns to the spandrel. The retrofitting scheme thus successfully transformed a weak-column strong beam frame into a strong column-weak beam frame. The optimum wing wall size could not be determined from the test, but it appears that significantly smaller wing walls would have achieved the same purpose. The retrofitted frame exhibited good ductility even though high shear was present in the spandrel.

Since a second retrofitting scheme was to be tested using the same frame, damage to the frame had to be limited. The

frame was, therefore, not loaded far into the inelastic range. This was not a substantial drawback because the desired information was collected before the test had to be stopped.

#### 4.1.4 Retrofitting with a Steel Bracing System.

Following the testing of the wing wall scheme, the wing walls were cut out and the frame was restored to its "bare frame state" for the testing of the bracing scheme [28]. The braced frame is shown in Fig. 4.1.5. The braces were modified wide-flange sections (Grade 36) with an effective slenderness ratio around 80. Collectors transferring lateral load from the frame to the bracing system were structural tees and steel channels, which were attached to the columns. All the connections between steel members were field welded to allow for adjustments. Epoxy grouted dowels were used to connect the steel members to the concrete frame.

The braced frame was submitted to static cyclic lateral loading to failure. The loading history consisted of four series of three cycles to a specified peak lateral drift (0.10%, 0.17%, 0.23%, and 0.36%) followed by three cycles at increasing peak drifts. The drift levels were measured between the first and third levels, and represent, therefore, the average drift of the first and second story.

Cracking of the columns appeared at 0.10% drift, but was not significant until 0.40% drift. The compression brace of the

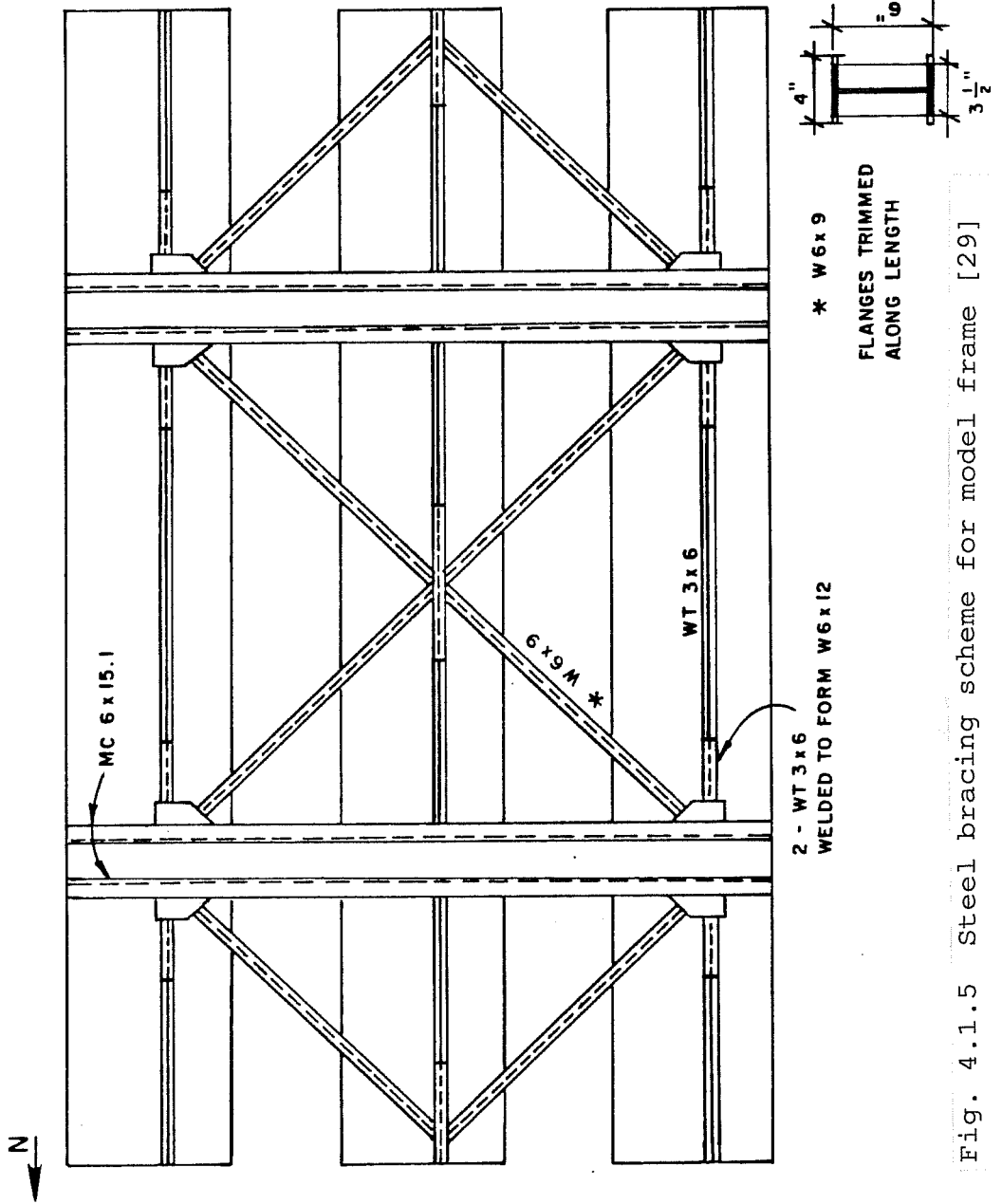


Fig. 4.1.1.5 Steel bracing scheme for model frame [29]

interior bay of the second story started buckling at about 0.50% drift in the north direction. All further inelastic behavior in subsequent cycles was concentrated in the second story. The four braces of the second story experienced buckling and yielding reversals. Meanwhile, cracking and stiffness deterioration of the columns was important, but the strength was maintained due to the vertical steel channels. The spandrels showed very little cracking. The ultimate load was reached in the north direction when the connection weld of a tension brace failed suddenly. The loss of the diagonal steel member resulted in a load redistribution in which the second story columns were overloaded and failed in shear. Figures 4.1.6 and 4.1.7 show the braced frame after the test; the buckling of the braces of the second story can be seen.

The hysteretic load-drift relationship for the steel braced frame is shown in Fig. 4.1.8. Although cycling the load reduced the stiffness, a new peak load was reached with every new peak displacement until failure. The strength of the braced frame was about six times the expected strength of the frame. A maximum effective interstory drift of over 1% was reached before failure. The connections of the bracing system proved to be the weak link of the scheme. High local deformations were generated at the connections when the braces alternately buckled in

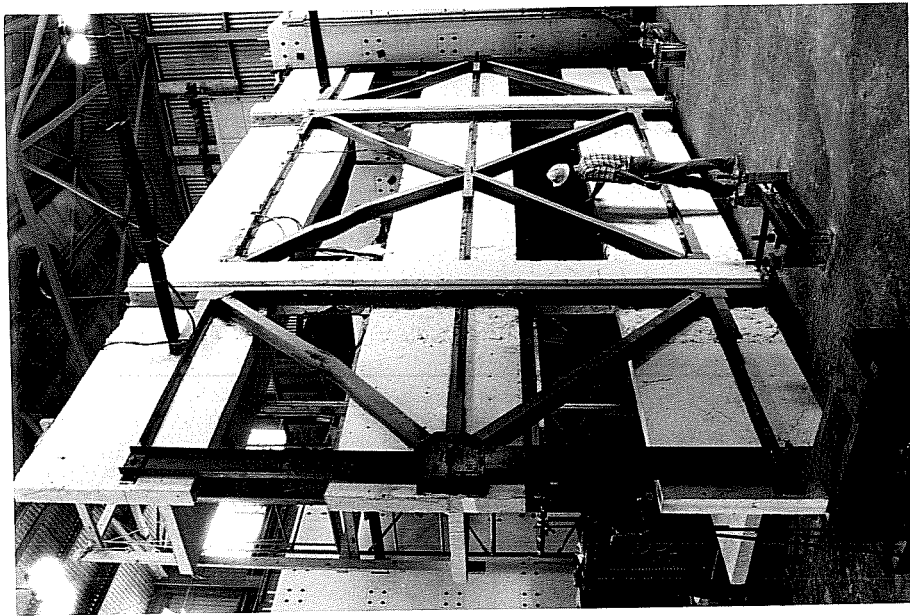


Fig. 4.1.6 Braced frame after test



b) Shear failure of composite column



a) Buckling of brace



Fig. 4.1.7 Damage to the braced frame

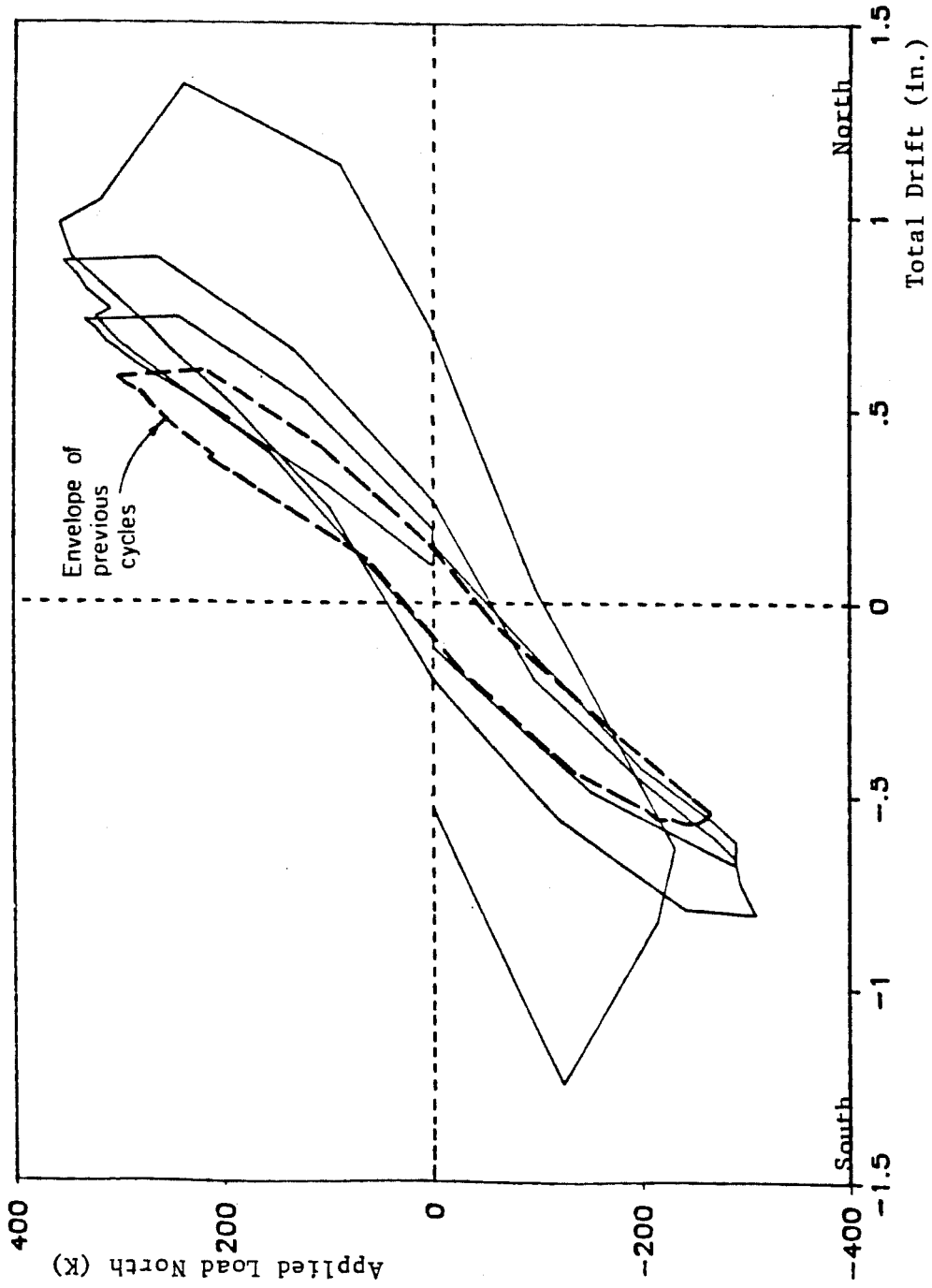


Fig. 4.1.1.8 Experimental load-drift relationship for the braced frame model [29]

compression and yielded in tension. The quality of the connection detailing and welding determined the strength and, particularly, the ductility of the steel braced frame.

Due to the configuration of the columns in the frame, the diagonal members of the bracing scheme were not continuous from one bay to another (See Fig. 4.1.5). Steel channels were attached to the columns to introduce the vertical component of the truss forces in the column. This created composite columns with an unusual cross section (see Fig. 4.1.9). The first story braces were removed to test the strength of the undamaged composite columns. The columns were submitted to monotonic static lateral loading up to 3.8% interstory drift. The plot of Fig. 4.1.9 shows that the channels substantially improved the column behavior. The lateral capacity of the column was increased by an estimated 50% and enough confinement was provided to transform the brittle short column into a relatively ductile column. Attaching channels to the columns could in some cases constitute a retrofitting scheme by itself [29].

#### 4.2 The Computer Program

This section describes the computer program used in the analytical study carried out in Chapters 6 and 7. The program had to reproduce closely the inelastic behavior of a steel braced reinforced concrete frame under cyclic lateral loading, and

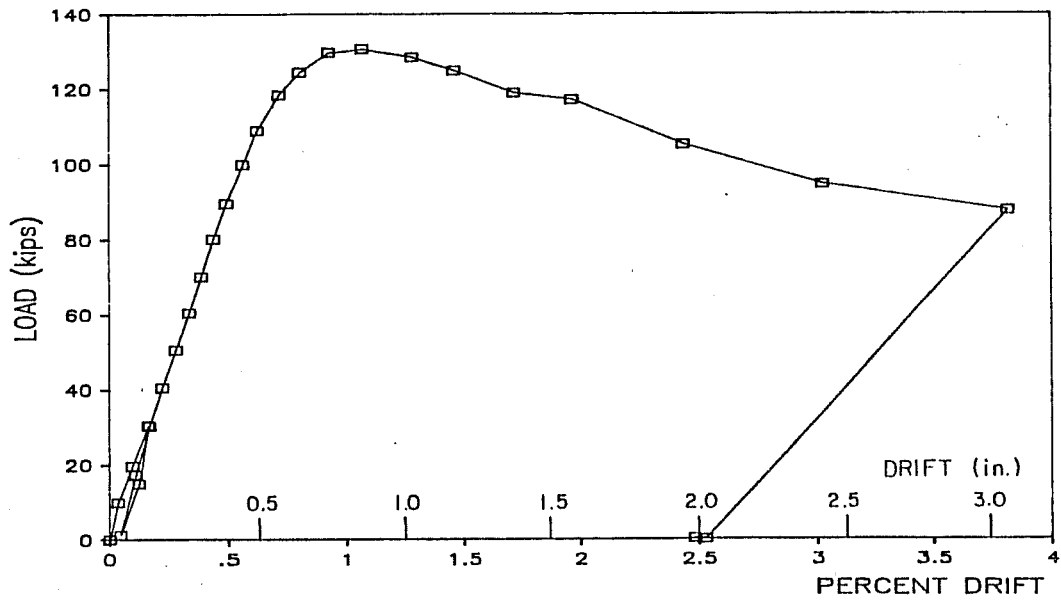
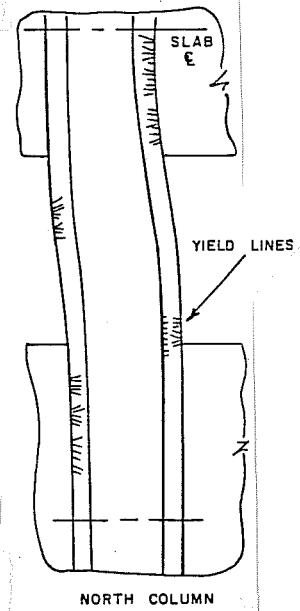
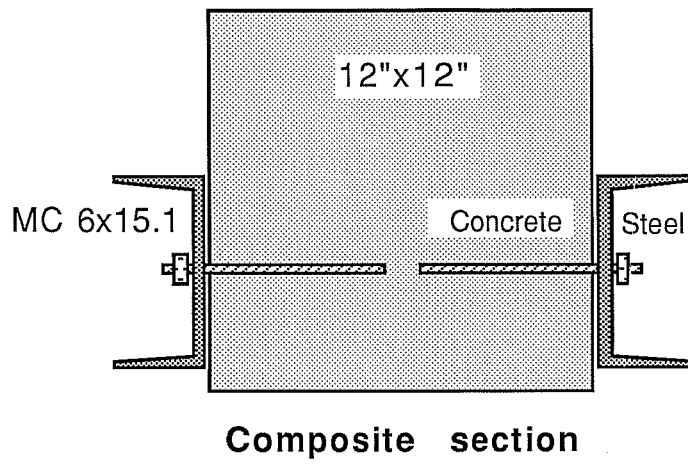


Fig. 4.1.9 Composite column

therefore had to include analytical models featuring nonlinear hysteresis rules for reinforced concrete frame members and steel braces.

A variety of analytical models have been developed for the nonlinear seismic analysis of structures [30]. A finite element approach can be used. However, a large number of degree of freedom is necessary to model a steel braced reinforced concrete frame with finite elements. The required computation effort, to obtain useful results is very large, especially if the hysteretic behavior is to be reproduced. The finite element approach is thus not well-suited for the purpose of this study.

Another approach is to use phenomenological models for the columns, beams, and braces. Phenomenological models are based on simplified hysteretic rules that mimic observed behavior. The models consist of a single line element with a limited number of degrees of freedom. The computational problem is thus reduced to a tractable size. Currently phenomenological modeling provides the best approach to the nonlinear hysteretic analysis of braced structures. The modeling approach makes use of the available experimental data. Experimental work is often conducted on a component basis, thus producing data which can be used readily in phenomenological models. The nonlinear hysteretic behavior of the columns and beams of reinforced concrete frames has been widely investigated experimentally.

Significant experimental data on the nonlinear hysteretic behavior of braces is available also (See Sec. 1.4.2). The phenomenological modeling approach was adopted for this study.

Rather than developing a new computer program, an existing program for nonlinear seismic analysis of structures was selected and extended for the particular need of this study. Among the several research computer programs available, DRAIN-2D [31] was selected as base code. DRAIN-2D is a general purpose computer program for the inelastic response of plane structures subjected to earthquake loading. It was developed by Kannan and Powell at the University of California at Berkley. It consists of a series of base routines carrying out step-by-step analysis and of subroutines modeling various structural elements. The program is organized for easy addition of subroutines for new element models.

DRAIN-2D was developed for dynamic analysis and had to be modified to also perform static analysis. This involved implementing the option to impose a desired load or displacement vector increment at each step of the analysis. Any desired static loading history can thus be specified. The inertial forces were canceled by setting all masses to zero.

DRAIN-2D was chosen over other programs for seismic analysis of structures because of its library of available

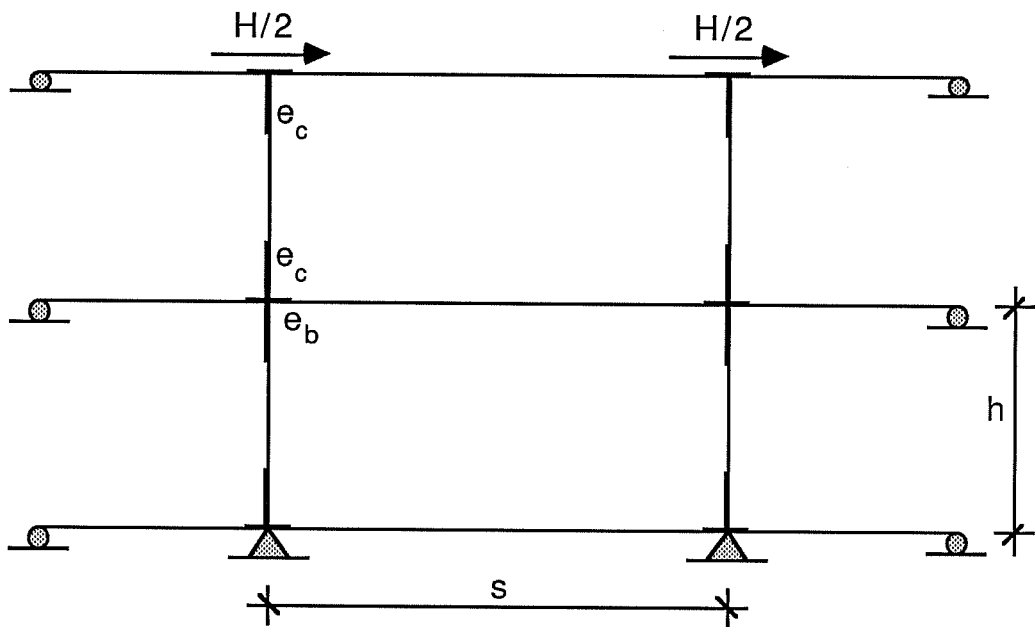
element models and the possibility of adding further element models. The two element models used for the columns and beams of the reinforced concrete frame (Element EL 7) and for the steel brace (Element EL 10) are described in Appendix A. The program is a research tool, and may not be efficient for most design tasks.

### 4.3 Duplication of the Experimental Data

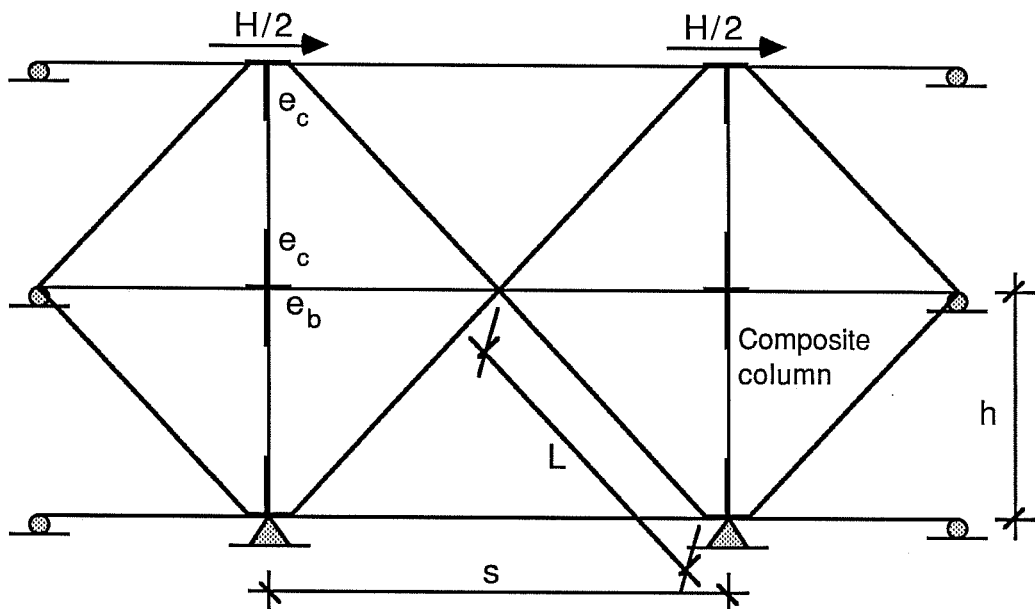
4.3.1 Bare Frame. The experimental tests described in Section 4.1 provided experimental data which was used to evaluate and calibrate the computer program.

First the load-deformation curve obtained on the bare frame was duplicated analytically. Figure 4.3.1a shows the analytical model established to reproduce the experimental initial stiffness of the bare frame. The geometrical and structural properties of the bare frame are given in Figs. 4.1.3 and 4.1.4. The beams and columns were modeled with element model EL 7 (See Sec. A.1). The following was assumed:

- The uncracked stiffness of the spandrel beams and columns was used. One-third of the slab was considered participating with the spandrel beam.
- The concrete modulus of elasticity was  $E_c = 3600$  psi, with  $f'_c = 4000$  psi.
- A rigid zone of length  $e_c$  was introduced in the



a) Bare frame



b) Braced frame

Fig. 4.3.1 Analytical models



column (Fig. 4.3.1) to account for the high stiffness of the beam-column joint. The effect of the beam rigid length  $e_b$  was neglected ( $e_b = 0$ ).

- The shear deformations were considered.
- The supports were considered infinitely stiff.

The column rigid zone length,  $e_c$ , is the single most important parameter and cannot be determined with accuracy. The difficulty stems from the particular geometry of the beam-column joints of the frame. The out-of-plane width of the columns is twice that of the beams, and the column and beam axes are offset (See Fig. 4.1.4). As was observed during testing, the columns experienced some curvature within the depth of the spandrel beams when the frame was subjected to lateral loading. This means that  $e_c$  is less than half the spandrel depth (i.e.  $e_c < 24"$ ). The experimental data were used to obtain an approximate value of  $e_c$ .

The initial stiffness values for different values of  $e_c$  are compared with the experimental data in Fig. 4.3.2. The frame stiffness is very sensitive to small variations of  $e_c$ . Two factors combine to cause this sensitivity. First, the stiffness of the column varies with the square of the free column height ( $h-2e_c$ ) which is very sensitive to a variation of  $e_c$ . Second, the spandrel beams are so stiff that most of the frame flexibility lies in the columns.

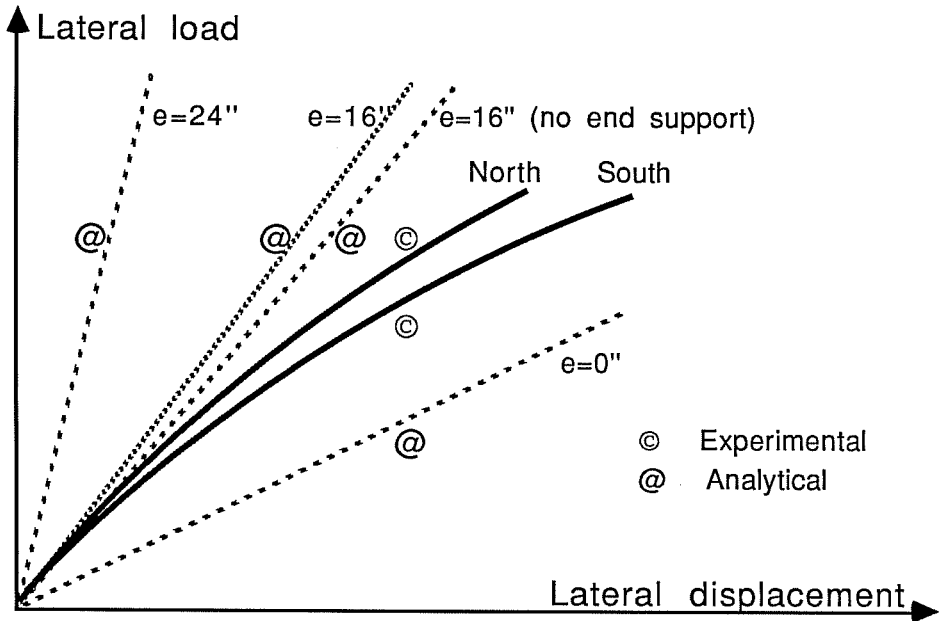


Fig. 4.3.2 Comparison of initial stiffness

A value of  $e_c$  around 16" gives the best agreement between analytical and experimental results. This value seems appropriate in light of the observed joint behavior at later stages where the frame was loaded into the inelastic range. With  $e_c = 16"$ , the beams contribute only one-fifth of the frame flexibility. In terms of stiffness the frame approaches the case of a frame with infinitely stiff beams. As a result of the seating and fitting tolerances in the support mechanism, the spandrels of the exterior bays may have had no support in the early stages of loading. A computer run established that such a loss of support results in a relatively small decrease in frame initial stiffness (about 15% increase, See Fig. 4.3.2).

4.3.2 Braced Frame. The next step is the duplication of the test results for the braced frame to evaluate the ability of the computer program to predict the strength and hysteretic load-deformation curve of a steel braced reinforced concrete frame.

The geometrical and structural properties of the bracing scheme are given in Fig. 4.1.5. The calibrated analytical model for the bare frame was extended to model the braced frame (see Fig. 4.3.1b). The column rigid zone,  $e_c$ , was kept at 16". The beam rigid zone,  $e_b$ , proved to have little influence in this case also and was set to zero. The specified load deformation curve for the composite columns was based on the experimental curve of

Fig. 4.1.9. The braces were modeled with element model EL10 (See Sec. A.2). The brace yield load was calculated using the yield stress obtained from coupon tests ( $f_y = 44.5$  ksi,  $P_{yp} = 109K$ ). The buckling load was set as the average of the maximum brace compression measured during the test ( $P_{yn} = 88K$ ). The effective slenderness ratio was evaluated at  $Kl/r < 80$  with  $K = 0.50$ .

The model was subjected to monotonic and cyclic loading. The specified cyclic loading history consisted of five cycles with increasing peak loads. The loading reproduces the character of the experimental loading history.

The computed load deformation curves for monotonic and cyclic loading are shown in Fig. 4.3.3. The predicted strength is 13% lower for the cyclic loading case. The analytical and experimental envelopes of the cyclic response are plotted together in Fig. 4.3.4. The two envelopes compare very favorably until failure of the bracing system. The predicted strength is within two percent of the observed strength in the north direction. There are two reasons for this favorable comparison. First, the specified strength for the members of the analytical model were largely drawn from the experimental test. A good correspondence between analytical and experimental results was therefore expected. Second, the computer program correctly reproduced the reduction in strength and stiffness associated

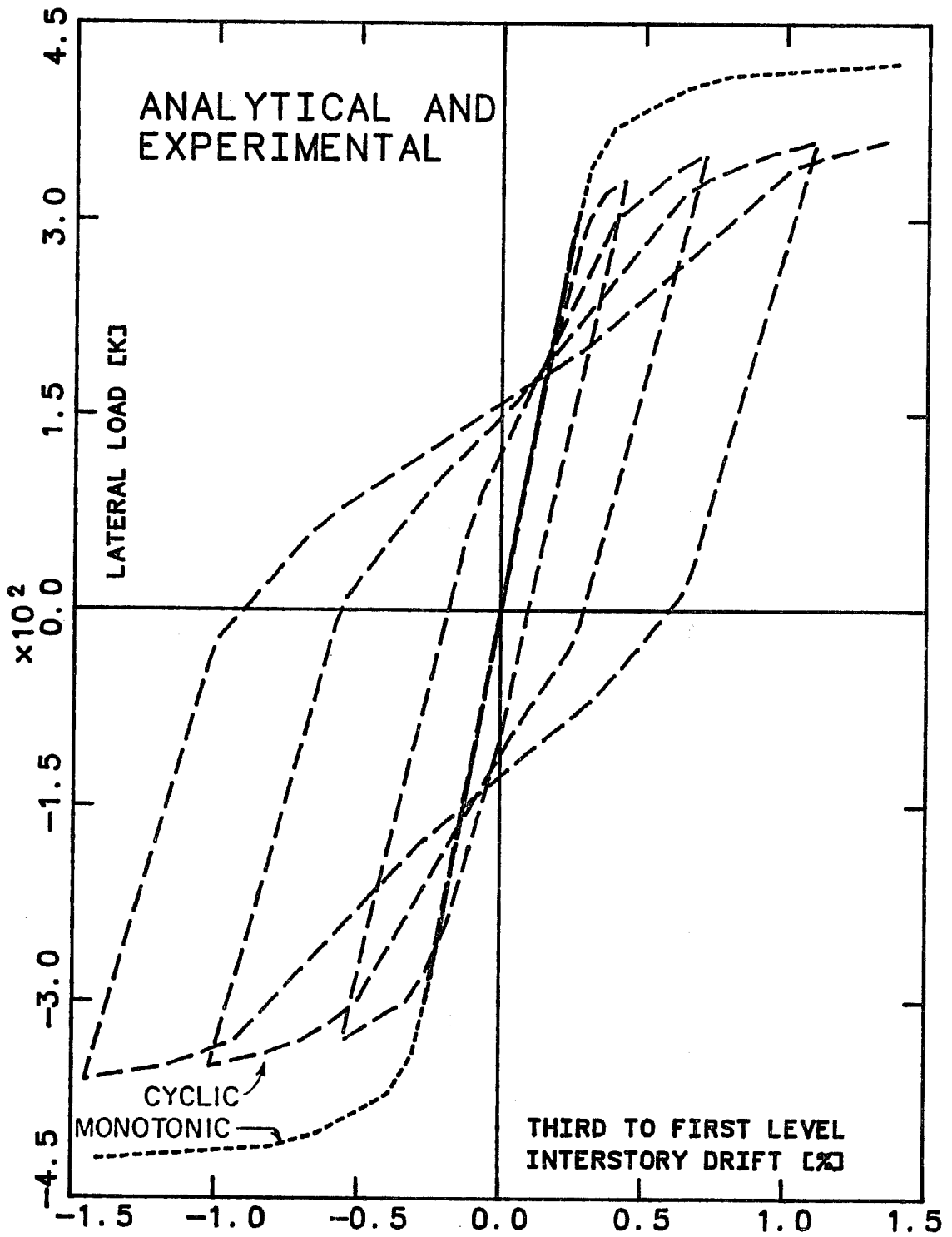


Fig. 4.3.3 Analytical load-drift relationship for the braced frame

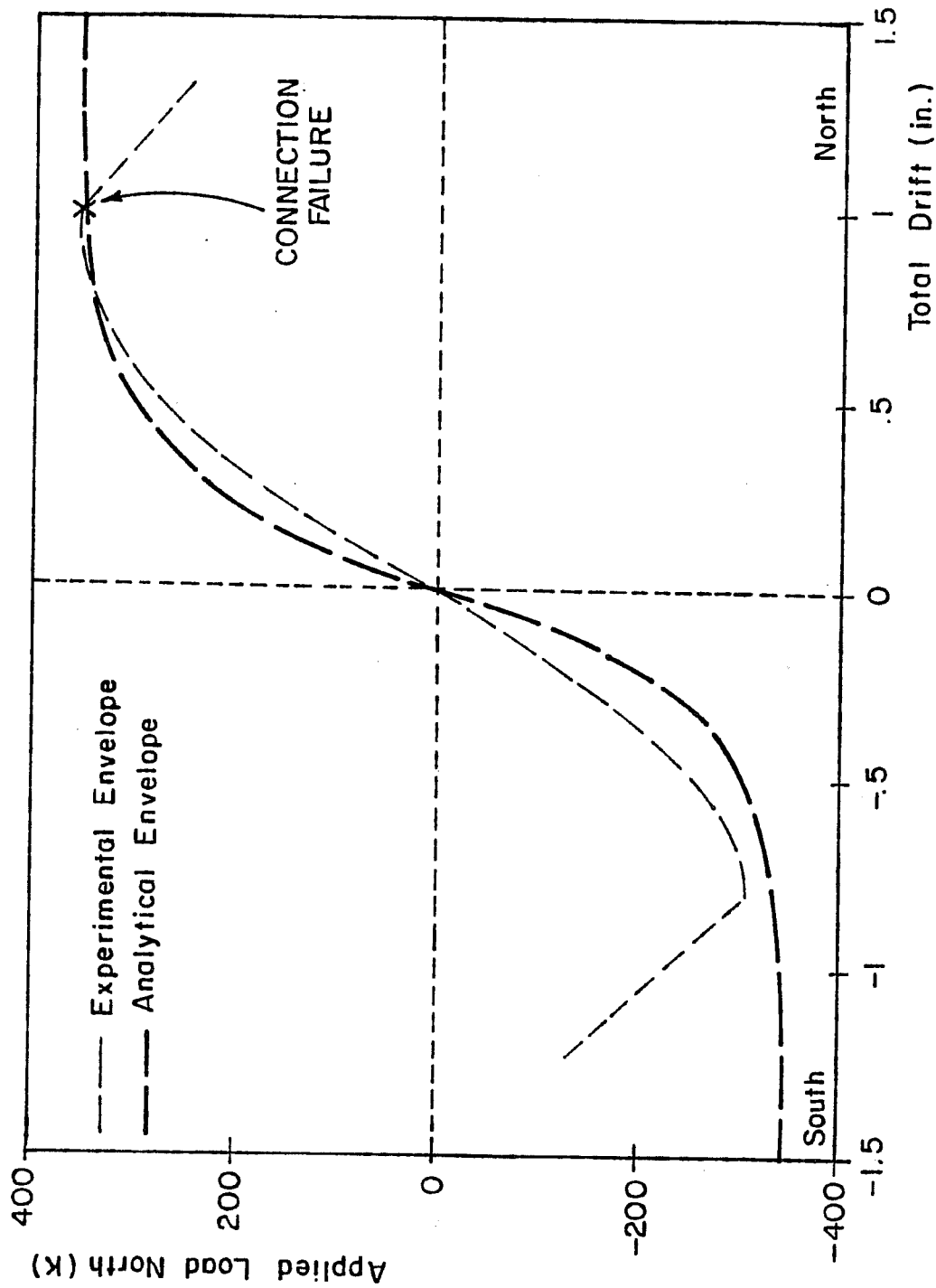


Fig. 4.3.4 Experimental and analytical load-drift envelopes

with cyclic loading. The monotonic curve (Fig. 4.3.3) overestimates the strength of the frame under cyclic loading by about 15%. Part of the discrepancy between the analytical and experimental curves of Fig. 4.3.4 is due to the fact that the onset of inelastic behavior (cracking, buckling and yielding) which is gradual in reality, is modeled as one event in the analysis. This explains why the loss of stiffness begins at a higher drift level in the analytical curve than in the experimental one.

The correct estimation of the loss of strength and stiffness associated with cyclic loading is important. It confirms the adequacy of the computer program for the study of the inelastic cyclic behavior of a steel braced reinforced concrete frame. A further confirmation is that the predicted failure sequence corresponds to the observed one. First column cracking occurred, followed by buckling of the compression member and finally yielding of the tension brace. The spandrels remained elastic.

In the test, the braced frame suddenly lost one-third of its capacity at an effective interstory drift of about 1%, when a brace connection failed in tension after fifteen cycles. The analytical model failed to predict this event because it assumed unlimited deformation capacity of the braces and their connections. Including quantitative limitation of the hysteretic

ductility of the bracing system in the analysis is difficult. As long as the possibility of connection failure is not excluded, the predicted behavior after a certain number of cycles in the inelastic range may be in doubt. If such failures are prevented through careful detailing, the analysis should be valid far into the inelastic range.



## CHAPTER 5

### PARAMETRIC STUDY

#### 5.1 Introduction

The parametric study introduced here complements the experimental work presented in Chapter 4 and the conceptual work of Chapters 2 and 3. The parametric study is carried out with the computer program described in Section 4.2. The goal of the study is to gain a better understanding of the behavior of a laterally loaded steel-braced reinforced concrete frame. The results of the parametric study are presented in Chapter 6.

The parametric study is performed on a so-called "subassemblage." The subassemblage is a simple structural unit representative of a braced frame. It is retained as basic study unit throughout the parametric investigation. In order to gain insight in the difference between the behavior under monotonic and cyclic loading, the subassemblage is submitted to three types of lateral loadings. Only horizontal components of the seismic loading are considered in this study. The variables of the study are the two main parameters controlling the behavior of the bracing system.

#### 5.2 Subassemblage

The two-dimensional subassemblage used in the parametric study is shown in Fig. 5.2.1. The subassemblage features a

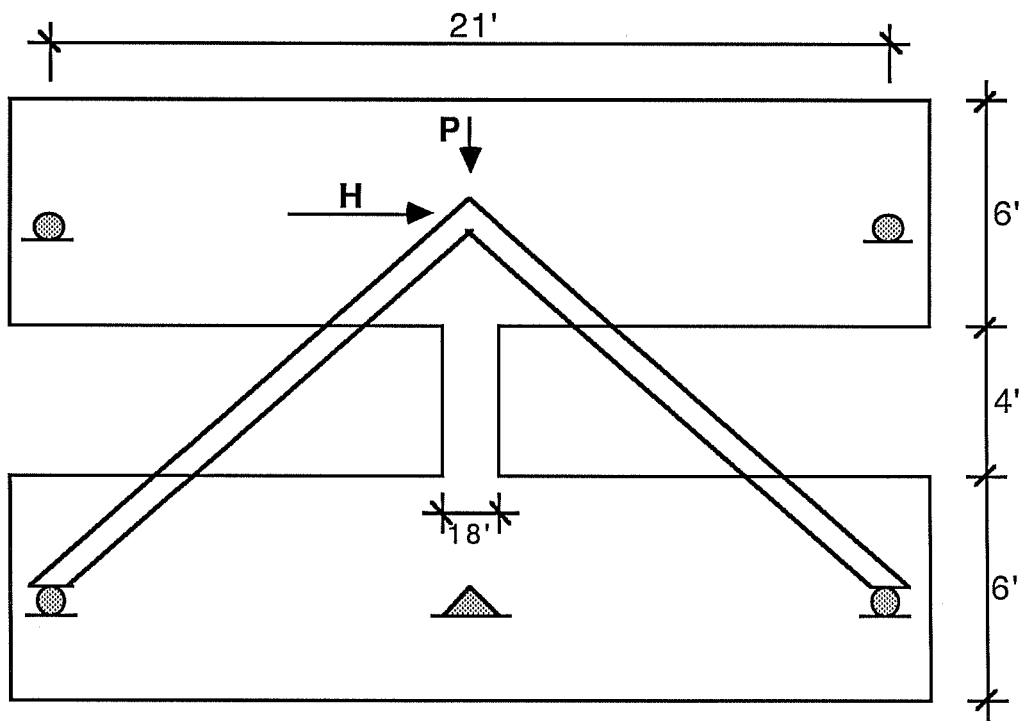


Fig.5.2.1 Subassemblage

column, two beams and two braces. The subassemblage conditions reproduce the situation of a braced interior column of a laterally loaded frame (see Fig. 5.2.2). The beams are supported by rollers at the inflection point of the spandrel beams when the frame deforms laterally. The inflection point is assumed to be at midspan. The reinforced concrete frame is braced with a pair of steel braces. At the upper end the braces are attached to the frame at the center point of the beam-column joint. At the lower end, they are attached to the beams with the vertical force component going to the roller supports.

The lateral loading is applied with a point load through the center point of the upper beam-column joint. The center point of the bottom beam column joint is restrained against vertical and lateral movement. A vertical force is introduced on the column to account for the  $P-\delta$  effects of the gravity load of the stories above. There are no gravity loads on the spandrels.

The subassemblage was chosen for the following reasons:

- The goal of the analytical work is to study the basic behavior under cyclic lateral loading of a steel braced reinforced concrete frame. More specifically, to study the impact of brace parameter variations and frame alterations on this behavior. The chosen subassemblage is the simplest possible structural unit on which to

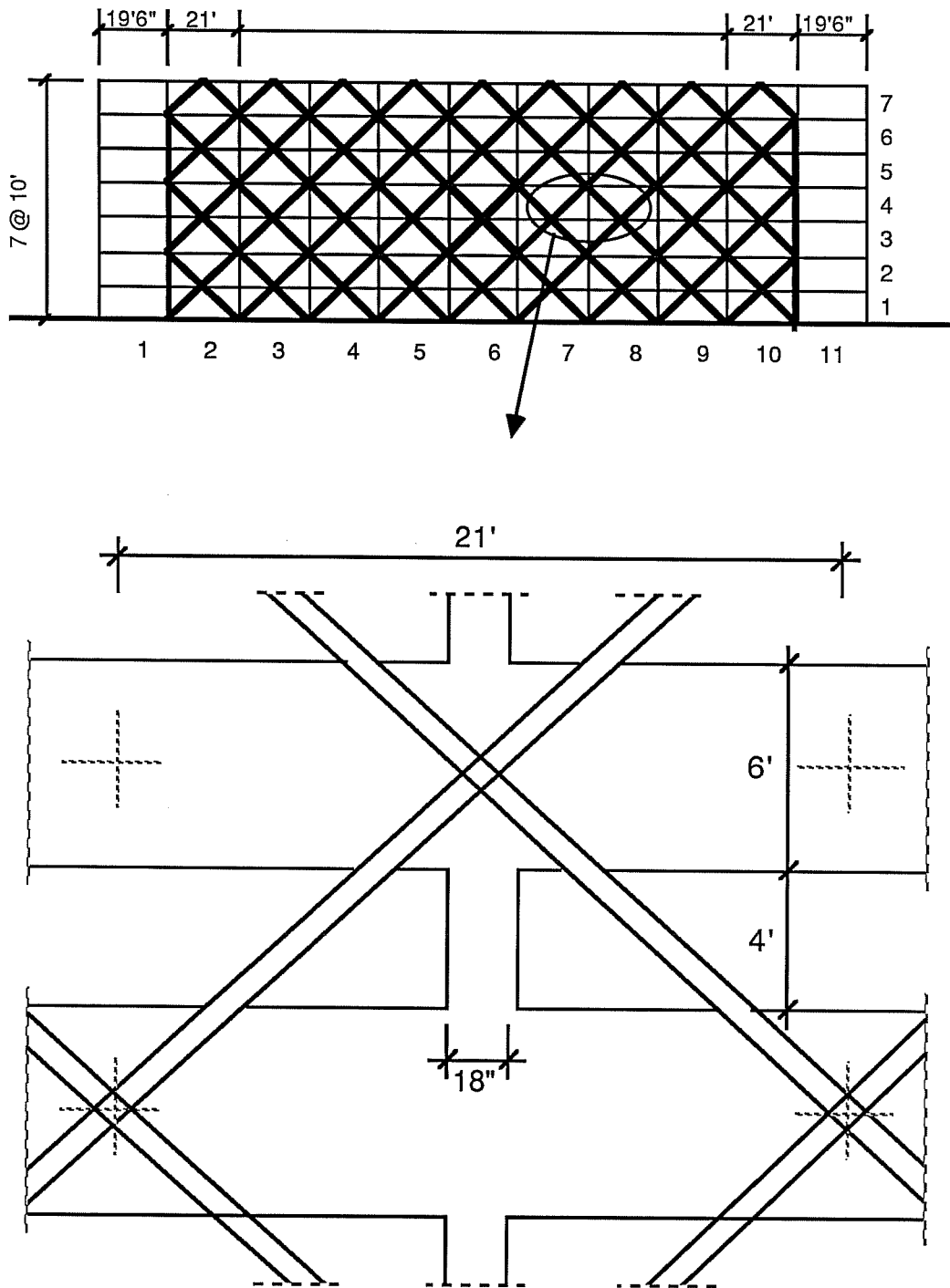


Fig. 5.2.2 Braced column of the prototype frame

model this behavior. This simplicity is both a conceptual and computational advantage.

- The subassemblage for the analytical study is well-suited for experimental study also. The analytical study could be useful in the determination of future experimental research.

The subassemblage geometry and structural properties are modeled on the prototype structure for the experimental study. The experience and understanding gained from the test and from the duplication of the test results (Chapter 4) can thus be used. The bracing configuration of the subassemblage is different from that of the test specimen (Fig. 4.1.5) in that the braces go through the center point of the frame beam-column joint. There are no vertical steel elements in the subassemblage. Most of the insight gained from the study of this particular subassemblage is relevant for retrofitting situations with different geometrical and structural characteristics.

An elastic design criterion is used for the subassemblage braces. The portion of the equivalent static design shear attributed to the bracing system is to be resisted without yielding or inelastic buckling. For typical values of  $kl/r$ , the criterion means that the design of the bracing system is done on the basis of the brace buckling stress.

### 5.3 Analytical Model of the Subassemblage

An analytical model of the subassemblage (Fig. 5.3.1) was prepared for the parametric study. The modeling of the subassemblage column, beams, and braces is described below.

Column. The subassemblage column is identical to those of the prototype building. Its geometrical and structural properties can be found in Fig. 4.1.2 and 4.1.3a. The column axial force  $P$  replacing the gravity load from the stories above was evaluated at 250k. The ultimate lateral capacity  $V_u$  can be computed with the equation of Fig. 3.6.4 for axially loaded short columns. The values of the parameters are:  $a = 24$  in.,  $d' = 16$  in.,  $f'_c = 3000$  psi,  $N = 250$ k,  $I = 8.750$  m<sup>4</sup>,  $A_g = 144$  in<sup>2</sup>,  $A_s/A_g = 0.235$ ,  $s_h = 18$  in.,  $A_v = 0.60$  in<sup>2</sup>, and  $f_{ys} = 40$  ksi. Because of the special configuration of the prototype beam-column joint, only part of the column width participates in the compression strut. The effective width was evaluated at  $b' = 10$ -in. With the values above, the column ultimate shear capacity is estimated to be  $V_u = 75$ k. Under a lateral load of 75k, only 60% of the calculated nominal flexural capacity of the column is developed. This confirms that the subassemblage column is a short column.

The beam-column joint of the prototype is 72-in. deep, but because of its particular configuration the depth of the rigid zone for the column is less. It was established in Sec.

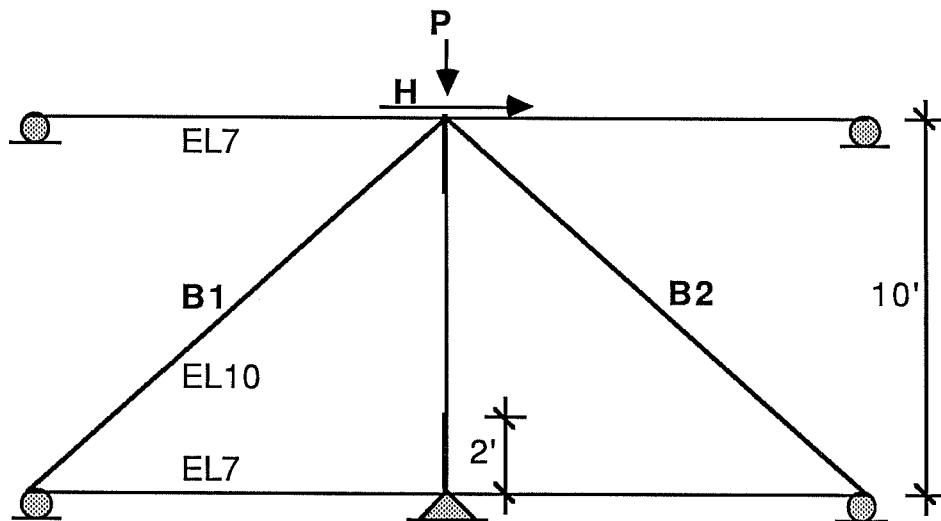


Fig. 5.3.1 Analytical model of the subassemblage

4.3.2 that the effective height of the rigid zone is two-thirds of the spandrel depth, i.e.  $e = 48$  in. The true height of the column for stiffness considerations is therefore:

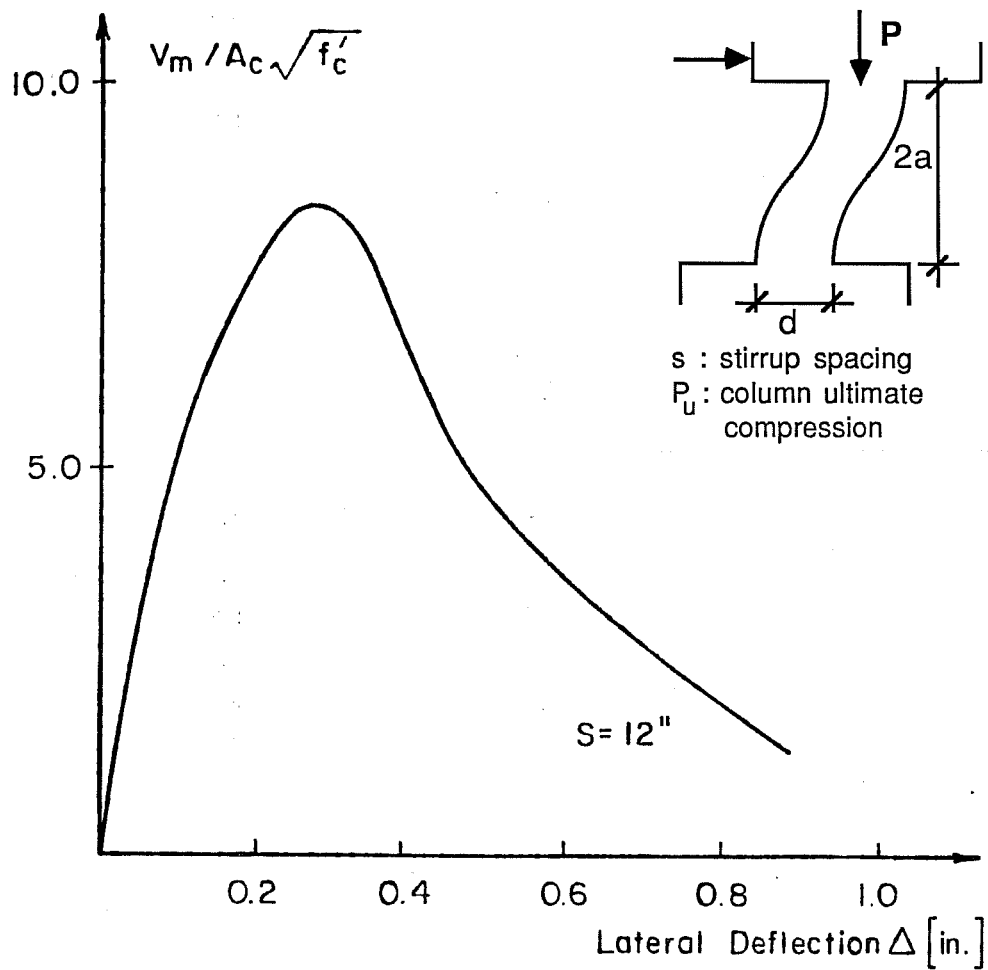
$$h' = 2a + (d - e) = 48 \text{ in.} + 24 \text{ in.} = 72 \text{ in.}$$

The column drifts are calculated with  $h' = 72$  in.

The shape of the load-deformation curve for the column was modeled on the basis of experimental work [23]. Figure 5.3.2 shows the envelope of the load-deformation curve for a short column under cyclic lateral loading. The test column had a shear span-to-depth ratio ( $2a/d$ ), confinement ( $d/s$ ), and axial loading ( $P/P_u$ ) similar to the subassemblage column. Because of those similarities, the shape of the load-deformation curve for the prototype column (Fig. 5.3.3) was assumed to be the same as the shape of the curve of Fig. 5.3.2.

The assumed load-deformation envelope for the prototype column was modeled with element EL7 (Appendix A.1). The broken line of Fig. 5.3.3 was used to define the moment-rotation relationship for the inelastic spring of the element model. The spring has an initial stiffness equal to half the column uncracked stiffness. At a shear equal to 60% of the ultimate shear, the stiffness is reduced to one-fifteenth of the uncracked stiffness (point A). The degrading part of the load-deformation curve (Segment BC) has a negative slope of minus 15% of the initial stiffness. Because of the lack of experimental data, the





	$2a/d$	$d/s$	$P/P_u$
Woodward Test	$36''/12'' = 3$	$12''/12'' = 1.0$	$\frac{140}{880} = 1/6.2$
Subassemblage Column	$48''/18'' = 2.7$	$18''/18'' = 1.0$	$\frac{250}{1300} = 1/5.2$

Fig. 5.3.2 Experimental load-deflection relationship for a short column similar to the prototype column [23]

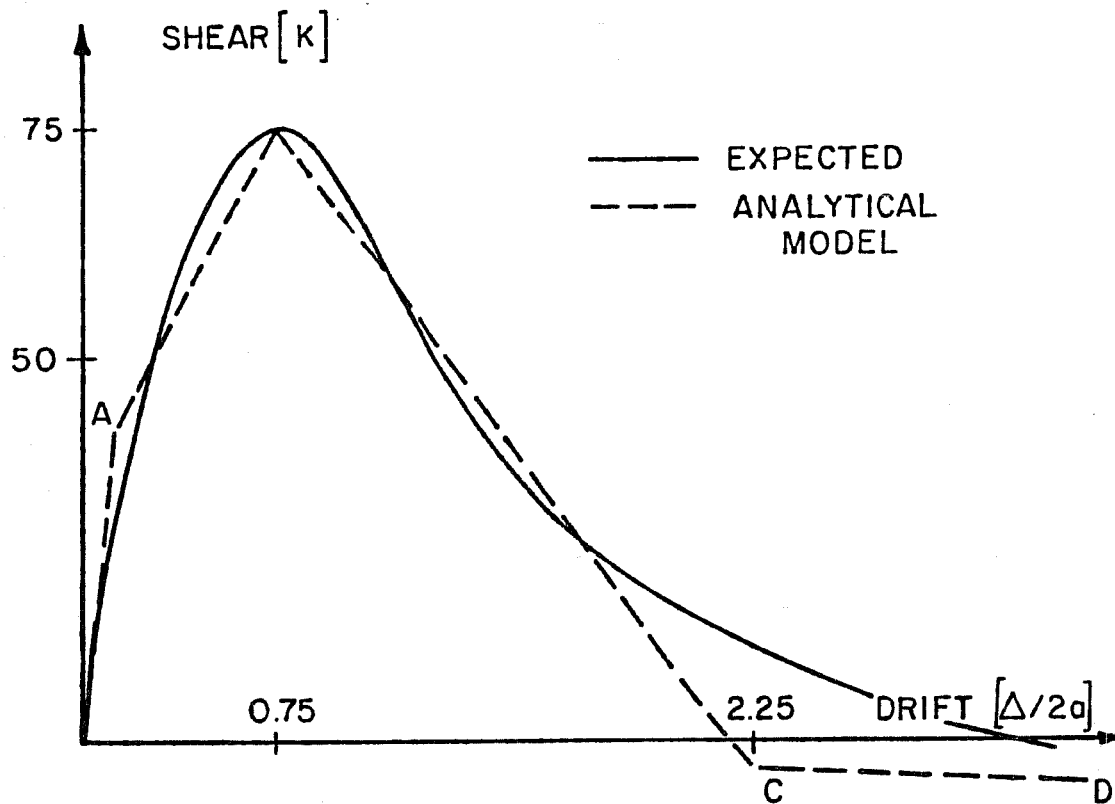


Fig. 5.3.3 Assumed load-drift relationship for the prototype column

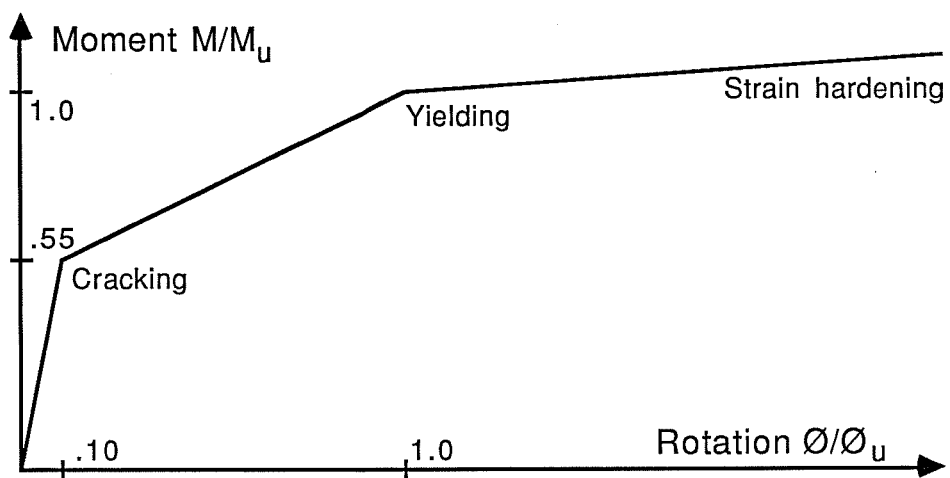


Fig. 5.3.4 Moment-rotation relationship for the beam inelastic spring

5.4.1 Design Ratio n. The ratio  $n$  is a measure of the increase in strength desired in the design of the bracing system. The value of  $n$  is the ratio of the design strength of the braced frame to the strength of the original frame. The ratio  $n$  is defined for a given story  $i$ :

$$n_i = H_i^R / V_{ui}^O$$

$H_i^R$  is the design lateral shear for story  $i$  of the retrofitted structure  $V_{ui}^O$  is the ultimate shear capacity of story  $i$  of the original structure. The determination of  $n$  is illustrated in Fig. 5.4.1 for the 2nd story of a structure retrofitted with a bracing system. On that story, two of the five bays are braced.

The ratio  $n$  is a design parameter. By the choice of  $n$ , the designer determines the design lateral load of the structure. Typically for wind and seismic loading, equivalent static loads are used and each story is designed separately. The ratio  $n$  is defined to accommodate this design approach. The ratio  $n$  is nondimensional, the strength of the existing structure is taken as a reference value.

$H_i^R$  is the design lateral shear for the retrofitted story  $i$ . The original structure may or may not be counted on to resist the design load, and the design criterion may be elastic or inelastic, depending on the retrofitting scheme. For the subassembly used in the parametric study  $H^R$  is defined in the following manner:

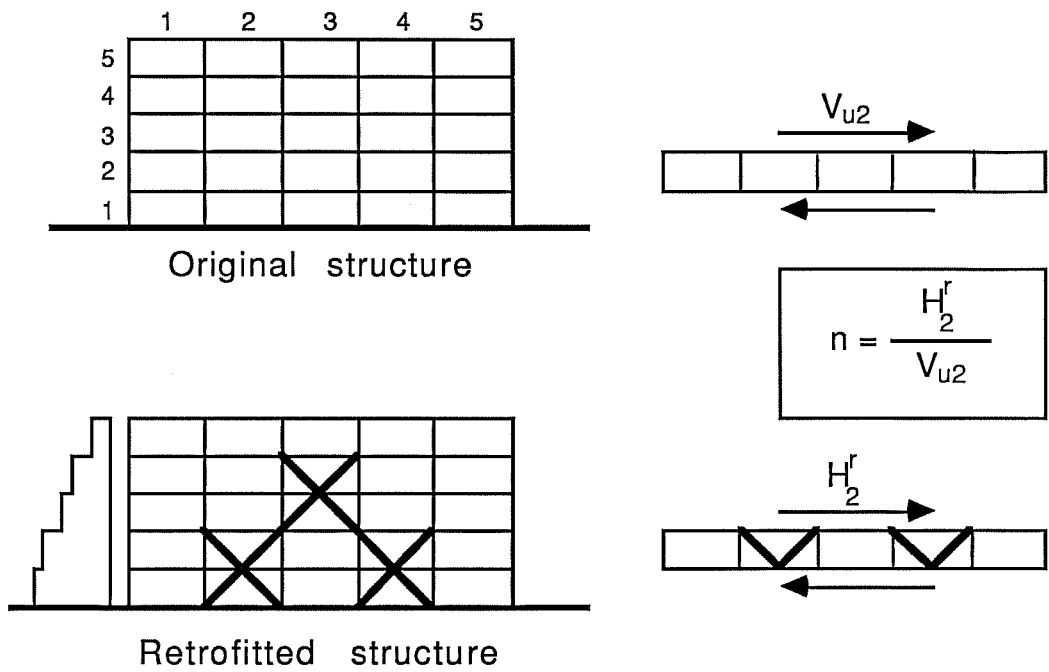


Fig. 5.4.1 Ratio  $n$  for a frame retrofitted with a steel bracing system

$$H^r = V_u^f + H^{bs}$$

$V_u^f$  is the ultimate shear capacity of the column.  $H^{bs}$  is the design load for the bracing system (see end of Sec. 5.2 for definition of design criteria).  $H^{bs}$  can be included in the equation for  $n$ :

$$n = H^r/V_u^f = (V_u^f + H^{bs})/V_u^f = 1 + H^{bs}/V_u^f$$

$$H^{bs} = (n - 1)V_u^f$$

The design load,  $H^{bs}$ , for the bracing system is  $(n - 1)$  times the strength of the frame.

5.4.2 Load Ratio  $m(\delta)$ . The load ratio  $m(\delta)$  is defined similarly to  $n$ , except that the design load for the retrofitted structure is replaced by the lateral load at drift  $\delta$ :

$$m(\delta) = V_1^f(\delta)/V_{ui}^o$$

$V_1^f(\delta)$  is the lateral shear on story  $i$  of the retrofitted structure at drift  $\delta$ .  $V_{ui}^o$  is the ultimate shear capacity of story  $i$  of the original structure.

The meaning of the  $n$  and  $m(\delta)$  ratios is illustrated in Fig. 5.4.2 with the lateral load-drift curves of the original and retrofitted structure. To produce  $m(\delta)$ , the load-drift curve of the retrofitted structure is normalized with the ultimate shear capacity  $V_{ui}^o$  of the original structure. The curve,  $m(\delta)$ , is thus a normalized load-drift curve. While the  $n$ -ratio reflects the design strength,  $m(\delta)$  is a measure of the effective strength of

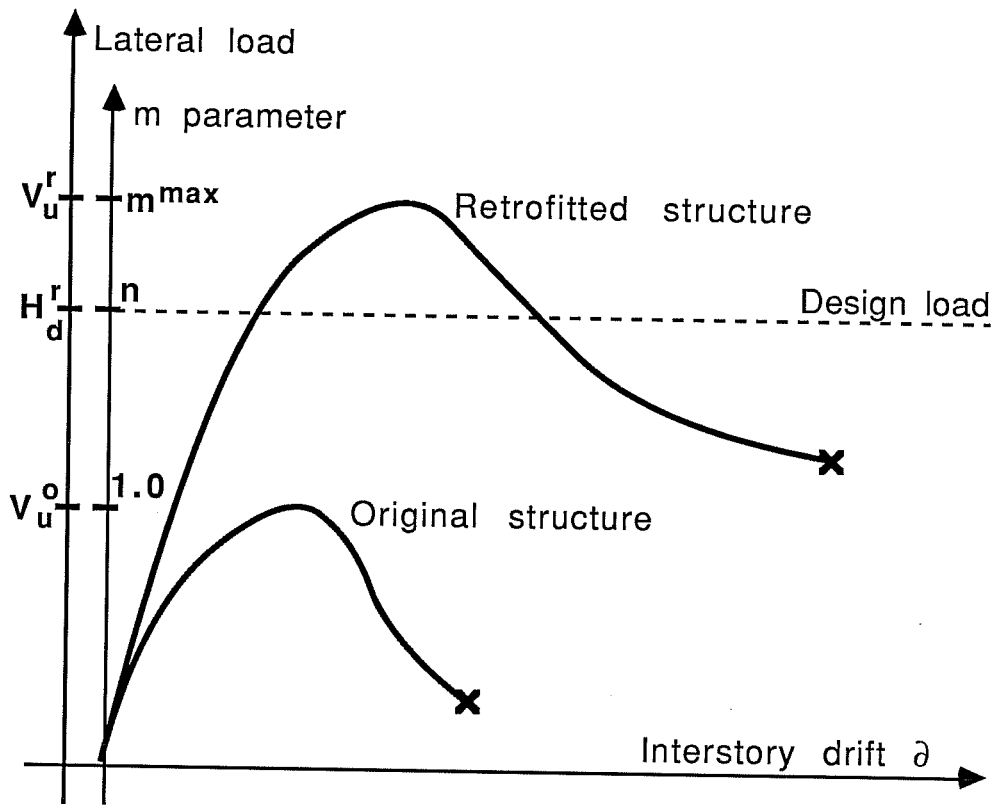


Fig. 5.4.2 Design ratio  $n$  and load ratio  $m$

the retrofitted structure. Comparing the  $n$  and  $m(\delta)$  ratios helps close the gap between design of the bracing system and actual behavior of the braced frame. For example, the beam peak  $m(\delta)$  value  $m^{\max}$  should be larger than  $n$  to guarantee adequate strength. In Chap. 6,  $m(\delta)$  curves for the subassemblage of Sec. 5.2 have been computed for different values of  $n$ . This set of curves can help the designer of a bracing scheme to select the appropriate design ratio  $n$  which will produce the desired effective strength and ductility. The  $n$  and  $m(\delta)$  ratios are dimensionless, allowing easy comparison of various retrofitting situations.

## 5.5 Loadings and Variables of the Parametric Study

5.5.1 Loadings. The subassemblage was studied under three types of static lateral loading. The first one is monotonic, the other two are cyclic.

Monotonic Loading. A monotonically increasing interstory drift is imposed on the subassemblage. This loading case helps understand the basic behavior of a steel braced reinforced concrete frame under lateral loading. This is relevant for both wind and seismic loading. Also an envelope within which cyclic loadings are located is obtained.

Reversed Loading. The subassemblage is subjected to a single cycle of lateral drift. There is one loading reversal in

each direction at an interstory drift of 1.2%, far into the inelastic range. This loading is not a realistic loading case, but it is useful in understanding the basic behavior of a steel braced frame under cyclic loading.

Cyclic Loading. The cyclic loading history consists of five cycles of increasing peak interstory drifts. This loading reproduces the main character of a true seismic loading.

The computer program could be used for dynamic loading. Such a loading is, however, outside the scope of this study. The inelastic dynamic response of a braced frame for specific input data can be computed, but by nature, earthquake loading is largely nondeterministic and cannot be predicted with certainty. The basic characteristic of seismic loading is that the building is subjected to cyclic lateral loading. The primary goal of this study is to investigate the behavior under cyclic lateral loading of a steel braced reinforced concrete frame. This purpose can be achieved better with a static loading.

5.5.2 Brace Variables. The intent of the parametric study is to determine the behavior of a laterally loaded steel braced reinforced concrete frame for various values of the two main brace parameters: the n-ratio which controls the relative strength of the frame and the bracing system, and the slenderness ratio  $k\ell/r$  which controls the buckling and hysteretic behavior of



the braces. The parametric study focuses on bracing system parameters because the designer can select bracing geometry.

n-parameter. The n-ratio is the ratio of the design strength of the retrofitted structure to the strength of the existing structure. It is thus a measure of the design load of the bracing system. As shown in Sec. 5.4.1, the bracing system design strength is  $n-1$  times the strength of the reinforced concrete frame. The higher the n ratio, the more dominant the bracing system.

Integer values of n from 1 to 4 were used in this study. Those values cover a wide range of practical retrofitting applications. At  $n = 1$ , the brace section area is zero. This trivial bracing case is provided for reference, it is the original, bare, structure. Values of n between 1 and 2 represent a structure with a light retrofitting. This could, for example, be the case of a structure with adequate strength but in need of stiffening for wind or seismic loading. Values of n between 2 and 3 are representative of a typical bracing retrofit design. A building with an inadequate lateral resisting system is braced with a system designed to carry the entire lateral load. The strength of the building is thus more than doubled. Values of n above 3 would be exceptional. They occur if the strength of the existing building is a small fraction of the required strength.

This can occur, for example, if the structure has been severely damaged in a previous earthquake.

5.5.3 Slenderness Ratio  $k\ell/r$ . The slenderness ratio  $k\ell/r$  is an important parameter of the bracing system. The experimental results of presented in Sec. 1.4.2 show that the buckling load and hysteretic behavior of the braces are a function of  $k\ell/r$  (See Fig. 1.4.3). The slenderness ratio depends on the bracing configuration and brace type chosen by the designer. It can cover a wide range of values. The three  $k\ell/r$  values chosen for the parametric study aim at covering this wide range:

- |                 |   |
|-----------------|---|
| $k\ell/r = 40$  | The brace has a high buckling load (about 95% of yield load) and good hysteretic behavior.            |
| $k\ell/r = 80$  | The buckling load is still relatively high (about 80% of yield), but the hysteretic behavior is poor. |
| $k\ell/r = 120$ | The slender brace has a low buckling load (about 55% of yield) and a very poor hysteretic behavior.   |

## CHAPTER 6

### RESULTS OF THE PARAMETRIC STUDY

#### 6.1 Monotonic Loading

The results of the parametric study for the monotonic loading case are presented and discussed briefly. For simplification, the "steel braced reinforced concrete frame" is referred to as "braced frame," the "interstory drift  $\delta$ " as "drift  $\delta$ " and when "strength," "load," or "resistance" are used, the lateral strength, load, and resistance are implied.

6.1.1 Failure Sequence. The failure sequence for the analytical model of the bare frame under monotonic loading is as follows (see Fig. 6.1.1):

0-1: Elastic behavior

1: Cracking of the columns ( $\delta = 0.05\%$ ,  $H = 38k$ )

2: Cracking of the spandrels ( $\delta = 0.15\%$ ,  $H = 50k$ )

3: Shear failure of the column ( $\delta = 0.40\%$ ,  $H = 75k$ )

4: Column lateral capacity reduces to zero ( $\delta = 1.00\%$ )

From point 3 to 4, the spandrels are unloaded as the lateral load decreases because the column is losing capacity. At point 4, the overall lateral capacity has become negative because of the P- $\delta$  effect on the column. The load-drift curve for the column by itself (with fixed ends) is also plotted for evaluating the influence of the spandrel on frame behavior.

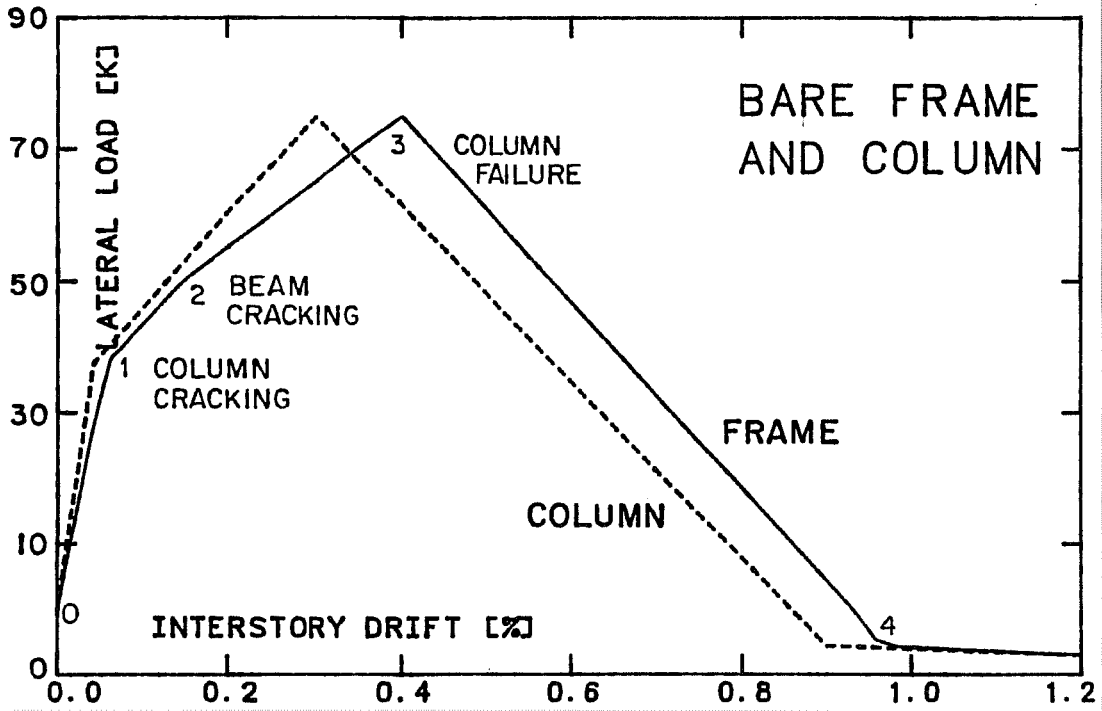


Fig. 6.1.1 Bare frame and column under monotonic loading

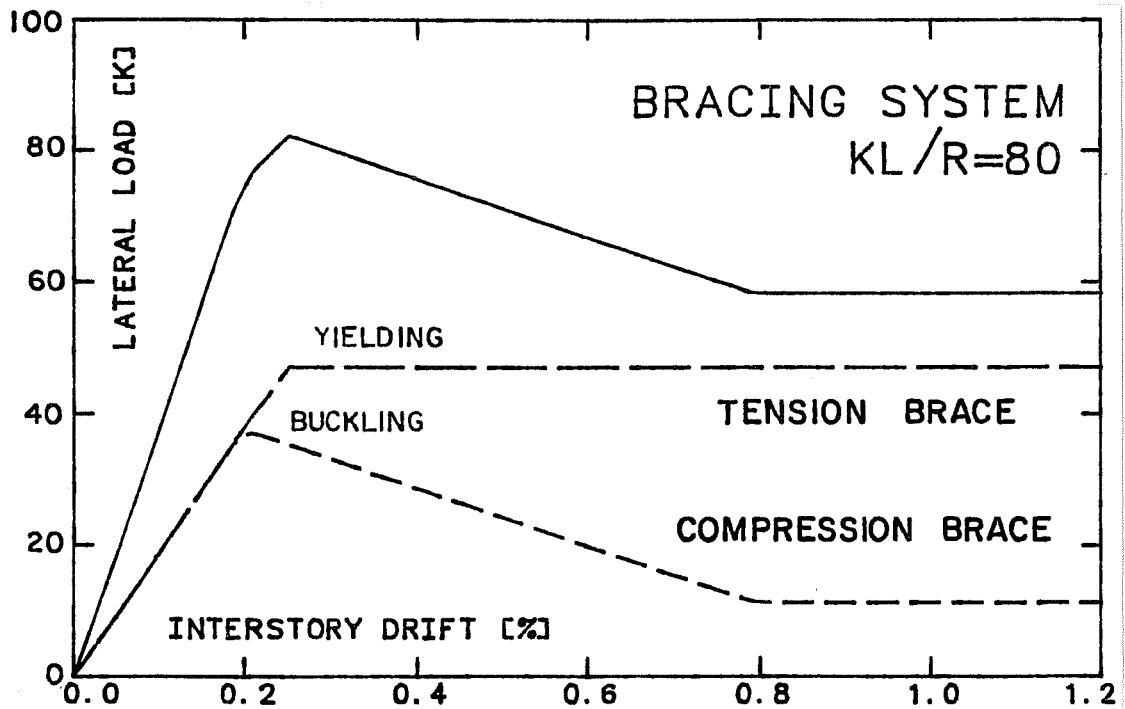


Fig. 6.1.2 Bracing system under monotonic loading

The contribution of the bracing system to the subassembly strength is plotted in Fig. 6.1.2 for a brace slenderness of 80. The individual contribution of the two braces to the lateral resistance is shown. The bracing system was designed to remain elastic (i.e. no buckling or yielding of the braces) under the design lateral load of 75k. Following buckling at  $H = 75k$  and  $\delta = 0.20\%$ , the contribution of the compression brace drops from 50% to 20% in the post-buckling range ( $\delta > 0.80\%$ ).

The computed load drift curve for the braced frame with  $n = 2$  and  $kl/r = 80$  under monotonic loading is plotted in Fig. 6.1.3. The  $m$ - $\delta$  plane is used, which means that the load-drift relationship for the braced frame is normalized with the strength of the original structure to produce the dimensionless curve  $m(\delta)$  (see Sec. 5.4.2 for definition of the  $m(\delta)$  ratio). As explained in Sec. 5.4.1,  $n = 2$  means that the elastic design load for the bracing system is equal to the ultimate lateral capacity of the bare frame. In this case, the design ratio  $n$  matches very closely the peak effective strength ratio:  $n = 2.00$  and  $m_{max} = 2.01$ . The contribution of the frame (i.e. the shear carried by the column) and the bracing system (i.e. the sum of the horizontal component of the brace axial forces) to the lateral strength of the braced frame are plotted separately. The failure sequence is as follows (see Fig. 6.1.3):

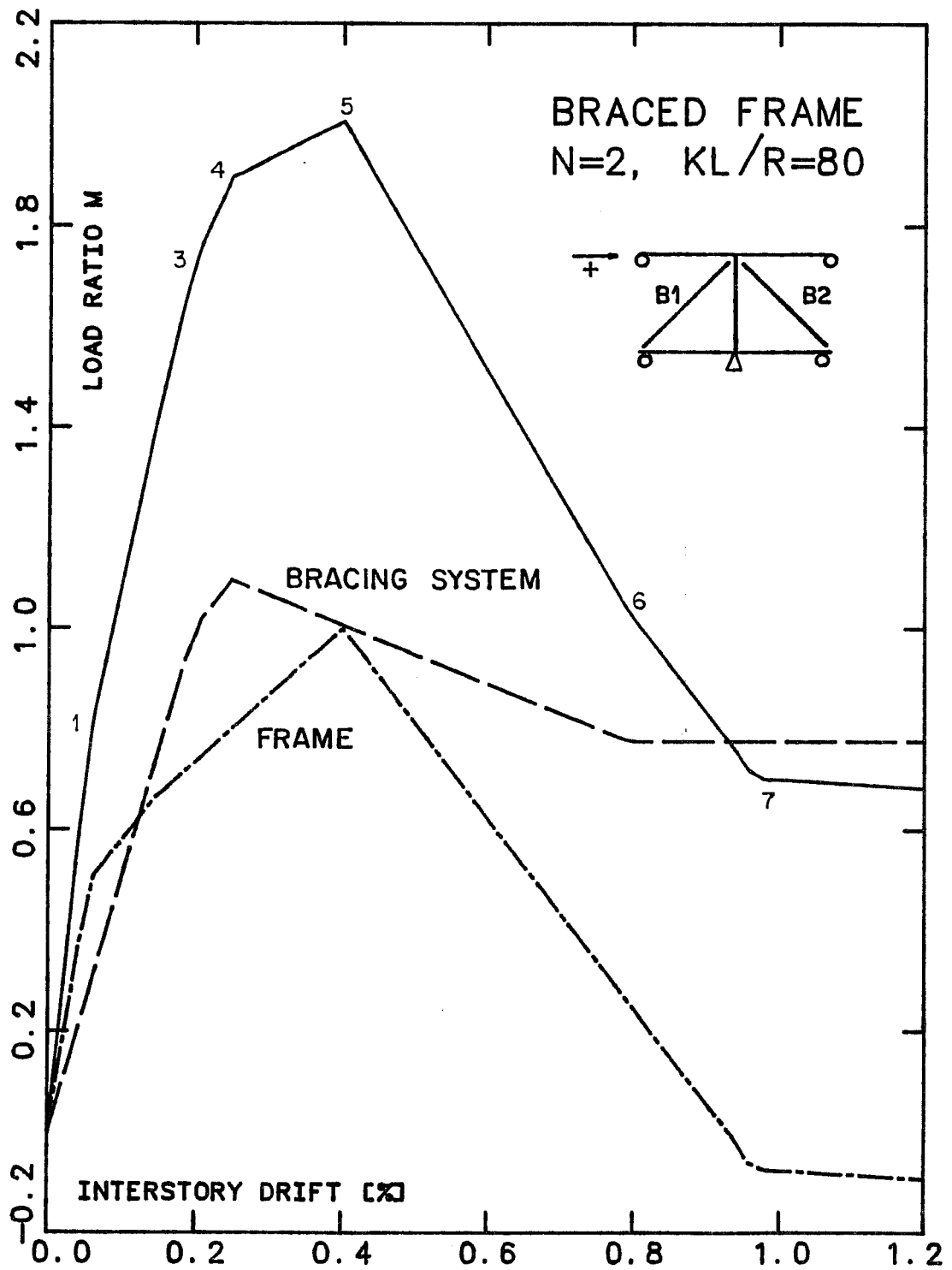


Fig. 6.1.3 Normalized load-drift relationship for a braced frame under monotonic loading

0-1: Elastic behavior

- 1: Cracking of the columns ( $\delta = 0.05\%$ )
- 2: Cracking of the spandrel ( $\delta = 0.15\%$ )
- 3: Buckling of compression brace B2 ( $\delta = 0.20\%$ )
- 4: Yielding of tension brace B1 ( $\delta = 0.25\%$ )
- 5: Shear failure of the column ( $\delta = 0.40\%$ )
- 6: Compression brace reaches post-buckling strength  
( $\delta = 0.80\%$ )
- 7: The column lateral strength reduces to zero ( $\delta = 1.00\%$ )

From point 5 to 7 the braced frame loses 65% of its lateral strength as the column fails in shear and the compression brace buckles. The bracing system and the frame are well-matched in terms of their relative deformability (see Sec. 3.3). When the bracing system buckles and enters the inelastic range ( $\delta = 0.20\%$ ) a large portion (about 75%) of the frame's lateral strength has been mobilized, but the lateral drift can be doubled before the columns fail. The braced frame thus has a high serviceability strength and a good margin against column damage.

6.1.2 Variation of  $n$  and  $k\ell/r$ . The influence of brace parameters  $n$  and  $k\ell/r$  on the monotonic behavior is shown in Figs. 6.1.4 to 6.1.6. The  $m-\delta$  curve for  $n = 1$  represent the bare frame case. The higher the  $n$ -ratio, the more dominant the bracing system, since the steel bracing is roughly  $n-1$  times

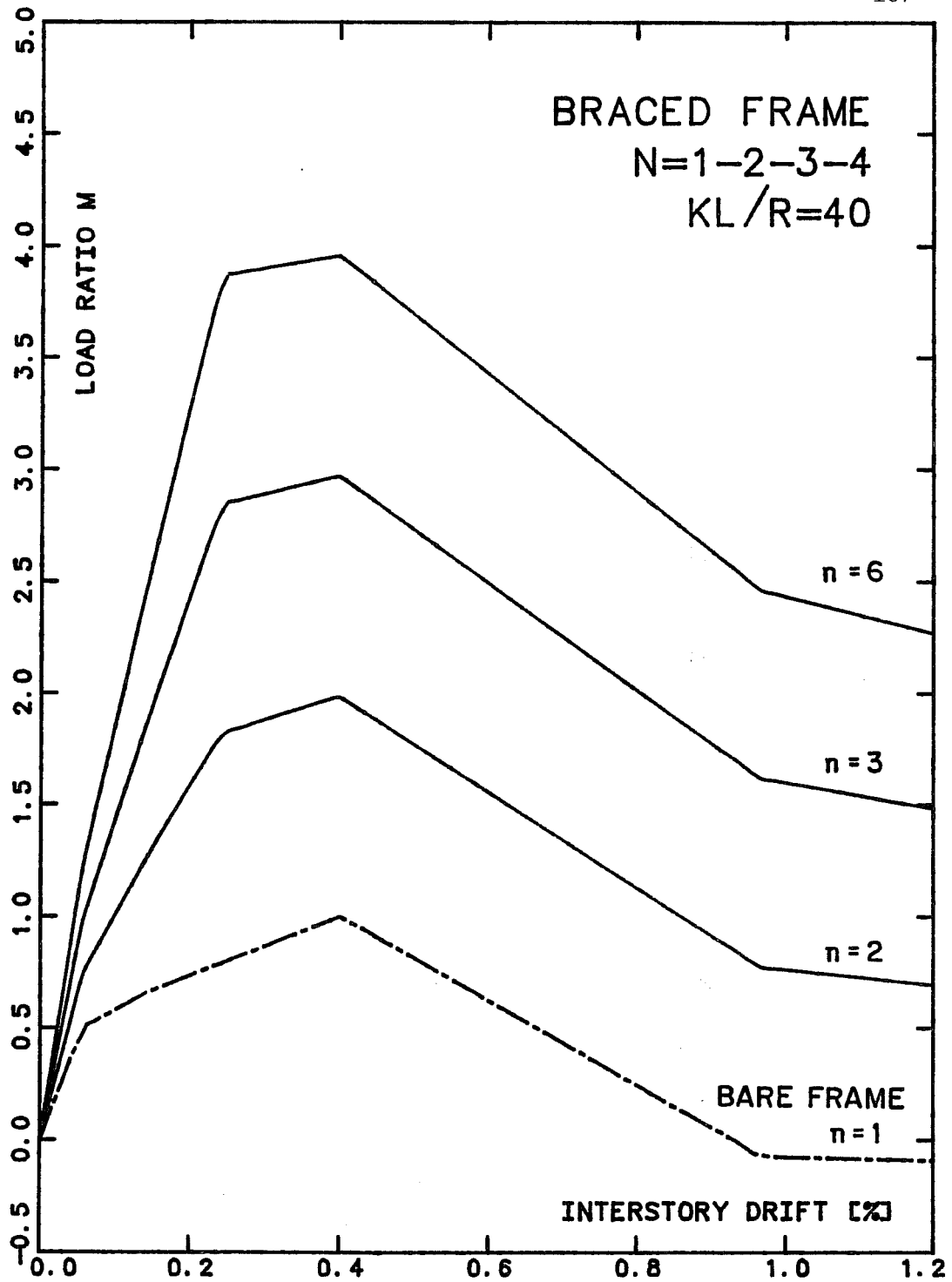


Fig. 6.1.4 Braced frame under monotonic loading  
- n=1,2,3 and 4, and kl/r=40



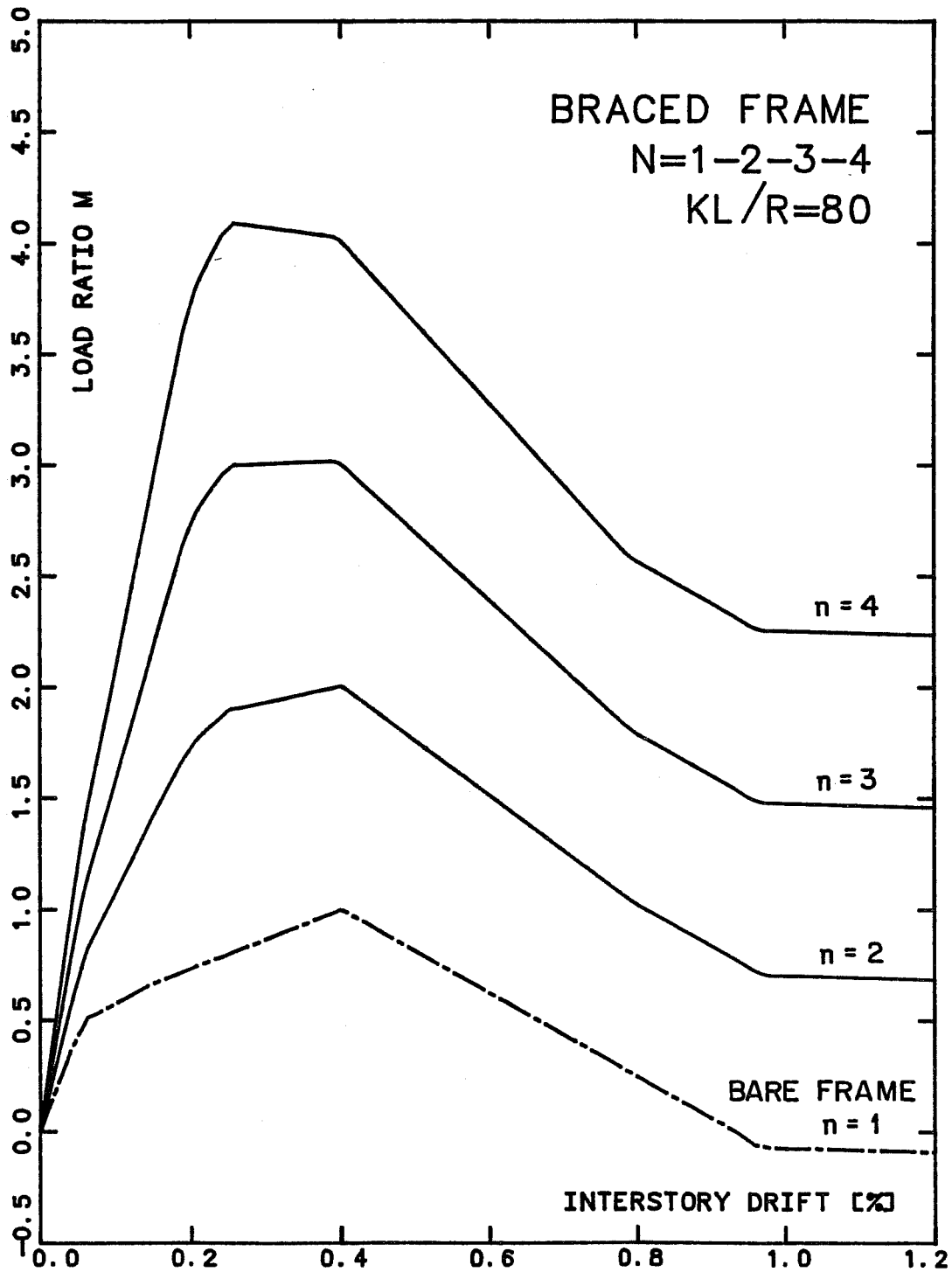


Fig. 6.1.5 Braced frame under monotonic loading  
- n=1,2,3 and 4, and  $kl/r=80$

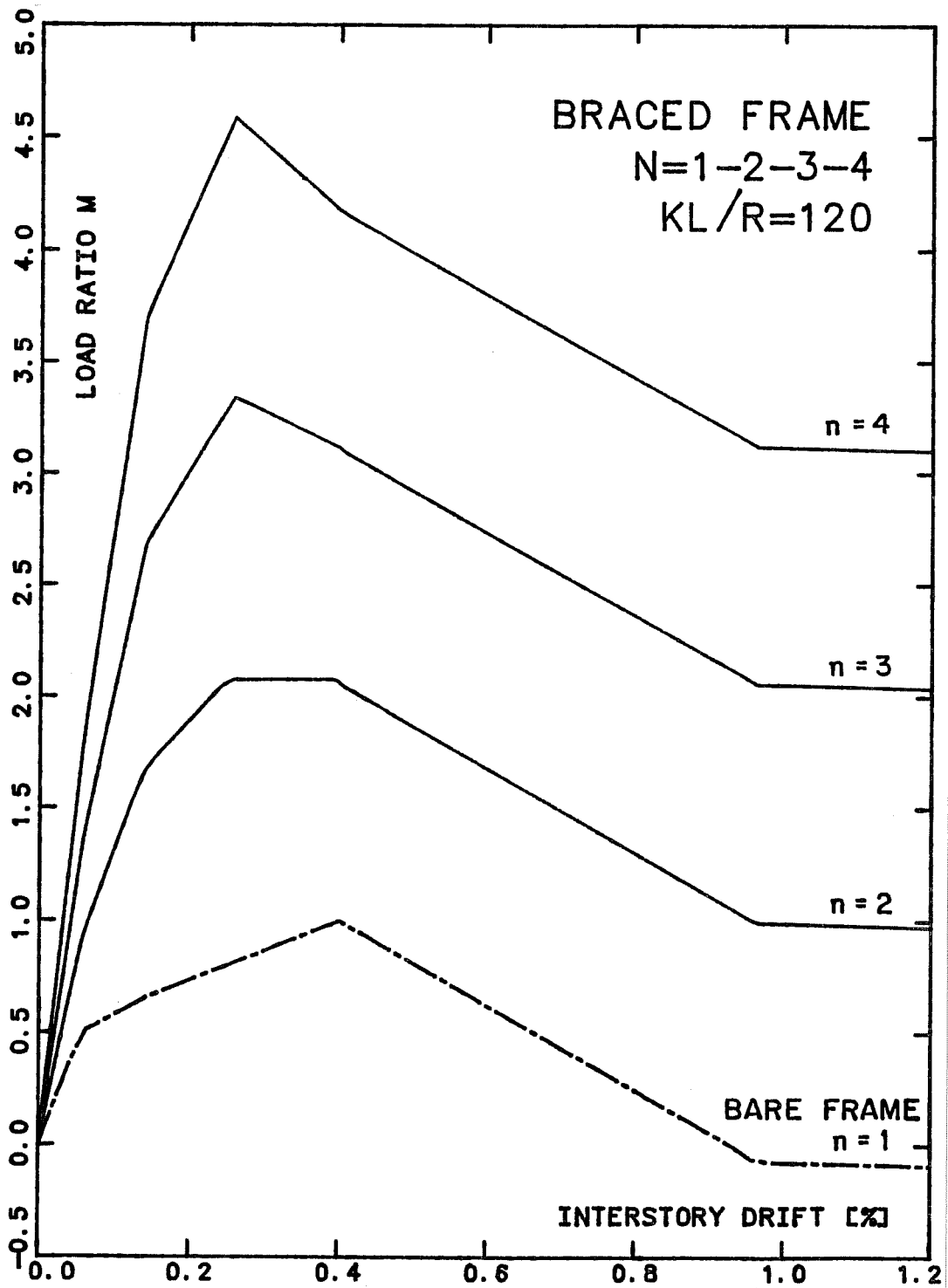


Fig. 6.1.6 Braced frame under monotonic loading  
- n=1,2,3 and 4, and  $kl/r=120$

stronger than the frame. All the  $m$ - $\delta$  curves display a pronounced drop of strength following the peak strength. The peak strength is reached either when the column fails at a drift of 0.40% (for  $kl/r = 40$ ) or when the tension brace yields at a drift of 0.25% (for  $kl/r = 120$ ). For a slenderness value of 120, the compression brace reaches its post-buckling strength before the column fails in shear. For a slenderness of 40 the loss of strength following buckling is more gradual and the post-buckling range is reached after the column has lost all lateral strength. The failure sequence of the braced frame is thus dependent on the braces slenderness ratio.

In Fig. 6.1.7, the three sets of  $m$ - $\delta$  curves are plotted together for comparison. The highest effective strength for a given design ratio  $n$ , is obtained for braced frames with  $kl/r = 120$ . The peak  $m(\delta)$  value matches  $n$  very closely for  $kl/r = 40$  and 80, but is significantly higher for  $kl/r = 120$  ( $m^{\max} = 4.6$  for  $n = 4.0$ ). The reason is the chosen elastic design criteria for the bracing system. The braces are designed on the basis of the buckling load  $P_{yn}$  rather than the yield load  $P_{yp}$ . For  $kl/r = 120$ ,  $P_{yp}$  is much higher than  $P_{yn}$  ( $P_{yn}/P_{yp} = 0.55$ ), so that there is substantial reserve in the tension brace when the design load is reached. Also, because of the low  $P_{yn}/P_{yp}$  ratio, the contribution of the compression brace to the lateral resistance of the braced frame is relatively small and the 70% loss of

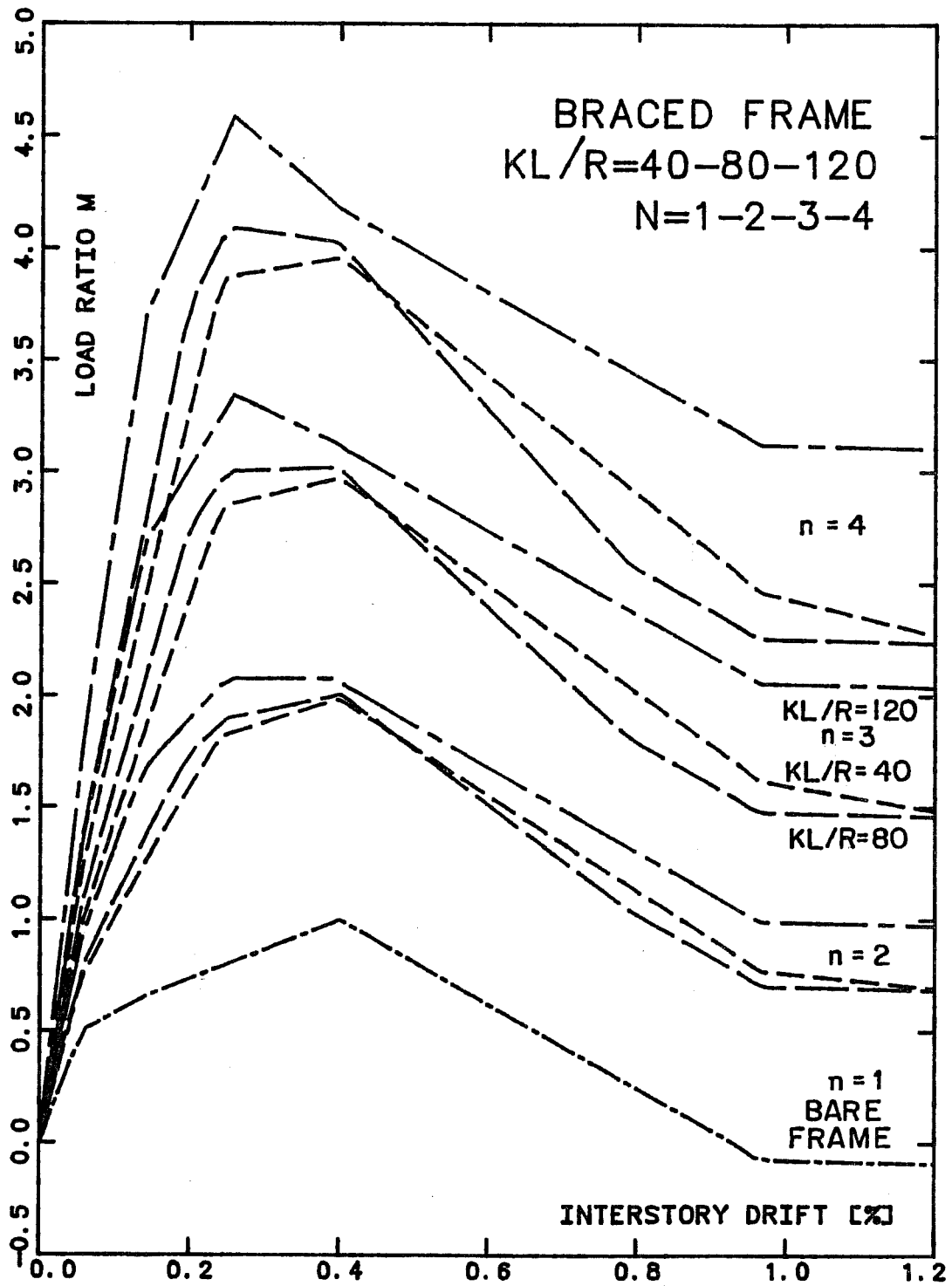


Fig. 6.1.7 Braced frame under monotonic loading  
 -  $n=1,2,3$  and  $4$ , and  $kl/r=40,80$  and  $120$

compression strength due to buckling has a reduced impact. This explains the higher  $m$  values for  $k\ell/r = 120$  in the post-buckling drift range.

Figures 6.1.4 to 6.1.6 show how the initial lateral stiffness of the braced frame increases with  $n$ . The elastic design criteria for the bracing system also explains why the highest initial stiffness, for a given  $n$  ratio, braced frame with  $k\ell/r = 120$  (see Fig. 6.1.7). The larger the slenderness, the lower the buckling stress (which is the basis of the brace design), the larger the resulting brace section, and the larger the elastic stiffness of the bracing system.

## 6.2 Reversed Loading

The results of the parametric study for the reversed loading case (one cycle of loading with reversal at drift 1.2% and -1.2%) are presented and commented on here.

6.2.1 Braces under Reversed Loading. The plot of Fig. 6.2.1 illustrates the influence of slenderness on cyclic behavior of the brace (as modeled by element EL10 of Appendix A.2). The brace is subjected to a full cycle of axial deformation (with reversals far into the inelastic range) starting with compression. To conform with the implication of the bracing system design criteria, the brace has the same buckling load for all three values of  $k\ell/r$  (40, 80, and 120). Since the buckling

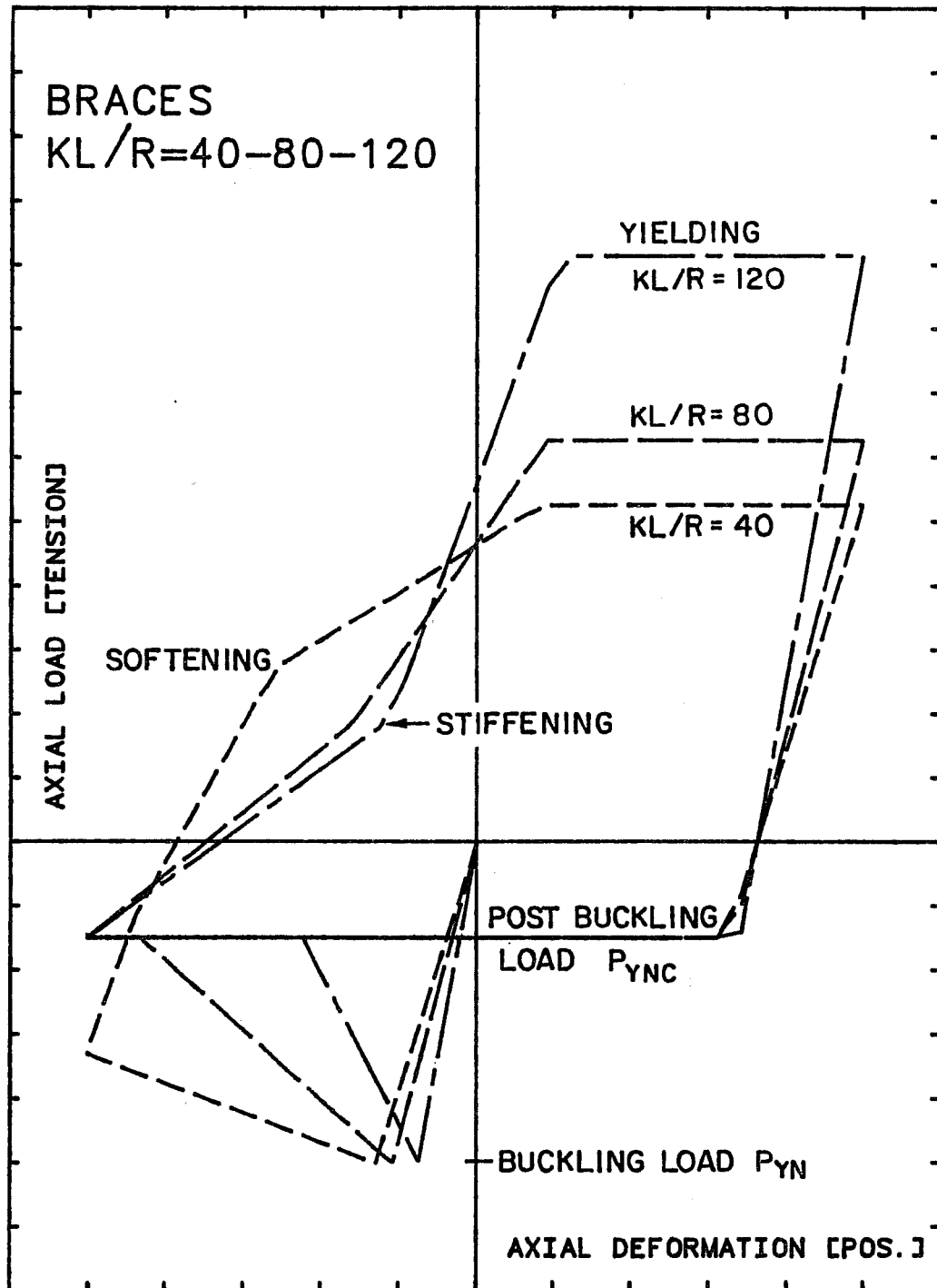
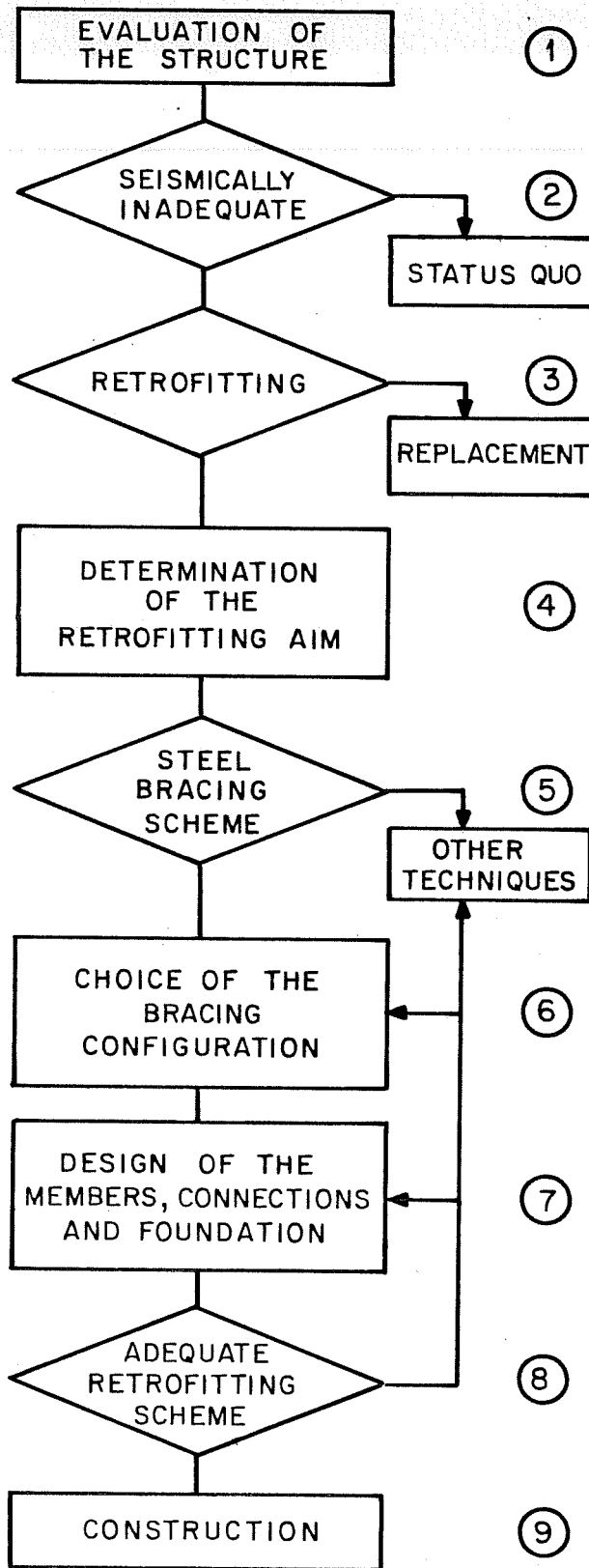


Fig. 6.2.1 Brace under reversed loading  
 -  $kl/r=40,80$  and  $120$



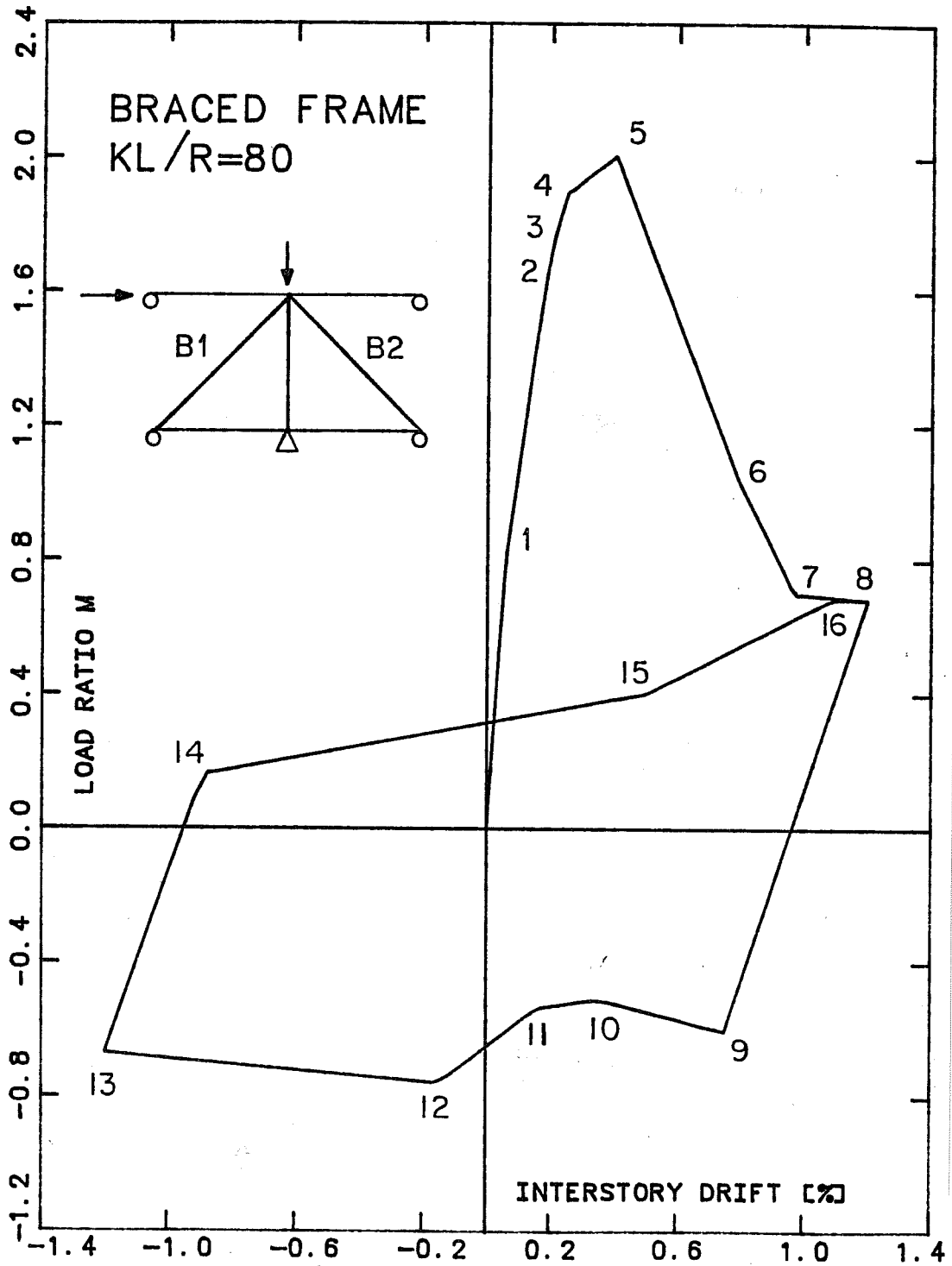


Fig. 6.2.2 Braced frame under reversed loading



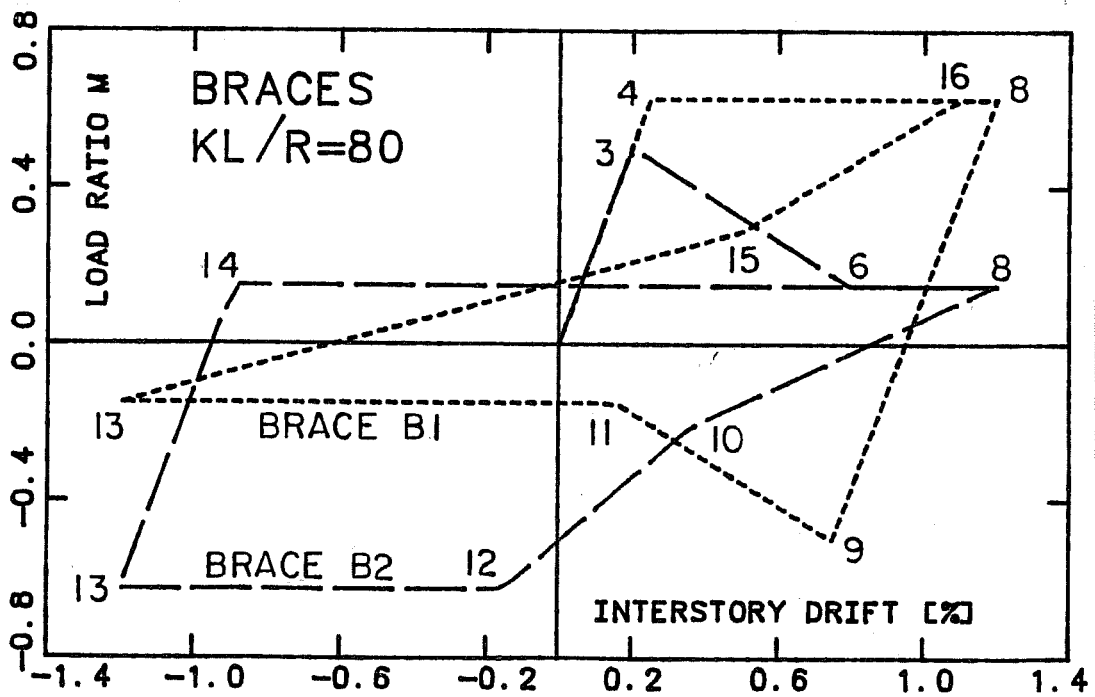
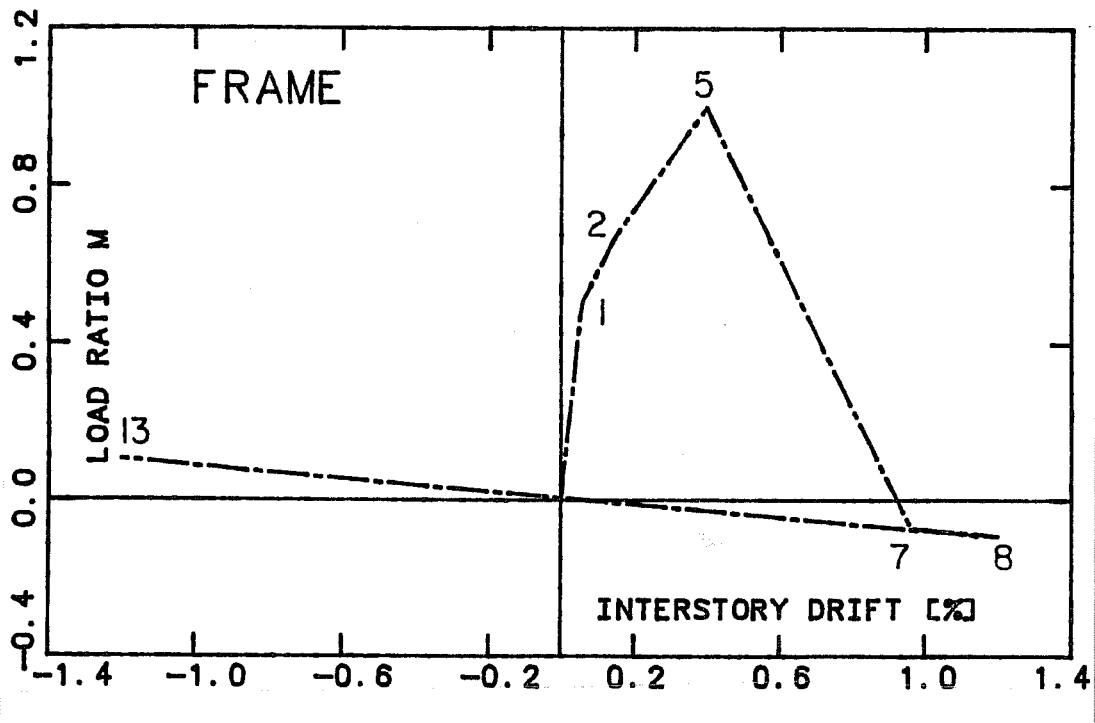


Fig. 6.2.3 Frame and brace contributions under reversed loading

lost all its strength in the initial (positive) loading direction, it has no strength in the reversed (negative) loading direction (see Sec. A.1). The behavior of the braced frame is controlled entirely by the bracing system from point 7 onward.

At reversal (Point 8,  $\delta = 1.20\%$ ) brace B1, which has yielded considerably in the initial direction, goes into compression and buckles at a positive drift level of 0.75% (Point 9). At a drift of 0.15% (point 11), brace B1 reaches the post-buckling plateau. Meanwhile, brace B2 which buckled in the positive direction straightens as it goes from compression to tension and yields when the negative drift range is entered (point 12). In the initial loading direction, the yielding of B1 (point 4) closely follows the buckling of B2 (point 3). In the reversed direction, the buckling (point 9) and yielding (point 12) are widely apart in terms of drift. This difference in behavior explains why the bracing system peak strength in the initial direction ( $m_{\max}^+ = 1.10$ ) is not matched in the reversed direction ( $m_{\max}^- = 0.80$ ). After the second loading reversal (Point 13), brace B2 buckles (Point 14) at the post-buckling load level. As the deformation of the braced frame is returned to the positive drift region, brace B1 stiffens (Point 15) and then yields (Point 16).

The curve of Fig. 6.2.2 shows the loss of strength and stiffness associated with cyclic loading of a braced frame. In

the initial loading in the positive direction a strength  $m$  of 2.0 is mobilized at drift 0.40%. In the second loading in the same direction (after two reversals at high drift levels),  $m$  is only 0.40 at that same drift. The initial peak strength ( $m_{\max} = 2.00$ ) cannot be maintained because of shear failure of the column and buckling of the brace. In the reversed direction the peak strength is  $m^{\max} = 0.80$ . The peak strength  $m^{\max} = 0.80$  is maintained in subsequent cycles because the brace yield and post-buckling strength in subsequent cycles do not change with increasing drift or cycling.

6.2.3 Variation of  $n$  and  $kl/r$ . The influence of the ratio  $n$  on the behavior of the braced frame under reversed loading is shown in Figs. 6.2.4 to 6.2.6. The higher the  $n$  value, the less the loss of the column strength impacts the braced frame behavior and the more stable the hysteresis loops become. It is clear from the three sets of  $m(\delta)$  curve that the failure sequence is not dependent on the ratio  $n$ , but is influenced by the slenderness. This is logical since the drift at which the buckling related inelastic events occur in the braces depend on  $kl/r$ . For  $kl/r = 120$ , the failure sequence is the same as the one described in Sec. 6.2.2 for  $kl/r = 80$ , but somewhat different for  $kl/r = 40$ . Because of the comparatively low buckling rate of a brace with  $kl/r = 40$ , the post-buckling

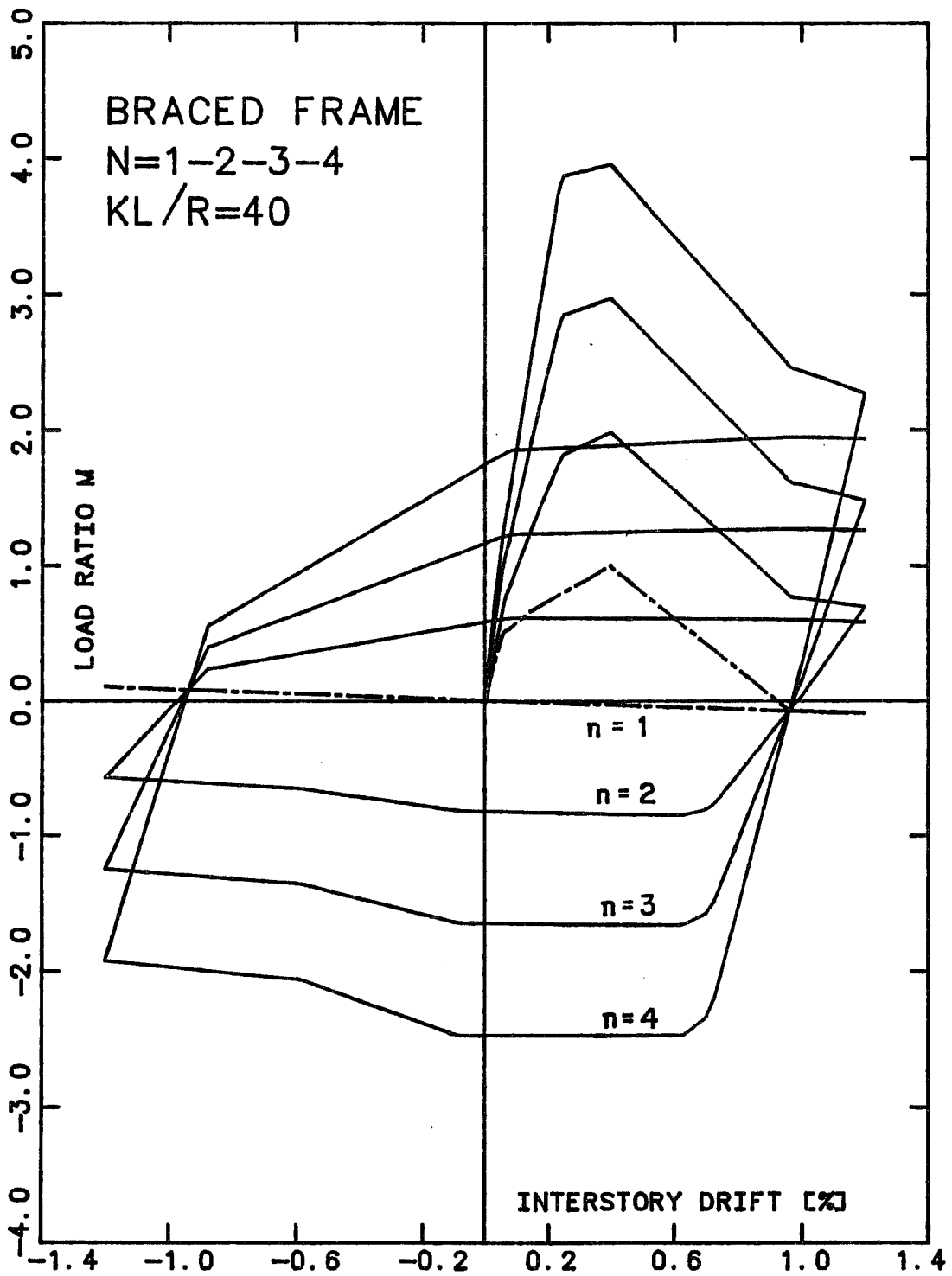


Fig. 6.2.4 Braced frame under reversed loading  
 -  $n=1, 2, 3$  and  $4$ , and  $kl/r=40$

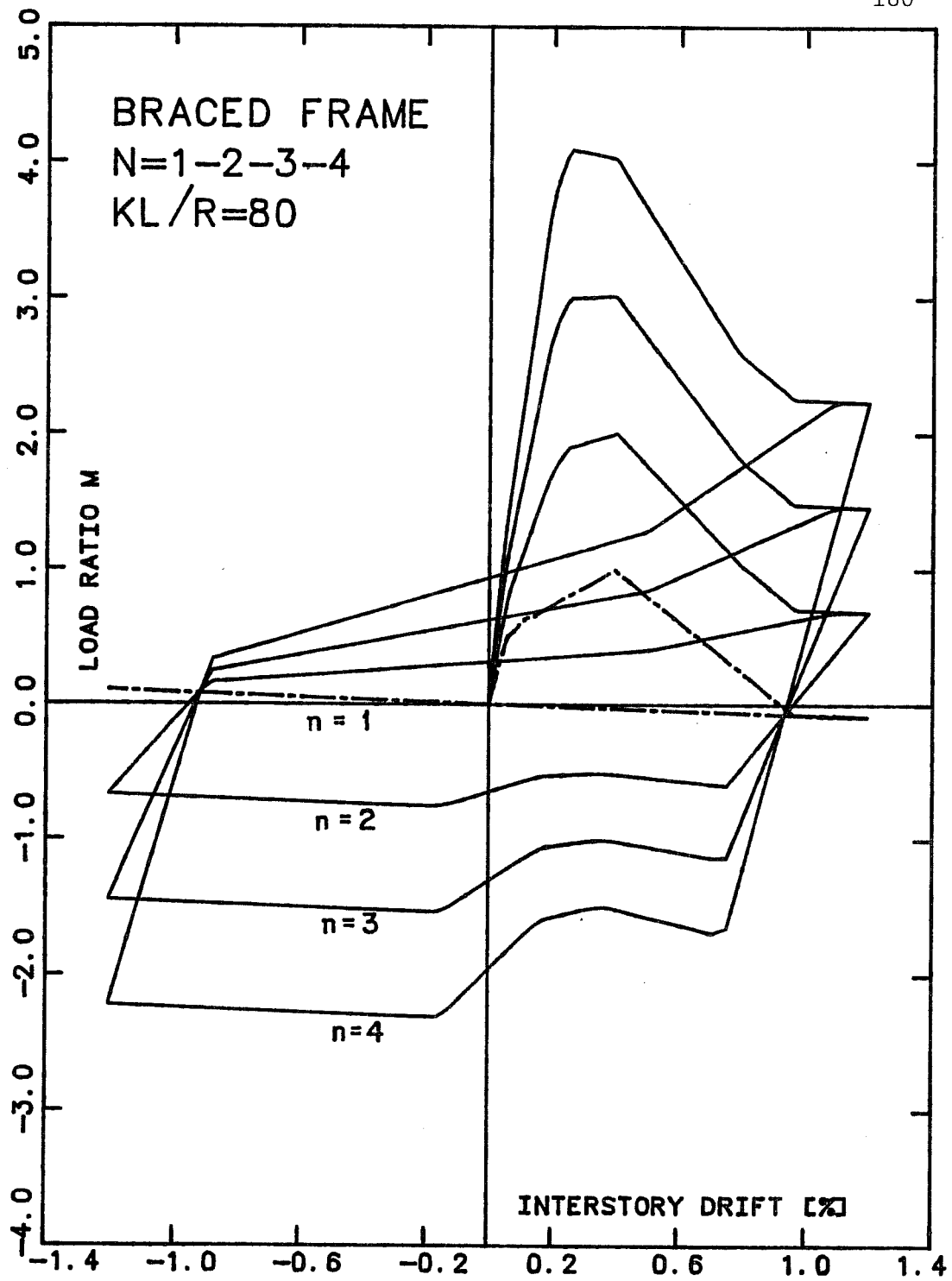


Fig. 6.2.5 Braced frame under reversed loading  
- n=1,2,3 and 4, and kl/r=80

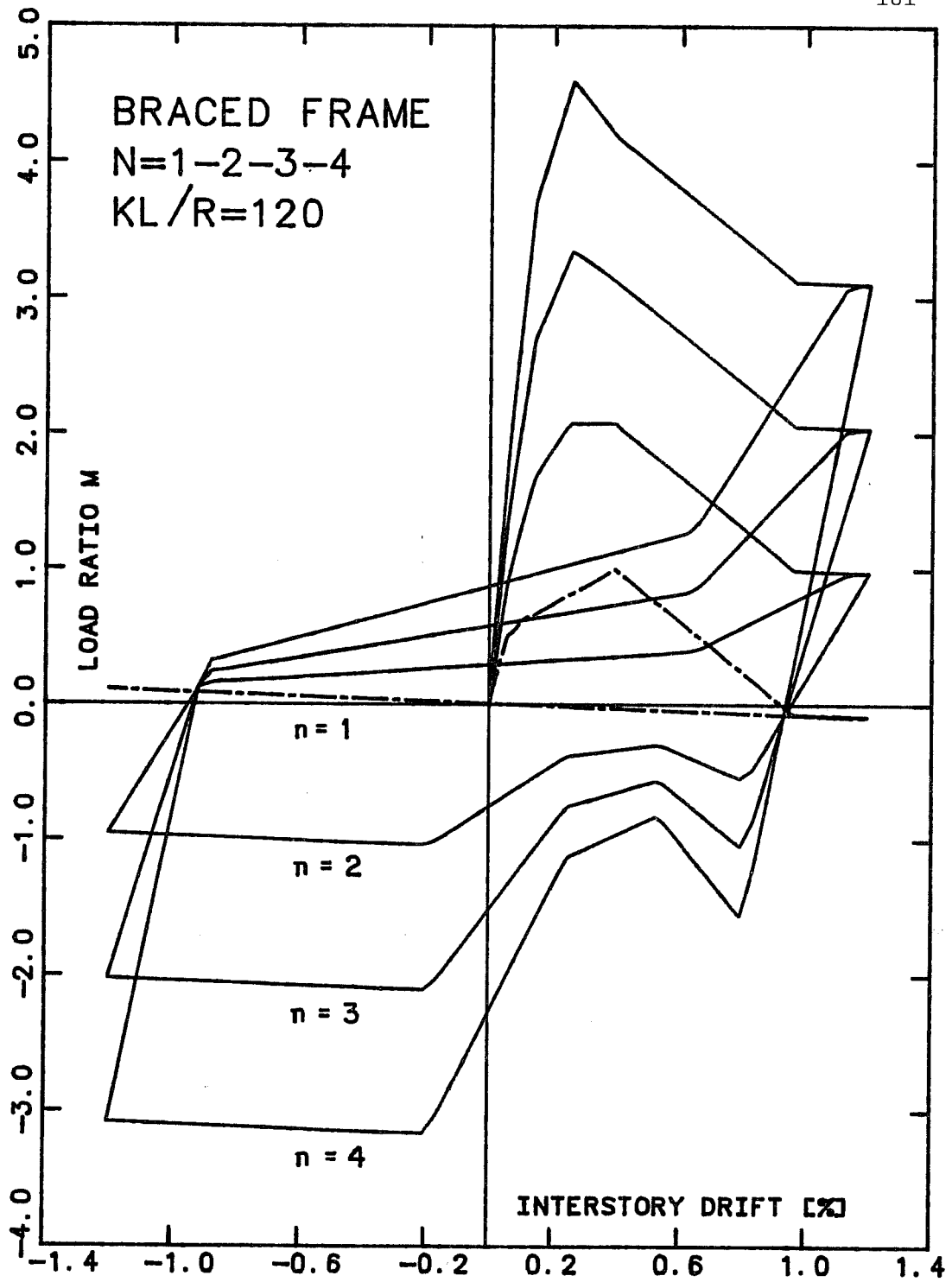


Fig. 6.2.6 Braced frame under reversed loading  
-  $n=1, 2, 3$  and  $4$ , and  $kl/r=120$

force level has not been reached in brace B2 at the point of load reversal ( $\delta = +1.20\%$ ). For the same reason, post-buckling of brace B1 in the reversed load direction is reached after yielding of brace B2 (points 11 and 12 in Figs. 6.2.2 and 6.2.3 are, therefore, reversed). Also, instead of a stiffening of brace B2 and brace B1 at points 10 and 15 of Fig. 6.2.2, there is a softening for  $k\ell/r = 40$  (see Fig. 6.2.1 also).

In Fig. 6.2.7, the  $m(\delta)$  curves for  $k\ell/r = 40$  and 120, and  $n = 4$  are plotted together for better evaluation of the influence of the slenderness on the cyclic behavior of the braced frame. The hysteresis loop for  $k\ell/r = 40$  is better balanced than for  $k\ell/r = 120$ , because of better behavior of the braces when the load is reversed. Under reversed loading, the braced frame with  $k\ell/r = 120$  reaches a first peak ( $m = -1.55$ ) at  $\delta = 0.80\%$  when brace B1 buckles and a second peak ( $m = -3.20$ ) when brace B2 yields at  $\delta = -0.20\%$ . The hysteresis loop exhibits behavior similar to "pinching" of reinforced concrete members with shear dominated failure in that the strength at zero drift, after a few reversals in the inelastic range, is very low. In terms of energy dissipation (i.e. area of the hysteresis loop), the curves for  $k\ell/r = 40$  and  $k\ell/r = 120$  are equivalent. But the material use is substantially less efficient for  $k\ell/r = 120$  because low buckling stress results in a large required brace section.

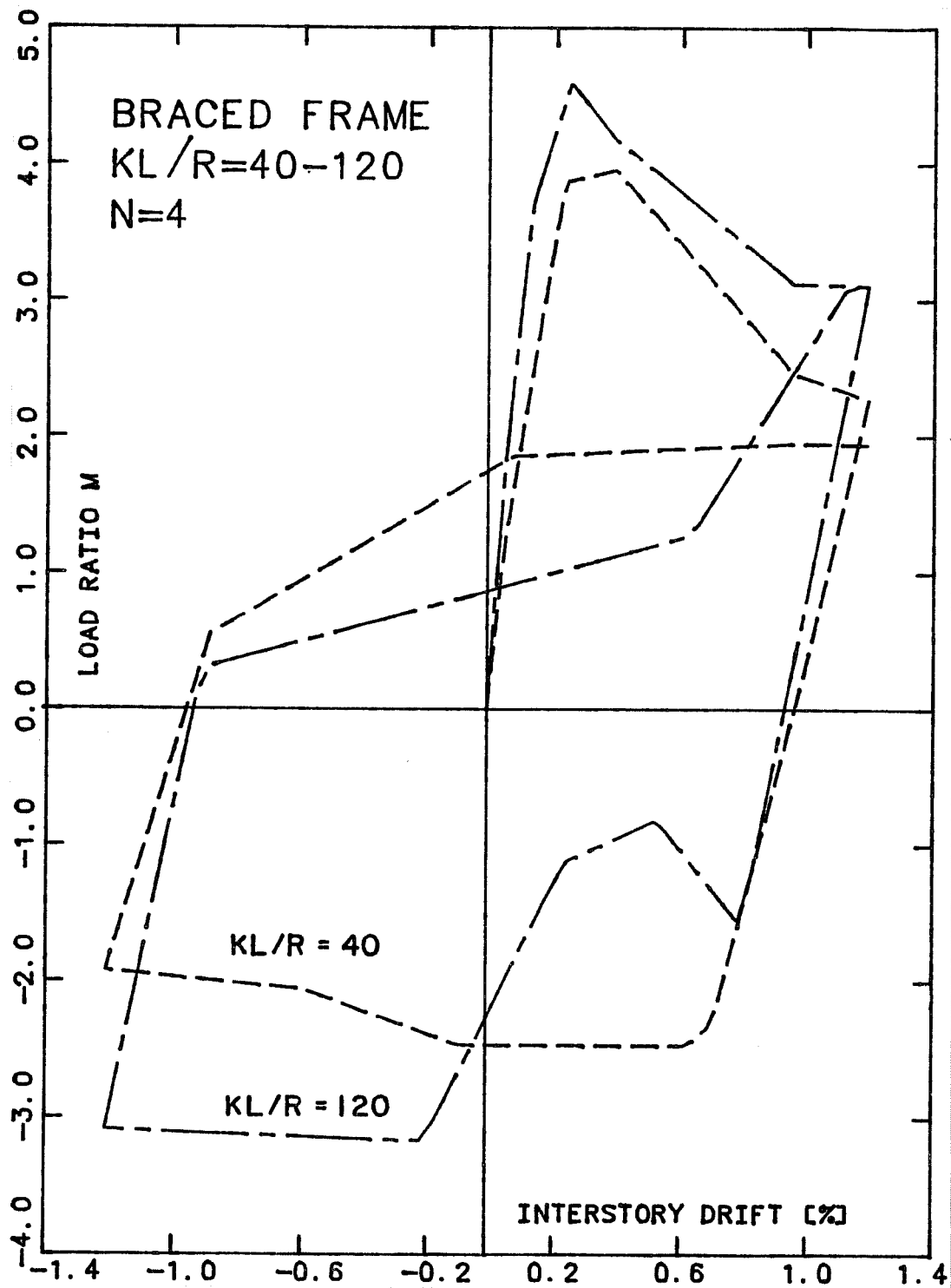


Fig. 6.2.7 Braced frame under reversed loading  
 -  $n=4$ , and  $kl/r=40$  and  $120$



6.2.4  $k\ell/r = 0$  and  $k\ell/r = \infty$ . It is interesting to study the braced frame behavior for  $k\ell/r = 0$  and  $\infty$  and compare with the "typical" situation for  $k\ell/r = 80$ . The braced frame with  $k\ell/r = 0$  (Fig. 6.2.8) exhibits an excellent hysteretic behavior. Buckling is prevented and the braces yield in compression. The rectangular hysteresis loop of the bracing system has maximum energy dissipation capacity.

The hysteretic behavior is much less favorable for  $k\ell/r = \infty$  (Fig. 6.2.9). The buckling load is zero so that only the tension brace can carry load. For a buckling stress of zero, the design criteria of Sec. 5.2 produces an infinite brace section. But  $k\ell/r = \infty$  the buckling is elastic and causes no damage. The brace is like a cable and the design can be based on the yield stress rather than the buckling stress. The required brace section is then double that of the same bracing system with  $k\ell/r = 0$ , because only the tension brace contributes to the lateral strength. Furthermore the braced frame with  $k\ell/r = 0$ , although using half the steel displays twice as much energy dissipation capacity (compare the hysteresis loop areas of Fig. 6.2.10). The effectiveness of the bracing system is reduced by a factor 4 in terms of cyclic energy dissipation if the slenderness goes from 0 to  $\infty$ , i.e. if the braces pass from "buckling prevented" to "no buckling strength." Both cases,  $k\ell/r = 0$  and  $\infty$ , have interesting practical applications which are discussed in Sec. 6.5.

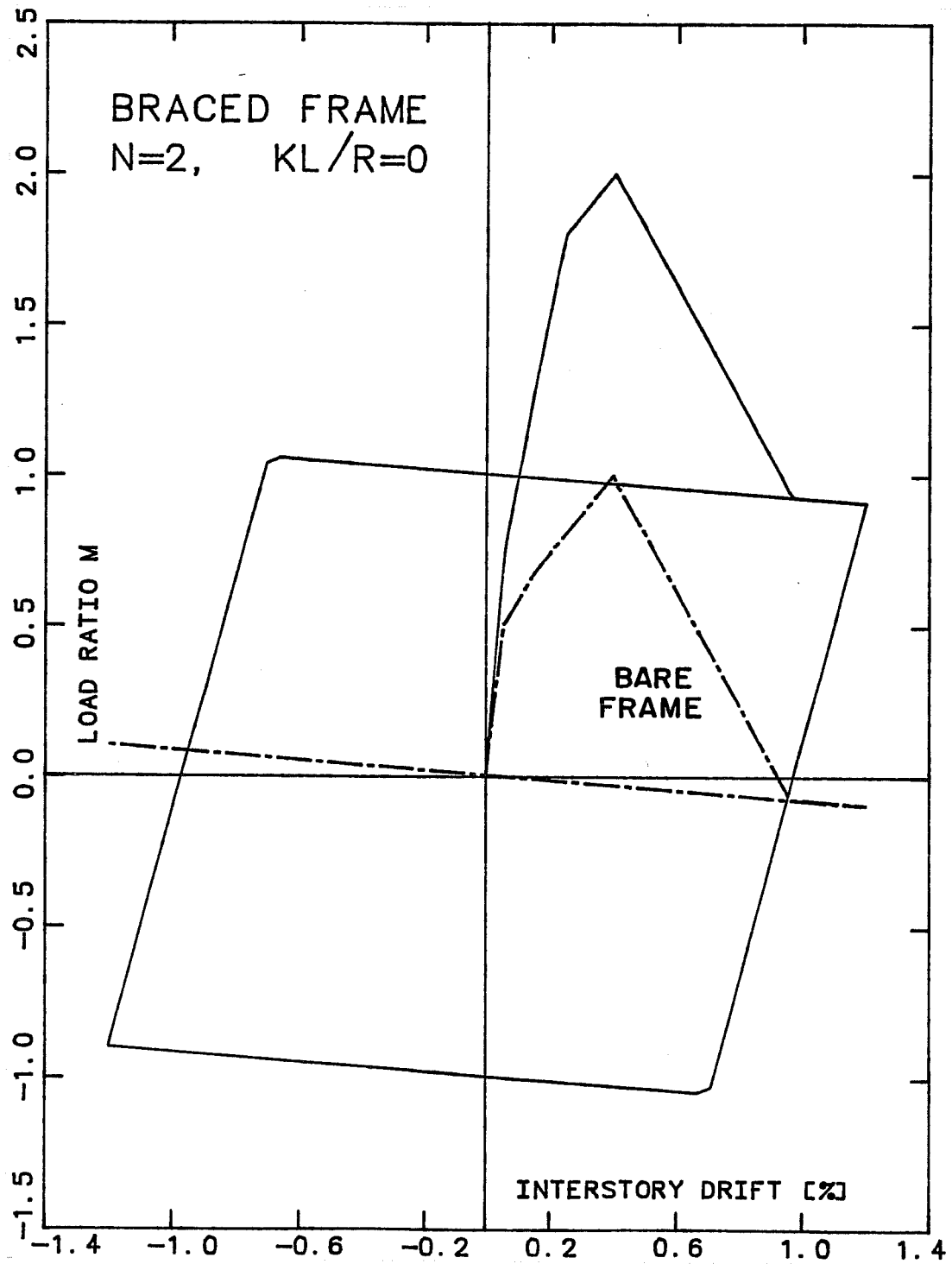


Fig. 6.2.8 Braced frame under reversed loading  
-  $n=2$ , and  $kl/r=0$

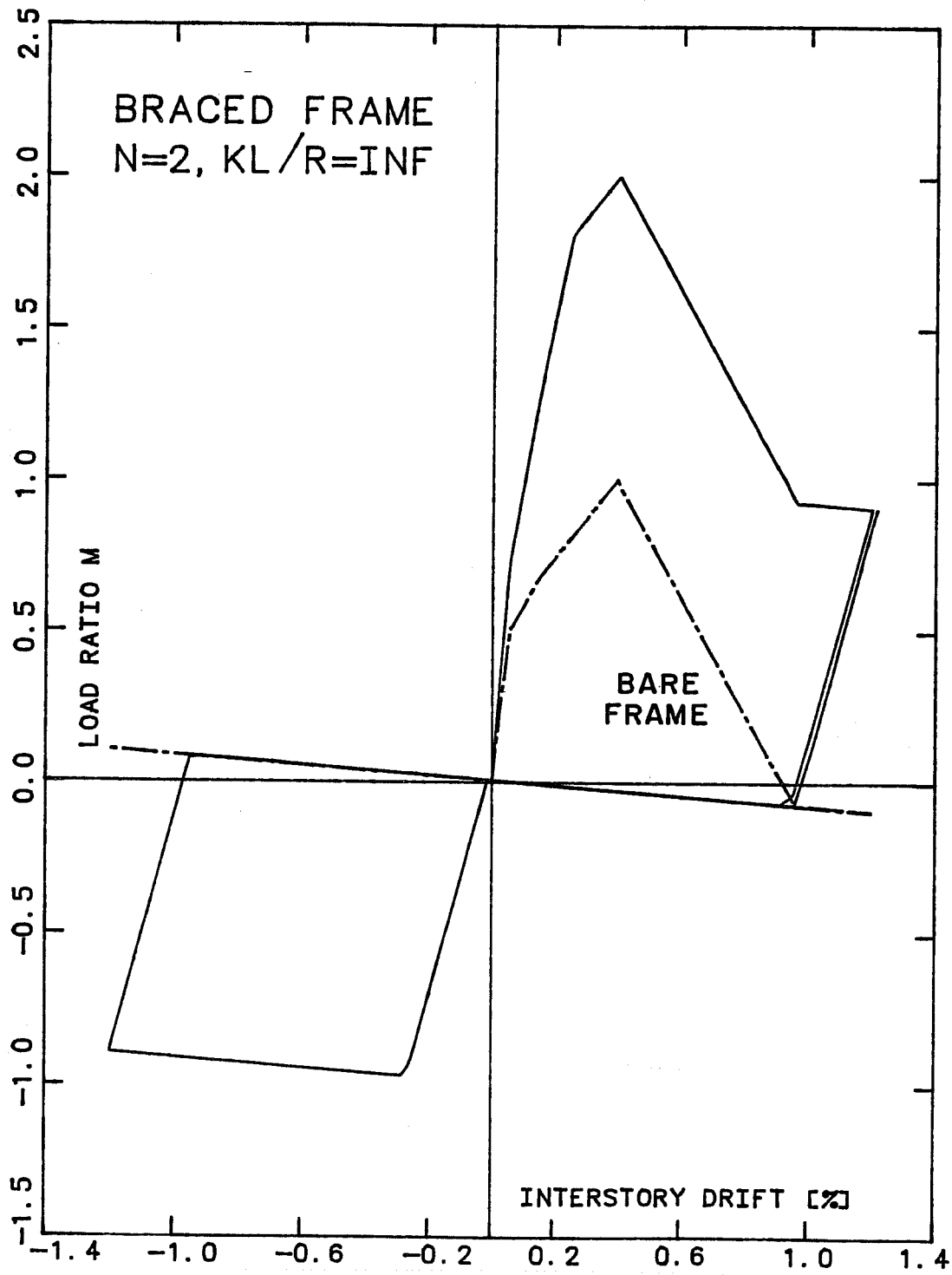


Fig. 6.2.9 Braced frame under reversed loading  
-  $n=2$ , and  $kl/r=\text{infinity}$

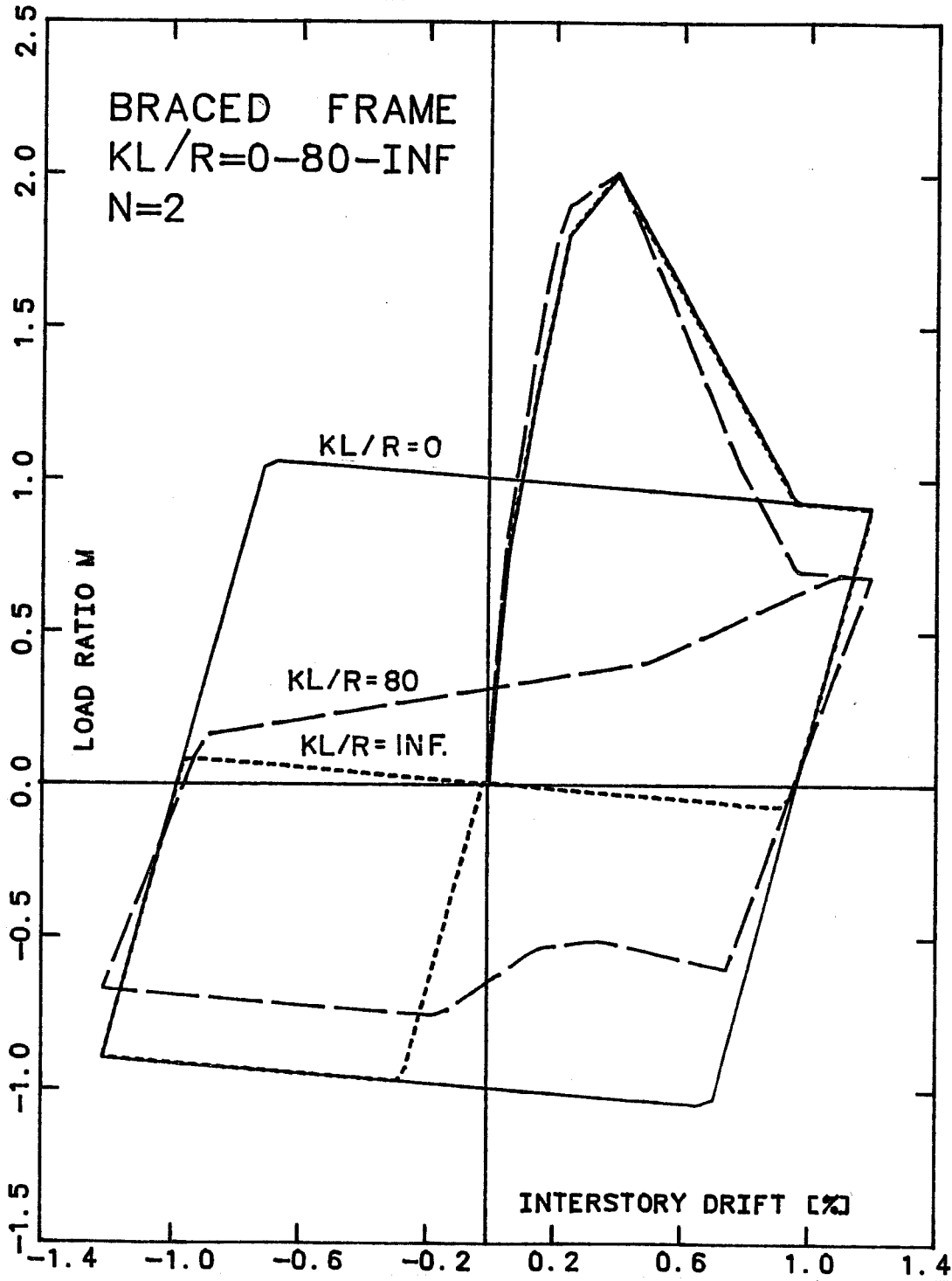


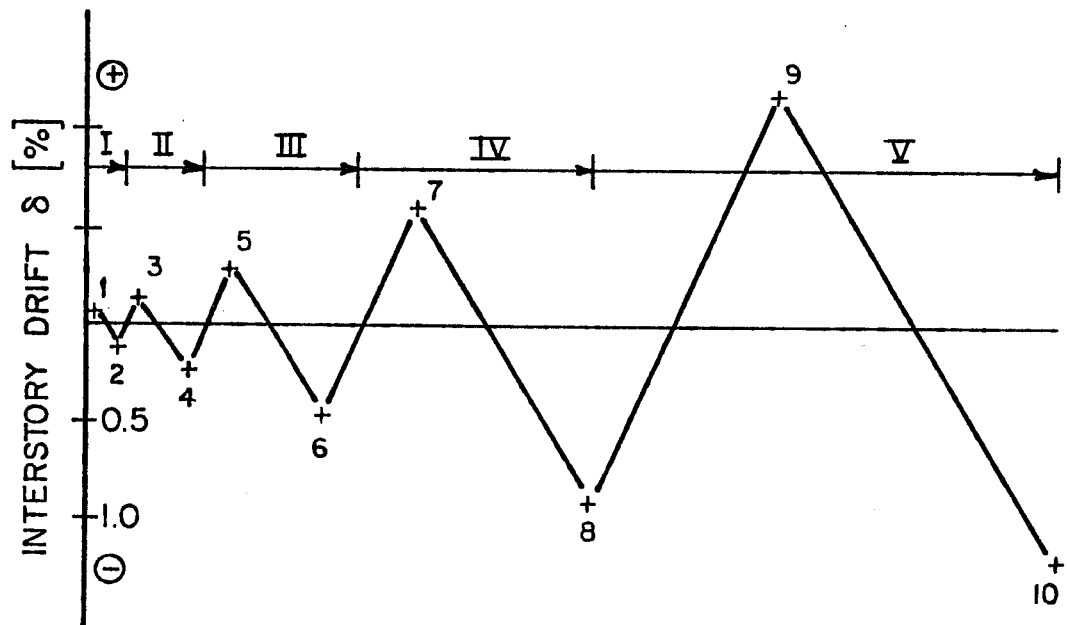
Fig. 6.2.10 Braced frame under reversed loading -  $n=2$ , and  $kl/r=0, 80$  and infinity

The unbalance in the forces of the tension and compression brace for  $kl/r = \infty$  generates a compression load in the column. The maximum extra column compression for the subassembly is  $(P_{yp} - P_{ync}) \sin \alpha$ . For  $kl/r = 0$ ,  $P_{yp}$  and  $P_{ync}$  are equal and their vertical components cancel each other. But for  $kl/r = \infty$ ,  $P_{ync}$  is zero so that the extra compression is  $P_{yp} \sin \alpha$ , which can be quite large and may overload the column.

### 6.3 Cyclic Loading

6.3.1 Development of the Inelastic Behavior. The response of the braced frame ( $n = 2$ ,  $kl/r = 80$ ) to the cyclic loading history of Fig. 6.3.1 is plotted in Fig. 6.3.2. Figures 6.3.3 and 6.3.4 show the contribution of the bare frame and the bracing system. As the peak drift is increased from cycle to cycle, there is a progression of inelastic behavior. This progression is followed below from one reversal point to the next.

- 1 : Column cracked in the positive direction.
- 2 : Column cracked in the negative direction.
- 3 : Spandrels cracked in the positive direction.
- 4 : Spandrels cracked in the negative direction; brace B1 buckled.
- 5 : Brace B2 buckled and brace B1 yielded.



CYCLE	PEAK INTERSTORY DRIFT $\delta$ [%]		LOAD REVERSAL
	$\delta^{\oplus}$	$\delta^{\ominus}$	
I	0.075	-0.113	1 2
II	0.150	-0.225	3 4
III	0.300	-0.450	5 6
IV	0.600	-0.900	7 8
V	1.200	-1.700	9 10

Fig. 6.3.1 Cyclic loading history

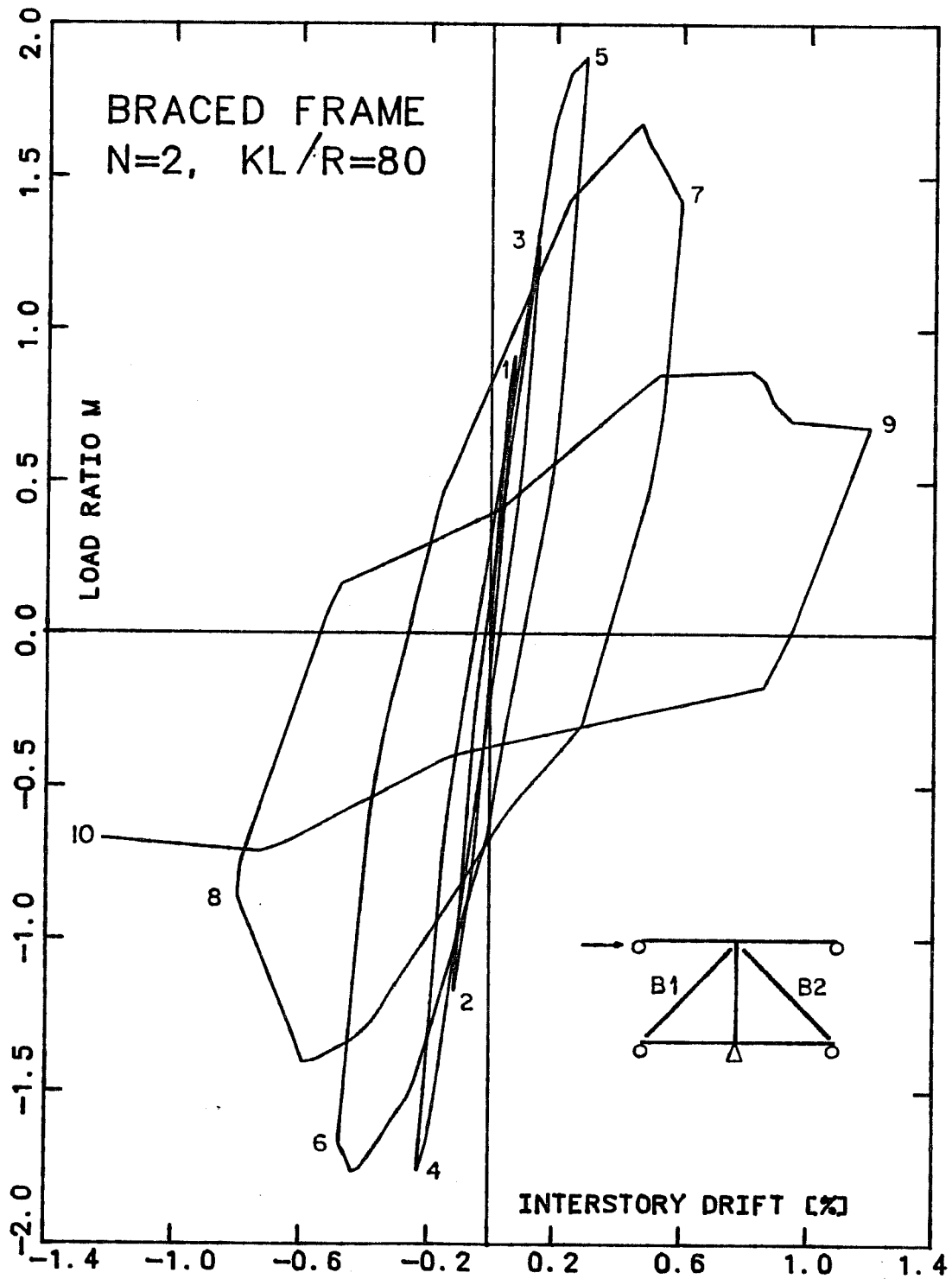


Fig. 6.3.2 Braced frame under cyclic loading

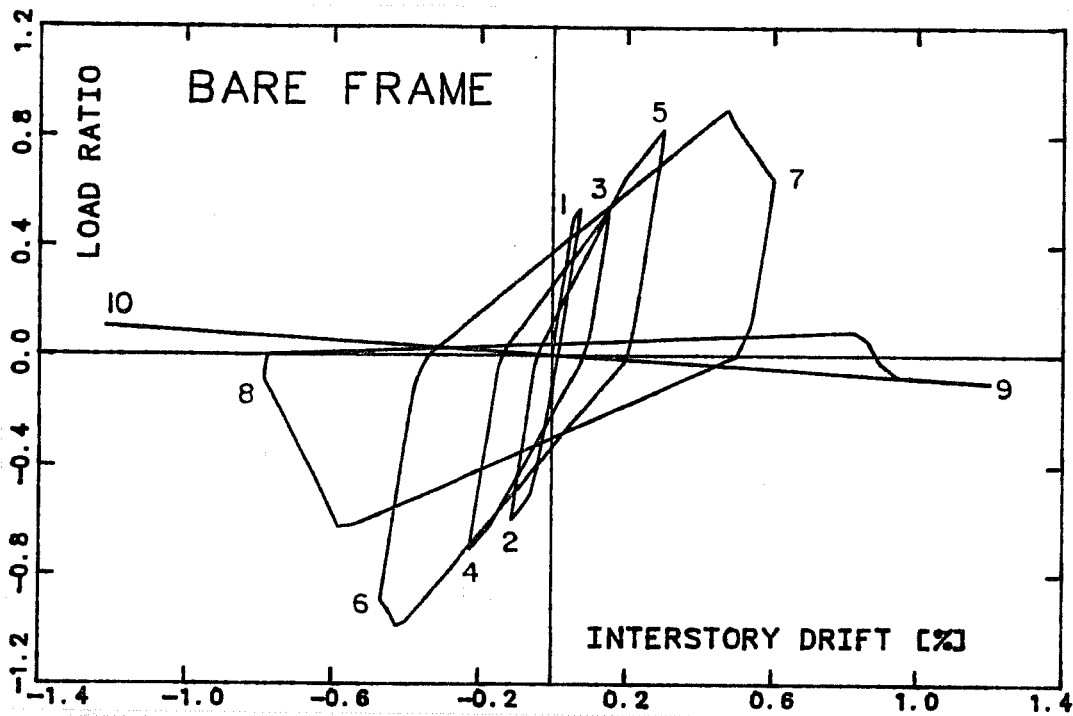


Fig. 6.3.3 Frame contribution under cyclic loading

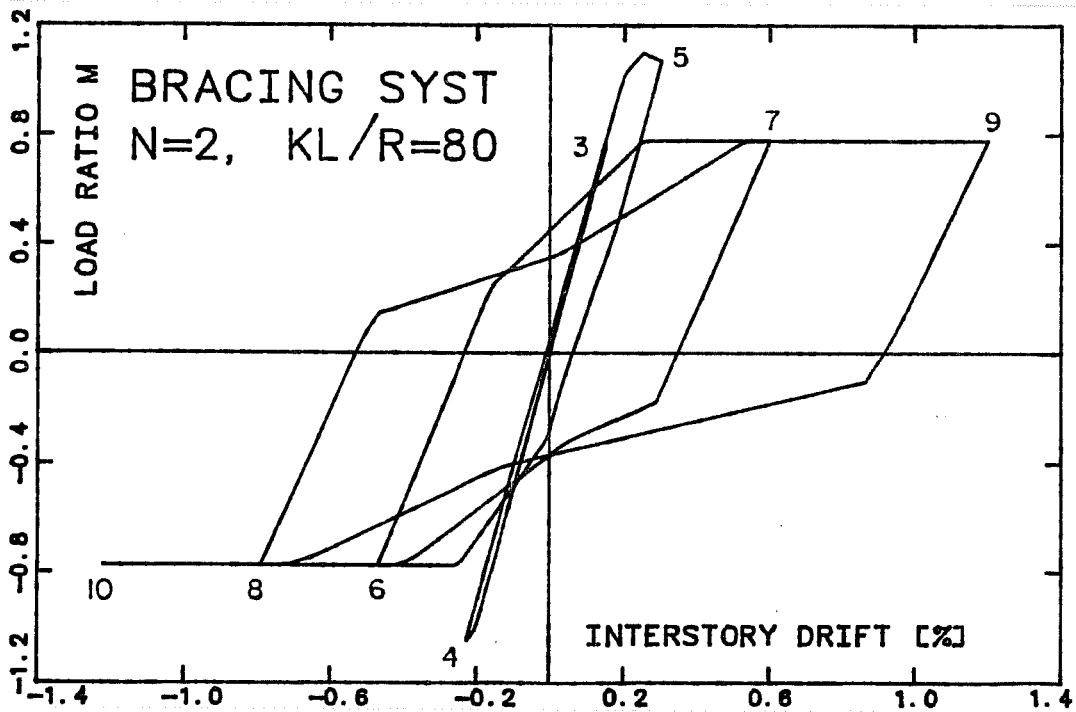


Fig. 6.3.4 Bracing system contribution under cyclic loading



- 6 : Column failed in negative direction; brace B1 buckled at post-buckling load level and B2 yielded.
- 7 : Column failed in positive direction; brace B2 buckled at post-buckling load level and B1 yields.
- 8 : Same as 6.
- 9 : Column lost all lateral strength, same as 7 for braces.
- 10 : Same as 9 for column; same as 6 for braces.

The hysteretic behavior of Fig. 6.3.2 has to be described as poor. From point 5 on, every cycle brings with it a substantial loss of strength and stiffness. This is no surprise when the response of the bare frame and of the bracing system are considered. The behavior of the bare frame (Fig. 6.3.3) is controlled by the column and is best understood by studying the hysteresis rule of element model EL7 for short columns (see Sec. A.1). The frame behavior is characterized by the rapid degradation of strength and stiffness of the column when it is cycled past the shear failure drift (0.40% in this case). The bracing system does not suffer as much degradation (Fig. 6.3.4). Once the braces have buckled more than once, the cyclic behavior is stable.

6.3.2 Variation of  $n$  and  $k\ell/r$ . The response of the braces to cyclic loading is plotted in Figs. 6.3.5 to 6.3.14 for nine combinations of  $n$  and  $k\ell/r$ . For better evaluation of the

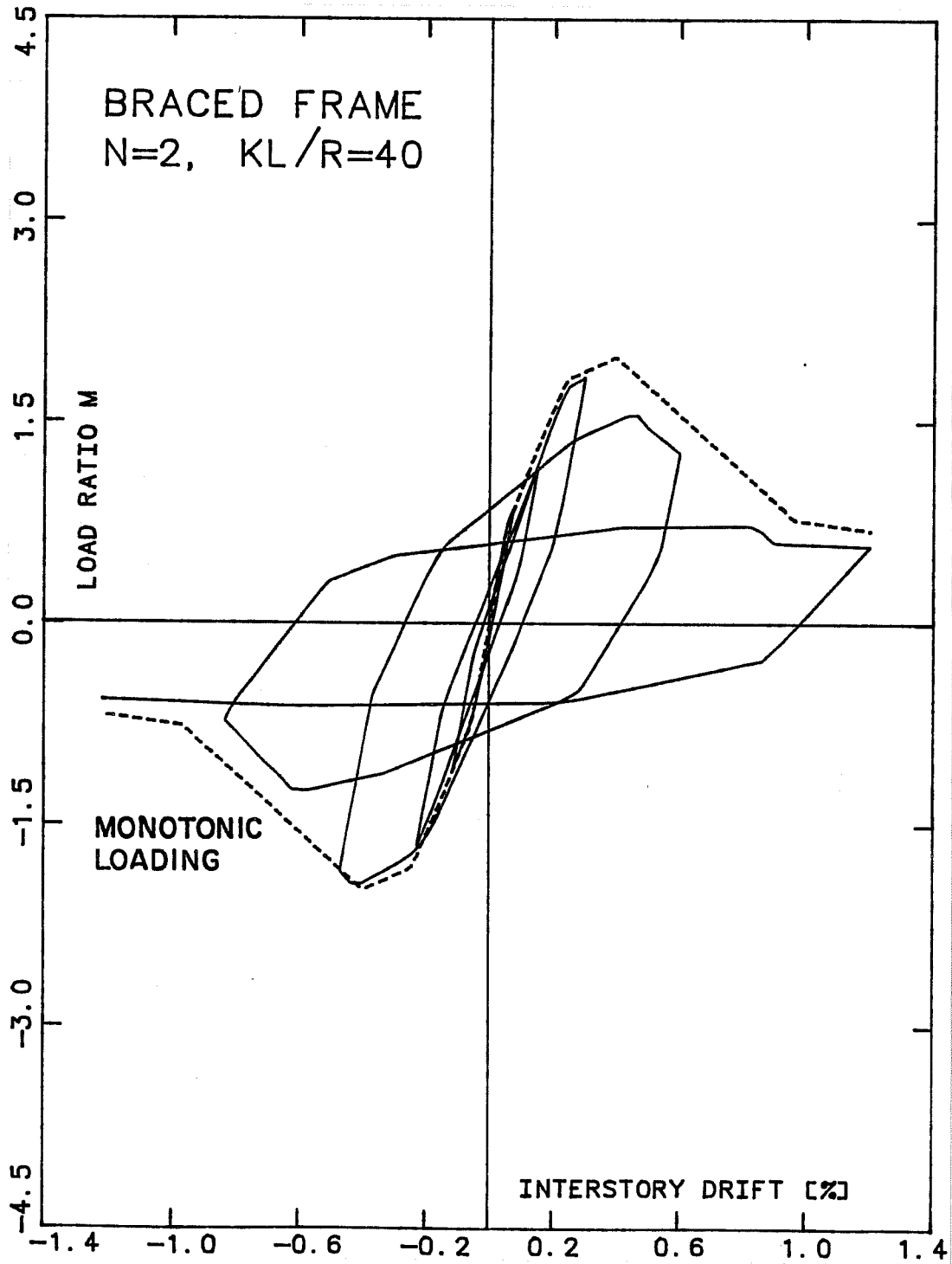


Fig. 6.3.5 Braced frame under cyclic loading  
-  $n=2$  and  $kl/r=40$

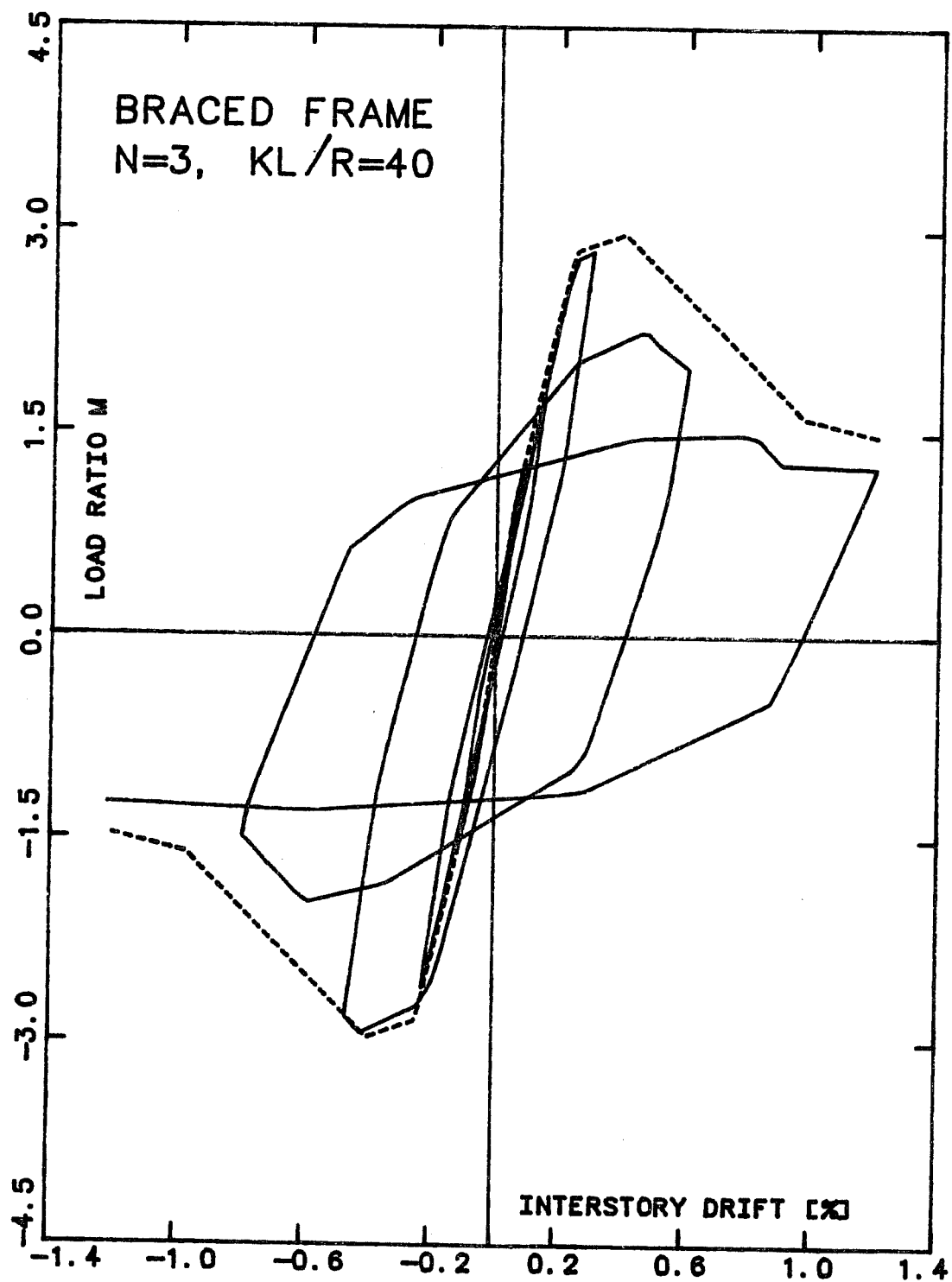


Fig. 6.3.6 Braced frame under cyclic loading  
-  $n=3$  and  $kl/r=40$

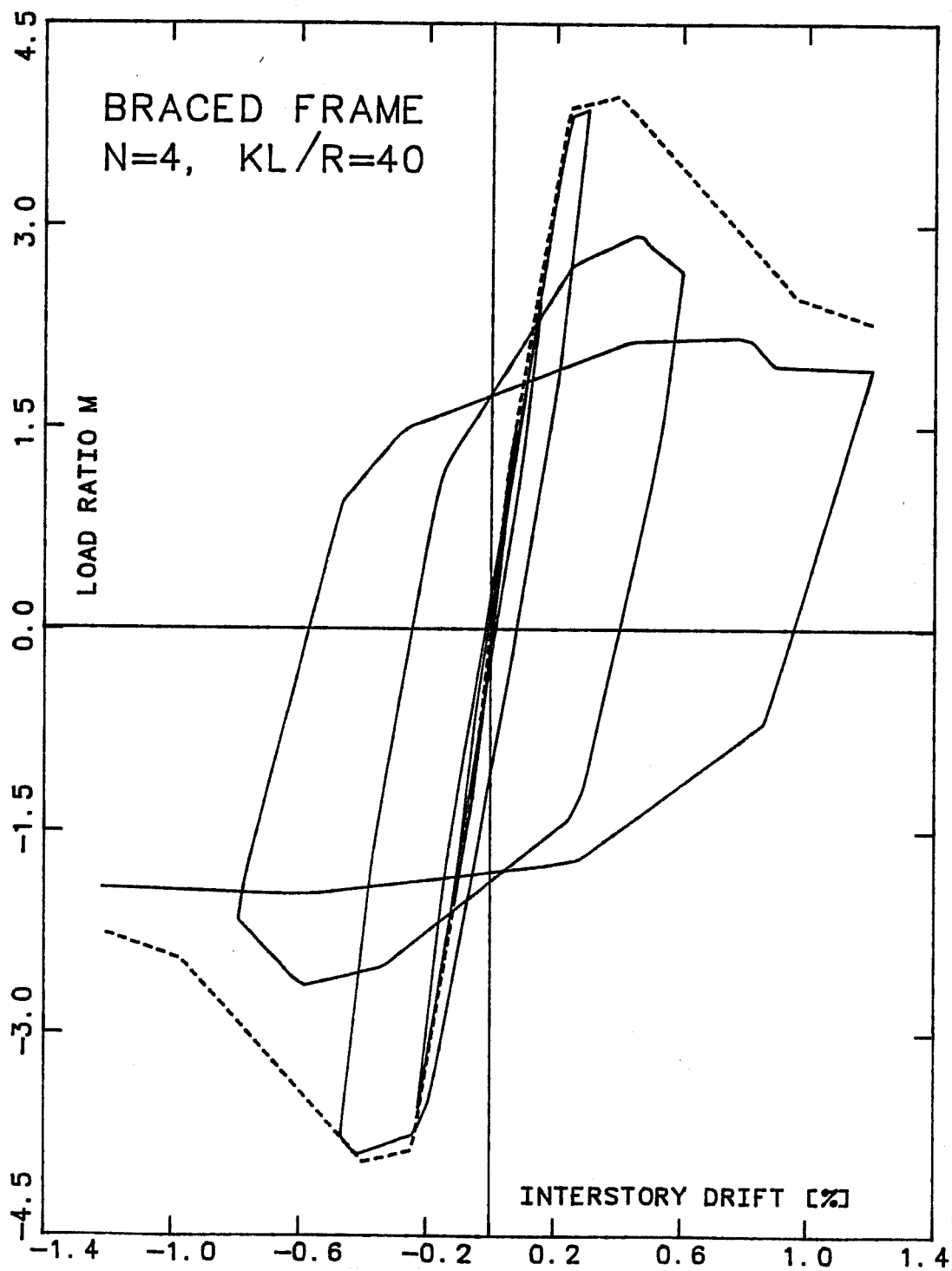


Fig. 6.3.7 Braced frame under cyclic loading  
-  $n=4$  and  $kl/r=40$

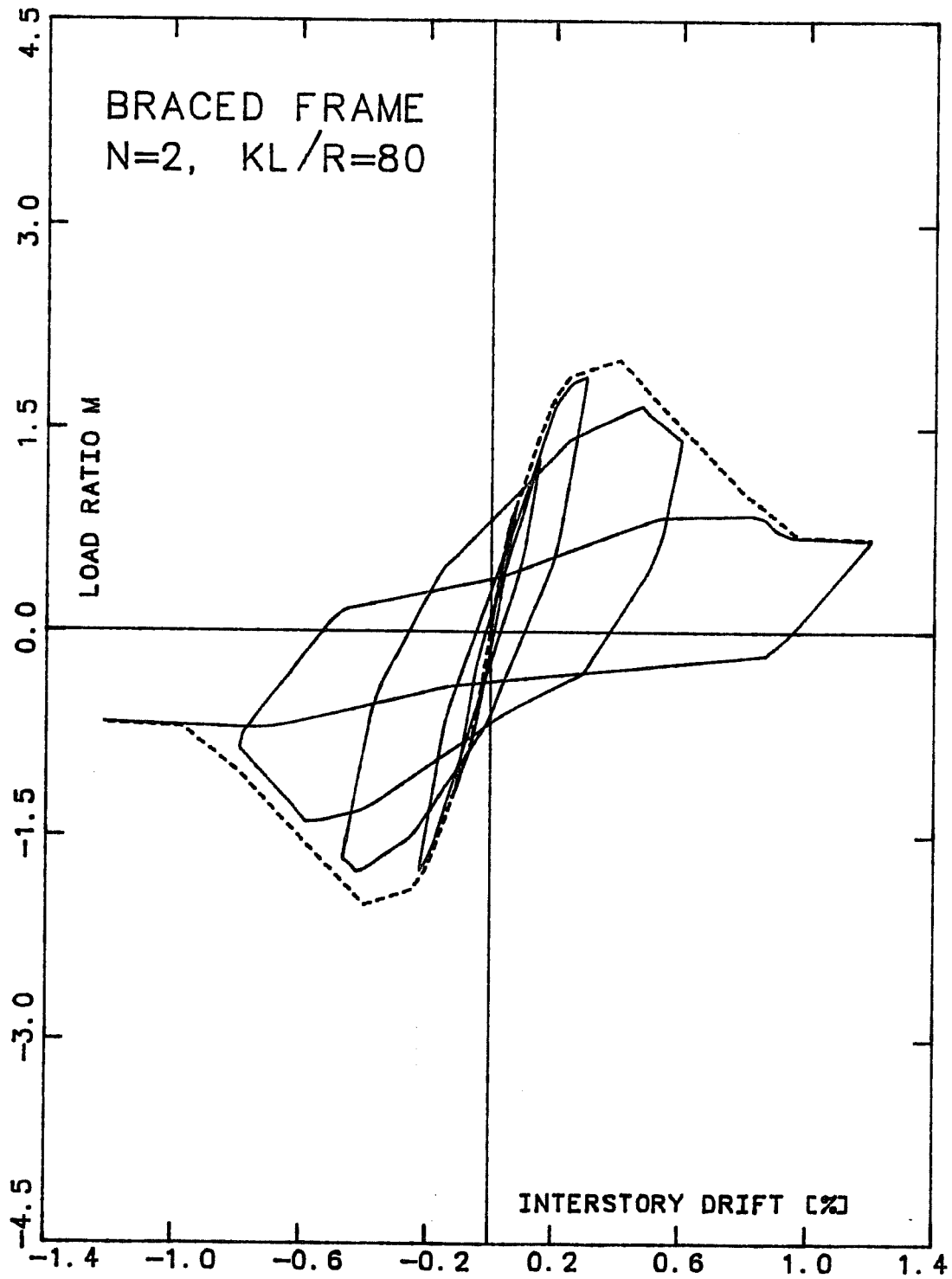


Fig. 6.3.8 Braced frame under cyclic loading  
-  $n=2$  and  $kl/r=80$

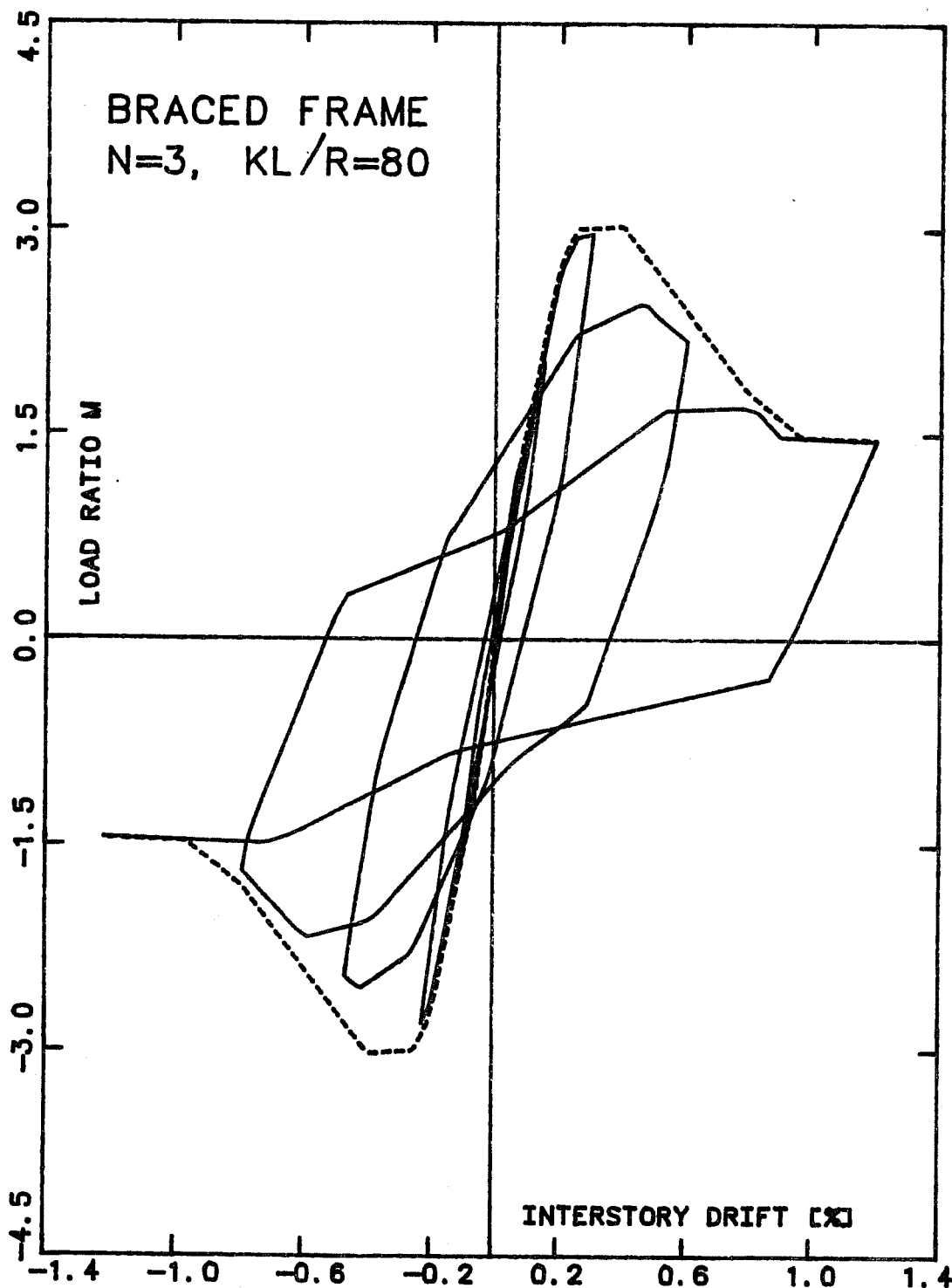


Fig. 6.3.9 Braced frame under cyclic loading  
- n=3 and kl/r=80

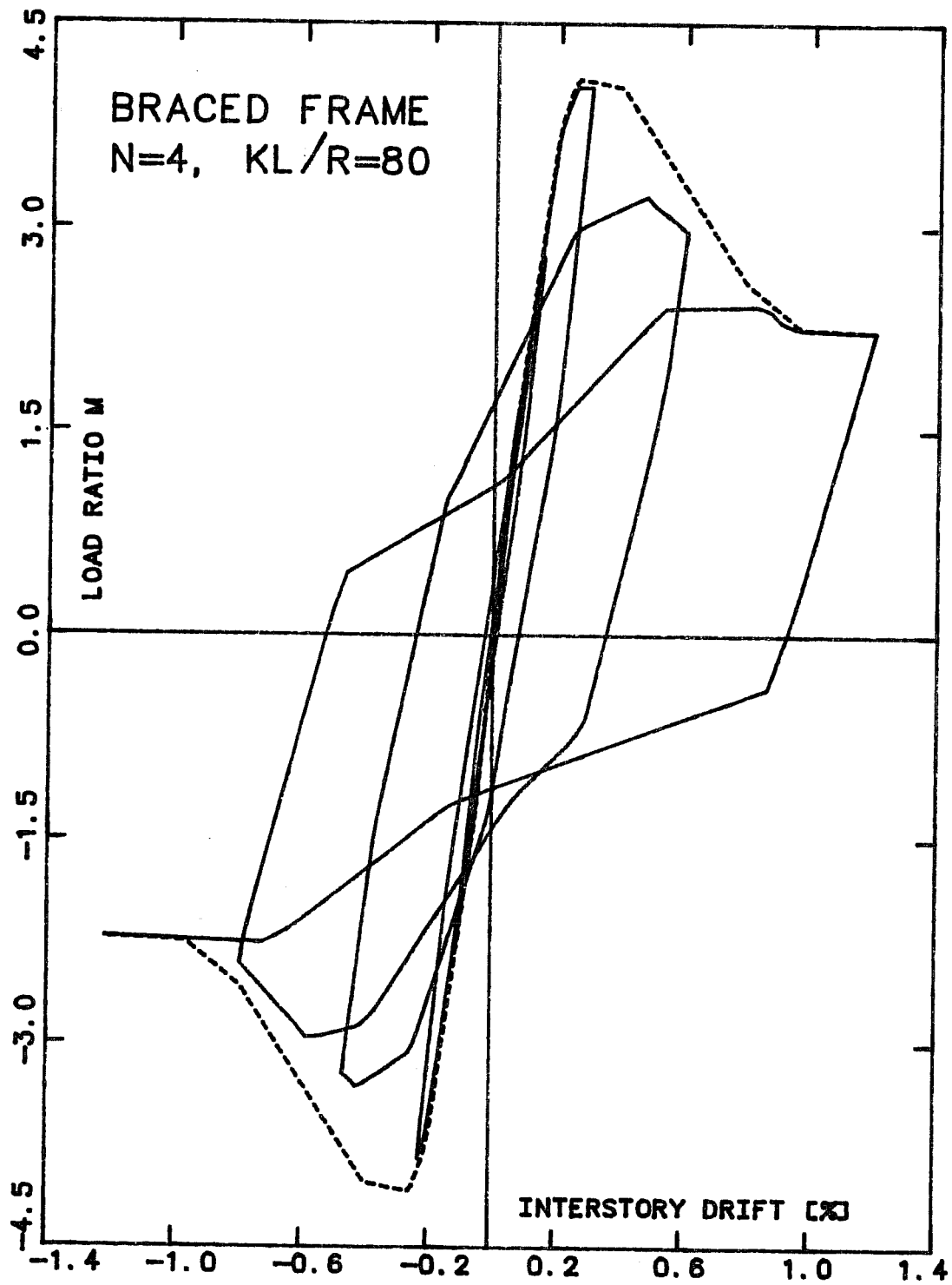


Fig. 6.3.10 Braced frame under cyclic loading  
-  $n=4$  and  $kl/r=80$

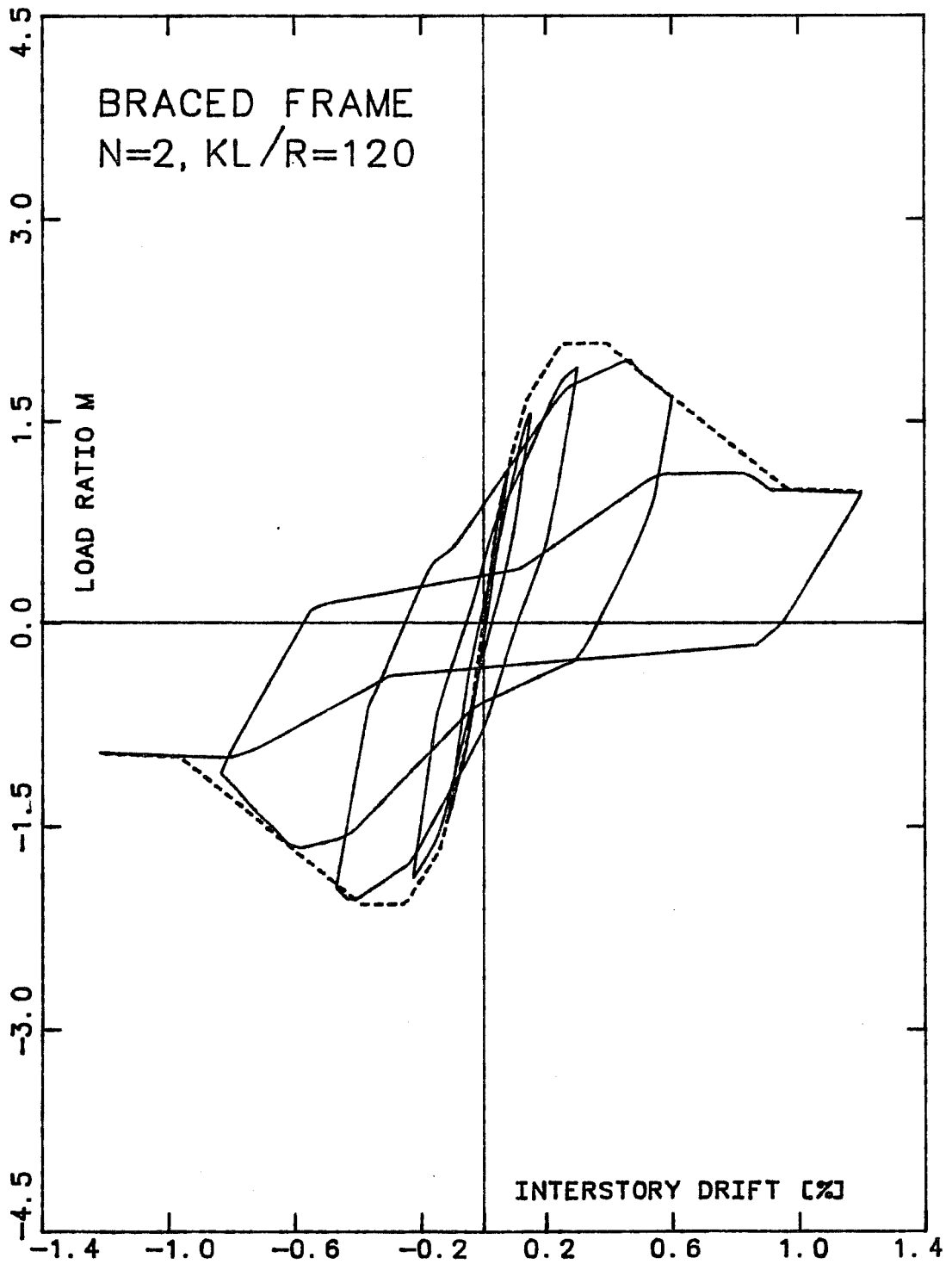


Fig. 6.3.11 Braced frame under cyclic loading  
-  $n=2$  and  $kl/r=120$



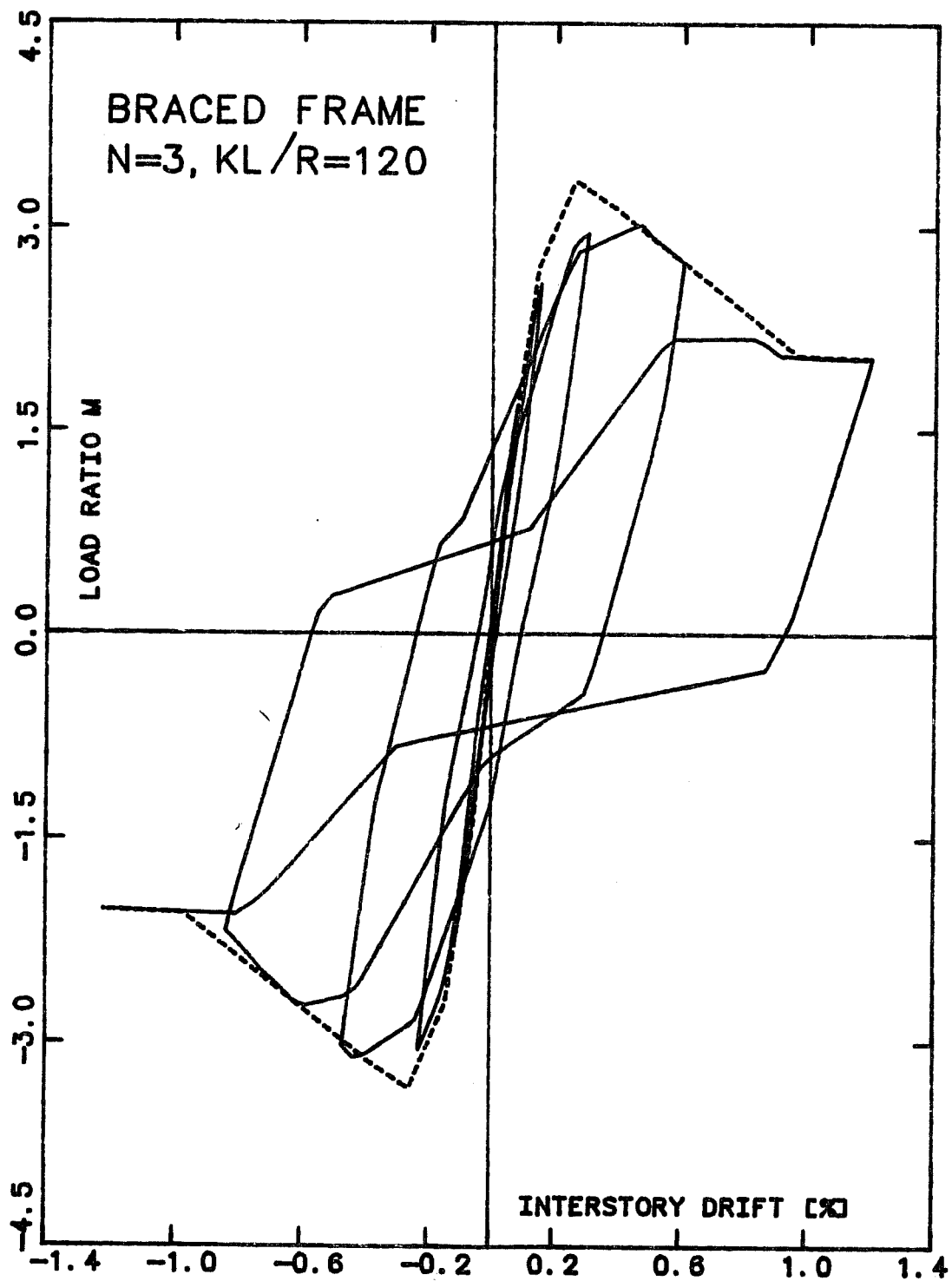


Fig. 6.3.12 Braced frame under cyclic loading  
-  $n=3$  and  $kl/r=120$

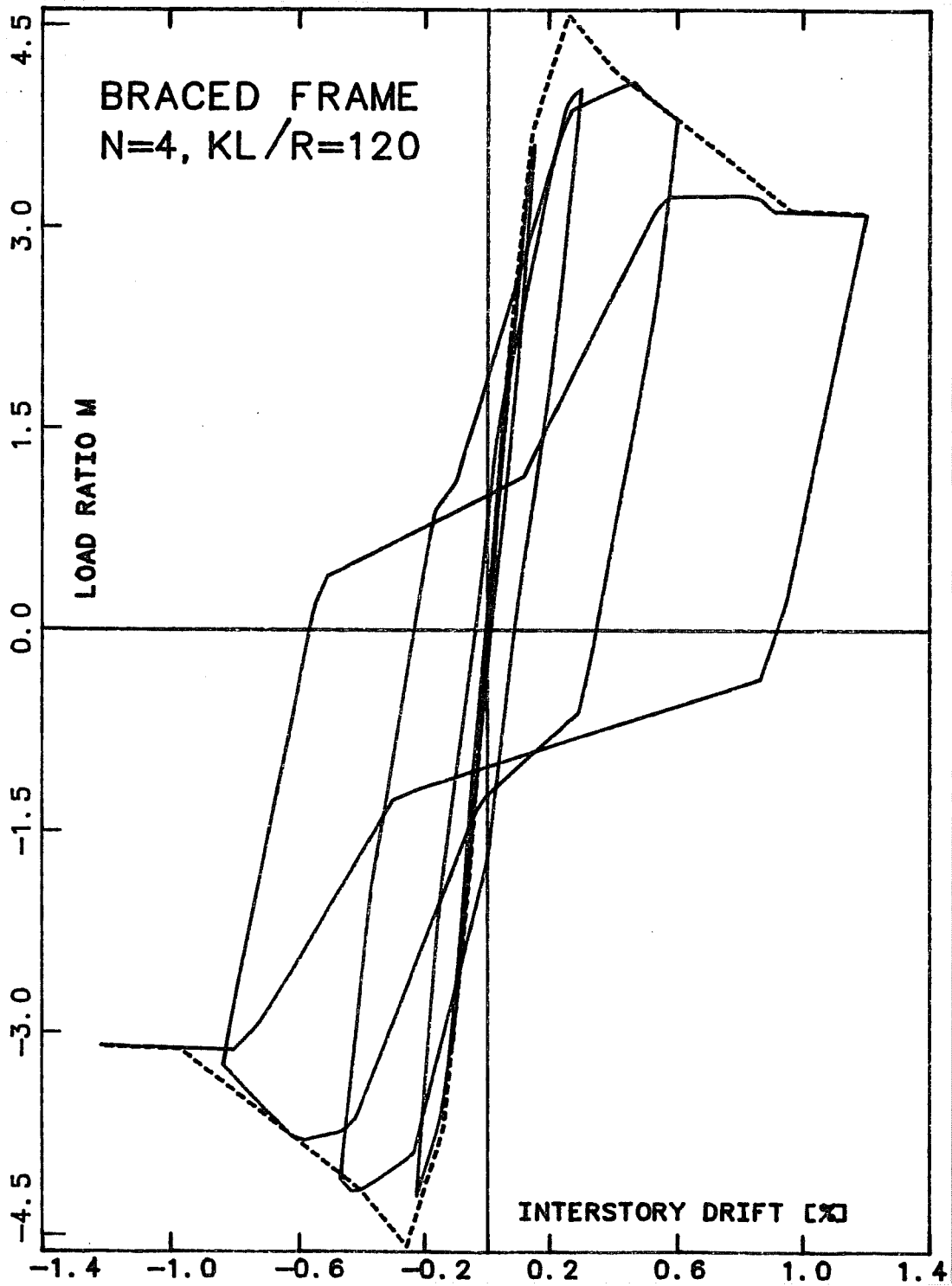


Fig. 6.3.13 Braced frame under cyclic loading  
-  $n=4$  and  $kl/r=120$

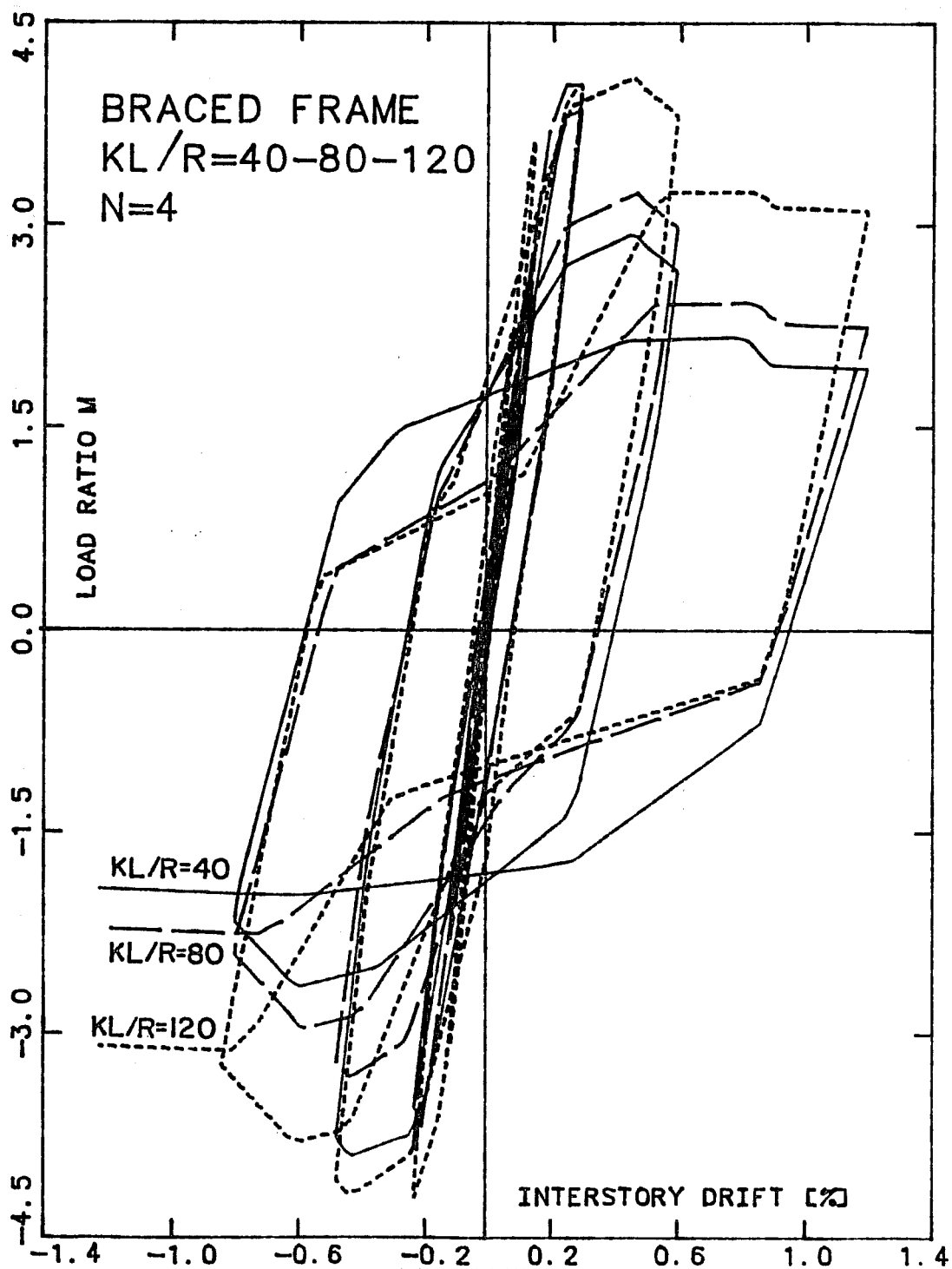


Fig. 6.3.14 Braced frame under cyclic loading  
-  $n=4$  and  $kl/r=40, 80$  and  $120$

effects of the cycling on behavior, the load-deformation curve under monotonic loading is included (see interrupted line). The envelope of the cyclic response follows the monotonic curve relatively closely. The largest difference is in cycles 4 and 5 for  $kl/r = 40$ , in cycle 4 for  $kl/r = 80$ , and in cycle 3 for  $kl/r = 120$ . Even more than under monotonic loading, the peak strength  $m^{\max}$  under cyclic loading matches the design strength ratio  $n$ . This is true for all three values of the slenderness.

With increasing  $n$  values, the loss of column strength and stiffness decreases in overall impact and the hysteretic behavior of the braced frame is more and more controlled by the bracing system. In Fig. 6.3.15, the last two cycles of the response for two values of  $kl/r$  are plotted together. The hysteresis loop for  $kl/r = 40$  is found to be significantly "fatter" than that for  $kl/r = 120$  which tends to exhibit a "pinching" behavior.

#### 6.4 Evaluation of the Steel Bracing Scheme

6.4.1 Introduction. The purpose of this section is to discuss the strengths and weaknesses of the bracing retrofitting scheme. The discussion is based on understanding gained from the parametric study (Secs. 6.1 - 6.3) and from the conceptual study (Chapter 3). The ability to improve the strength, stiffness, and ductility of the structure is evaluated and design

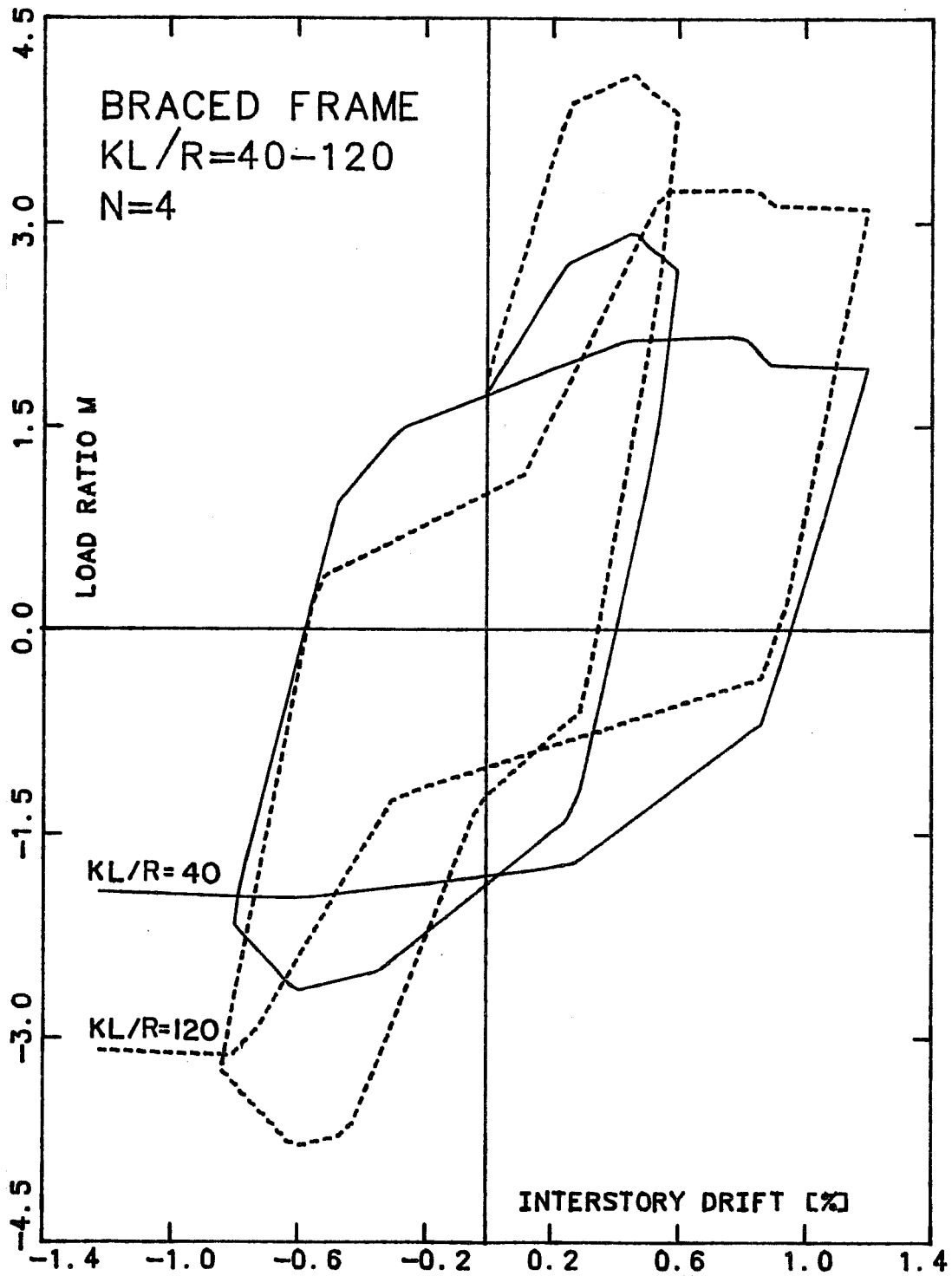


Fig. 6.3.15 Last two cycles of the loading history  
-  $n=4$  and  $kl/r=40$  and  $120$

implications are discussed. The discussion assumes a scheme with braces with a typical slenderness ratios, i.e. braces which carry substantial loads and buckle inelastically in compression.

6.4.2 Strength. The retrofitting scheme is very well-suited to improve the strength of a structure. The bracing system and the frame are basically two independent lateral resistance systems adding their strength and stiffness. The additional strength and stiffness increase is provided by a new system, which does not have to rely on the existing system. The level of strength or stiffness increase can be regulated with maximum freedom by the choice of the design strength or design stiffness for the bracing system. In the parametric study, the design criterion for the bracing system was strength and the desired level of strength was given by the ratio  $n$ . The peak effective strength was found to match the design strength for the braced frame, especially for the cyclic loading case.

Because the bracing system remains elastic almost up to its peak strength, the added strength is mostly in the elastic range. If the two systems are well-matched (see Sec. 3.6), the braced frame strength which can be mobilized without damage to the frame or the bracing system is close to the peak load. This is advantageous for the seismic performance of the retrofitted structure.

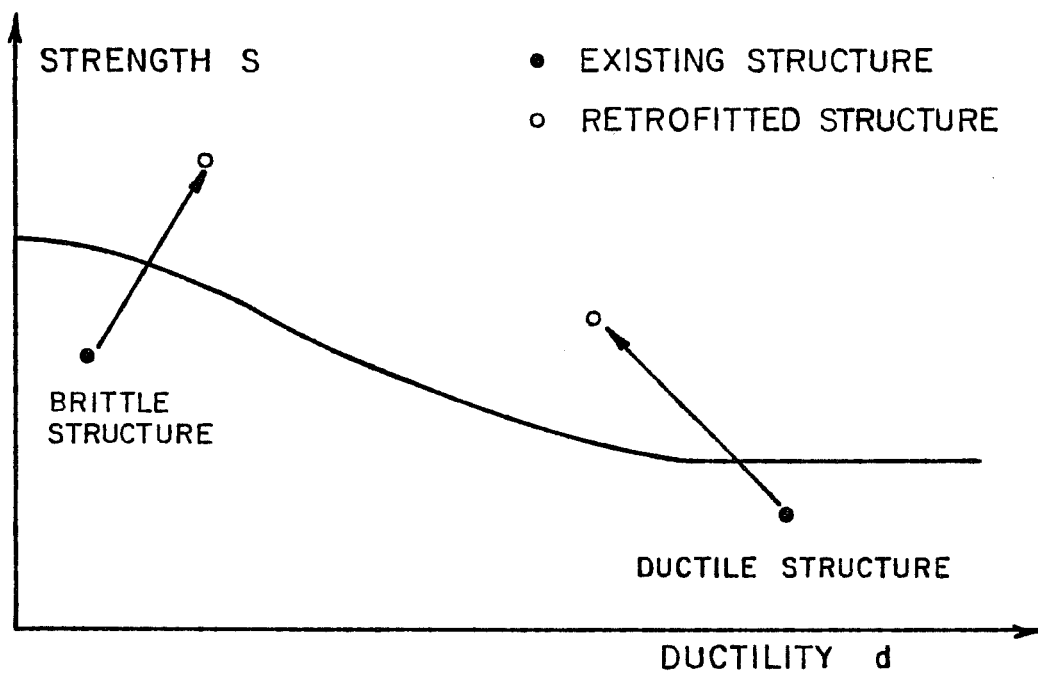


Fig. 6.4.1 Retrofitting with a steel bracing system

steel which yields. The limiting factor on the lateral deformation capacity of a braced frame with short columns may then be the loss of the vertical load-carrying function of the frame rather than failure of the bracing system (see discussion in Sec. 3.6).

6.4.5 Design Implications for the Bracing System. The major advantage of the bracing retrofitting scheme is its ability to increase the elastic strength and stiffness of the retrofitted structure. The ductility increase is significant if the scheme is used on a brittle structure. But unless inelastic buckling is prevented, the hysteretic ductility of a steel-braced frame has low reliability and should be evaluated conservatively. The retrofitting scheme is thus best-suited for retrofitting operations aimed primarily at strengthening and/or stiffening.

The braced frame should be designed elastically. The braces should not buckle inelastically in a design earthquake. It was shown in Sec. 3.3 that the elastic strength of a well-matched braced frame is not much smaller than the peak strength; it is thus not overconservative to design the bracing system elastically. The braced frame hysteretic behavior in the inelastic range may not be ideal but the frame can be prevented from entering the inelastic range because high elastic strength is provided.



If the retrofitted structure is to remain in the elastic range, it must be designed using the seismic forces for a strength reliant structure. Those forces are higher than if inelastic behavior is allowed and ductility can be counted on in design (see Sec. 3.5). This, however, is largely compensated for by the advantages of keeping the structure in the elastic range. First, structural damage is prevented and the strength and stiffness degradation linked with the cycling of the structure in the inelastic range is avoided. Second, the deformations are limited, and nonstructural damage is likely to be minimized. One school of thought in earthquake engineering even suggests that all structures should remain elastic for the design earthquake. The idea is that ductility may well prevent the collapse of the structure, but is not adequate in terms of usability after the earthquake. Prevention of collapse, which aims at preserving life is only one of the requirements for a structure. Engineers are increasingly coming to the realization that many structures need to satisfy more stringent seismic performance requirements, even (or especially!) in a strong earthquake. There is a growing class of buildings for which very little, if any, damage to the structure itself or the activities, processes or installations it supports, is acceptable. This class of building includes, for example, hospitals, industrial complexes and information processing centers (computers) which are vital to the functioning

of society and thus have a very short or no acceptable "shut down time." Some defense installations could be classified in the same group, because they are vital to military readiness. Also, many industrial installations must be designed for very low damage levels because of the potential for environmental disaster in case of damage. In an increasingly technical society, there are more and more buildings in which the "structural component" should not be the weak link in terms of operational safety. The cost of "maximum seismic safety" is small in comparison to the economical, societal, military, or environmental importance of their safety. Clearly, such buildings should be designed for elastic behavior and with narrow drift control criteria. Because of its ability to increase the elastic stiffness and strength of a structure, the steel bracing scheme may be especially well-suited for retrofitting of existing buildings of this type.

In summary, the steel bracing scheme can be used to produce structures which can meet a wide range of seismic performance requirements based on strength and/or stiffness. It can be used for preventing collapse and is also well-suited for more demanding retrofitting tasks such as drift control. Two characteristics of the bracing system combine to produce this versatility. First, most of the strength and stiffness added by the bracing system is elastic. This is "quality" increase in

strength and stiffness because it can be mobilized without damage. Second, the level of strength and stiffness increase can be set with maximum freedom because it is introduced by a new system, the bracing system, which is basically independent from the existing one in its lateral resistance mechanism.

## 6.5 Prevention of Inelastic Buckling

6.5.1 Introduction. The buckling of the compression brace is the primary obstacle to good hysteretic ductility of a braced frame. The negative effects from inelastic buckling can be alleviated by using braces with either a very low or a very large slenderness ratio. Figure 6.5.1 shows qualitatively the hysteretic behavior of a steel brace as  $kl/r$  is varied from zero to infinity. If the slenderness ratio is very low, the brace compression yield load is lower than the buckling load and inelastic buckling is prevented. If the slenderness ratio is very high, such as in cables, the brace buckles elastically and inelastic buckling is prevented also. Those two approaches to buckling prevention are discussed in Secs. 6.5.2 and 6.5.3.

6.5.2 Very Low Slenderness. The parametric study confirms that low brace slenderness is advantageous for hysteretic behavior. The designer of the bracing system should thus keep the unbraced length of the braces as short as possible. If the slenderness ratio is low enough, the brace yields in

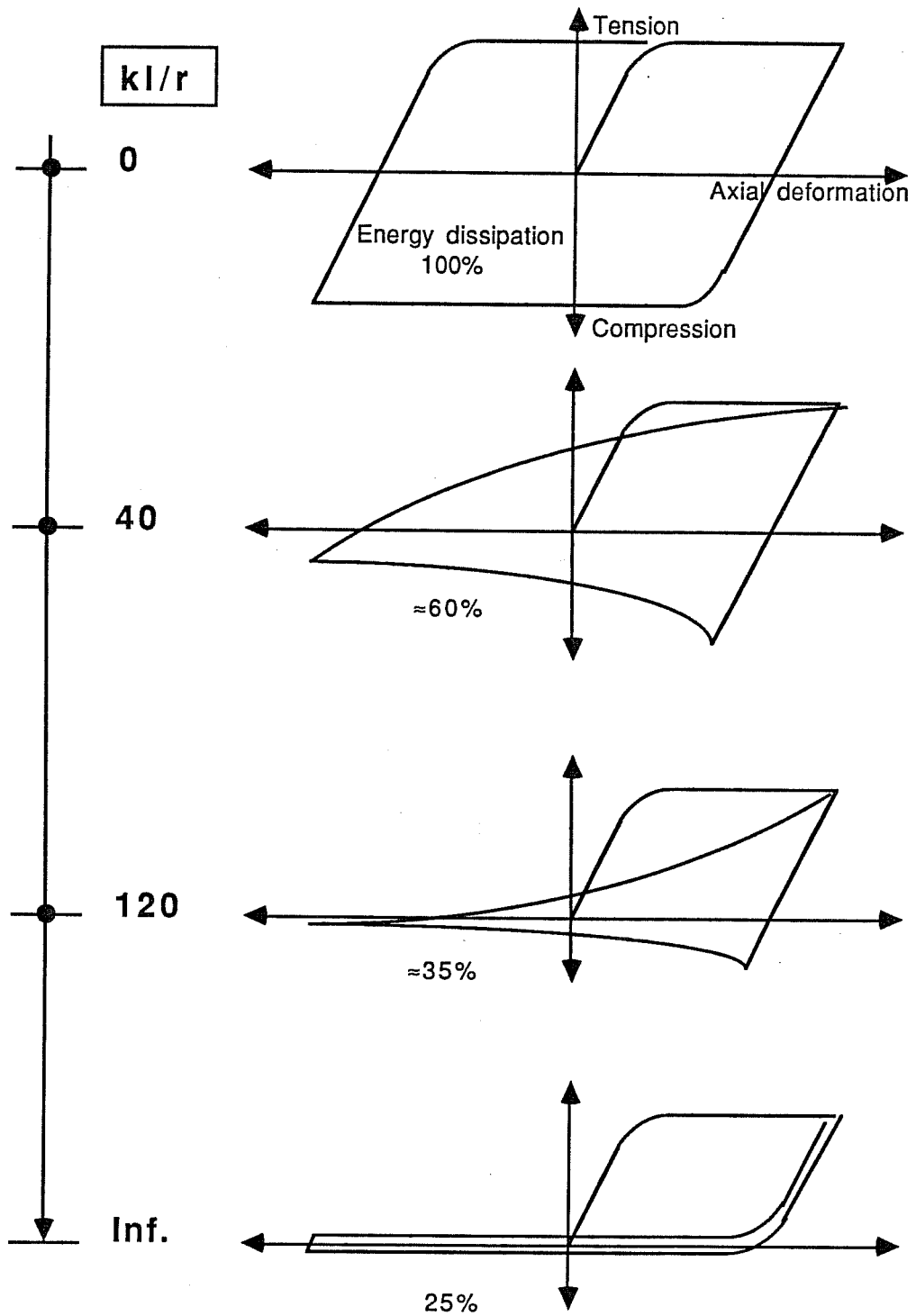


Fig. 6.5.1 Qualitative influence of brace slenderness ratio  $kl/r$  on hysteretic behavior

compression rather than buckles. The bracing system displays favorable hysteretic behavior, as illustrated by Fig. 6.2.8 for the  $kl/r = 0$  case. In a typical retrofitting, however, it is not possible to brace the diagonal elements closely enough (in-plane and out-of-plane) to fully prevent buckling.

So-called "fused braces" have been proposed for new buildings. Such braces feature a friction device designed to "slide" at a load smaller than the buckling load. The brace is prevented from buckling in compression and yielding in tension. The inelastic behavior is limited by the friction device. Tests [32] on braced steel frames with "fused braces" showed that excellent hysteretic behavior (energy dissipation) can be achieved but the cost effectiveness and reliability of using the system is unproven, both for new structures and for retrofitting operations.

6.5.3 Very Large Slenderness Ratio. High  $kl/r$  values normally result in bracing systems with undesirable inelastic hysteretic behavior. The low buckling load means (1) low energy dissipation capacity (see Fig. 6.2.9 for a braced frame with  $kl/r = \infty$ ) and (2) large inelastic buckling deformations which may produce failure under cyclic loading. But if cables are used, buckling is elastic and nondestructive, and the second problem disappears. Using cables for bracing existing reinforced concrete frame structures is an idea which needs experimental

investigation, especially in regard to energy dissipation. To guarantee maximum energy dissipation, the cables should yield in as many locations as possible when the braced frame is subjected to large lateral deformations. The cables should, therefore, be bonded to the frame at intervals over the building height, at every story for example. This would, however, increase the construction effort and make replacement of the cables more difficult. Construction and replacement may be simplified if threaded bars, which can be connected to one another and to the frame with a mechanical coupling device are used instead of cables. These anchors could be placed at every story to increase yielding of the tension bars when the braced frame deforms inelastically. It would be necessary to guarantee that the bars behave like cables, i.e. that they buckle without damage.

The cables could be prestressed to increase the initial stiffness of the bracing system. Stiffening is generally desirable since it limits drifts. Figure 6.5.2 shows the braced frame forces generated by prestressing the cables with a force  $P$ . Shifting the axis of the load-deformation curve of the cables associated with the prestressing is illustrated in Fig. 6.5.3. The prestressed cable has an apparent compression strength equal to the prestressing force,  $P$ , and an apparent yield strength in tension equal to the yield strength  $P_{yp}$  minus the prestress force

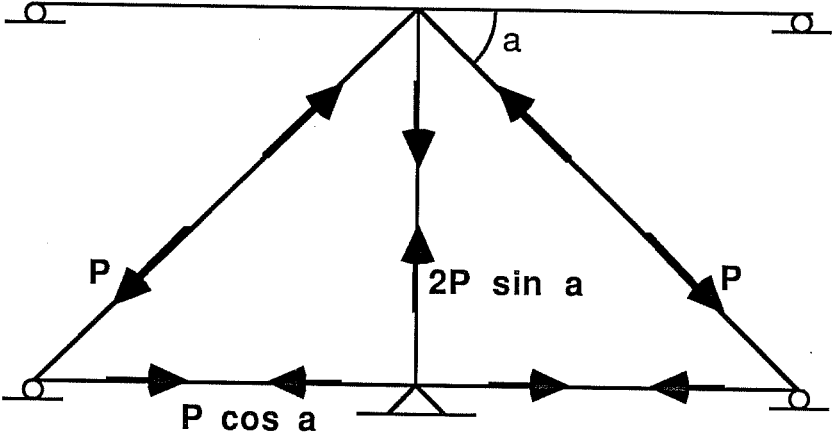


Fig. 6.5.2 Prestressing forces in the braced frame

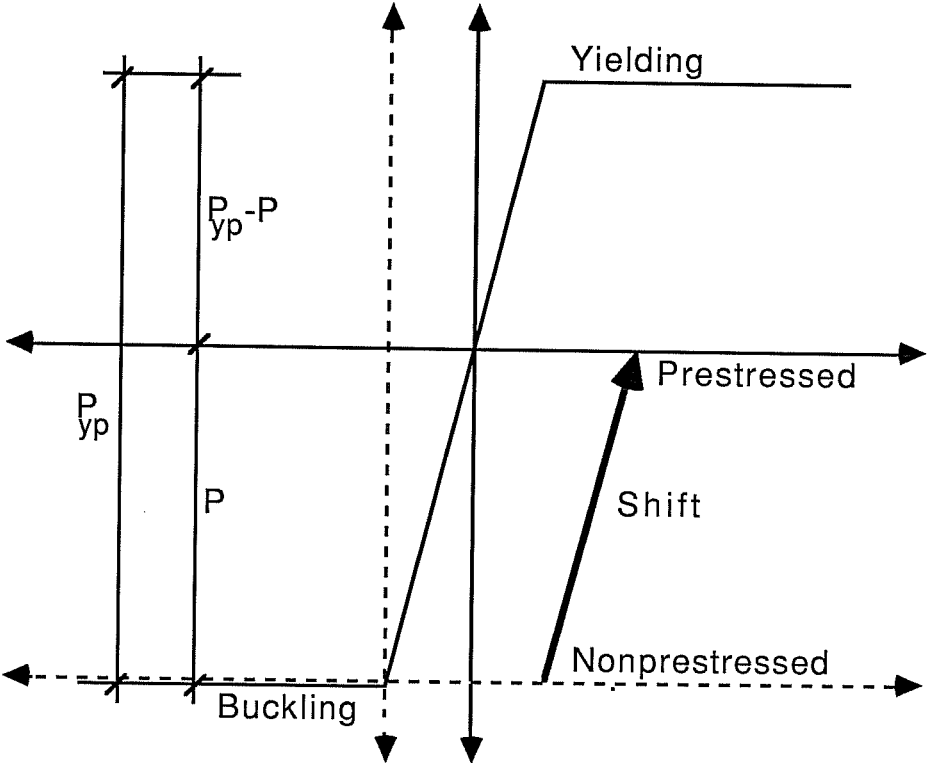


Fig.6.5.3 Load deformation curve for a cable, nonprestressed and prestressed

P. The brace initial stiffness is thus the same in compression and tension.

The influence of prestressing on the bracing system load-deformation curve is shown in Fig. 6.5.4 for  $P = 0.4 P_{yp}$ . Through prestressing, the load producing buckling of brace B2 is shifted from 0 to  $2P \sin \alpha = 0.8 P_{yp} \sin \alpha$ . In the load range between 0 and  $2P_{yp} \cos \alpha$ , both braces B1 and B2 contribute to the lateral stiffness of the bracing system which is, therefore, double that of the unstressed case. If the load is increased beyond  $0.8 P_{yp} \sin \alpha$ , the stiffness is reduced by half because the compression brace is buckling. Prestressing does not change the bracing system ultimate load; tension brace B1 yields when  $P_{yp} \cos \alpha$  is reached.

The optimum prestressing level  $P$  for the cable is half the yield strength  $P = 0.5P_{yp}$  (actually somewhat more because of relaxation of the prestress). With such a prestressing level, brace B1 yields and B2 buckles simultaneously when the bracing system ultimate load is reached. The bracing system lateral stiffness is thus double that of the unstressed case over the entire elastic range.

If the cables are prestressed, the effect of the resulting compression forces in the reinforced concrete beams and columns must be considered (see Fig. 6.5.1). The compression is generally welcome in the beams. In the columns it depends on the



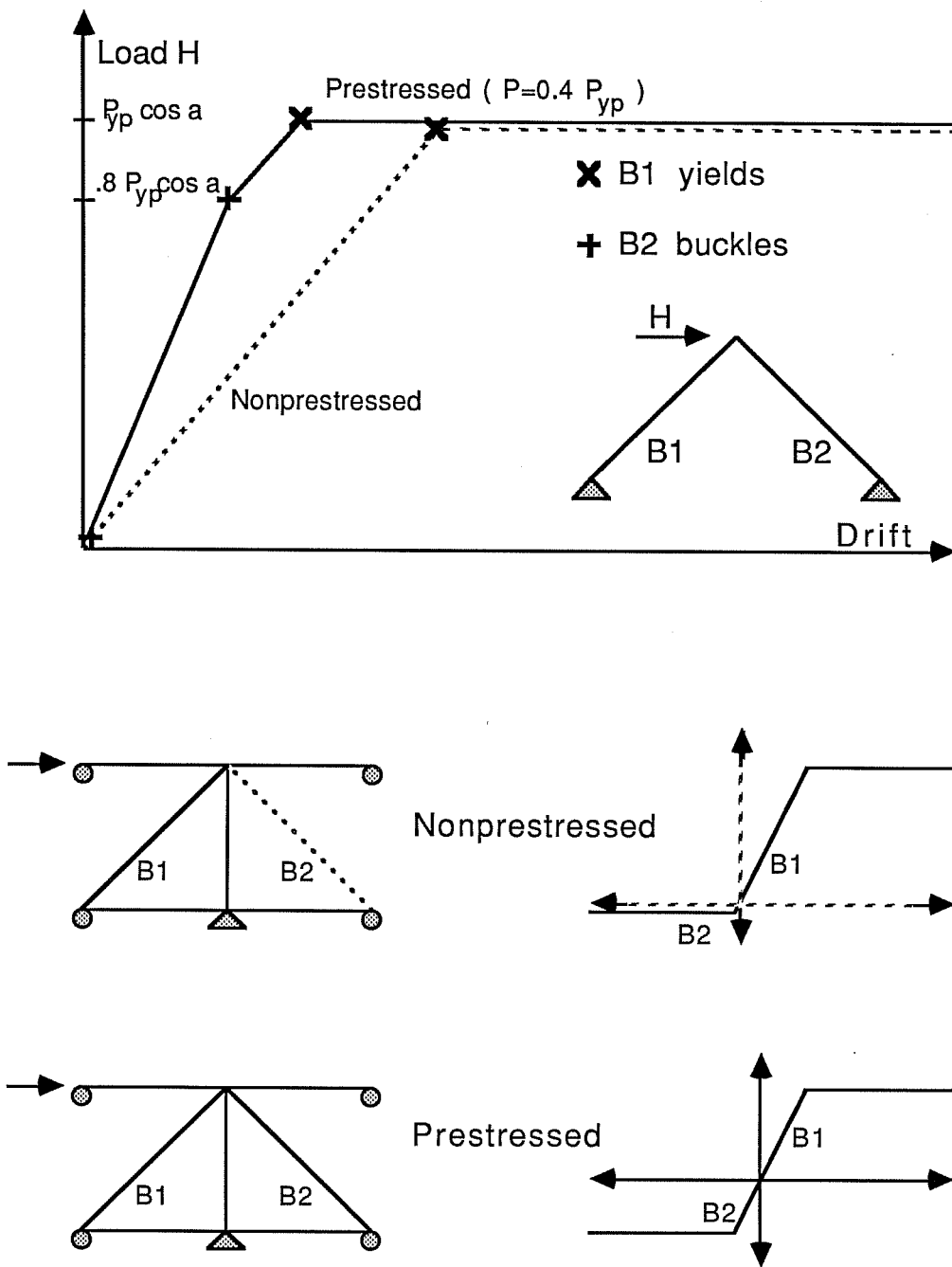


Fig. 6.5.4 Effect of prestressing

level of compression from gravity loads. The additional compression is generally favorable, but if the compression from gravity is high (above balance load) the columns could be overloaded. In such a case, the columns should be strengthened. The extra compression could be reduced by reducing the prestress. But the column compression from prestressing cannot exceed the compression generated in the column in the unprestressed case when a lateral drift is imposed which brings the tension brace to yield. If the column is overloaded by prestressing the braces, it would be overloaded if the unprestressed bracing system enters the inelastic range. The difference is that the additional compression is permanent in the prestressed case while it only appears under lateral loading in the unprestressed case.

The use of cables (or threaded bars) seems to have potential, especially for interior frames. The advantage of the cable is elastic buckling, which does not create the problems encountered under repeated cyclic loading when using braces which buckle inelastically. Using braces may also simplify construction and open the possibility of using high strength material.

The behavior of the braced frame in the elastic range can be improved by prestress of the cable, It should however not be overlooked that the favorable effect of prestressing is lost if the inelastic range is ever entered, because once the cables

yield, the prestress is lost. The weakness of a cable system is the low energy dissipation capacity under cyclic inelastic deformations (see comparison of bracing system with  $k\ell/r = 0$  and  $k\ell/r = \infty$  in Section 6.2.4).

## CHAPTER 7

### BEAM WEAKENING IN FRAMES WITH WEAK COLUMNS

#### 7.1 Introduction

The seismic performance of a steel braced reinforced concrete frame at ultimate depends on the failure mechanism of the frame. The prototype frame for this study is an example of a frame with an undesirable failure mechanism. The failure of the frame is controlled by weak short columns which fail in shear at a drift of about 0.5%. Beyond that drift the frame rapidly loses lateral capacity and damage to the columns also reduces the vertical carrying capacity. The key to a favorable failure mechanism of multistory frames under lateral loading is to force failure away from the columns into the beams. Such a frame is called a strong column - weak beam frame. Figure 7.1.1 shows the difference in failure mechanism between a strong column - weak beam frame, and a weak column - strong beam frame. The energy dissipation is significant if plastic hinges develop in the beams rather than in the columns. Also, if the inelastic behavior is limited to the beams, the columns are able to carry the vertical loads even under large lateral drifts. Weak column-strong beam frames are often seismically inadequate and in need of seismic retrofitting. Bracing such frames improves the lateral strength and stiffness but not the failure mechanism of

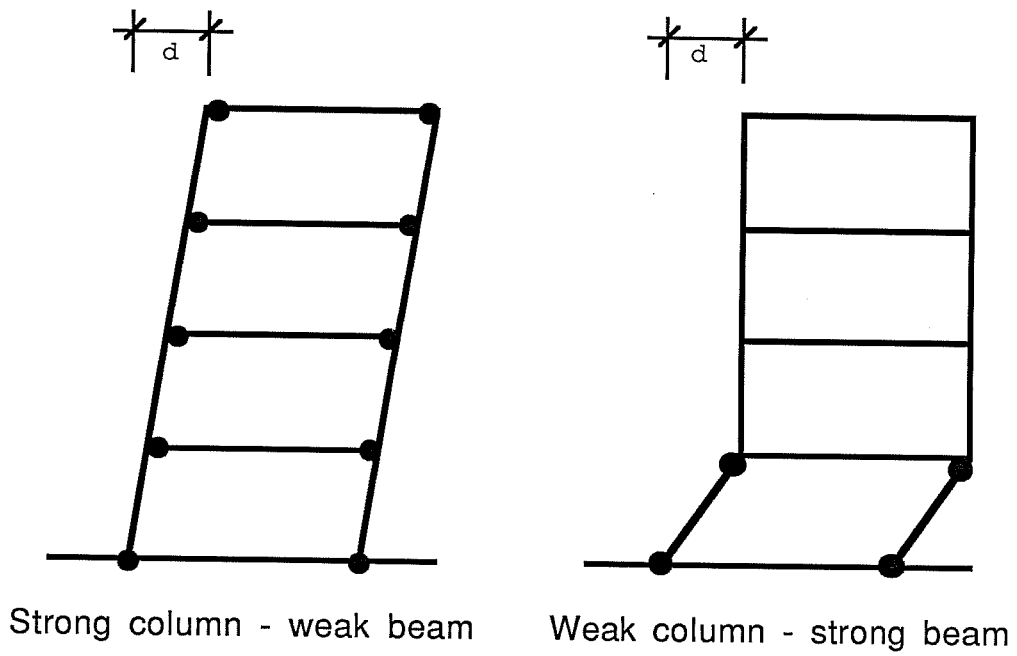


Fig. 7.1.1 Frame lateral failure mechanism

the frame. The bracing system can be made strong and stiff enough to prevent the frame from reaching drift levels which would produce failure under a design earthquake. However, the random nature of seismic loading demands that the failure mechanism be acceptable in an earthquake larger than the design one.

It is, therefore, interesting to consider complementing the bracing of a weak column - strong beam frame with measures to improve its failure mechanism. The aim of such measures should be to move failure away from the columns into the beams, i.e. to transform the frame into a strong column - weak beam frame. This can be achieved either by strengthening the columns or by weakening the beams. Strengthening the columns has the added advantage of increasing the lateral strength and stiffness of the frame. In the case of a retrofitting scheme using a bracing system, this increase has relatively little value, since the bracing system can be designed to provide almost any desired level of lateral strength and stiffness increase at little extra cost. In combination with providing bracing, weakening the beams is usually an attractive improvement measure because it is much easier to carry out than column strengthening.

The object of this chapter is to investigate the idea of combining bracing of reinforced concrete frames with weak columns with weakening of the beams. The prototype structure is used for

the case study. The bracing of a frame with strong columns and weak beams complements the study of Chapter 6 in which the behavior of braced frames with weak short columns was studied. Frames with strong columns typically exhibit adequate ductility, but may need to be braced for inadequate strength and/or stiffness.

## 7.2 Weakening Parameters

7.2.1 Conceptual Representation of the Idea. The retrofitting of the Sendai School Building (see Sec. 1.3.2) is a practical example of combining bracing of a weak column - strong beam frame with weakening of its beams. The idea is illustrated in Fig. 7.2.1 using the representation developed in Section 2.4. The original frame is seismically inadequate both in strength and ductility. In retrofitting approach II, bracing of the frame is preceded by weakening the beams. The beam weakening transforms the brittle weak column - strong beam frame into a ductile strong column - weak beam frame. The lateral strength of the altered frame is lower than that of the original structure because the beams hinge at a lateral load smaller than the column failure load. But the ductility of the frame is increased significantly because the failure mechanism is changed. The improved frame still needs the strengthening and stiffening of the bracing system, but Fig. 7.2.1 shows that the required bracing system

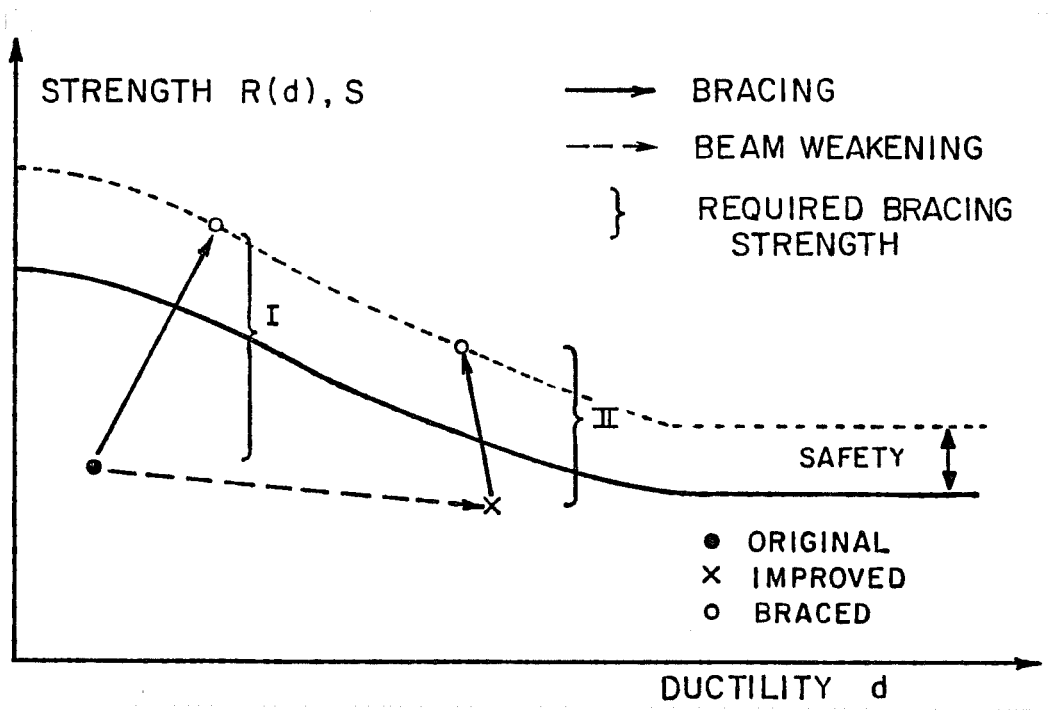


Fig. 7.2.1 Retrofitting with and without beam weakening



strength is reduced. The frame with weakened beams is safer at ultimate state, because it has substantially higher ductility. The lateral deformation capacity of the braced frame in this case may actually be limited by the steel bracing system rather than the reinforced concrete frame. Weak column - strong beam frames are sometimes referred to as frames with captive columns. Through the weakening of the beams the columns are "deactivated."

7.2.2 The r and q ratios. Two ratios are defined here to facilitate a quantitative discussion of the beam weakening scheme.

Ratio q. For a frame member submitted to double curvature,  $q$  is defined as the ratio of the shear  $V_{US}$  leading to shear failure over the shear  $V_{UF}$  leading to flexural failure (see Fig. 7.2.2). The  $q$  ratio is thus a measure of the "brittleness" of the member. Values of  $q$  above 1 indicate a ductile failure with flexural hinges. If  $q$  is smaller than one, the failure is shear dominated. The smaller the  $q$  value, the more brittle the behavior. The  $q$  ratio is particularly important for the columns of weak column - strong beam frames because columns with  $q \leq 1$  lose their lateral and possibly axial capacity at large lateral drifts.

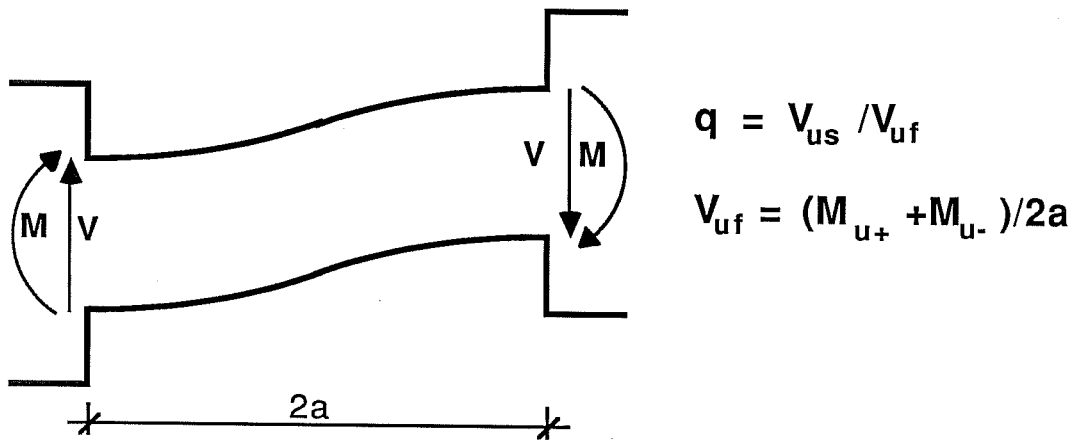


Fig. 7.2.2 Ratio  $q$  for a member in double curvature

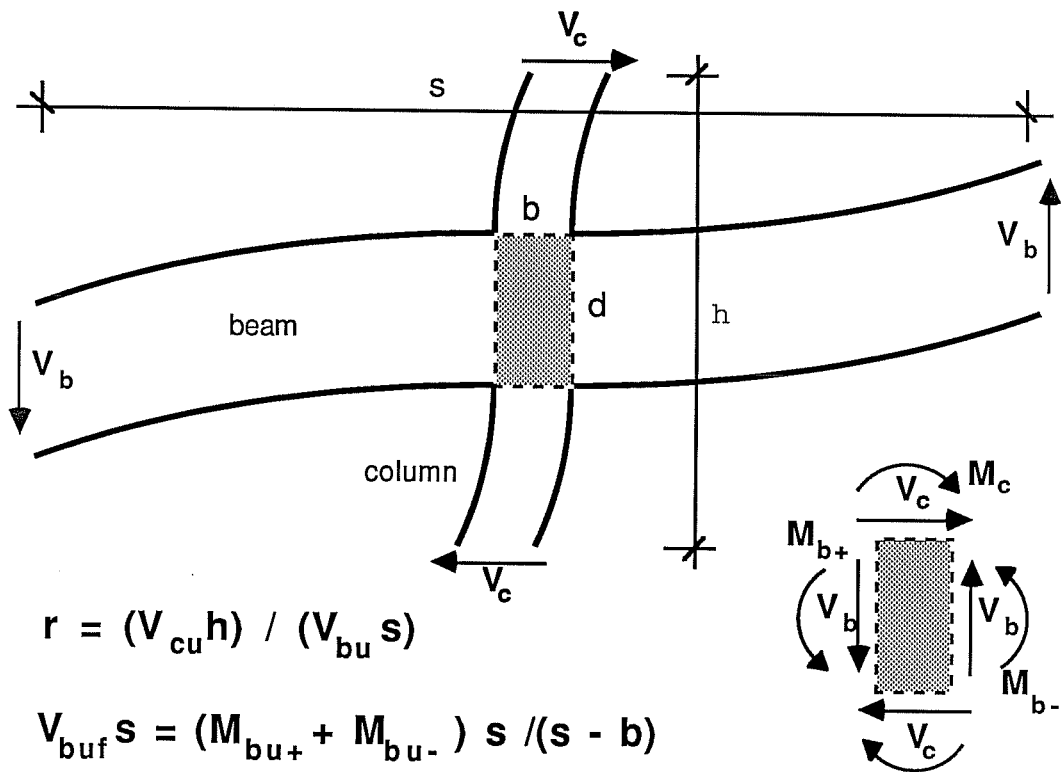


Fig. 7.2.3 Ratio  $r$  for a beam column joint

Ratio r. Figure 7.2.3 shows a beam column assemblage under lateral loading. If  $V_{cu}^*h$  is the moment leading to column failure and  $V_{bu}s$  the moment leading to beam failure,  $r$  is defined as the ratio of  $V_{cu}^*h$  to  $V_{bu}^*s$ .  $V_u$  is equal to  $V_{us}$  if  $q$  is smaller than one. If  $q$  for the beam is larger than one, then  $V_{bu} = (M_{bu+} + M_{bu-})/(s - b)$ , where  $M_{bu+}$  and  $M_{bu-}$  are the beam positive and negative moment capacities at the face of the joint.

The ratio  $r$  is a measure of the relative strength of the columns and beams at a joint under lateral loading. A value of  $r$  below one indicates that the columns are weaker than the beams. As was seen above, frames with weak columns have an undesirable failure mechanism. Weakening the beams should be considered as a means of producing a strong column - weak beam frame. The beam strength can be reduced to produce an  $r$  ratio above one. The higher the  $r$  value, the lower the likelihood of yielding or failure of the column in an earthquake. The ratio  $r$  can be interpreted as the safety factor against column failure under lateral loading.

The Prototype Frame. The  $q$  ratio for the columns and beams of the prototype frame and the  $r$  ratio for the beam - column joint are calculated below. The structural properties of the prototype frame are given in Sec. 4.1.2.

$$\begin{aligned}
 V_{cus} &= 75 \text{ k} & V_{bus} &= 123 \text{ k} \\
 M_{cu} &= 255 \text{ k-ft} & M_{bu+} &= 650 \text{ k-ft} \\
 & & M_{bu-} &= 308 \text{ k-ft} \\
 h &= 10 \text{ ft} & s &= 21 \text{ ft} \\
 d &= 6 \text{ ft} & b &= 1.5 \text{ ft} \\
 2a &= 4 \text{ ft} & 2a &= 19.5 \\
 V_{cuf} &= 128 \text{ k-ft} & V_{buf} &= 49 \text{ k ft} \\
 q_c &= V_{cus}/V_{cuf} & q_b &= V_{bus}/V_{buf} \\
 &= 75\text{k}/128\text{k} = \underline{0.59} & &= 123\text{k}/49\text{k} = \underline{2.51}
 \end{aligned}$$

$$\begin{aligned}
 r &= V_{cuh}/V_{bus} = (75\text{k} \cdot 10 \text{ ft})/(49\text{k} \cdot 21 \text{ ft}) \\
 &= 1/1.37 = \underline{0.73}
 \end{aligned}$$

The calculation confirms that the prototype frame is a weak column - strong beam frame ( $r = 0.73 < 1$ ) with shear dominated failure of the column ( $q_c = 0.59 < 1$ ).

7.2.3 Weakening Parameters. Figure 7.2.4 illustrates weakening of the beams of the prototype frame. The beams are altered to reduce the moments they can transfer to the columns. Cuts are typically located at the face of the column where the moments are highest under lateral loading. The depth of the cut is  $u$  for a cut on top of the beam and  $v$  for a cut on the bottom of the beam. The length of the cut is  $w$ . The primary reduction in flexural capacity comes from removal of the reinforcement, but

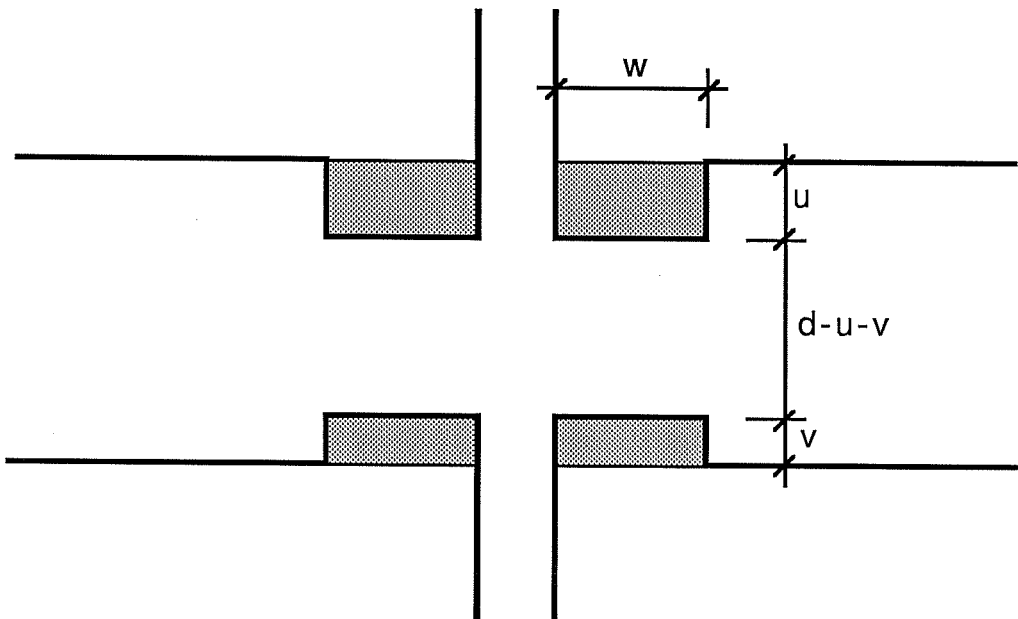


Fig.7.2.4 Weakening parameters  $u$ ,  $v$  and  $w$

there is also a reduction due to the change in section depth from  $d$  to  $d - u - v$ .

Weakening increases the effective free height of the column from  $2a$  to  $2a + u + v$ . Since the flexural capacity of the column is unchanged, the ratio  $q_c$  is increased by a factor  $(2a + u + v)/2a$ . This increase is favorable for a brittle column ( $q_c < 1$ ) because it reduces the brittleness but not the strength ( $V_{us}$  is not affected). But for a column with a flexure dominated failure ( $q > 1$ ), the increase in  $q$  corresponds to a proportional decrease in strength.  $V_{uf}$  is reduced by a factor  $(2a + u + v)/2a$  as a result of the increased column free height.

Practical examples of beam weakening are shown in Fig. 7.2.5 for a joint of the prototype frame (reinforcement detailing in Fig. 4.1.3). Weakening can be carried out by cutting or coring through the reinforced concrete beam. Coring can be used to remove a particular layer of reinforcement. The coring scheme of Fig. 7.2.5 is weakening scheme 3b of Sec. 7.4; in this scheme the second layer of negative reinforcement is removed. If the beams are cut, small values of  $u$  and  $v$  result in large reductions of the beam flexural capacity because most of the reinforcement is located on top and bottom of the beams. The effective length  $w$  of the weakened section is larger than the spacing of the two extreme cuts or corings because of the anchorage length of the cut reinforcement. The length  $w$  is

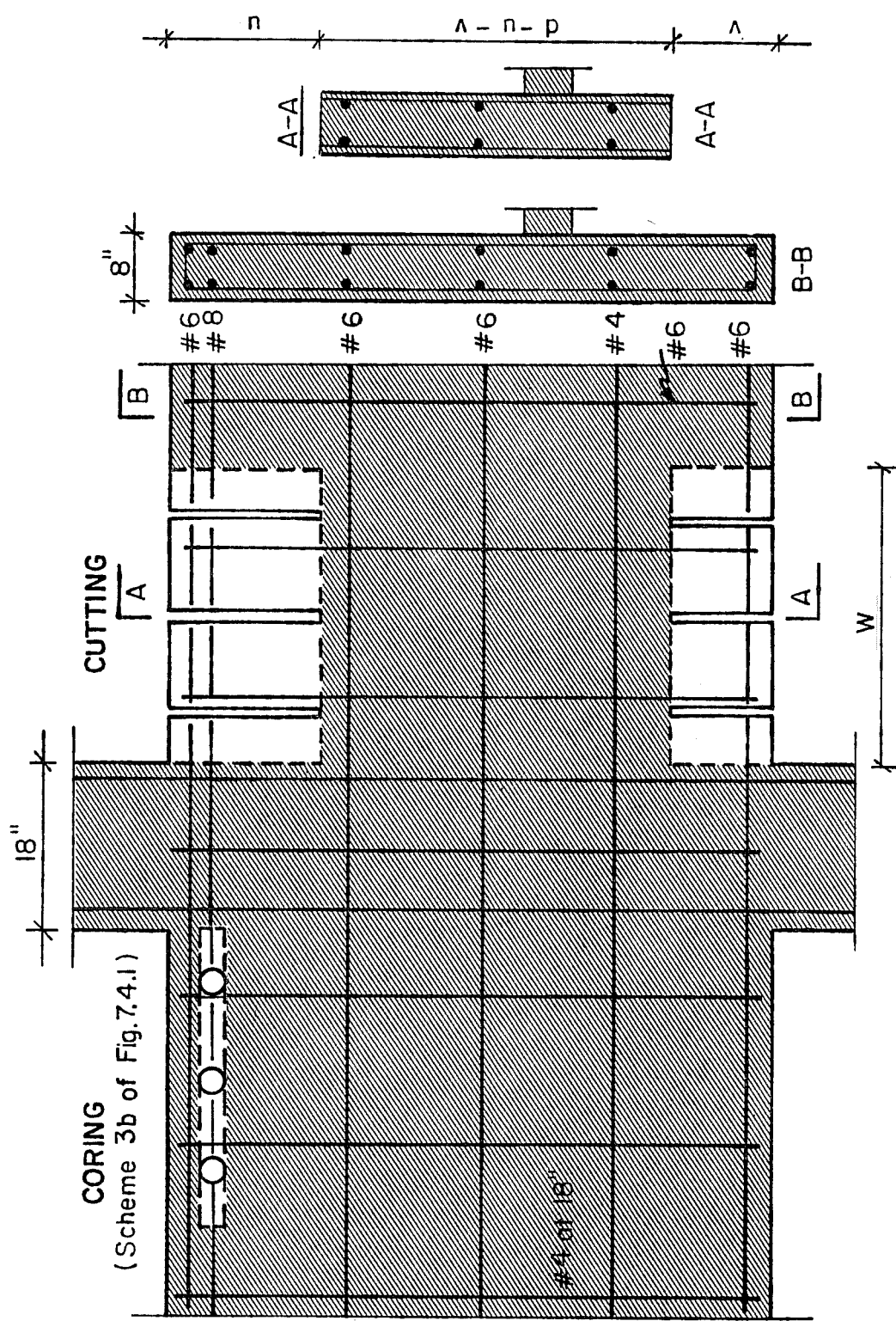


Fig. 7.2.5 Beam weakening schemes for prototype frame

important for the energy dissipation capacity of the flexural hinge which develops in the weakened section at ultimate. If  $w$  is too small, yielding and cracking cannot spread and the rotation capacity is limited;  $w$  should be larger than half of the effective section depth  $d - u - v$ .

The designer must check that the weakened beams can perform their primary function, which is to carry the gravity loads to the column. In the case of the prototype, the beams of the prototype frame are much stronger than required for gravity loading and can be weakened significantly. The spandrel beams have sufficient positive flexural capacity to carry the gravity loads as simple beams. The weakened section could, therefore, lose all moment capacity, but it must retain adequate shear strength. Figure 7.2.6 shows the shear transfer mechanism through the weakened zone of the prototype beam (same weakening scheme as in Fig. 7.2.5). A truss model is useful in choosing a weakening scheme which preserves an adequate shear transfer mechanism through the weakened zone. The model shows that cutting the shear reinforcement must be avoided.

### 7.3 Braced Frame with Weakened Beams

The influence of weakening the beams on the behavior of the braced frame under monotonic, reversed, and cyclic loading is studied in this section. The subassemblage developed for the



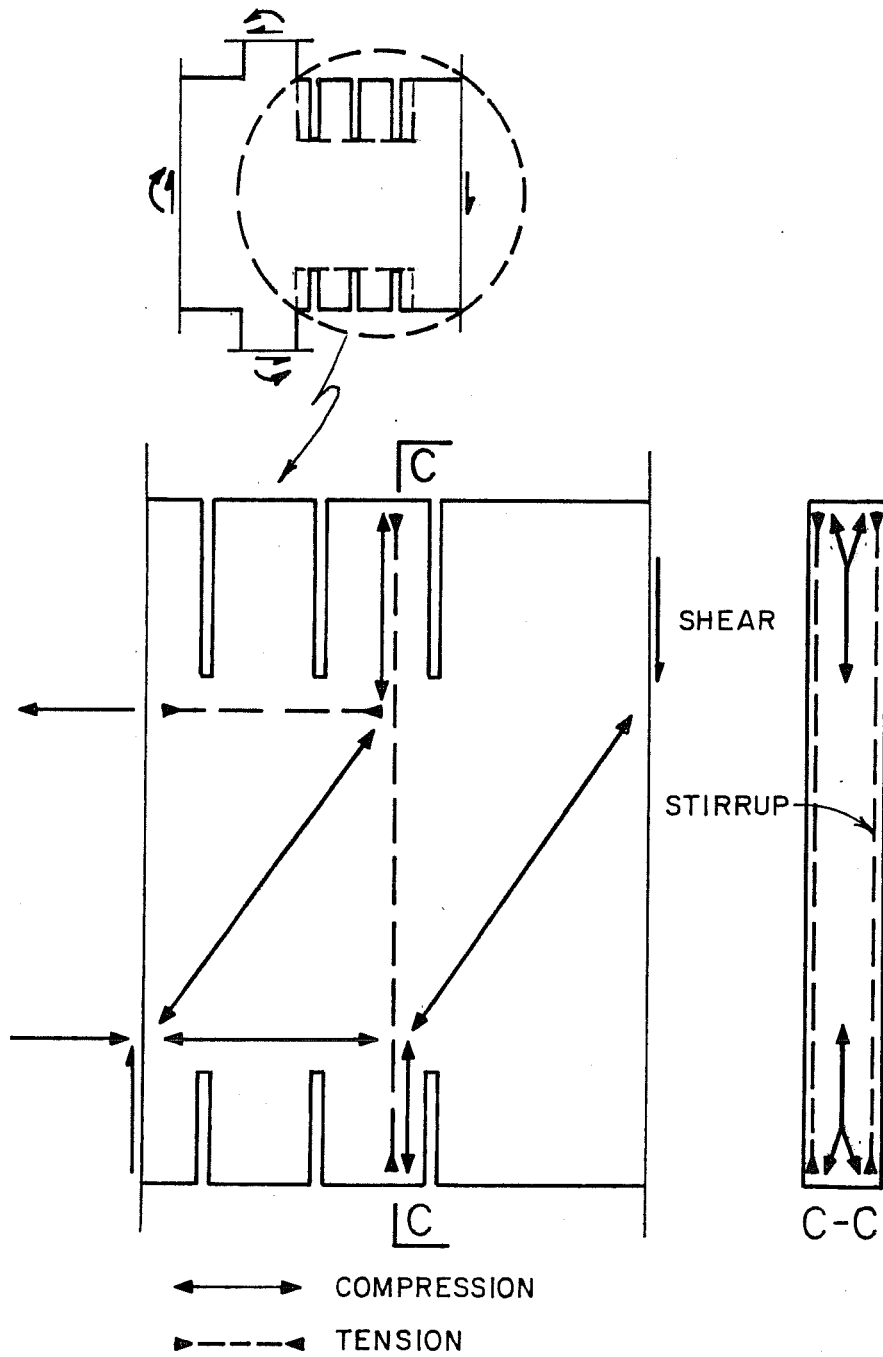


Fig. 7.2.6 Shear transfer in weakened beam

parametric study of Chapter 6 is used (see Fig. 5.3.1). The brace design strength ratio is  $n = 2$  and the slenderness ratio is  $k\ell/r = 80$ . For this example, the weakening parameters are those of scheme 3b in which the second layer of negative reinforcement is cored (see Figs. 7.2.6 and 7.4.1). The monotonic lateral load - drift relationships  $m(\delta)$  for the frame with and without beam weakening are compared in Fig. 7.3.1. In the original frame, cracking of the columns and beams is followed by failure of the column and the loss of the frame lateral capacity. The failure sequence of the improved frame is different once the beams crack. The beams hinge at 90% of the load which produces failure of the column in the original frame. At larger drift, the lateral strength is maintained and, in fact, increased because of strain hardening in the beams. The weak column - strong beam frame with  $r = 0.73$  is transformed into a strong column - weak beam frame with  $r = 1.21$ . The improved frame has better deformability (see Sec. 3.3) since the ultimate load is reached at a drift 20% higher than in the original frame. The reduction of the frame initial stiffness is insignificant.

The influence of beam weakening on the braced frame behavior is shown in Fig. 7.3.3. The small loss in peak strength is more than compensated by the stability of strength beyond peak drift and by the protection provided against column damage.

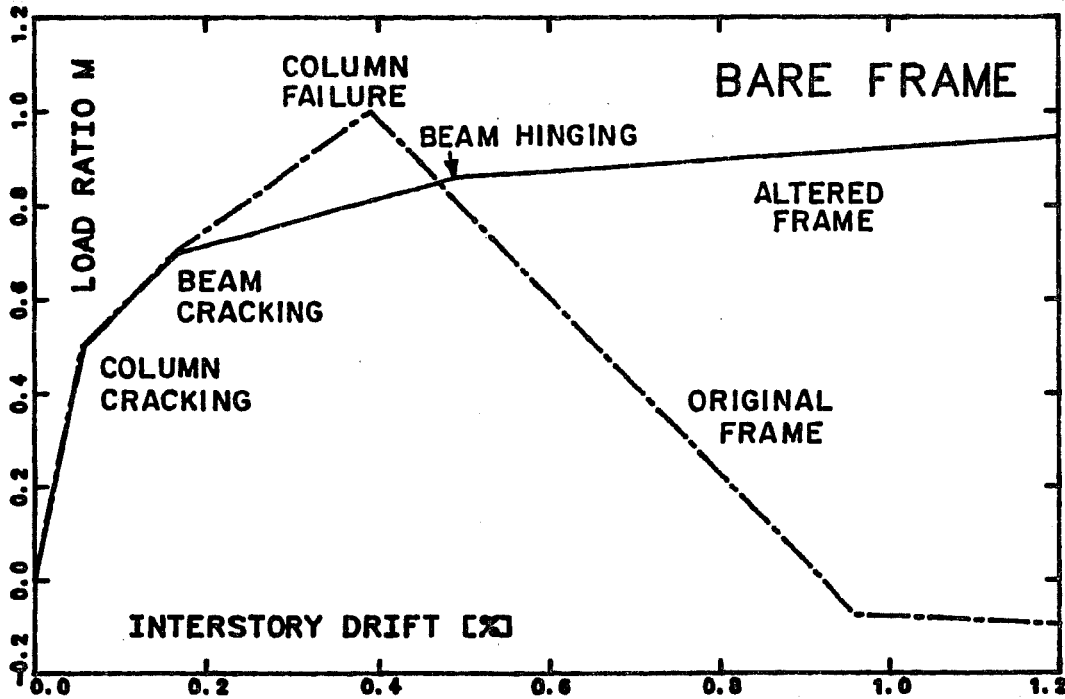


Fig. 7.3.1 Altered frame under monotonic loading

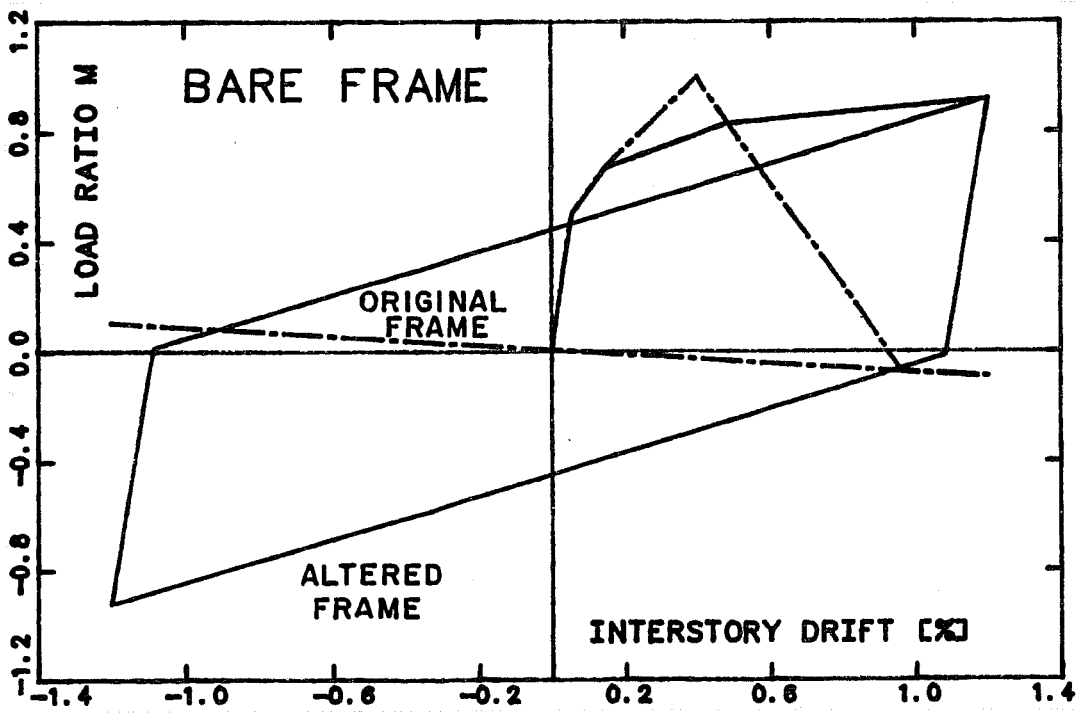


Fig. 7.3.2 Altered frame under reversed loading

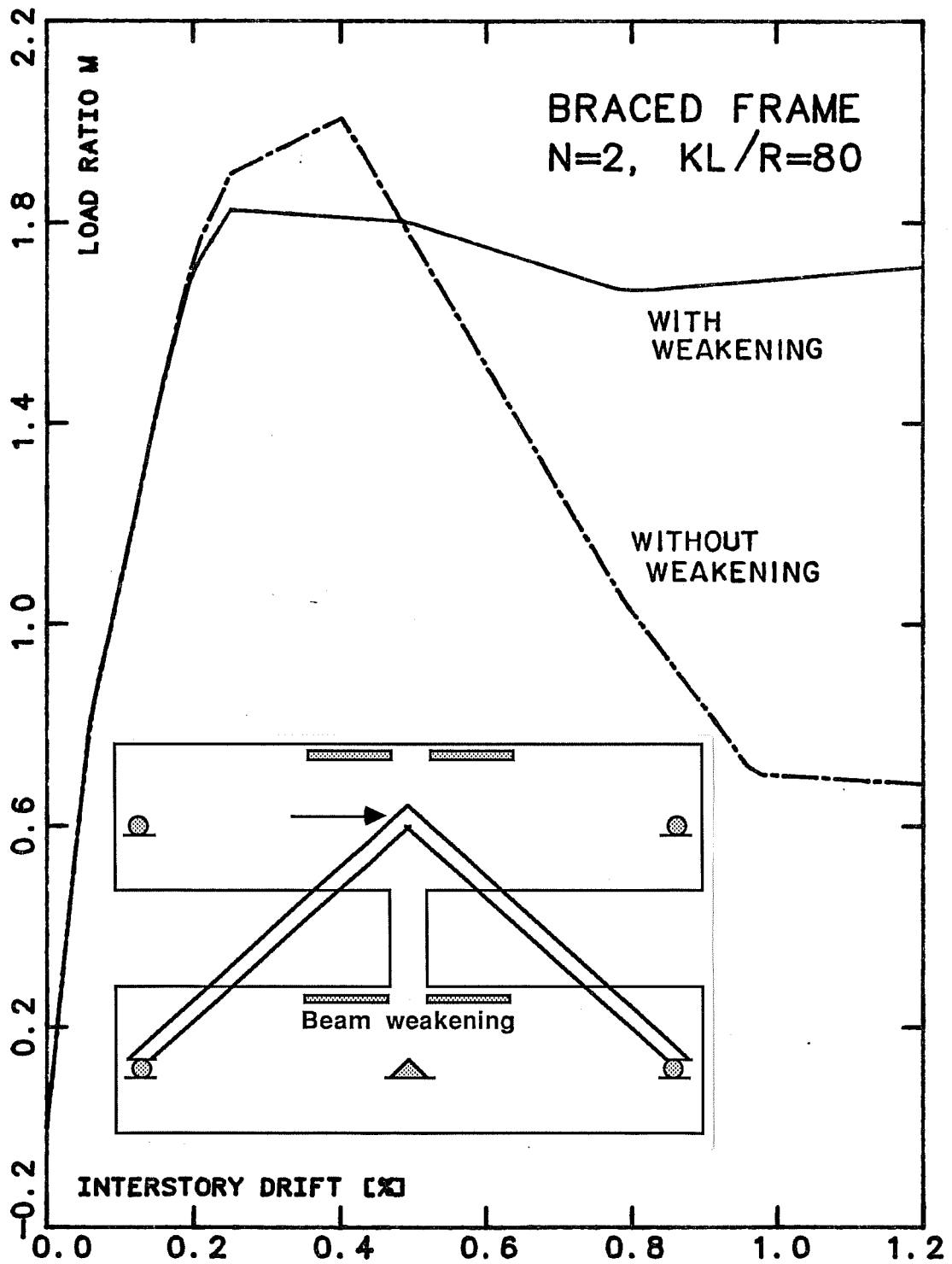


Fig. 7.3.3 Braced frame under monotonic loading, with and without beam weakening

The positive impact of the weakening scheme on frame behavior under reversed loading is shown in Fig. 7.3.2. The original frame has no strength in the reversed direction because loss of short column strength in one direction results in an equivalent loss in the other loading direction. The improved frame, the beam flexural hinges loses stiffness but not strength under large deformation. As a result, the energy dissipation capacity of the braced frame under reversed loading is higher if the beams are weakened (see Fig. 7.3.4). The improved hysteretic behavior of the braced frame with weakened beams is also observed in the cyclic loading case (see Fig. 7.3.5).

In summary, the beam weakening scheme 3b for the prototype frame:

- increases the  $r$  ratio at the frame joints from 0.73 to 1.21. The likelihood of column damage is thus substantially reduced.
- does not reduce the elastic stiffness of the frame significantly.
- maintains sufficient gravity load carrying capacity in the beams. Does not the beam gravity loads.
- requires only a modest construction effort.
- does not reduce the aesthetic quality or disrupt the function of the building.

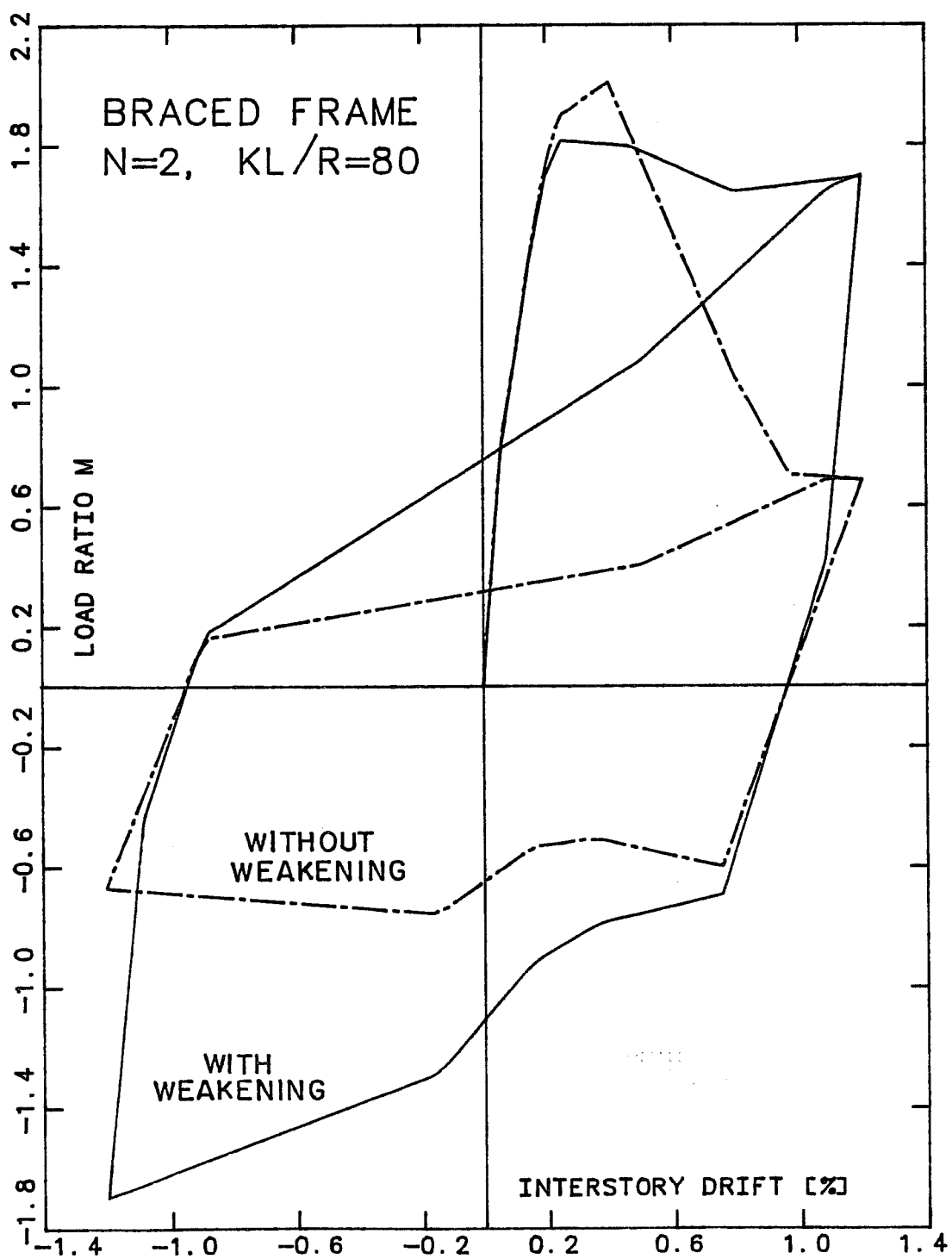


Fig. 7.3.4 Braced frame under reversed loading, with and without beam weakening

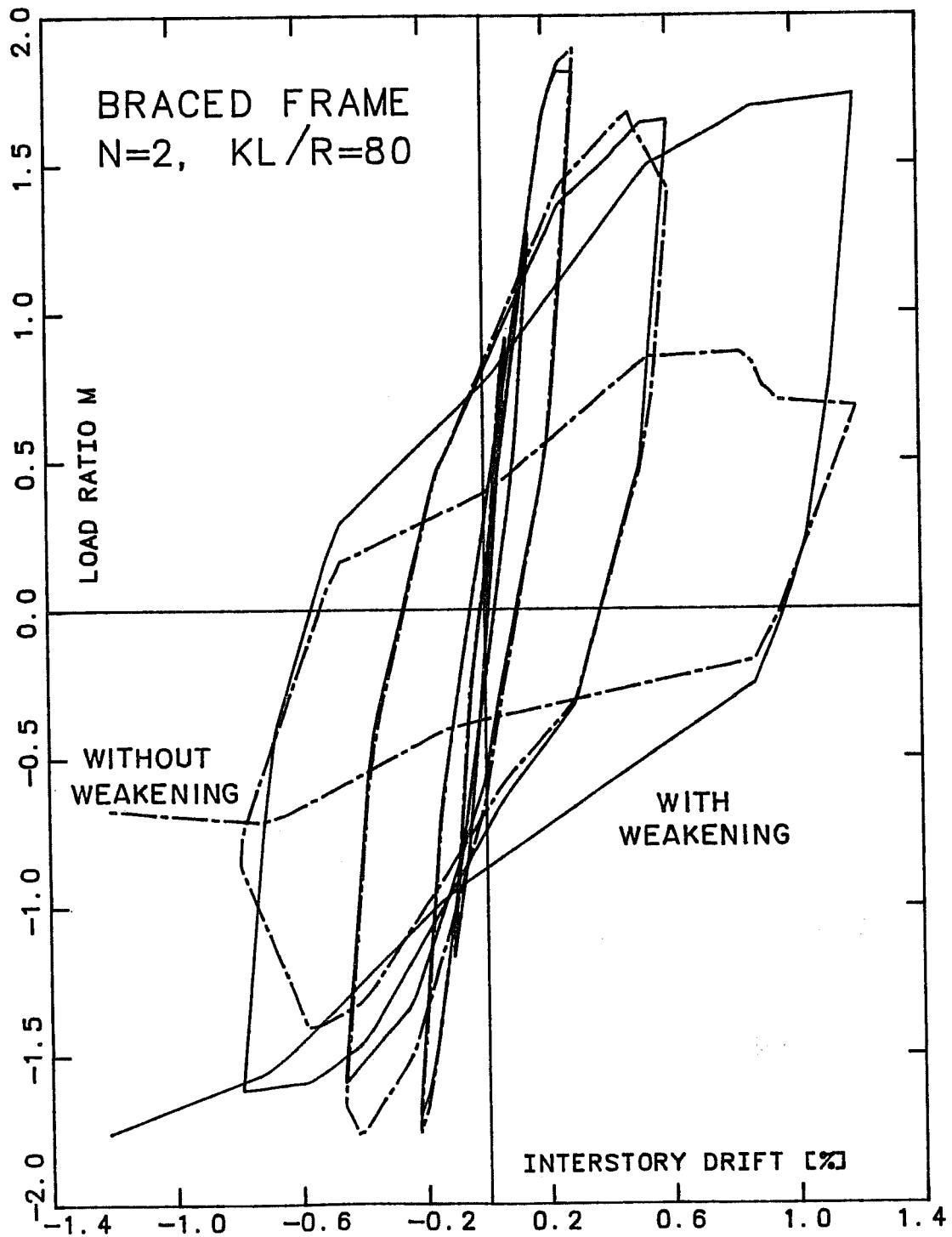


Fig. 7.3.5 Braced frame under cyclic loading, with and without beam weakening

## 7.4 Parametric Study

7.4.1 Variation of Parameters u and w. Twelve different beam weakening schemes for the prototype frame are shown in Fig. 7.4.1. The weakening parameters  $u$  and  $v$  are varied to cover a wide range of possible weakening schemes. The length  $w$  of the weakened sections is fixed at 36". The lateral load drift curves  $m(\delta)$  for the frames with weakened beams and for the original frame are compared in Figs. 7.4.2 to 7.4.4.

Set 1, Weakening on Top of the Beam Only (see Fig. 7.4.2). The depth  $u$  of the cut is varied from 6" to 24". In all four schemes, the main negative reinforcement is cut and the spandrel beams are weakened substantially. For  $u = 6"$ , the beam moment capacity is reduced by 60% and the safety factor against column failure is  $r = 1.76$ . The main effect of deepening the cut depth  $u$  to more than 6" is to reduce the lever arm for the positive moment reinforcement. The  $r$  ratio increases, therefore, only to  $r = 2.28$  when  $u$  is increased to 18". A new layer of negative reinforcement is cut if  $u$  is deepened to 24", resulting in a jump of  $r$  to 2.95. The  $q$  ratio, an indication of the brittleness of the column (definition in Sec. 7.2.1), is also influenced by the value of  $u$ . It is improved from  $q = 0.59$  for  $u = 0"$  to  $q = 0.88$  for  $u = 24"$ . The required depth of top cut to bring  $q$  above 1.0 is  $u = 34"$ .



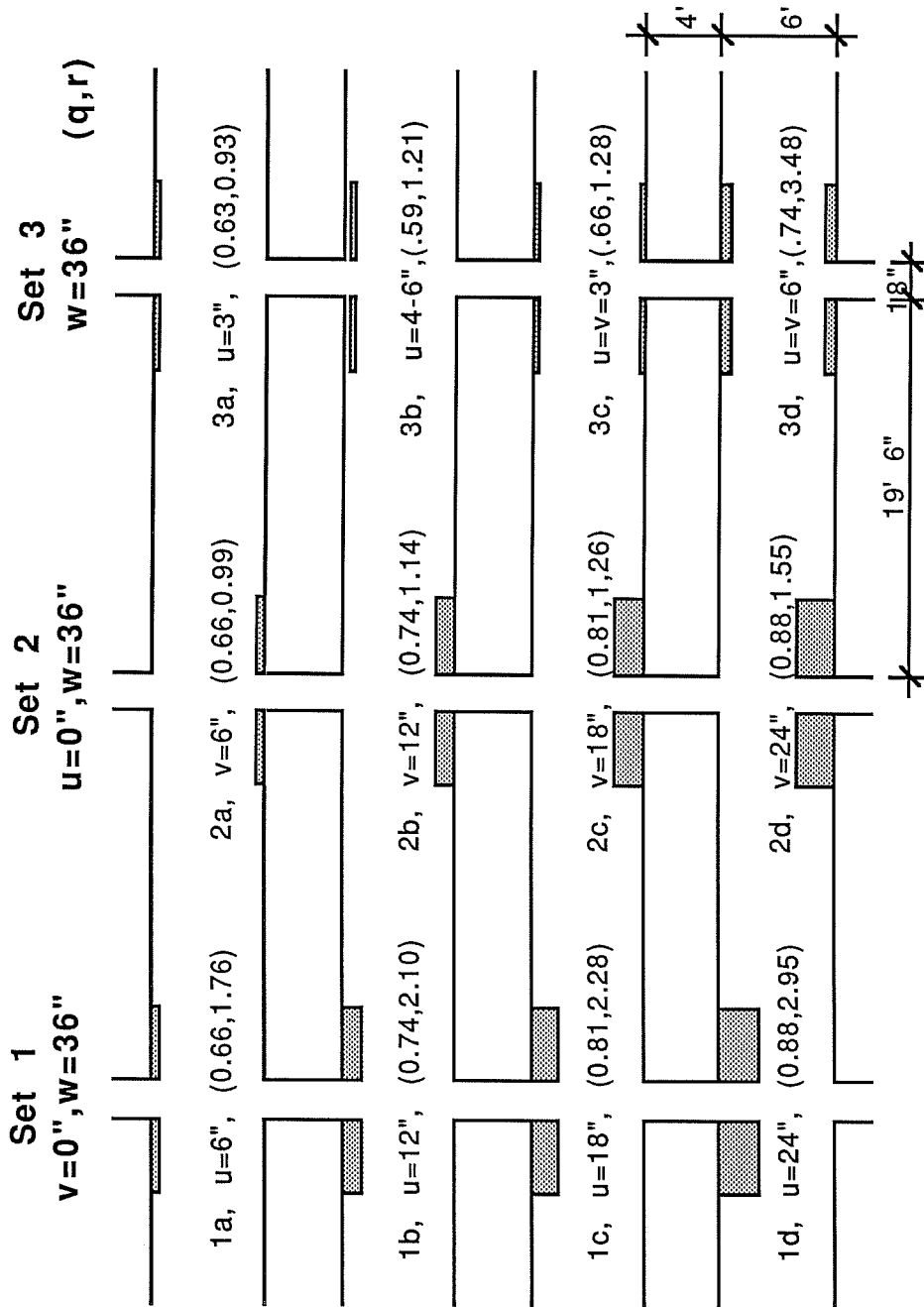


Fig. 7.4.1 Weakening schemes for the prototype frame

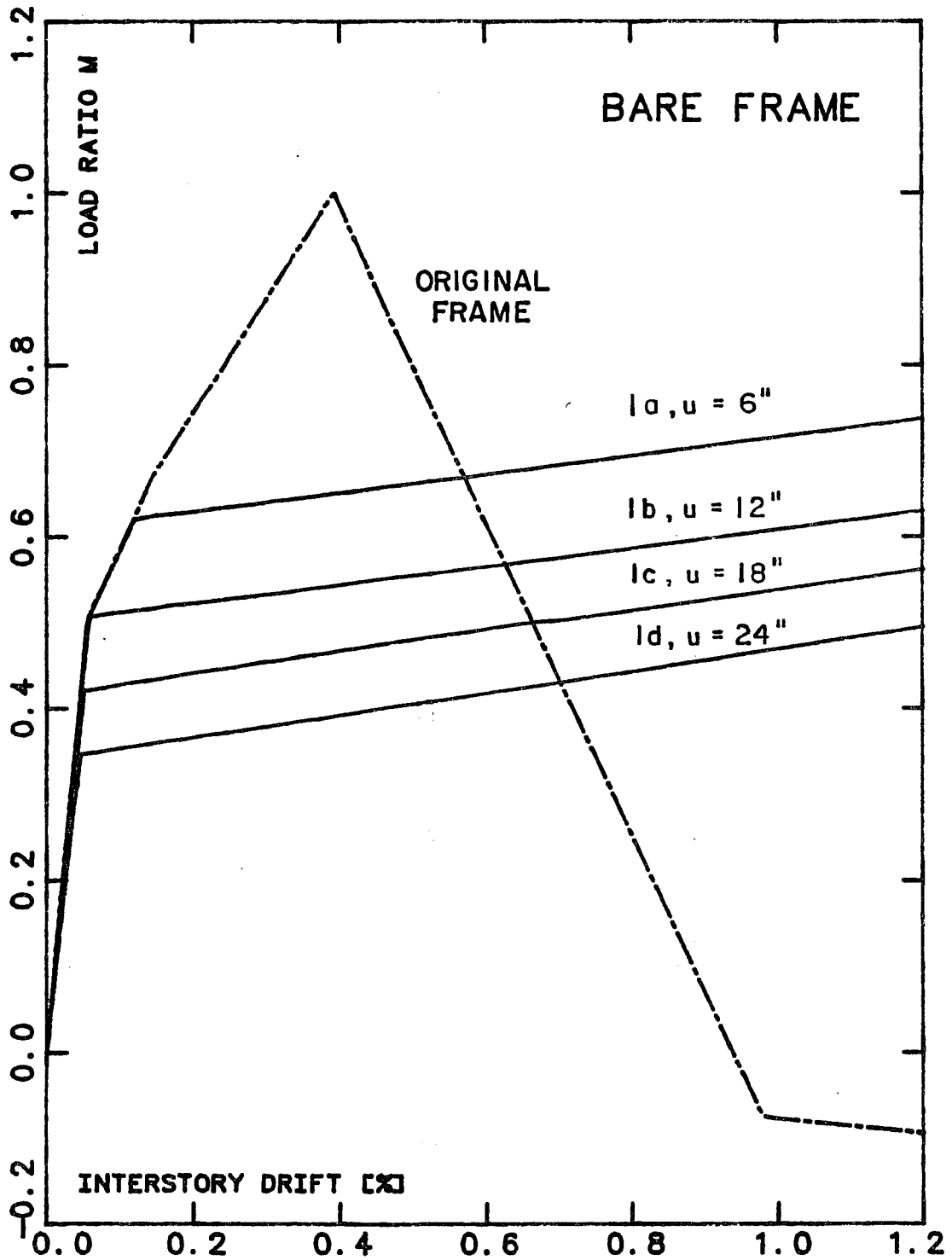


Fig. 7.4.2 Load-drift relationships for weakening schemes of Set 1

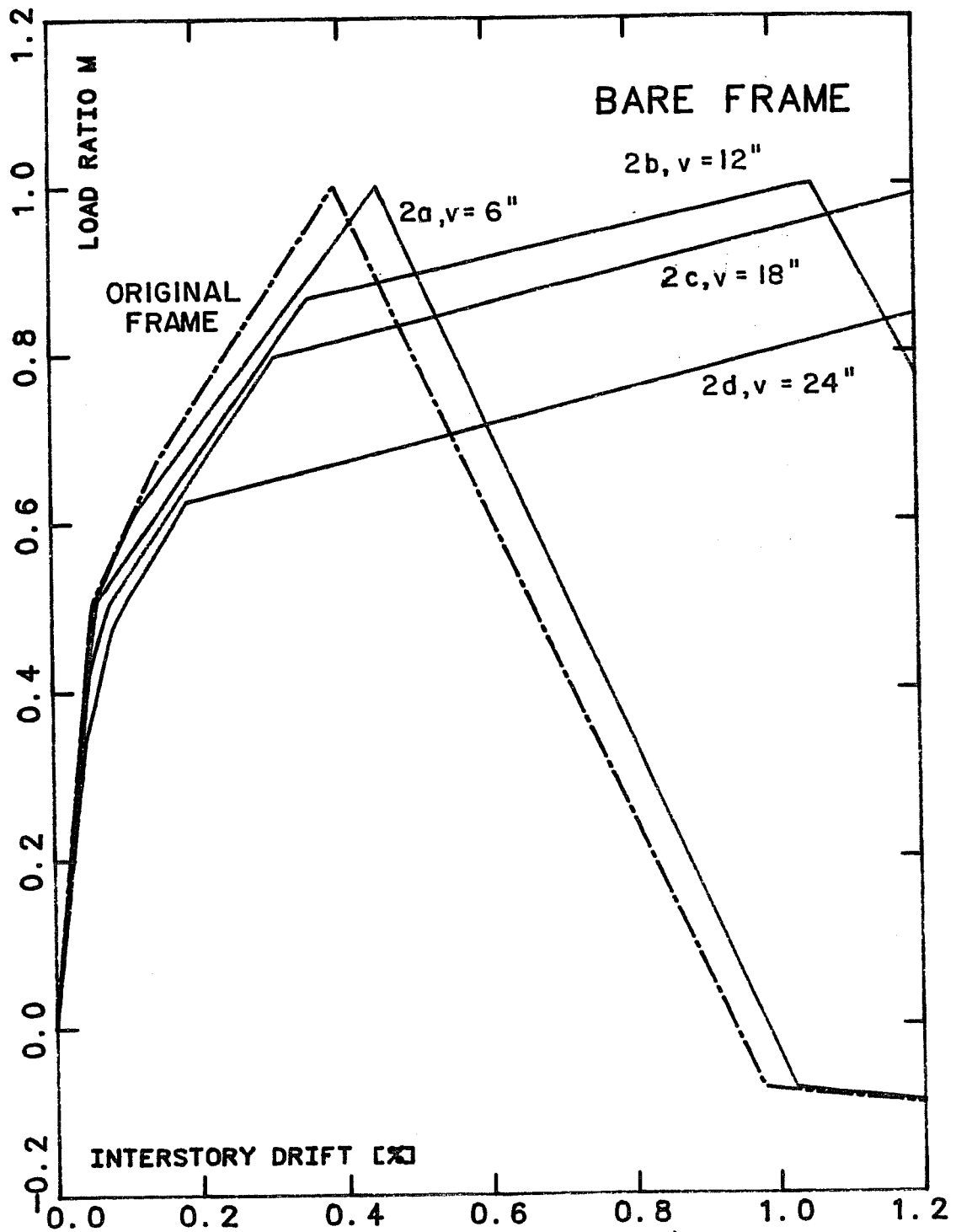


Fig. 7.4.3 Load-drift relationships for weakening schemes of Set 2

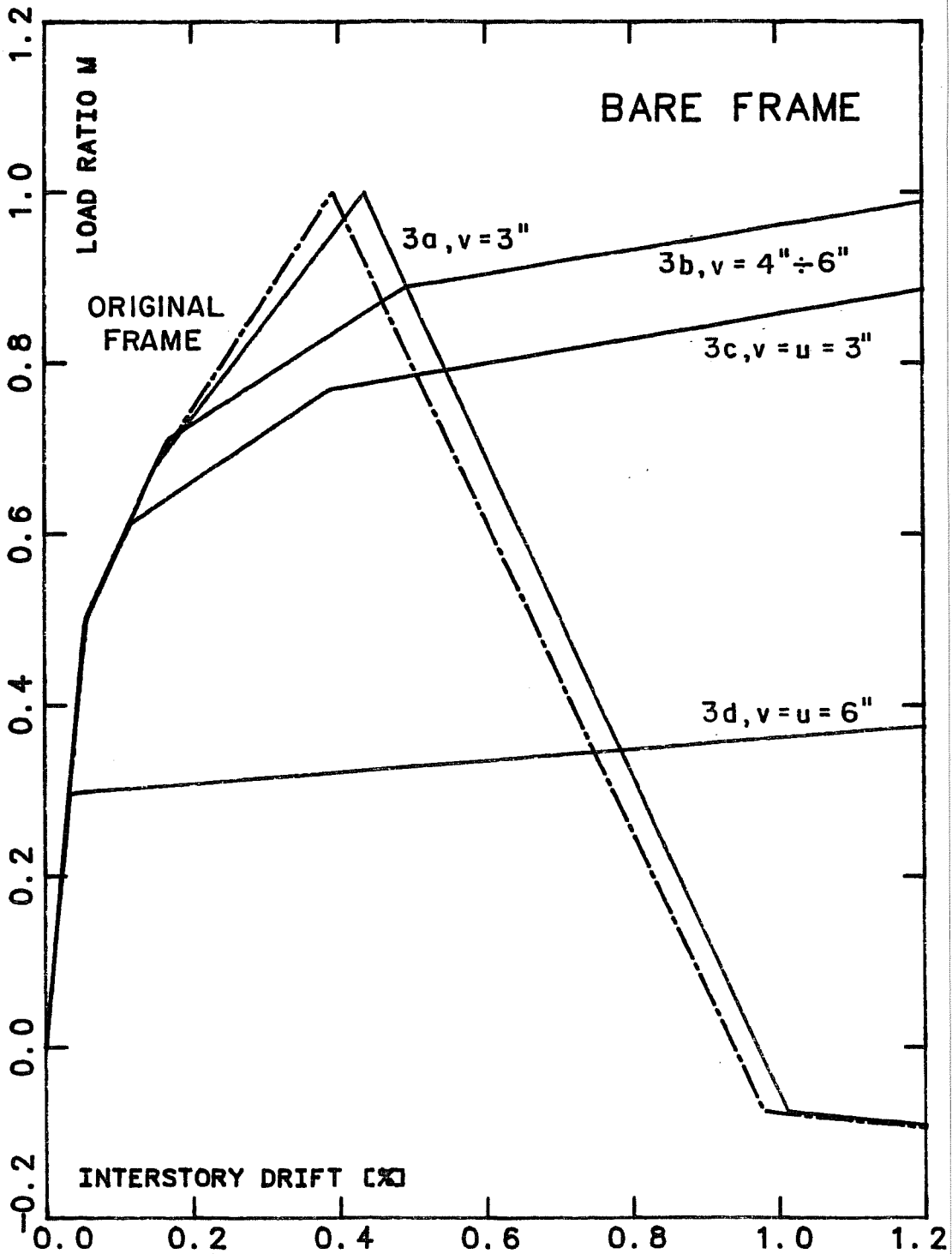


Fig. 7.4.4 Load-drift relationships for weakening schemes of Set 3

The influence of the depth of weakening on the initial stiffness of the frame can be seen in Fig. 7.4. The passage from  $u = 0$ " to  $u = 24$ " reduces the beam stiffness under double curvature by 61%, but the frame lateral stiffness by only 24% (see Sec. 7.5 for discussion of the stiffness of the weakened frame). Because of the large ratio of beam-to-column stiffness, a beam strain hardening ratio of 3% results in a frame strain hardening ratio of 10%.

Cutting the negative reinforcement produces a greatly underreinforced section. The negative cracking moment  $M_{cr-}$  is larger than the negative yield moment  $M_{u-}$ . This could be a problem for the gravity loading of the beams, which could theoretically fail without warning. But there is enough flexural capacity at midspan for redistribution to guarantee that the ultimate gravity load is larger than the cracking load. For seismic loading, the energy dissipation capacity rather than the peak strength determines the safety at ultimate. A large cracking moment does not in itself limit the energy dissipation of a flexural hinge,  $M_{cr} > M_u$  is thus acceptable. If underreinforcement is a problem for gravity loading, the concrete section can always be reduced by additional coring around the reinforcement. For simplification  $M_{cr}$  was lowered to the  $M_u$  value for the schemes where  $M_{cr} > M_u$ . In those cases, the frame goes directly from the elastic range into strain hardening.

Set 2, Weakening on Bottom of the Beam (see Fig. 7.4.3).

This set of weakening schemes is similar to the first one, except that the bottom of the beam is weakened. The positive reinforcement is smaller than the negative, so that a cut of  $v = 6$ " (Scheme 2a) increases the  $r$  ratio to only 0.99. A value of  $r$  below 1.00 means that the column fails before the beams hinge. The failure sequence and load - drift curve  $m(\delta)$  of frame 2a is, therefore, similar to that of the original frame. The failure is still controlled by the brittle failure of the short columns. The failure drift is larger because of the weaker beams. If  $v$  is increased to 12" (scheme 2b), the beams hinge ( $r = 1.14$ ). But the columns nevertheless fail at an interstory drift of 1% because of the large strain hardening in the beams. The  $r$  ratio is computed at the onset of strain hardening.  $r$  should be larger than 1.2 to prevent column failure at high drift levels because strain hardening in the beams can easily increase the moment transferred to the column by 10 or 15%. Parameter  $v$  has to be increased to 24" for  $r$  to exceed 1.5.

Set 3, Miscellaneous (see Fig. 7.4.4). In scheme 3a ( $u = 3$ ") the top layer of negative reinforcement is cut (see Fig. 7.2.6). The resulting  $r$  ratio is below 1.0 ( $r = 0.93$ ), so that the frame behavior at ultimate is dominated by brittle column failure. Combining  $u = 3$ " with  $v = 3$ " (scheme 3c) achieves the

goal of moving failure to the column ( $r = 1.28$ ). Scheme 3b, which consists of cutting the second layer of top negative reinforcement (two #8 bars) results in a  $r$  ratio of 1.21. This scheme was studied in Section 7.3 under reversed and cyclic loading. Finally, if the top and bottom reinforcement is cut (Scheme 3d,  $u = v = 6$ "), the beams lose 80% of their strength and are highly underreinforced ( $M_{CR}/M_U = 1.79$ ). The resulting ratio  $r = 3.48$  is unnecessarily high.

7.4.2 Choice of Parameters  $u$ ,  $v$ . The choice of the weakening scheme depends on the desired level of safety against column damage. The defined  $r$  ratio dictates the choice of  $u$  and  $v$ . In the section on seismic design the ACI Code [25] gives a minimum design requirement for the ratio of column to beam strength. Section A.4.2.2 requires that  $\Sigma M_e / \Sigma M_g \geq 1.2$ , where  $M_e$  is the flexural design strength of the columns (taking axial load into account) and  $M_g$  is the design flexural strength of the beams. Expressed in terms of the  $r$  ratio (with nominal rather than factored beam and column strength) the requirement becomes  $r \geq 1.2 (0.9 \cdot 0.7) = 1.54$ . In the "Recommendations for Design of Beam-Column Joints", ACI Committee 352R-85 proposes to reduce the minimum required  $r$  ratio to 1.40 for joints which are part of the primary system for resisting lateral loads. Paulay [33] has suggested that for a number of reasons it is improbable that the ACI requirement of A.4.2.2 "would fulfill its intent which is to

reduce the likelihood of yielding in the columns." The main reason is that the ACI Code does not consider the enhancement of the beam strength, due to the slab reinforcement and to strain hardening. Paulay recommends designing for  $r$  values between 2 and 2.5.

The twelve weakening schemes investigated above produce  $r$  values ranging from 0.93 to 3.48. The designer of the retrofit scheme can "tune" the safety level against column damage as desired. A high safety level is particularly desirable in the case of brittle short columns. The lower the ratio  $q$  (brittleness factor), the higher the  $r$  ratio should be. Producing the desired  $r$  ratio may not always be possible because it would threaten the ability of the beam to carry gravity loads to the columns. In such a case, any increase of the  $r$  ratio is welcome. In this respect all twelve weakening schemes of Sec. 7.6.1 are better than "no beam weakening." Schemes 2a, 2b, and 3a ( $r = 0.99, 1.14, \text{ and } 0.93$ ) would probably fail to achieve the primary goal of weakening which is to prevent column failure in a strong earthquake, but they would nevertheless improve the failure mechanism. Values of  $r$  above 2.0 are unnecessarily high. A value of  $r$  between 1.5 and 2.0 is recommended for retrofitting involving weakening of the beams.



### 7.5 Stiffness of the Weakened Frame

For a given column stiffness, the frame lateral stiffness is a function of the beam stiffness. The influence of the ratio of beam-to-column stiffness on the frame lateral stiffness is shown in Fig. 7.5.1. The beam and column stiffness are the flexural stiffness of the member under double curvature. Only flexural deformations were considered in the calculation of the frame stiffness. The frame stiffness is normalized with the stiffness of the frame with infinitely stiff beams. If the beams have no stiffness, the frame lateral stiffness is zero (like a pinned column). If the beams are infinitely stiff, the frame stiffness is that of the column with fixed ends. In the case of the prototype frame, the beam stiffness under double curvature is about three times that of the columns. The resulting frame stiffness is about 79% that of the frame with infinitely stiff beams. Figure 7.5.1 shows that the high relative stiffness of the beam places the frame in the portion of the curve where the slope is small. Changes in beam stiffness result in comparatively small changes in frame stiffness. Most of the frame flexibility is in the column.

Figure 7.5.2 shows the impact of weakening scheme 1d (see Sec. 7.4.1) on the frame stiffness. The 24" deep and 36" long cut reduces the beam stiffness by 61% and results in a loss of frame stiffness of only 24%. The other weakening schemes

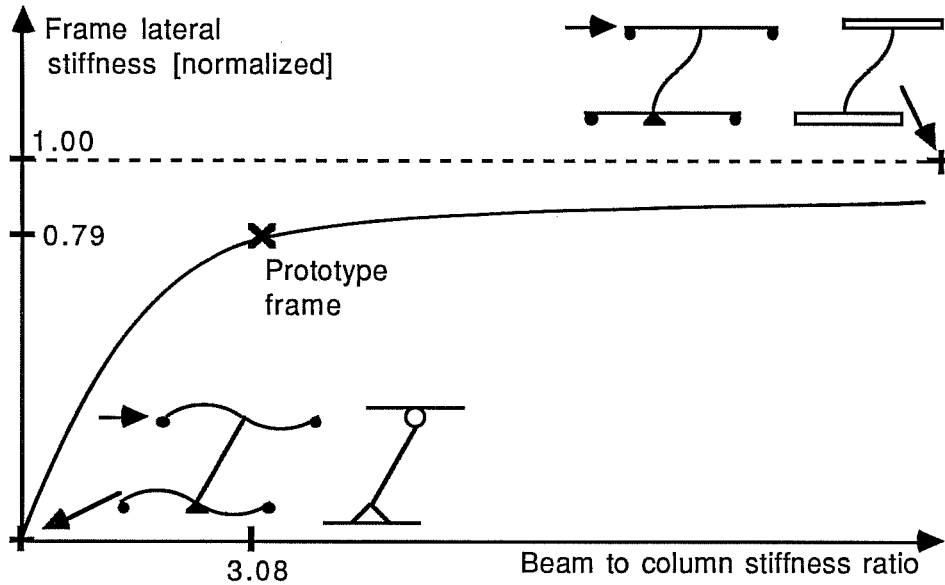


Fig. 7.5.1 Influence of beam to column stiffness ratio on frame lateral stiffness

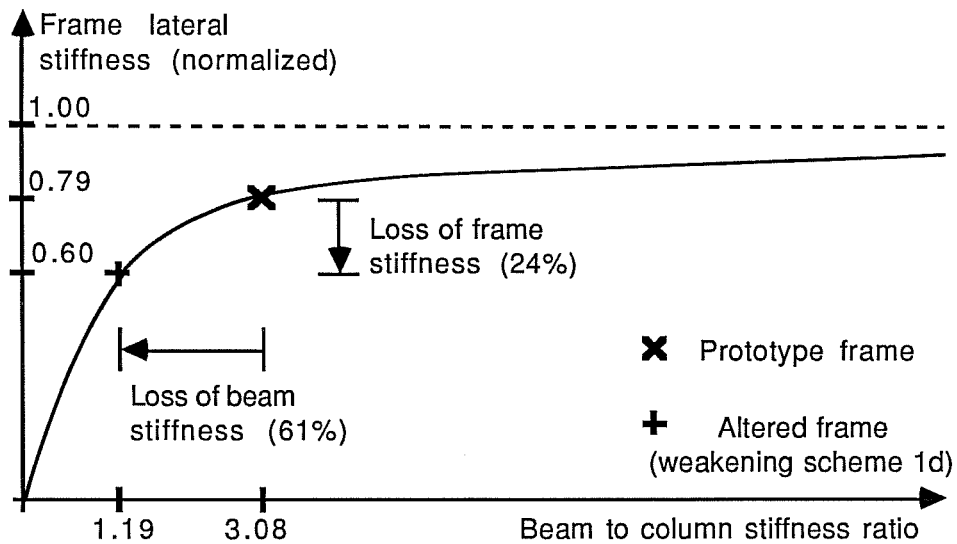


Fig. 7.5.2 Loss of frame lateral stiffness, beam weakening scheme 1d

all cause smaller reduction in frame stiffness. If the length  $w$  of the cut is increased from 36" to 60", the loss in frame stiffness is still small (about 30%).

## CHAPTER 8

### SUMMARY AND CONCLUSIONS

#### 8.1 Summary

The intent of the study is to examine problems faced in the design of the retrofitting of a reinforced concrete frame with a steel bracing system.

The first portion of the study is not limited to steel bracing schemes. Concepts are studied which are useful for the discussion of any retrofitting operation. The evaluation of the seismic adequacy of a structure is discussed and various approaches for seismic retrofitting of inadequate structures are studied. Means are developed to assess the impact of retrofitting on the seismic safety of the structure. The aim of retrofitting is defined in terms of strength, stiffness and ductility.

The rest of the study is specific to the retrofitting of reinforced concrete frames with steel bracing systems. Applications and previous research are reviewed. A simple approximate analytical model for a braced frame is developed. The selection of frames and bays to be braced and of a bracing pattern is discussed. The advantages of matching the deformability of the bracing system and the existing frame are

investigated. A parametric study is carried out to find the best weakening scheme for the beams of the prototype frame.

## 8.2 Conclusions

The study of the retrofitting of reinforced concrete frames with steel bracing systems leads to the following conclusions. Information gained from the experimental portion of the project and reported in [29] is included.

### 8.2.1 Design Considerations.

Retrofitting Aim. The choice of the retrofitting technique and configuration depends on the specific structural deficiencies and properties of the structure. The weaknesses must be corrected without introducing new ones. Improvements in strength should not be the sole consideration. Changes in the ductility, stiffness, and natural periods of vibration of the structure also affect the seismic performance of the structure.

Adequacy of the Bracing Scheme. Steel bracing systems are very well-suited for retrofitting operations aimed toward strengthening and/or stiffening reinforced concrete structures. The retrofitted structure can be designed to respond in the elastic range because most of the strength added by the bracing system is elastic (for brace slenderness ratios below 100). The strength and stiffness of the bracing system can be adjusted to

good hysteretic behavior of the braced frame. Tests show that the alternate buckling and yielding of the brace is linked with large local deformations at the brace connections which may lead to failure. Even if buckling does not lead to failure, it limits the brace energy dissipation capacity. To avoid the problems associated with inelastic buckling, it is recommended that the bracing system be designed to respond in the elastic range. The connections of the bracing system should nevertheless be detailed for ductile behavior in case the design loads are exceeded. It is also recommended that the effective brace slenderness ratio be kept below 80 to encourage good hysteretic performance.

Prevention of Inelastic Buckling. There are two ways to prevent braces from buckling inelastically. One is for the brace slenderness ratio to be low enough for yielding to take place instead of buckling. Such braces display excellent hysteretic behavior and provide the braced frame with very significant energy dissipation capacity. The slenderness ratio of a brace can be lowered artificially by the use of a "buckling fuse." The other way to prevent inelastic buckling is for the brace slenderness ratio to be large enough for buckling to be elastic, as in cables. Large hysteretic energy dissipation cannot be expected from a system with braces buckling elastically. The cables could be prestressed to improve the serviceability

obtained by the simple superposition of the load-drift curve for the reinforced concrete frame and the bracing system. The buckling length of the braces should be adjusted to account for the restraint provided by the frame.

The basic behavior of a steel braced frame under cyclic lateral loading can be studied adequately using a simple subassemblage representing an elemental unit of the frame and bracing system. The use of that basic unit may also be advantageous in experimental research.

### 8.2.3 Nonstructural Considerations

Disruption. The bracing system is typically attached to the exterior of the perimeter frames. The disruption to the operation of the building during and after construction is minimized in comparison to other schemes which require construction work in the interior of the building. No modification to the window is necessary. Interior furnishing could possibly be left untouched.

Construction. The bracing system can be prefabricated and erected rapidly with a minimum of manpower and equipment. But close quality control is essential, especially with respect to weld inspection, and a moderate to high level of labor skill is necessary. Large fitting tolerances must be allowed because of expected variation in actual frame dimensions.

Aesthetics. The configuration and proportions of an exterior bracing system must be chosen carefully to avoid damaging the appearance of the building. The retrofitted building should not "advertise" that it was "fixed", that the bracing system was added. The bracing system should appear to be a natural component of the structure. The configuration, detailing, and color of the bracing system can be used to give personality to an otherwise plain building. It may often be possible to enhance the aesthetic quality of a building with a carefully shaped exterior bracing system.

### 8.3 Suggestions for Research

The conceptual and analytical study suggests the need for experimental research in the following area:

Connections. The connections in the bracing system and between the bracing system and the frame must not be the weak link in the structure under cyclic loading. Research on the detailing of those connections is needed to improve their reliability under seismic loading.

Use of Cables. The idea of using cable as bracing elements must be researched, particularly in regards to energy dissipation. The possibility of prestressing the cables to improve the behavior at serviceability should be investigated.



Axial Capacity of Short Columns Loaded Laterally. At large lateral drifts short columns suffer damage which can substantially reduce their axial capacity. At large lateral drifts the bracing system may provide adequate lateral strength, but the frame may not be able to carry the gravity loads. The lack of available experimental data on this problem hinders evaluation of the seismic safety of a braced frame with short columns.

Beam Weakening. Experimental research is necessary to confirm the effectiveness of improving the seismic performance of a braced frame with weak columns by weakening the beams. Various possible weakening techniques should be investigated. Guidelines for the design of weakening schemes could be developed.

The goal of future experimental research should be to provide information for the development of design guidelines for the retrofitting of reinforced concrete frames with steel bracing system. Research is also required to ascertain the cost effectiveness of the retrofitting scheme and improve the construction techniques. The need for research must be evaluated in view of the growing demand for seismic retrofitting of existing structures in the U.S. The photograph of Fig. 8.3.1 is witness to the upcoming need for seismic retrofitting with bracing systems.

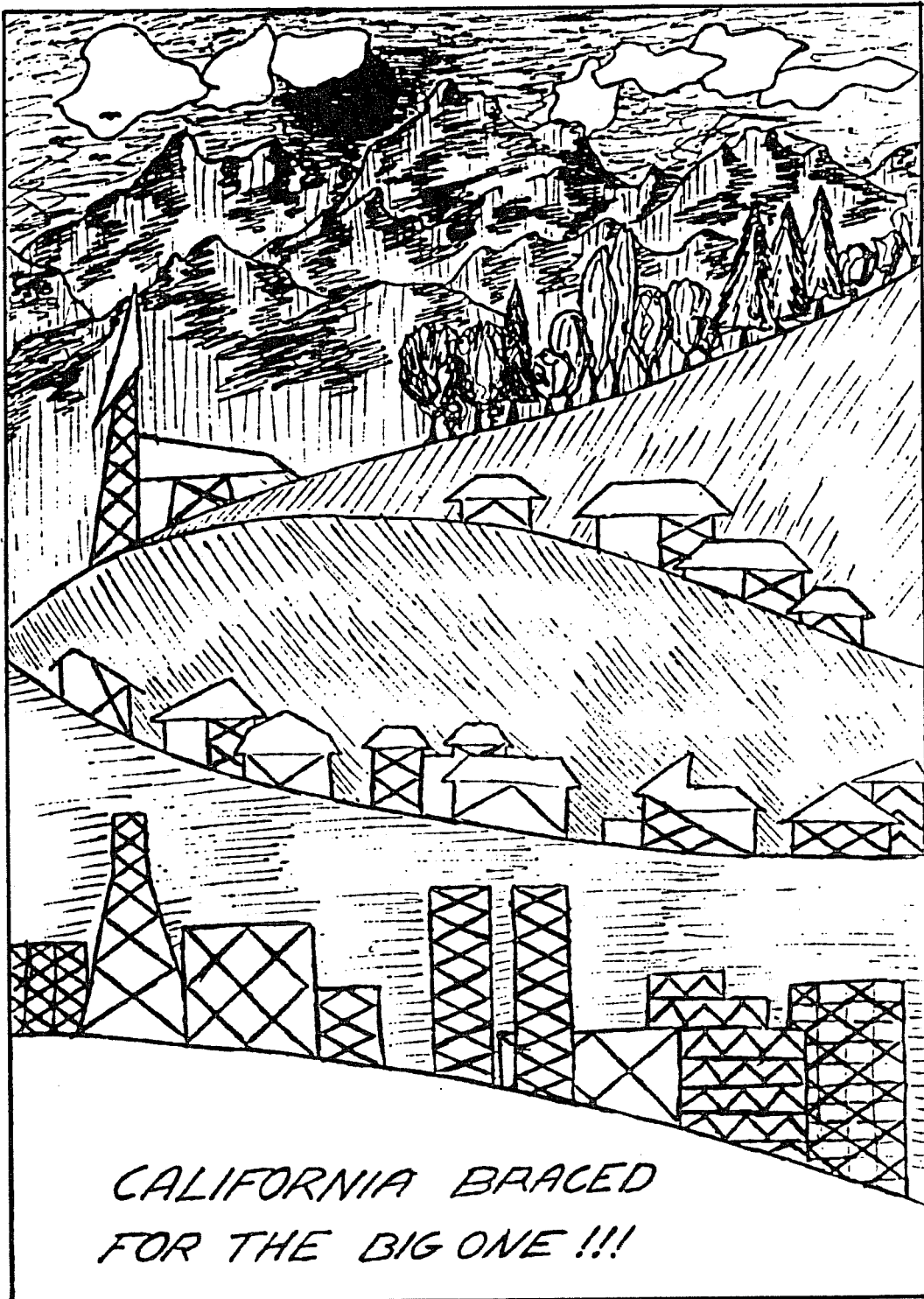


Fig. 8.3.1 California in the year 2000!

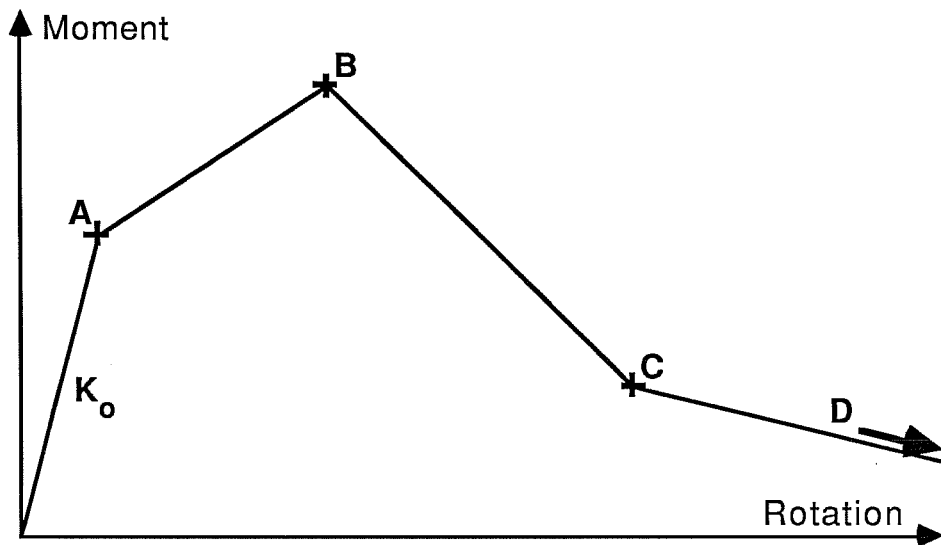
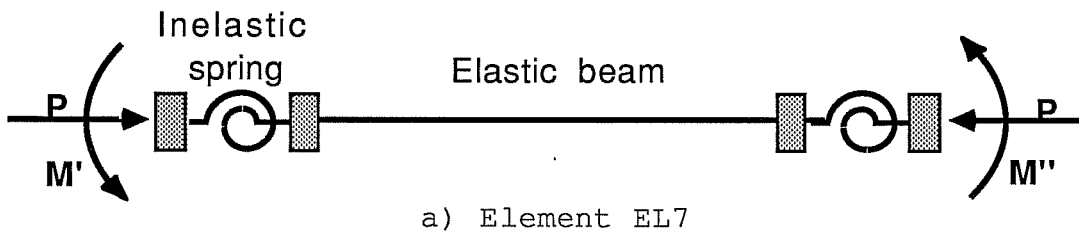
## APPENDIX A

### A.1 Beam Column Element EL7

Beam column element EL7 was developed for this study to model reinforced concrete column and beam behavior under cyclic loading. EL7 was created by modifying library beam element EL6 [31]. The modification was necessary because EL6 can not adequately reflect the behavior of short columns under lateral loading (Sec. 3.7). EL7 has a more sophisticated inelastic component than EL6: it is quadrilinear instead of bilinear and can accommodate negative stiffness.

Element EL7 possesses flexural and axial stiffness, but the moment-axial force interaction is not reproduced. Shear deformation,  $P-\delta$  effects and rigid joints can be modeled. EL7 is a single component model in flexure. A perfectly elastic beam is in series with two end springs (Fig. A.1.1). The nonlinear hysteretic behavior is reproduced by those two rotation springs.

EL7 can be used for modeling short columns (See Sec. 3.6). Since the inelastic behavior is reproduced by the end rotational springs, the model's behavior has to be controlled through the end moments rather than the shear. For a column under double curvature and with the inflection point in the middle, the end moment and the shear are proportional. EL7 can then be used adequately to model a shear-controlled behavior.



b) Moment-rotation relationship for the inelastic spring

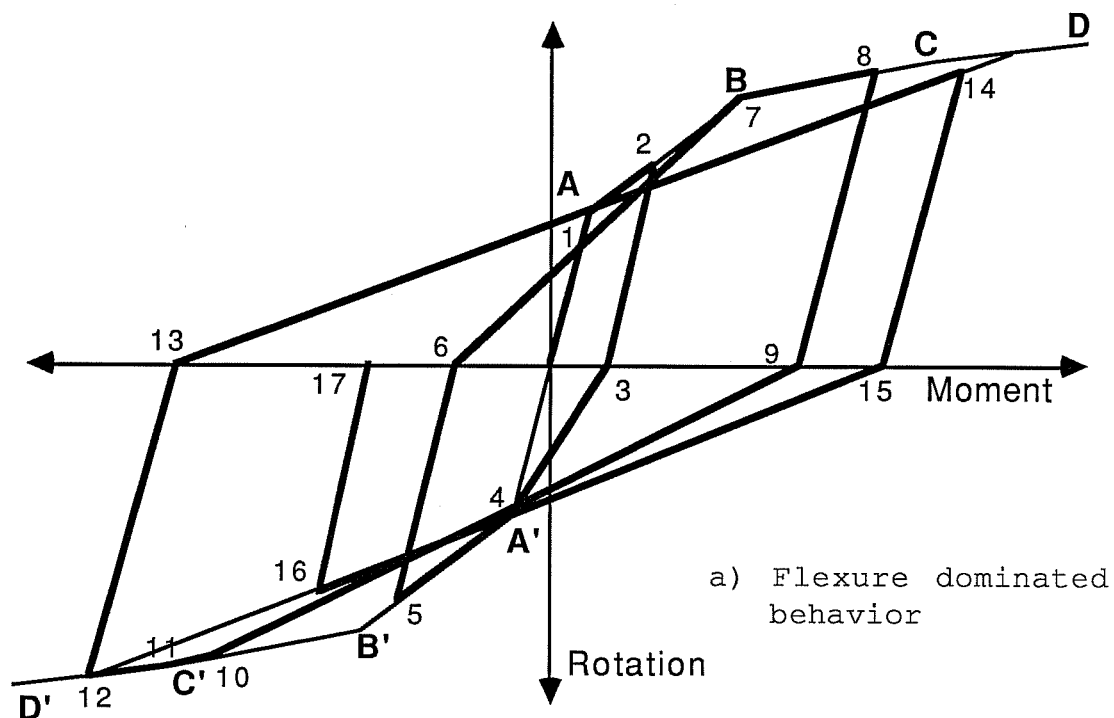
Fig. A.1.1 Beam column element EL7

But the further the inflection point is from midheight, the more the end moments and the shear diverge, and the less appropriate it becomes to use EL7 for the modeling of a shear-dominated component. Fortunately, for most frames under seismic loading, it is reasonable to assume a midheight position of the column inflection point.

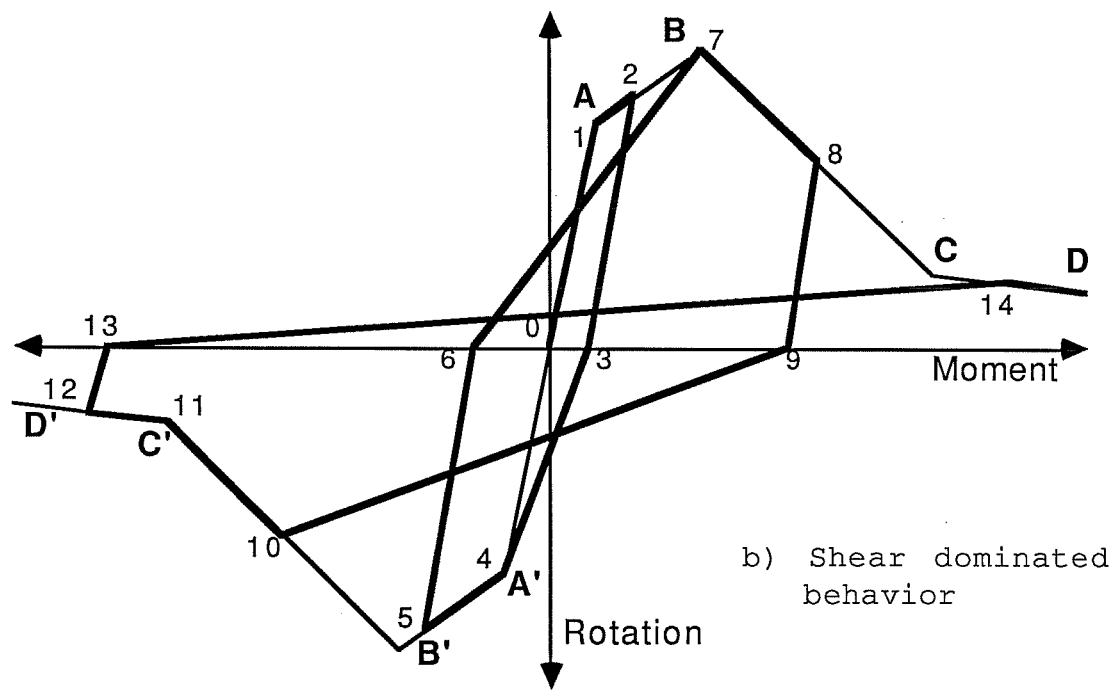
The constitutive hinge moment relationship for the flexural springs is shown in Fig. A.1.1. The length and the slope of segments OA, AB, and BC can be defined freely. This gives the user much liberty in the shaping of the spring "backbone curve." EL7 is thus a versatile element: it can model a flexure-dominated behavior (see Fig. A.1.2a), or a shear-dominated behavior (e.g. short column) (see Fig. A.1.2b).

The hysteretic behavior of the spring is based on the Takeda model and reflects observed experimental behavior for reinforced concrete components (including Bauschinger effects). The hysteretic rules are shown in Fig. A.1.2 both for the flexure and shear dominated behavior. The quadrilinear backbone curve described above is used as an envelope for the cyclic moment-rotation relationship.

A reinforced concrete component submitted to cyclic loading loses stiffness. The hysteretic model reproduces this stiffness degradation. When the load changes sign, the reloading stiffness depends on the amount of accumulated nonlinear



a) Flexure dominated behavior



b) Shear dominated behavior

Fig. A.1.2 Hysteretic rules for beam column element EL7

rotation. The bigger the inelastic rotation, the lower the loading stiffness  $K_l$ . If the reversal point is on segment AB of the envelope (points 2 and 5 in Fig. A.1.2), the loading stiffness  $K_l$  in the following cycle (segment 6-7) is computed with point B as "aim point." For a load reversal on segment BC or CD of the envelope (point 8), the "aim point" for loading in the reversed direction (segment 9-10) is the point with opposite rotation and moment, i.e. symmetric with respect to the origin. This feature was introduced to reproduce the observed behavior of a short column under cyclic lateral loading. If the column is cycled past the peak shear load, on the softening part of the load-deformation curve, any strength loss in one direction results in comparable strength loss in the other direction. The experimental curve of Fig. A.1.3 illustrates this behavior. This feature gives acceptable hysteretic behavior for the flexure-dominated element also (see Fig. A.1.2a).

The amount of pinching is controlled by parameter  $\alpha$ . If  $\alpha = 0$ , the unloading stiffness  $K_u$  is equal to the initial stiffness, and there is no pinching. If  $\alpha = 1.0$ , the pinching is maximum because  $K_u$  is computed for the hysteresis loops to have a zero width at the origin.  $\alpha$  typically lies between 0.0 and 0.4.

The main shortcoming of hysteretic model EL7 is its failure to reproduce the stiffness degradation of a reinforced

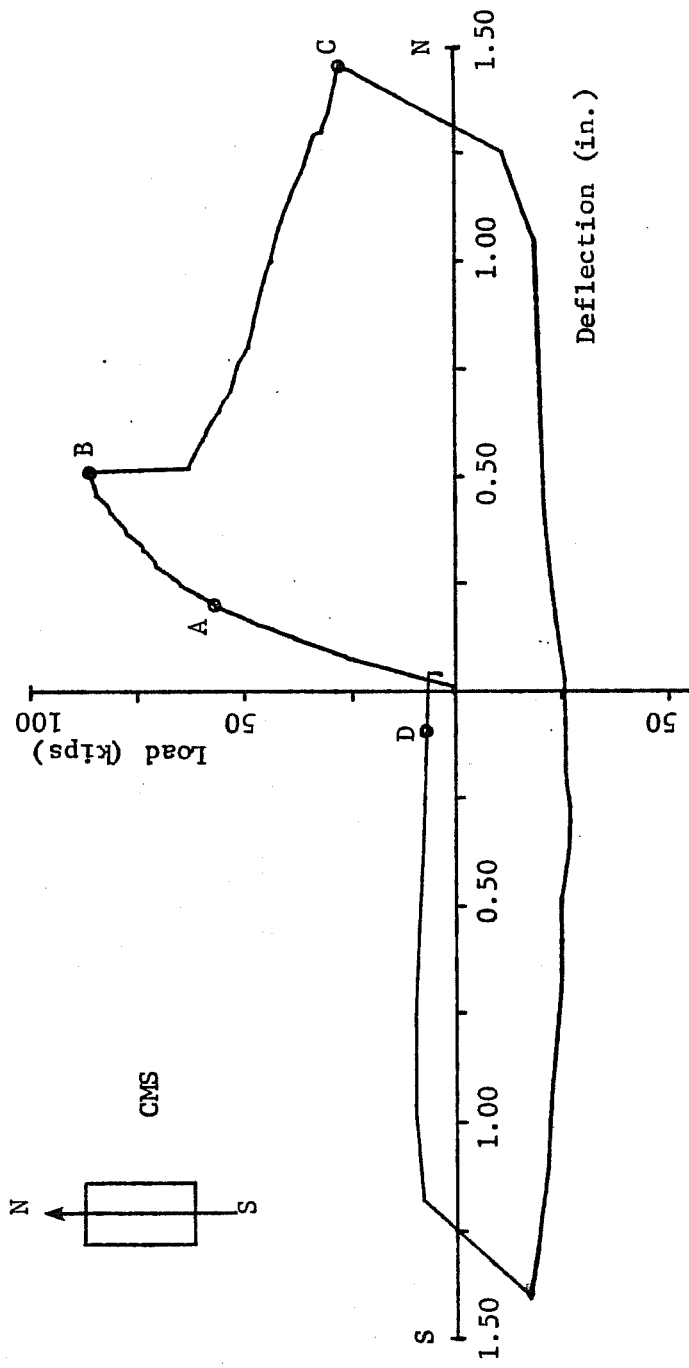


Fig. A.1.3 Experimental load-deflection for a short column [24]



concrete element which is cycled several times to a given inelastic displacement. This model only introduces stiffness degradation when the peak displacement is increasing from one cycle to the next.

## A.2 Buckling Element EL10

End moment buckling element EL10 [16] was developed for use with DRAIN-2D. It models steel members, with fixed ends, subjected to cyclic loading. The model is based on experimental work described in Sec. 1.2. EL10 has flexural and axial stiffness. In flexure, EL10 is a two component model: a perfect elasto-plastic component is paralleled by a perfectly elastic component. The elastic component models strain hardening. The end moment axial force interaction diagram for the elasto plastic element is shown in Fig. A.2.1.

The axial hysteresis behavior of the element is shown in Fig. A.2.1. The energy dissipation capacity under cyclic loading is controlled primarily by the post-buckling load level P<sub>YNC</sub>, which is typically between 0.3 and 0.6 of the buckling load P<sub>YN</sub>. After the first cycle, the maximum compression load is P<sub>YNC</sub>. The location of point F is a function of the slenderness ratio  $kl/r$ .

In the original element EL10, the rate of capacity degradation after first buckling is independent of the slenderness ratio. In other words, the slope BC in Fig. A.2.1 is



independent of  $Kl/r$ . This was changed for the study herein; the change was based on experimental work [11]. Fig. 1.4.6 shows that the loss of capacity following buckling is "faster" for slender members. A new equation is introduced which gives a steeper slope BC for a slender member:

$$SBC = 3 * (80/(kl/r)) * (1/(1 - PYNC/PYN))$$

The effect of the change in the computation of slope BC on the modeled brace behavior can be seen in Fig. 6.2.1.

The main shortcoming of the model is its failure to reproduce the progressive decrease of the buckling load in the first 5-10 cycles. Recent research has produced more sophisticated models, but axial hysteresis of EL7 strikes a good balance between numerical simplicity and complex experimental behavior.

## REFERENCES

1. Wyllie, L., "Seismic Strengthening Procedures for Existing Buildings", Strengthening of Building Structures - Diagnosis and Theory, IABSE Symposium, Venice, Italy, 1983, pp. 363-370.
2. Kawamata, S. and Masaki, Q. "Strengthening Effect of Eccentric Steel Braces to Existing R.C. frames," Proceedings 7th World Conf. on Earthquake Eng., Istanbul, 1980.
3. Del Valle, E., "Some Lessons from the March 14 Earthquake in Mexico City," Proceedings 7th World Conf. on Earthquake Eng., Istanbul, 1980.
4. Sugano, S., and Fujimura, M., "Aseismic Strengthening of Existing Reinforced Concrete Buildings," Proceedings of the Seventh World Conference on Earthquake Engineering, Part I, Vol. 4, Istanbul, Turkey, 1980, pp. 449-456.
5. Sugano, S., "An Overview of the State-of-the-Art in Seismic Strengthening of Existing Reinforced Concrete Buildings in Japan", Proceedings of the Third Seminar on Repair and Retrofit of Structures, Ann Arbor, Michigan, 1982, pp. 328-349.
6. Higashi, Y., et al., "Experimental study of Strengthening Reinforced Concrete Structures by Adding Shear Wall," Seventh World Conference on Earthquake Engineering, Istanbul, Turkey, 1980, V. 7., pp. 173-180.
7. Sugano, S. and Endo, T., "Seismic Strengthening of Reinforced Concrete Building in Japan," Strengthening of Building Structures - Diagnosis and Theory, IABSE Symposium, Venice, Italy, 1983, pp. 371-378.
8. Sugano, S. and Fujimura M., "Aseismic Strengthening of Existing Reinforced Concrete Buildings," Seventh world Conference on Earthquake Engineering, Istanbul, Turkey, 1980, V. 4, pp. 449-456.
9. Higashi, Y., Endo, T., and Shimizu, Y., "Experimental Studies on Retrofitting of Reinforced Concrete Structural Members," Proceedings of the Second Seminar on Repair and Retrofit of Structures, Ann Arbor, MI, 1981, pp. 126-155.

10. Aoyama, H., Yamamoto, Y., "Seismic Strengthening of Existing R.C. Buildings." Proceedings from the U.S.-Japan Joint Seminar on Composite and Mixed Construction, ASCE, July 1984.
11. Black, G., Wenger, W., and Popov, E., "Inelastic Buckling of Steel Structures Under Cyclic Load Reversals," UCB/EERC Report - 80/40, Berkeley, CA, October 1980.
12. Gugerli, H. and Goel, S., "Inelastic Cyclic Behavior of Steel Bracing Members," UMEE Report 82R1, Ann Arbor, MI, January 1982.
13. Zayas, A.Z., Shing, P.B., Mahin, S.A. and Popov, E.P., "Inelastic Structural Modeling of Braced Offshore Platforms for Seismic Loading," Report No. UCB/EERC-81/04 Earthquake Engineering Research center, University of California Berkeley, CA., January 1981.
14. Ikeda, K., and Mahin, S.A., and Dermitzakis, S.N., "Phenomenological Modeling of Steel Braces Under Cyclic Loading," Report No. UCB/EERC-84/09, Earthquake Engineering Research Center, University of California, Berkeley, CA, May 1984.
15. Ikeda, K., Mahin, S.A., "A Refined Physical Theory Model for Predicting the Seismic Behavior of Braced Steel Frames", Report No. UCB/EERC-84/12, Earthquake Engineering Research Center, University of California, Berkeley, CA, July 1984.
16. Jain, A.K., and Goel, S.C., "Hysteresis Models for Steel Members Subjected to Cyclic Buckling or Cyclic End Moments and Buckling," University of Michigan Research Report UMEE 78R6, Ann Arbor, December, 1978.
17. Sugano, S., "Guidelines for Seismic Retrofitting (Strengthening, Toughening, and/or Stiffening) Design of Existing Reinforced Concrete Buildings," Proceedings of the Second Seminar on Repair and Retrofit of Structures, Ann Arbor, MI, 1981, pp. 189-237.
18. Aoyama, H., "A Method for the Evaluation of the Seismic Capacity of Existing Reinforced Concrete Buildings in Japan." Bulletin of the New Zealand National Society for Earthquake Engineering, Vol. 14, No. 3, September 1981.

19. Newmark, N.M., Hall, W.J., "Procedures and Criteria for earthquake Resistant Design", Building Practice for Disaster Mitigation, Building Science Series 45, National Bureau of Standards, Washington, D.C., 1973.
20. Kelly, J.M., "The Economic Feasibility of Seismic Rehabilitation of Buildings by Base Isolation", Report No. UCB/EERC-83/01, Earthquake Engineering Research Center, University of California, Berkeley, CA, 1983.
21. Hanson, R.D., Bergman, D.M., Ashour, S.A., "Supplemental Mechanical Damping for Improved Seismic Response of Buildings", Proceedings Third U.S. National Conference on Earthquake Engineering, EERI, Charleston, South Carolina, 1986.
22. Popov, E.P., Malley, J.O., "Design of Links and Beam-to-Column connections for Eccentrically braced Steel Frames", Report UCB/EERC-83/03, Earthquake Engineering Research Center, University of California, Berkeley, CA, 1983.
23. Woodward, K. and Jirsa, J.O., "Influences of Reinforcement on R.C. Short Column Lateral Resistance," ASCE Journal of Structural Eng., vol. 110, Jan. 1984.
24. Umehara, H., Jirsa, J.O., "Shear Strength and Deterioration of Short Reinforced Concrete Columns Under Cyclic Deformations", PMFSEL 82-3, The University of Texas at Austin, 1982.
25. American Concrete Institute, Building Code Requirements for Reinforced Concrete (ACI 318-83), Detroit, MI, 1983.
26. Bush, T., Roach, C., Jones, E. and Jirsa, J., "Behavior of a Strengthened Reinforced Concrete Frame," Proc., Third U.S. Natl. Conf. on Earthquake Eng., EERI Publ., 1986.
27. Roach, C., "Seismic Strengthening of a Reinforced Concrete Frame Using Reinforced Concrete Piers," unpublished master's thesis, The University of Texas at Austin, May 1986.
28. Jones, E., "Seismic Strengthening of a Reinforced Concrete Frame Using Structural steel Bracing," unpublished Master's thesis, The University of Texas at Austin, december 1985.

29. Bush, T., "Seismic Strengthening of a Reinforced Concrete Frame," unpublished Ph.D. dissertation, The University of Texas at Austin, May 1987.
30. Keshavarzian, M., Schnobrich, W.C., "Analytical Models for the Nonlinear Seismic Analysis of Reinforced Concrete Structures", Engineering Struct., 1985, Vol. 7.
31. Kanaan, A.E., Powell, G.H., "DRAIN-2D, A General Purpose Computer Program for Dynamic Analysis of Inelastic Plane Structures", Report EERC 73-6 and EERC 73-22, University of California, Berkeley, CA.
32. Filiatrault, A., Cherry, S., "Seismic Tests of Friction Damped Steel Frames", Proceedings Third Conference of the Engineering Mechanics Division of ASCE, University of California, Los Angeles, 1986.
33. Paulay, T., "A Critique of the Special Provisions for Seismic Design of the Building Code Requirements for Reinforced Concrete (ACI 318-83)", ACI Journal, Vol. 83, No. 2, April 1986, pp. 274-283.

V I T A

Marc Eric Badoux was born in Bern, Switzerland, on October 5, 1961, the son of Jean-Claude Badoux and Eliane Badoux. He attended high school in Lausanne, Switzerland. He entered the Swiss Federal Institute of Technology in Zurich in October 1979 and received the degree of bachelor of civil engineering in December, 1983. In January 1984 he entered the graduate school of The University of Texas at Austin.

Permanent Address:                   12 Beau-Site  
  CH-1004 Lausanne  
  Switzerland

The dissertation was typed by staff of Ferguson Structural Engineering Laboratory.